

# EXPLORING THE POTENTIAL OF NATURAL PRODUCTS THROUGH ADVANCED TECHNIQUES AND GREEN SOLVENTS

EDITED BY: Mauricio A. Rostagno, Ana Carolina De Aguiar,  
Gerardo Fernández Barbero and Marta Ferreiro González  
PUBLISHED IN: Frontiers in Chemistry





# frontiers

## Frontiers eBook Copyright Statement

The copyright in the text of individual articles in this eBook is the property of their respective authors or their respective institutions or funders. The copyright in graphics and images within each article may be subject to copyright of other parties. In both cases this is subject to a license granted to Frontiers.

The compilation of articles constituting this eBook is the property of Frontiers.

Each article within this eBook, and the eBook itself, are published under the most recent version of the Creative Commons CC-BY licence.

The version current at the date of publication of this eBook is CC-BY 4.0. If the CC-BY licence is updated, the licence granted by Frontiers is automatically updated to the new version.

When exercising any right under the CC-BY licence, Frontiers must be attributed as the original publisher of the article or eBook, as applicable.

Authors have the responsibility of ensuring that any graphics or other materials which are the property of others may be included in the CC-BY licence, but this should be checked before relying on the CC-BY licence to reproduce those materials. Any copyright notices relating to those materials must be complied with.

Copyright and source acknowledgement notices may not be removed and must be displayed in any copy, derivative work or partial copy which includes the elements in question.

All copyright, and all rights therein, are protected by national and international copyright laws. The above represents a summary only. For further information please read Frontiers' Conditions for Website Use and Copyright Statement, and the applicable CC-BY licence.

ISSN 1664-8714

ISBN 978-2-88966-406-1

DOI 10.3389/978-2-88966-406-1

## About Frontiers

Frontiers is more than just an open-access publisher of scholarly articles: it is a pioneering approach to the world of academia, radically improving the way scholarly research is managed. The grand vision of Frontiers is a world where all people have an equal opportunity to seek, share and generate knowledge. Frontiers provides immediate and permanent online open access to all its publications, but this alone is not enough to realize our grand goals.

## Frontiers Journal Series

The Frontiers Journal Series is a multi-tier and interdisciplinary set of open-access, online journals, promising a paradigm shift from the current review, selection and dissemination processes in academic publishing. All Frontiers journals are driven by researchers for researchers; therefore, they constitute a service to the scholarly community. At the same time, the Frontiers Journal Series operates on a revolutionary invention, the tiered publishing system, initially addressing specific communities of scholars, and gradually climbing up to broader public understanding, thus serving the interests of the lay society, too.

## Dedication to Quality

Each Frontiers article is a landmark of the highest quality, thanks to genuinely collaborative interactions between authors and review editors, who include some of the world's best academicians. Research must be certified by peers before entering a stream of knowledge that may eventually reach the public - and shape society; therefore, Frontiers only applies the most rigorous and unbiased reviews.

Frontiers revolutionizes research publishing by freely delivering the most outstanding research, evaluated with no bias from both the academic and social point of view. By applying the most advanced information technologies, Frontiers is catapulting scholarly publishing into a new generation.

## What are Frontiers Research Topics?

Frontiers Research Topics are very popular trademarks of the Frontiers Journals Series: they are collections of at least ten articles, all centered on a particular subject. With their unique mix of varied contributions from Original Research to Review Articles, Frontiers Research Topics unify the most influential researchers, the latest key findings and historical advances in a hot research area! Find out more on how to host your own Frontiers Research Topic or contribute to one as an author by contacting the Frontiers Editorial Office: [researchtopics@frontiersin.org](mailto:researchtopics@frontiersin.org)

# EXPLORING THE POTENTIAL OF NATURAL PRODUCTS THROUGH ADVANCED TECHNIQUES AND GREEN SOLVENTS

Topic Editors:

**Mauricio A. Rostagno**, Campinas State University, Brazil

**Ana Carolina De Aguiar**, Campinas State University, Brazil

**Gerardo Fernández Barbero**, University of Cádiz, Spain

**Marta Ferreiro González**, University of Cádiz, Spain

**Citation:** Rostagno, M. A., De Aguiar, A. C., Barbero, G. F., González, M. F., eds. (2021). Exploring the Potential of Natural Products through Advanced Techniques and Green Solvents. Lausanne: Frontiers Media SA.  
doi: 10.3389/978-2-88966-406-1

# Table of Contents

- 04 Editorial: Exploring the Potential of Natural Products Through Advanced Techniques and Green Solvents**  
Gerardo Fernández Barbero, Ana Carolina de Aguiar, Marta Ferreira-González and Mauricio Ariel Rostagno
- 07 Deep Eutectic Solvent Micro-Functionalized Graphene Assisted Dispersive Micro Solid-Phase Extraction of Pyrethroid Insecticides in Natural Products**  
Xiaoyu Song, Rui Zhang, Tian Xie, Shuling Wang and Jun Cao
- 17 Transformation Characteristics of Hydrogen-Donor Solvent Tetralin in the Process of Direct Coal Liquefaction**  
Hai-zhou Chang, Jun-qi Li, Shuai Du, Kai-yuan Shen, Qun Yang, Han Yi and Ji-wei Zhang
- 23 Highly Efficient Adsorption of Phenylethanoid Glycosides on Mesoporous Carbon**  
Helin Xu, Wenjing Pei, Xueqin Li and Jinli Zhang
- 34 Selective Adsorption and Purification of the Acteoside in *Cistanche tubulosa* by Molecularly Imprinted Polymers**  
Xiaobin Zhao, Wenjing Pei, Ruili Guo and Xueqin Li
- 47 Fungi as a Potential Source of Pigments: Harnessing Filamentous Fungi**  
Rishu Kalra, Xavier A. Conlan and Mayurika Goel
- 70 Extraction of Flavonoids From Natural Sources Using Modern Techniques**  
Jaísa Oliveira Chaves, Mariana Corrêa de Souza, Laise Capelasso da Silva, Daniel Lachos-Perez, Paulo César Torres-Mayanga, Ana Paula da Fonseca Machado, Tânia Forster-Carneiro, Mercedes Vázquez-Espinosa, Ana Velasco González-de-Peredo, Gerardo Fernández Barbero and Mauricio Ariel Rostagno





# Editorial: Exploring the Potential of Natural Products Through Advanced Techniques and Green Solvents

Gerardo Fernández Barbero<sup>1\*</sup>, Ana Carolina de Aguiar<sup>2</sup>, Marta Ferreira-González<sup>1</sup> and Mauricio Ariel Rostagno<sup>3</sup>

<sup>1</sup> Department of Analytical Chemistry, Faculty of Sciences, University of Cadiz, Cadiz, Spain, <sup>2</sup> Laboratório de Engenharia de Processos, Departamento de Engenharia de Alimentos, Faculdade de Engenharia de Alimentos (LEP/DEA/FEA), University of Campinas, Campinas, Brazil, <sup>3</sup> Department of Analytical Chemistry, Faculty of Sciences, University of Cadiz, Cadiz, Spain

**Keywords:** natural products, green solvents, new technologies, extraction techniques, purification techniques

## Editorial on the Research Topic

### Exploring the Potential of Natural Products Through Advanced Techniques and Green Solvents

This Research Topic presents a brief overview on a number of relevant studies that focus on two main aspects, i.e., on the one hand, the potential of natural products of interest obtained through extraction, separation, purification, or transformation by applying novel and advanced extraction and conservation techniques and on the other hand, the study of green methodologies that intend to either minimize the use of harmful solvents or favor the use of green solvents.

A wide and complex range of plants, animals, insects, and microorganisms that can be found in nature exhibit the capacity to produce a broad range of chemical compounds with interesting properties regarding human health and are still to be explored from a diversity of approaches. These include the attempts to replace synthetic food additives for health concern reasons or the production of second generation ethanol from biomass, just to mention a couple of them. In this regards, Science is increasingly discovering the potential of natural products and gradually changing our world and reshaping the way our society contemplates them.

If the use of natural products is to become a reality, there are several aspects which must be taken into consideration. Thus, their effectiveness or even their possible negative effects on human health as well as other aspects such as the methodologies employed in their production, their processing costs and also their environmental impact are important matters of concern. At the same time, the varying form in which they can be found in nature and the specific requirements that to ensure their production according to a satisfactory standard quality so that they are generally accepted by consumers are some of the issues to be seriously considered.

Consequently, natural products are constantly gaining weight and leading to the emergence of new technologies, processes, and methodologies applied to their extraction, separation, purification, transformation or analysis.

Even though considerable advances are being made, the challenge to develop new techniques and more efficient, greener, more rapid and affordable methods is still a pressing need. The use of green solvents, such as CO<sub>2</sub>, water or biobased ones that intend to reduce environmental impact, while improving selectivity and yields, have proven to be of special interest, since they can largely contribute to perfect old production processes, particularly when combined with particularly advanced and innovative techniques. In this sense, supercritical fluid technology deserves special attention for its potential to do away with the use of the toxic or polluting solvents that have been traditionally used by other methods. The extraction of hydrophobic compounds using supercritical

## OPEN ACCESS

### Edited and reviewed by:

Valeria Conte,  
University of Rome Tor Vergata, Italy

### \*Correspondence:

Gerardo Fernández Barbero  
gerardo.fernandez@uca.es

### Specialty section:

This article was submitted to  
Green and Sustainable Chemistry,  
a section of the journal  
Frontiers in Chemistry

**Received:** 08 November 2020

**Accepted:** 16 November 2020

**Published:** 07 December 2020

### Citation:

Barbero GF, de Aguiar AC,  
Ferreira-González M and  
Rostagno MA (2020) Editorial:  
Exploring the Potential of Natural  
Products Through Advanced  
Techniques and Green Solvents.  
Front. Chem. 8:627111.  
doi: 10.3389/fchem.2020.627111

CO<sub>2</sub> or the hydrolysis of cellulose from biomass using subcritical water are only some of the examples of a great potential still to be further investigated. Ultrasound is another technology that has been widely used to enhance some old processes by combining it with a number of new technologies and methodologies. Microwaves and electric fields have also proven their efficiency as an alternative processing method with a great potential.

In order to truly and deeply understand the mechanisms involved, we should still gather a considerable amount of data that would allow us to determine the influence of the process parameters to be considered in relation to each technology; i.e., temperature, pressure, power input, processing time, raw material features, stability, etc. And such knowledge should lead us to a further and more successful development of those attractive and novel technologies.

"Exploring the Potential of Natural Products through Advanced Techniques and Green Solvents" is a special issue of *Frontiers in Chemistry* that intends to illustrate the state of the art in this field through six outstanding contributions.

Chaves et al. contribution consists on an exhaustive revision on the use of modern techniques for the extraction of flavonoids from natural sources. Flavonoids are natural phenolic compounds that are synthesized by some plants as secondary metabolites and can be widely found in the vegetable kingdom. They are responsible for the flavor, color, and pharmacological activities of plants and plant products. Flavonoids exhibit rather marked and interesting biological properties, such as antioxidant, anti-inflammatory or anti-tumor activities, among others. Those beneficial properties make of them the focus of interest for a large amount of projects and papers that are currently addressing a number of specific aspects, such as their biological synthesis, extraction, analysis or stability. In this review, the newest natural compound extraction techniques that are currently being used are addressed in detail. Those techniques intend to minimize solvent consumption, increase extraction yields, improve extraction selectivity, reduce processing times, and minimize the degradation of the target compounds, thus reducing process costs and environmental consequences. ultrasound assisted extraction (UAE), supercritical fluid extraction (SFE), microwave assisted extraction (MAE), pressurized liquid extraction (PLE) or accelerated solvent extraction-ASE), along with a combination of different techniques are among those novel techniques that are being employed to extract both flavonoids as well as bioactive compounds from natural sources (Barba et al., 2016).

In another study, Kalra et al. investigated fungi as a potential source of pigments. A growing concern related to the harmful effects of synthetic colorants on both human health and the environment has given place to a substantial interest in natural coloring alternatives. Thus, the world demand for natural colorants that can be used by the food, cosmetic and textile industries is rapidly increasing. At present, plants and microorganisms are the main source of dyes and pigments used by modern industries. Among other unconventional sources of dyes and pigments production, filamentous fungi and, particularly, ascomycete and basidiomycete (mushroom) fungi, and lichens, are known to produce an extraordinary range of colors that comprise several chemical classes of pigments

such as melanins, azaphilones, flavins, phenazines, and quinines. Filamentous fungi are an important source of a wide range of metabolites such as polyphenols, polyketides, carotenoids, terpenoids and a broad range of colored compounds. Selecting the extraction techniques is one of the crucial steps for the efficient recovery of these metabolites and it mainly depends on the nature of the metabolites of interest as well as on the location of such metabolites in the mushroom culture (Chadni et al., 2017). Some of the pigments are extracellular and in those cases, they are easily released into the fermentation broth, which makes their extraction generally more feasible than in the case of intracellular pigments, which require specialized extraction techniques to be removed from the biomass containing them. The use of inexpensive, efficient, and safe extraction methodologies for the recovery of natural pigments is one of the main challenges to be overcome in order to enable large-scale production. For easier and more feasible further processing, extracellular, and water-soluble pigments obtained by submerged cultures are preferred. For the extraction of hydrophobic and intracellular compounds, green extraction methods seem to be the most suitable, since they are free from organic solvents or require smaller amounts of the same and are, therefore, considered both safer and more environmentally friendly. Some of these extraction techniques can also be successfully used at low temperature. This contributes to the extraction of thermolabile pigments while avoiding their degradation. UAE, PLE, MAE, SFE, ionic liquid-assisted extraction and pulsed electric field (PEF) assisted extraction are among the latest techniques used to obtain fungal dyes.

With respect to original research articles, Song et al. extracted and synthesized five pyrethroid insecticides by applying, for the first time, deep eutectic solvent micro-functionalized graphene (DES-G) as the adsorbent of the dispersive micro solid-phase extraction (DMSPE). While food safety is generally a matter of major concern for most consumers, pesticides, and other additive residues have always been considered a serious problem when it comes to human safety. The use of certain pesticides such as organochlorine, organophosphorus or pyrethroid insecticides greatly contribute to the control of pests and to the increment of crop yields. However, airborne pesticides may accumulate on the surface of crops and enter the food chain causing considerable damage to consuming species. Pyrethroid insecticides are particularly toxic to mammals because of their low water solubility, high liposolubility, and a considerable capacity to pass through biofilms (Feo et al., 2010). It is therefore necessary to develop the adequate analytical methods that allow for the extraction and analysis of pyrethroid insecticides, especially from complex matrices. In this sense, in order to improve the detection efficiency of pyrethroid insecticide analytical methods and to reduce organic solvent consumption, a green and efficient microextraction method was to be developed. Thus, such a method has been developed in this research, where several DES-Gs have been synthesized by simple procedures and an optimum DES-G has been selected as the adsorbent of DMSPE. The developed method has been successfully applied to determine pyrethroid insecticides residues in beebread, *Curcuma wenyujin*

and *Dendrobium officinale* with recoveries in the range of 80.9–114.1%. Another article by Chang et al. described the production of the hydrogen-donor solvent tetralin by means of the direct liquefaction of coal. Pure tetralin liquid as well as mixture of tetralin and Wucuiwan coal (WCW) were separately reacted under a liquefaction conditions. Direct liquefaction of coal is an efficient option for the green use of coal, since it transforms solid coal into liquid solvents by adding hydrogen (Vasireddy et al., 2011). When tetralin is used as the hydrogen-donor solvent the liquefaction rate of WCW at 380 and 420°C reaches between 69.76 and 83.86%, respectively. Xu et al. have studied the extraction and purification of phenylethanoid glycosides (PhGs) from *Cistanche tubulosa*, by adsorption of its extracts. PhGs are the main active compounds in *Cistanche tubulosa*, which exhibit several pharmacological activities including the protection of neurons and liver, the regulation of the immunological system as well as anti-inflammatory and antioxidative properties. For the extraction and purification of these compounds a new adsorption material was tested, namely the mesoporous carbon (Qin et al., 2018). Three types of mesoporous carbons were tested and compared for PhGs extraction and purification: ordered mesoporous carbon (CMK-3), disordered mesoporous carbon (DMC), and three-dimensional cubic mesoporous carbon (CMK-8). The results indicated that CMK-3 showed the highest adsorption capacity due to its highly specific surface area, its large number of pores and its oxygen-containing functional groups. Finally, Zhao et al. also presented the purification of the acteoside (main PhG from *Cistanche tubulosa*) in its extracts by means of other adsorbing substances such as molecularly imprinted polymers (MIPs) (Lulinski et al., 2016). In their study, the MIPs

were designed and synthesized to selectively adsorb acteoside. The effects of different functional monomers, crosslinkers, and MIP solvents were investigated. The MIPs were studied in static adsorption, dynamic adsorption, and selectivity experiments. The results proved that MIPs can be employed as an adsorption material to purify the active ingredients that can be found in plant extracts.

In this Research Topic, we have tried to present the state of the art on the use of novel techniques for the extraction and/or purification of different natural compounds of interest for human health that can be found in a variety of plant matrices. A number of advanced techniques, new materials, and the use of green methodologies have been described and their promising results lead us to think that they will soon be replacing older, traditional methods that demand larger amounts of energy, time, and solvents, with the subsequent environmental and economic negative effects.

## AUTHOR CONTRIBUTIONS

GB, AA, MF-G, and MR contributed in handling the manuscripts as Guest/Associate guest editors and have also written the editorial. All authors contributed to the article and approved the submitted version.

## ACKNOWLEDGMENTS

The editors would like to thank the authors, co-authors, reviewers, and the Frontiers in Chemistry development team, whose efforts led to the success of this special topic.

## REFERENCES

- Barba, F. J., Zhu, Z., Koubaa, M., Sant'Ana, A. S., and Orlie, V. (2016). Green alternative methods for the extraction of antioxidant bioactive compounds from winery wastes and by-products: a review. *Trends Food Sci. Technol.* 49, 96–109. doi: 10.1016/j.tifs.2016.01.006
- Chadni, Z., Rahaman, M. H., Jerin, I., Hoque, K., and Reza, M. A. (2017). Extraction and optimisation of red pigment production as secondary metabolites from *Talaromyces verruculosus* and its potential use in textile industries. *Mycology* 8, 48–57. doi: 10.1080/21501203.2017.1302013
- Feo, M. L., Eljarrat, E., and Barceló, D. (2010). Determination of pyrethroid insecticides in environmental samples. *TrAC-Trend. Anal. Chem.* 29, 692–705. doi: 10.1016/j.trac.2010.03.011
- Lulinski, P., Bamburówicz-Klimkowska, M., Dana, M., Szutowski, M., and Maciejewska, D. (2016). Efficient strategy for the selective determination of dopamine in human urine by molecularly imprinted solid-phase extraction. *J. Separ. Sci.* 39, 895–903. doi: 10.1002/jssc.201501159
- Qin, G., Ma, J., Wei, W., Li, J., and Yue, F. (2018). The enrichment of chlorogenic acid from *eucommia ulmoides* leaves extract by mesoporous carbons. *J. Chromatogr. B* 1087–1088, 6–13. doi: 10.1016/j.jchromb.2018.04.036
- Vasireddy, S., Morreale, B., Cugini, A., Song, C., and Spivey, J. J. (2011). Clean liquid fuels from direct coal liquefaction: chemistry, catalysis, technological status and challenges. *Energy Environ. Sci.* 4, 311–345. doi: 10.1039/C0EE00097C

**Conflict of Interest:** The authors declare that the research was conducted in the absence of any commercial or financial relationships that could be construed as a potential conflict of interest.

Copyright © 2020 Barbero, de Aguiar, Ferreiro-González and Rostagno. This is an open-access article distributed under the terms of the Creative Commons Attribution License (CC BY). The use, distribution or reproduction in other forums is permitted, provided the original author(s) and the copyright owner(s) are credited and that the original publication in this journal is cited, in accordance with accepted academic practice. No use, distribution or reproduction is permitted which does not comply with these terms.



# Deep Eutectic Solvent Micro-Functionalized Graphene Assisted Dispersive Micro Solid-Phase Extraction of Pyrethroid Insecticides in Natural Products

Xiaoyu Song<sup>1</sup>, Rui Zhang<sup>1</sup>, Tian Xie<sup>1\*</sup>, Shuling Wang<sup>1\*</sup> and Jun Cao<sup>1,2\*</sup>

<sup>1</sup> Medical College, Hangzhou Normal University, Hangzhou, China, <sup>2</sup> College of Material Chemistry and Chemical Engineering, Hangzhou Normal University, Hangzhou, China

## OPEN ACCESS

### Edited by:

Mauricio A. Rostagno,  
Campinas State University, Brazil

### Reviewed by:

Mustafa Soylak,  
Erciyes University, Turkey  
Ali Mohammad Haji Shabani,  
Yazd University, Iran

### \*Correspondence:

Tian Xie  
xbs@hznu.edu.cn  
Shuling Wang  
wsling222@163.com  
Jun Cao  
caoj@hznu.edu.cn

### Specialty section:

This article was submitted to  
Green and Sustainable Chemistry,  
a section of the journal  
Frontiers in Chemistry

Received: 25 May 2019

Accepted: 09 August 2019

Published: 23 August 2019

### Citation:

Song X, Zhang R, Xie T, Wang S and  
Cao J (2019) Deep Eutectic Solvent  
Micro-Functionalized Graphene  
Assisted Dispersive Micro Solid-Phase  
Extraction of Pyrethroid Insecticides in  
Natural Products. *Front. Chem.* 7:594.  
doi: 10.3389/fchem.2019.00594

Deep eutectic solvent micro-functionalized graphene (DES-G) was synthesized and first applied as the adsorbent of dispersive micro solid-phase extraction (DMSPE) to extract five pyrethroid insecticides. In DMSPE, the target analytes were absorbed by DES-G and then desorbed by trace eluent, next, the treated samples were quantified via ultra-high performance liquid chromatography equipped with diode-array detection. A scanning electron microscope, transmission electron microscopy and Fourier transform infrared spectrometer were used to characterize the prepared DES-G. Furthermore, this method was verified under the selected conditions with the precision for retention times ranging from 0.43 to 0.57%, and repeatability ranged from 0.04 to 2.41% for peak areas. The developed method was successfully applied to determine pyrethroid insecticides residues in beebread, *Curcuma wenyujin* and *Dendrobium officinale* with the recoveries in the range of 80.9–114.1%.

**Keywords:** deep eutectic solvent, graphene, dispersive micro solid-phase extraction, pyrethroid insecticides, beebread, *Curcuma wenyujin* and *Dendrobium officinale*, ultra-high performance liquid chromatography

## INTRODUCTION

Graphene, similar to graphite, C<sub>60</sub> and carbon nanotubes in chemical structure composed of sp<sup>2</sup> hybrid carbon atoms, is a new carbon nanomaterial. It contains a two-dimensional (2D) single layer carbon sheet structure stacked by hexagonal honeycomb lattices (Liu et al., 2012). In recent years, graphene has been used as adsorbent due to its large surface area and ease of adsorbing multiple compounds (Geim, 2009; Chandra et al., 2010; Li et al., 2011; Zhao et al., 2011). However, the main disadvantage tending to agglomerate leads to the instability of graphene in aqueous phase and limits its wider application (Stankovich et al., 2006a). The agglomeration is caused by the effects of  $\pi$ -conjugated and van der Waals forces, so it is able to solve this problem through the functional modification of graphene (Hayyan et al., 2015). To date, a variety of materials have been used to functionally modify graphene, such as polyoxometalates (Camille and Bandosz, 2009; Zhou and Han, 2010), organic diazonium salts (Englert et al., 2011), poly (oxyalkylene) amines (Hsiao et al., 2010), ionic liquids (ILs) (Zhao et al., 2014), deep eutectic solvent (DES) and so on. DES, a new green solvent, is a two-component or three-component eutectic mixture consisting of hydrogen bond acceptors (HBA) and hydrogen bond donors (HBD) in a suitable stoichiometric



ratio. Choline chloride and betaine are commonly used as HBA of DES, while urea, polyols, and sugars are often used as HBD (Shishov et al., 2017). Owing to the low melting point, low toxicity, ease of synthesis, DES has been used to modify some materials such as cotton (Karimi et al., 2017), magnetic nanoparticles (Karimi et al., 2016) and graphene, and then applied as the sorbents in the micro-extraction methods. In particular, the DES functionalized graphene (DES-G) has good dispersibility and stability in the aqueous phase, and has enormous potential application in the field of analytical chemistry (Radosevic et al., 2015).

The direct determination of trace analytes is usually limited due to the low analyte contents and complicated sample matrix, so the sample pretreatment is extremely necessary to extract target compounds from various complex samples. Nowadays, the sample extraction methods including solid-phase extraction (SPE) (Yilmaz and Soyak, 2016; Yilmaz et al., 2018), pipette-tip solid-phase extraction (PT-SPE) (Wang et al., 2014), headspace solid phase micro-extraction (HS-SPME) (Farhadi et al., 2014), Quick Easy Cheap Effective Rugged Safe (QuEChERS) method (Zheng et al., 2013), liquid-phase microextraction (LPME), hollow fiber-based liquid-phase microextraction (HF-LPME), single-drop microextraction (SDME) and dispersive micro solid-phase extraction (DMSPE) have been reported. Among them, DMSPE introduced by Tsai et al. (2009) has attracted the attention of researchers because of its low consumption of organic solvents, and simple sample pretreatment manipulation (Kocot et al., 2013; Zheng et al., 2013). The process of DMSPE includes the sorption of compounds on adsorbent and following desorption by eluent at  $\mu\text{L}$  level. Therefore, the core of DMSPE is the choice of adsorbent. However, the use of DES-G as an adsorbent in DMSPE, as far as is known, has not been reported.

Food safety has always been a serious and controversial issue for the consumers, who paid close attention to the food safety-related events (Beulens et al., 2005). Pesticide residues and various additives have always been a hot topic in food safety. The use of pesticides such as organochlorine pesticides, organophosphorus pesticides, and pyrethroid insecticides, could control pests and increase crop yields. However, pesticides scattered in the air accumulated on the surface of crops and flowed into the food chain, causing serious damage to other species (Carvalho, 2006). Especially pyrethroids insecticides are more toxic for mammals due to their low water solubility, high liposolubility and ease of pass through biofilms (Feo et al., 2010). Therefore, some analytical methods were developed to extract and analyze pyrethroid insecticides in various complex matrices. For instance, Esteve-Turrillas et al. (2005) determined several pyrethroid residues in olive oils by SPE, in which the mixture of basic alumina and  $\text{C}_{18}$  was used as the adsorbent. Giroud et al. (2013) detected lambda-cyhalothrin, cypermethrin, deltamethrin, and esfenvalerate in bee bread at trace level using the method of acetonitrile-based extraction. The improved QuEChERS method was proposed by Li et al. (2016) for the detection of pyrethroid insecticides in fruits and vegetables. Torbati et al. (2018) analyzed ten pyrethroids in apple and strawberry by homogeneous liquid-liquid microextraction. In order to improve the detection

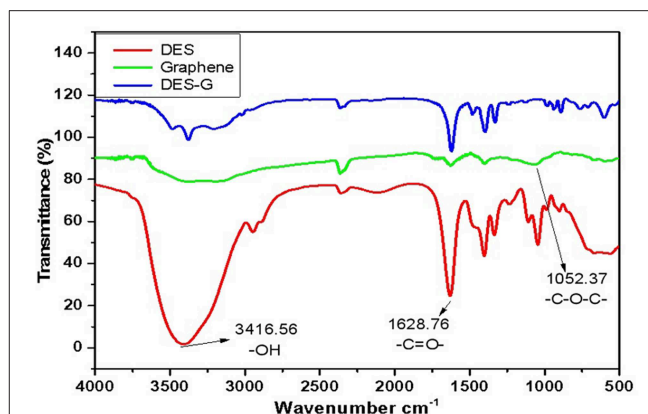


FIGURE 1 | FTIR spectra of DES, Graphene, and DES-G.

efficiency of pyrethroid insecticides and reduce organic solvent consumption, it is necessary to develop a green and efficient sample microextraction method.

In this work, several DES-Gs were synthesized by simple procedure and an optimum DES-G was selected as the adsorbent of DMSPE. Moreover, DES-G-based DMSPE method was investigated for the microextraction and determination of pyrethroid insecticides by ultra-high performance liquid chromatography (UHPLC). To confirm the reliability of this method, scanning electron microscope (SEM), transmission electron microscopy (TEM) and Fourier transform infrared spectrometer (FT-IR) were used for characterizing the functional changes of graphene. After a series of optimizations, the precision, repeatability, and linearity were studied under optimum conditions. Moreover, the proposed extraction approach was used for determining pesticide residues (fenpropathrin, ethofenprox, bifenthrin, fenvalerate, lambda-cyhalothrin) in natural products [bee bread, *Curcuma wenyujin* and *Dendrobium officinale* (*D. officinale*)].

## RESULTS AND CONCLUSIONS

### FTIR, SEM, and TEM Analysis

FTIR, capable of qualitative and quantitative analysis of samples, was conducted to confirm the synthesis of DES and compare the changes before and after functionalization of graphene. Figure 1 shows the FTIR spectra of DES (DES 5), graphene (monolayer GO) and DES-G (DES 5-functionalized monolayer GO) as examples. As shown in the FTIR spectra of DES, the bonds of  $3416.56\text{ cm}^{-1}$  and  $1628.76\text{ cm}^{-1}$  represented  $-\text{OH}$  of betaine and  $-\text{C}=\text{O}-$  of glycerol, respectively. It is concluded that betaine and glycerol synthesized a new compound. Comparing the FTIR spectra of DES-G with DES and graphene, the  $-\text{OH}$  of DES and  $-\text{C}-\text{O}-\text{C}-$  ( $1052.37\text{ cm}^{-1}$ ) of graphene were obviously weakened.

In order to explore the influence of DES on the morphology, composition and internal structure of graphene, several samples were analyzed by SEM and TEM. The SEM and TEM images of three types of graphene were exhibited in Figure 2. For the

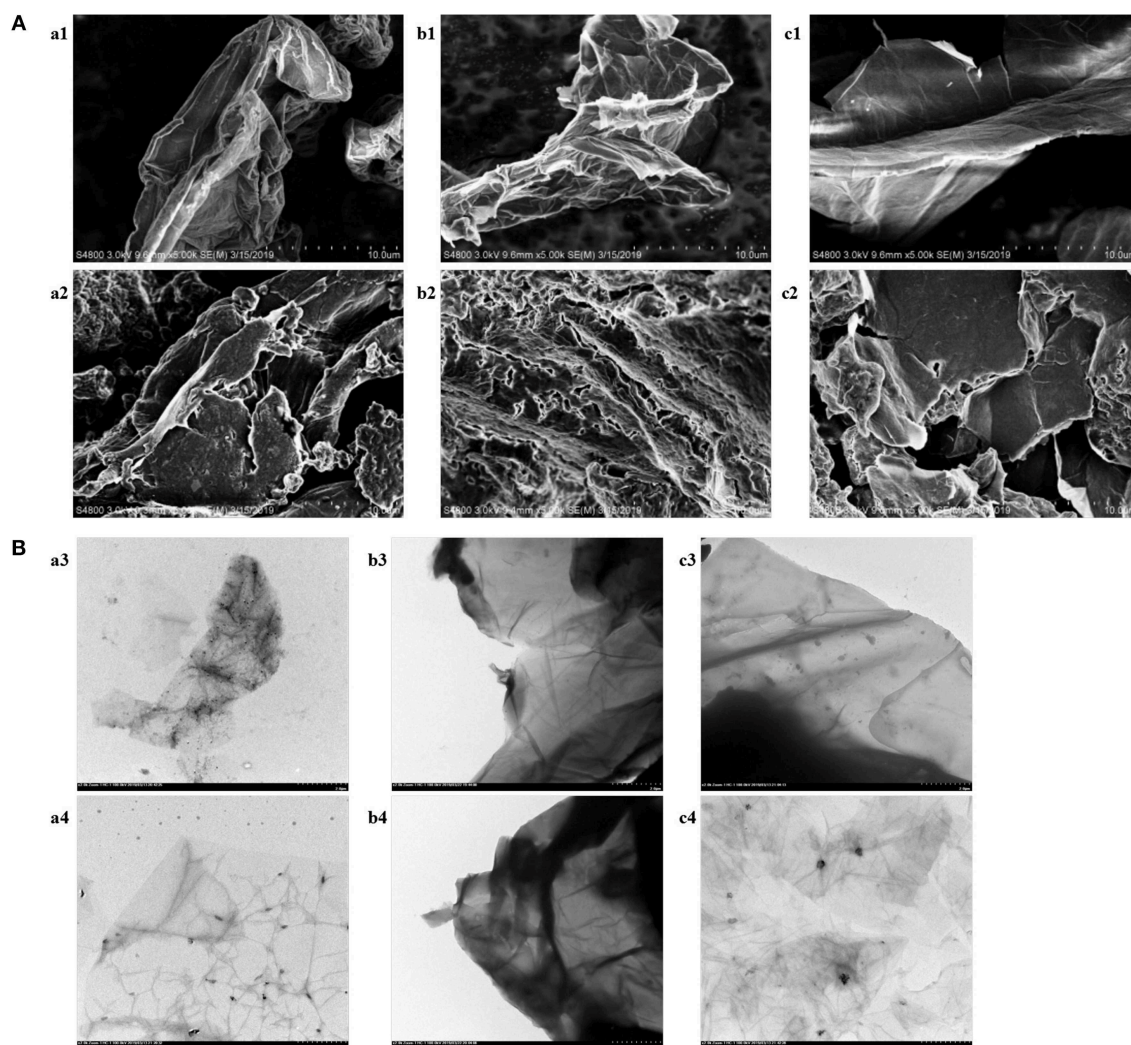


**FIGURE 2 | (A)** SEM images of monolayer GO (a1), rGO-TEPA (b1), GO-COOH (c1), DES-monolayer GO (a2), DES-rGO-TEPA (b2), and DES-GO-COOH (c2). **(B)** TEM images of monolayer GO (a3), rGO-TEPA (b3), GO-COOH (c3), DES-monolayer GO (a4), DES-rGO-TEPA (b4), and DES-GO-COOH (c4).

longitudinal comparison of **Figure 2A**, considerable differences were observed in the morphology of the three functionalized graphenes (a2, b2, c2) compared to the original graphenes (a1, b1, c1). The loose stacking of functionalized graphenes, a structural deformation caused by the modification of DES, contributed to the dispersion of graphene in water and improved the stability of graphene in the aqueous phase (Hayyan et al., 2015). The sheet structure of graphene was clearly shown in the TEM images of **Figure 2B**. As can be seen from the pictures (a4, b4, c4), the functionalized graphene had a thinner sheet shape, which was consistent with the loose structure shown in the SEM images. The further horizontal comparison of SEM and TEM images was shown in the section of “Choice of the Type of Graphene.”

### Optimization of Extraction Conditions

The extraction efficiency was affected by various factors. The study selected several major factors to optimize extraction

efficiency, starting with the initial conditions (1  $\mu\text{g/mL}$  of sample solution, 2.5  $\mu\text{g/mL}$  of graphene, shaking 2 min, 100  $\mu\text{L}$  of methanol as the elution solvent).

### Choice of Deep Eutectic Solvent

In order to select DES with good dispersion and suspension stability, six kinds of DES listed in **Table 1** were prepared and five DES-Gs were synthesized under the same conditions. The DES1 (choline chloride:glucose = 1:1) was discarded because it was easy to solidify and difficult to mix uniformly with graphene. Then the five DES-Gs were prepared into relatively high concentrations (1,000  $\mu\text{g/mL}$ ), sealed and stood still. **Figure S1** showed that all of the DES-Gs were dispersed homogeneously in water after sonication. However, the samples of Gr1 and Gr2 were precipitated rapidly only within 5 min and the Gr3 was precipitated gradually at 10 min. After standing for more than 48 h, Gr1, Gr2, and Gr3 were fully agglomerated and a clear

**TABLE 1** | Types and abbreviations of deep eutectic solvent.

Salt	HBD <sup>a</sup> type	Mole ratios of salt:HBD	Abbreviation (DES <sup>b</sup> )
Choline chloride	D-(+)-Glucose	1:1	DES1
	Propylene glycol + Water	1:1:1	DES2
	Glycerol	1:2	DES3
	Urea	1:2	DES4
Betaine	Glycerol	1:2	DES5
	Glycerol + Propylene glycol	1:1:1	DES6

<sup>a</sup>HBD, hydrogen bond donors.<sup>b</sup>DES, deep eutectic solvent.

water layer appeared. Meanwhile, Gr4 and Gr5 showed long-term stability. The results related to that the DES prepared by different mixtures had a discrepant dispersibility for graphene due to the different interaction of salts and HBDs, and the carboxyl functional group of betaine provided more oxygen atoms for forming hydrogen bonds with the HBD. So Gr4 and Gr5 were selected as the dispersant for extracting pesticide samples in subsequent dispersion studies. The result was shown in **Figure 3A** with the best extraction efficiency obtained by Gr4. This result was attributed to that the water-insoluble graphene was highly soluble in polyalcohol based-DES which had the least polarity (Zahrina et al., 2018). Consequently, the DES5 (Gr4) was selected for further research.

## Choice of the Type of Graphene

The structure of the base surface of graphene has a vital effect on its physicochemical properties such as the adsorption capability and solubility, which directly influence the concentration efficiency. To evaluate the effect of the type of graphene, monolayer GO, rGO-TEPA and GO-COOH were treated by DES5 under the same conditions. On the basis of the experimental results of **Figure 3B**, rGO-TEPA had the highest extraction efficiency for target analytes in comparison with monolayer GO and GO-COOH. That was because the base surface of monolayer GO mainly contained oxygen-containing functional groups, which changed the van der Waals force of the graphite molecules and affected their state in aqueous solution (Stankovich et al., 2006b). However, rGO-TEPA treated by DES began to precipitate at 30 min and showed visible delamination at 60 min (**Figure S2**). This phenomenon was likely attributed to the formation of intramolecular hydrogen bonds in rGO-TEPA, which competitively inhibited the interaction of graphene with DES, resulting in poor stability in water. It can be confirmed in **Figure 2**, the distinct sheet structures of functionalized rGO-TEPA that showed in the SEM images (b2) and its tightly stacked carbon layers resulted in a tendency to promote easy agglomeration. Additionally, no significant changes in the internal structure of functionalized rGO-TEPA (b4) compared to functionalized monolayer GO and GO-COOH (a4, c4) from the TEM images. The poor extraction efficiency of GO-COOH may be attributed that the carboxyl group of GO-COOH affected the adsorption of the target analytes by the

graphene sheet. From **Figure 3A**, the surface of the GO-COOH before and after modification (c1, c2) was relatively smooth, without much continuous fold and wrinkle, resulting in the weak adsorption capacity. Therefore, considering the suspension stability and the extraction efficiency, monolayer GO was chosen for the next work.

## Effect of Graphene Concentration

Due to the unique two-dimensional nanosheet structure with the porous surface, graphene was used as adsorbent for indirect enrichment of target analytes (Liu et al., 2012). Therefore, the amount of graphene had an essential influence on the extraction efficiency. The effect of graphene was studied by changing its concentration of 0.5, 1.5, 2.5, and 3.5  $\mu\text{g/mL}$ , respectively. From **Figure 3C**, the highest peak areas were achieved at the concentration of 1.5  $\mu\text{g/mL}$  and the peak areas were significantly decreased when the concentration exceeded 1.5  $\mu\text{g/mL}$ . This result was related to the adsorption saturation of the porous surface of graphene. It was well-known that the high concentration of graphene provided a large surface area and a large number of adsorption sites for the adsorption of the target analytes, thereby improving the concentration efficiency. However, the higher concentration of graphene produced stronger adsorption capability for the target compound that was difficult to be eluted by the eluent, resulting in poor concentration efficiency. So, in the following experiments, 1.5  $\mu\text{g/mL}$  of monolayer GO was added to 5 mL of sample solution for adsorption.

## Effect of Extraction Time

In the course of preliminary experiment, it was found that the extraction time had an essential influence on the concentration efficiency. Thus, in the study, the effect of extraction time was investigated by using the oscillating shaker at the maximum speed (500 r) for 1.0, 1.5, 2.0, and 2.5 min. As shown in **Figure 3D**, the peak areas of the five pyrethroid insecticides increased to a maximum when the mixture was shaken for 1.5 min. Adequate extraction time ensured sufficient contact of the compounds of the sample solution with the surface of graphene, and improved the adsorption efficiency of graphene to the target analytes. However, it was observed that the response progressively decreased with the extraction time changing from 1.5 to 2.5 min. The result was ascribed to the enhancement of the interaction between analytes and graphene induced by extended extraction time, making the analytes difficult to elute by the eluent, thus resulting in the loss of analytes and decreased response. Therefore, the extraction time of 1.5 min was selected for the subsequent experiments.

## Choice of Elution Solvent

The type of elution solvents is a critical parameter that directly affected the concentration efficiency in the DMSPE. The elution solvents should be miscible with the target compounds and elute the compounds easily from the graphene in a small volume. In addition, the pyrethroid insecticides are lipophilic compounds (Serôdio and Nogueira, 2005). In order to find the suited eluent solvents for the analytes, methanol, acetonitrile,



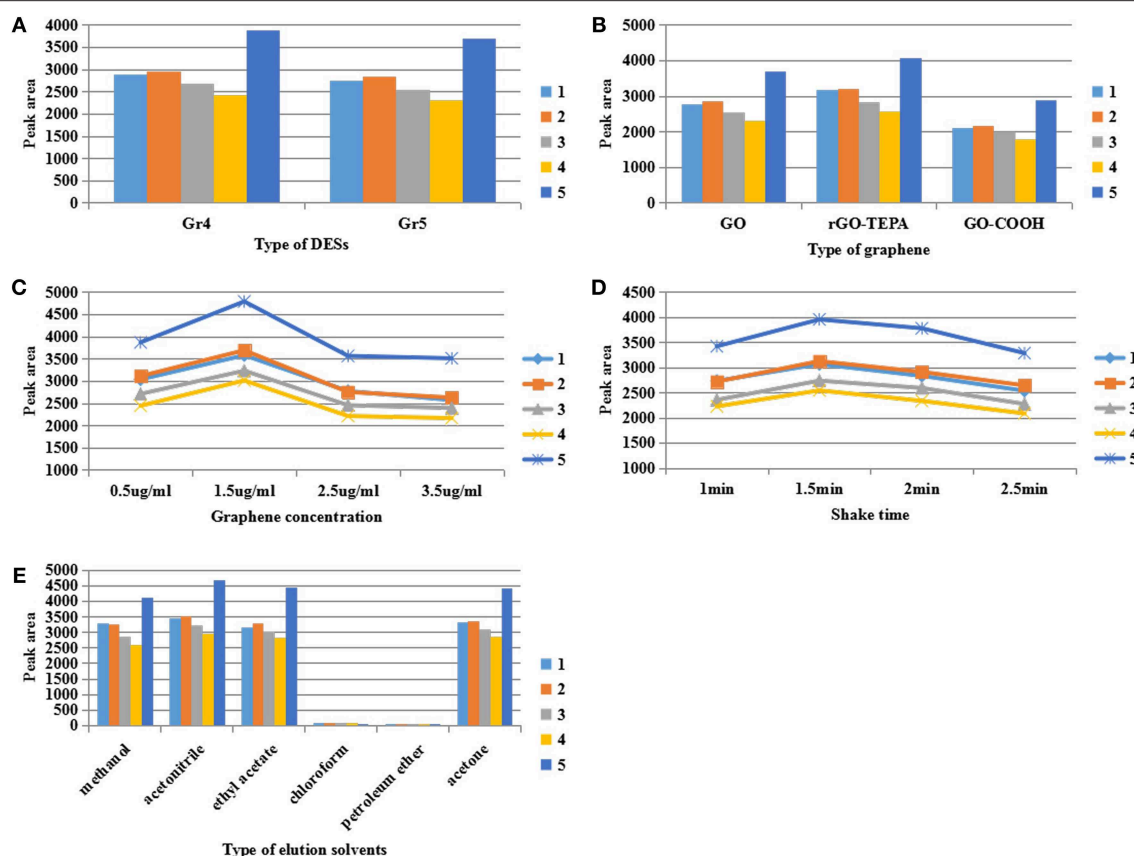


**FIGURE 3 |** Effect of (A) the type of deep eutectic solvent, (B) the type of graphene, (C) graphene concentration, (D) shake time, (E) the type of elution solvent on the extraction of pyrethroid insecticide. The initial conditions were as follow: 1  $\mu$ g/mL of sample solution, 2.5  $\mu$ g/mL of monolayer GO, shaking 2 min, 100  $\mu$ L of methanol as the elution solvent.

ethyl acetate, chloroform, petroleum ether and acetone were evaluated by comparing the response of the five compounds on the same condition (1  $\mu$ g/mL of sample solution, 1.5  $\mu$ g/mL of monolayer GO, shaking 1.5 min at 500 r, 100  $\mu$ L elution solvent). The result is shown in **Figure 3E**. It was observed that acetonitrile showed a relatively high peak areas for five pyrethroid insecticides, followed by acetone, ethyl acetate and methanol, whereas chloroform and petroleum ether provided a poor response which was barely detectable. This phenomenon can be explained by the high elution ability of acetonitrile and the poor solubility of chloroform and petroleum ether to pesticides. Based on the above experimental results, acetonitrile was selected as the optimum elution solvent for further studies.

## Analytical Performance

The methodology of DES-G-based DMSPE was examined and evaluated with respect to linearity, precision, repeatability, the detection limit (LOD) and the quantitation limit (LOQ) under the above optimal conditions, 1.5  $\mu$ g/mL of DES-G (as monolayer GO) used for adsorbing analytes, shaking 1.5 min at 500 r and 100  $\mu$ L acetonitrile as the elution solvent. The linearity was investigated for the concentration of target compounds in the range of 0.01–1.0  $\mu$ g/mL and the linear regression data was

presented in **Table 2**. Analytical performance data of the target analytes was shown in **Table 3**. The precision, calculated on the basis of the relative standard deviations (RSDs, %), was used to verify the stability of the instrument. The intra-day precision of the presented method was studied by using six replicates in a day ranged from 0.43% to 0.57% for retention time, and the inter-day precision was obtained by injecting two needles at the same time for three consecutive days in the range of 0.43–0.56% for retention time. In order to verify the reliability of the proposed method, the repeatability was measured by three parallel sample preparation steps of the sample solution. The repeatability values, expressed as RSDs (%), varied between 0.04 and 2.41% for peak areas. The LODs were 0.016–0.24 ng/mL for five pyrethroid insecticides at signal-to-noise ratio of 3 and the LOQs (S/N ratio of 10:1) were 0.054–0.784 ng/mL.

## Analytical Application

The real samples, including beebread, *Curcuma wenyujin* and *D. officinale* were determined and analyzed to examine the availability of the developed method. The experimental results of typical chromatograms displayed in **Figure 4**. In order to further study the effect of the sample matrix on the detection sensitivity of the method, the spiked recovery was studied by spiking three



levels of concentration (0, 0.05, and 0.5  $\mu\text{g/mL}$ ) of standard solution in real samples and the results were summarized in **Table 4**. The recoveries for beebread, *Curcuma wenyujin* and *D. officinale* were 80.9–112.9, 81.5–111.1, and 86.4–114.1%, respectively. The enrichment factor, as calculated by comparing the response of five compounds before and after the DES-G-based DMSPE process, was 46–59-folds (the concentration effect was shown in **Figure S3**). In addition, LC-MS/MS was performed to define the target analytes of real samples and the parameters were listed in **Table 4**.

## Comparison of DES-G-Based DMSPE With Other Methods

The proposed method was compared with other extraction methods that applied for the determination of pyrethroid insecticides. The characteristics of developed method and the comparison of the amount of adsorbent, the type and amount of extraction solvent, extraction time, RSD (%) and LOD were listed in **Table 5**. It can be seen that the LODs of this method were lower than those achieved by SPE (Esteve-Turrillas et al., 2005), LLE-DLLME (Farajzadeh et al., 2014), and MDSPE (Badawy et al., 2018). In comparison with other methods, the amounts of adsorbent and extraction solvent were obviously reduced: only 1.5  $\mu\text{g/mL}$  of DES-G and 100  $\mu\text{L}$  of acetonitrile. Furthermore, the extraction time of only 1.5 min significantly improved the extraction efficiency. It is worth mentioning that the RSD (%) was relatively low, which proved the stability of the method.

**TABLE 2** | Linear regression data of the investigated analytes.

Pyrethroid insecticide	Linear range ( $\mu\text{g/mL}$ )	Linear equation	Correlation coefficient ( $R^2$ )
Fenpropathrin	0.01–1	$y = 3493.5x - 87.577$	0.9985
Ethofenprox	0.01–1	$y = 3664.2x - 2.166$	0.9970
Bifenthrin	0.01–1	$y = 3444.0x + 15.584$	0.9948
Fenvalerate	0.01–1	$y = 3111.2x - 50.736$	0.9979
Lambda-cyhalothrin	0.01–1	$y = 4790.3x + 35.660$	0.9956

Conditions: 1  $\mu\text{g/mL}$  of sample solution, 1.5  $\mu\text{g/mL}$  of monolayer graphene oxide, shaking 1.5 min, 100  $\mu\text{L}$  of acetonitrile as the elution solvent.

Thus, DES-G-based DMSPE combined with UHPLC-DAD was rapid, stable, sensitive and environmentally friendly for the determination of pyrethroid insecticides in natural products.

## CONCLUSIONS

The method of DES-G assisted DMSPE with UHPLC-DAD was developed for the trace analysis of five pyrethroid insecticides in beebread, *Curcuma wenyujin* and *Dendrobium officinale*. In this work, the DES, easy to be produced and low toxicity, was a new type of functional reagent and effectively modified the graphene. Moreover, the graphene, micro-functionalized by DES, not only retained the high adsorption capacity of graphene, but weakened its main defect that was prone to agglomeration. After the optimization of a series of parameters, under optimized conditions, the sensitivity, reliability and practicability of this method were verified with the LODs were 0.016–0.24 ng/mL, the repeatability was 0.04–2.41% and the recovery ranged from 80.9 to 112.9%. Based on the above experimental results, the method was simple, rapid, sensitive, efficient and environmentally friendly. In addition, the functionalization method of graphene and the application of DES-G are worthy of further exploration. There is no doubt that the future of graphene in the field of analytical chemistry is still very bright and is full of potential.

## MATERIALS AND METHODS

### Reagents and Materials

Fenpropathrin, ethofenprox, bifenthrin, fenvalerate, lambda-cyhalothrin were produced by Shanghai Pesticide Research Institute Co., Ltd. (Shanghai, China). Trichloromethane and glycerol were purchased from Xilong Scientific Co., Ltd. (Shantou, China). Methanol (HPLC grade), acetonitrile (HPLC grade), ethyl acetate [analytical grade (AR)], petroleum ether (AR), acetone (AR), choline chloride (AR), and betaine (purity 98%) were provided by Sinopharm Chemical Reagent Co., Ltd. (Shanghai, China). D-(+)-Glucose was purchased from Shenggong Biological Engineering Co., Ltd. (Shanghai, China). Propylene glycol (99.8%) was purchased from Beijing Bailingwei Technology Co., Ltd. (Beijing, China). Ultrapure water was supplied by Hangzhou Wahaha Group Co., Ltd. (Hangzhou,

**TABLE 3** | Analytical performance data of the investigated analytes.

Pyrethroid insecticide	Intra-day precision <sup>a</sup> (RSD%, $n = 6$ )		Inter-day precision <sup>a</sup> (RSD%, $n = 6$ )		Repeatability <sup>a</sup> (RSD%, $n = 3$ )		LOD <sup>b</sup> (ng/mL)	LOQ <sup>b</sup> (ng/mL)
	Retention time	Peak area	Retention time	Peak area	Retention time	Peak area		
Fenpropathrin	0.571	0.442	0.560	1.847	0.039	2.220	0.045	0.151
Ethofenprox	0.514	0.433	0.502	2.751	0.048	2.406	0.067	0.223
Bifenthrin	0.538	0.439	0.527	3.129	0.046	1.951	0.240	0.784
Fenvalerate	0.501	0.457	0.492	2.556	0.051	1.403	0.110	0.381
Lambda-cyhalothrin	0.429	0.533	0.425	3.157	0.056	2.305	0.016	0.054

<sup>a</sup>Precision and repeatability are defined as the RSD (%).

<sup>b</sup>LOD and LOQ are calculated on the basis of the signal-to-noise ratio of 3 and 10, respectively.

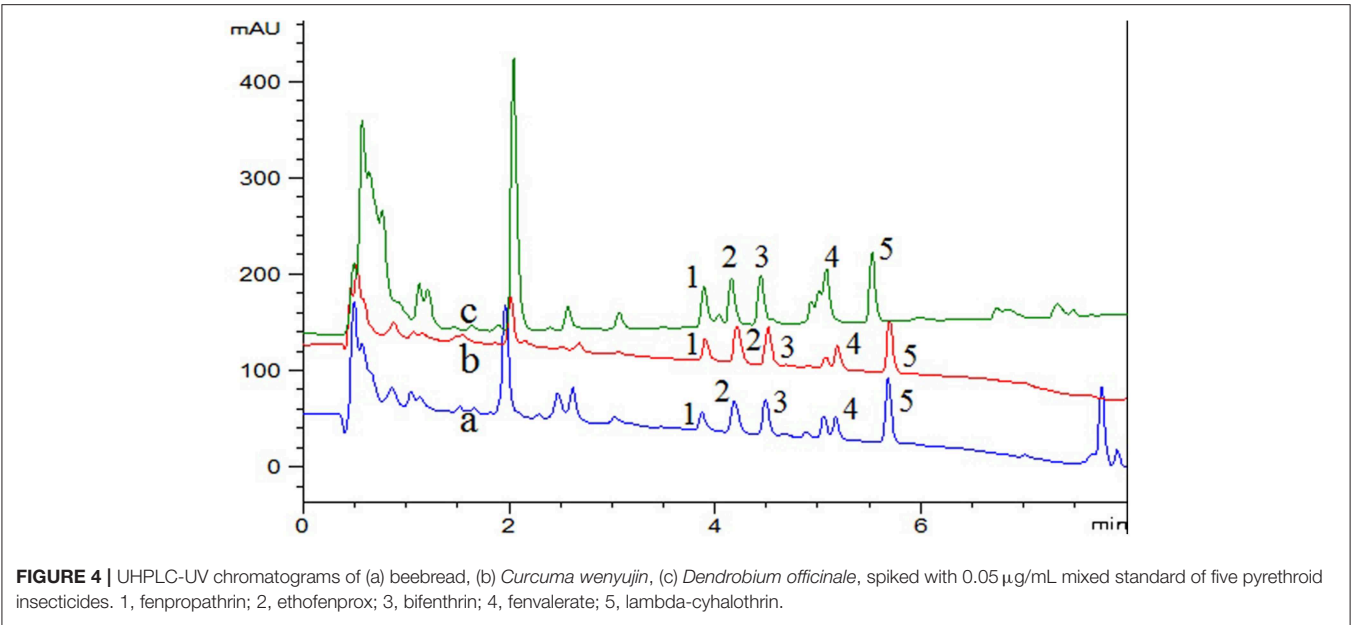


**TABLE 4 |** Determination of five pyrethroid insecticides in spiked samples.

Analyte	Added ( $\mu\text{g/mL}$ )	Beebread		<i>Curcuma wenyujin</i>		<i>Dendrobium officinale</i>		M	M+23
		Found ( $\mu\text{g/mL}$ )	Recovery <sup>a</sup> (%)	Found ( $\mu\text{g/mL}$ )	Recovery <sup>a</sup> (%)	Found ( $\mu\text{g/mL}$ )	Recovery <sup>a</sup> (%)		
Fenpropathrin	0	n.d. <sup>b</sup>	–	n.d. <sup>b</sup>	–	n.d. <sup>b</sup>	–	–	372.43
	0.05	0.0536	107.1	0.0459	91.9	0.0570	114.1		
	0.5	0.5019	100.4	0.5465	109.3	0.4320	86.4		
Ethofenprox	0	n.d. <sup>b</sup>	–	0.0094	–	n.d. <sup>b</sup>	–	–	399.49
	0.05	0.0451	90.3	0.0417	83.4	0.0535	106.9		
	0.5	0.5351	107.0	0.5138	102.8	0.4957	99.1		
Bifenthrin	0	n.d. <sup>b</sup>	–	n.d. <sup>b</sup>	–	n.d. <sup>b</sup>	–	–	445.86
	0.05	0.0436	87.3	0.0407	81.5	0.0563	112.6		
	0.5	0.5398	108.0	0.5503	110.1	0.5125	102.5		
Fenvalerate	0	n.d. <sup>b</sup>	–	n.d. <sup>b</sup>	–	n.d. <sup>b</sup>	–	–	442.90
	0.05	0.0457	91.4	0.0467	93.3	0.0542	108.5		
	0.5	0.4856	97.1	0.5555	111.1	0.4868	97.4		
Lambda-cyhalothrin	0	n.d. <sup>b</sup>	–	n.d. <sup>b</sup>	–	n.d. <sup>b</sup>	–	449.85	–
	0.05	0.0404	80.9	0.0490	98.0	0.0606	101.2		
	0.5	0.5643	112.9	0.5262	105.2	0.5034	100.7		

<sup>a</sup>Recovery (%) = (the amount found in the spiked sample – the amount found in the sample)  $\times$  100 / the amount added.  
<sup>b</sup>n.d., not detectable.

China). Monolayer graphene oxide (GO) was purchased from Suzhou Carbon Graphene Technology Co., Ltd. (Suzhou, China). Reduced graphene oxide-tetraethylene pentamine (rGO-TEPA) and carboxyl functionalized graphene oxide (GO-COOH) were supplied by Nanjing Xianfeng Nano Material Technology Co., Ltd. (Nanjing, China). Beebread, *Curcuma wenyujin* and *D. officinale* were purchased from local market in Beijing (Beijing, China), Wenzhou (Wenzhou, China) and Zhuji (Zhuji, China), respectively. All stock solutions of pyrethroid insecticides were dissolved by methanol at 1,000  $\mu\text{g/mL}$  and stored at 4°C.

Working solutions were obtained by diluting the stock solution with ultrapure water.

Instrumentation and Conditions

Agilent 1,290 series UHPLC system (Agilent Technologies Co., Ltd., USA) coupled with a high speed binary pump and a diode array detector (DAD) was used for the quantitative analysis of the pyrethroid insecticides. The separation of target analytes was carried out on Agilent SB-C<sub>18</sub> column (2.1  $\times$  100 mm, 1.8  $\mu\text{m}$ ). The detection wavelength was set

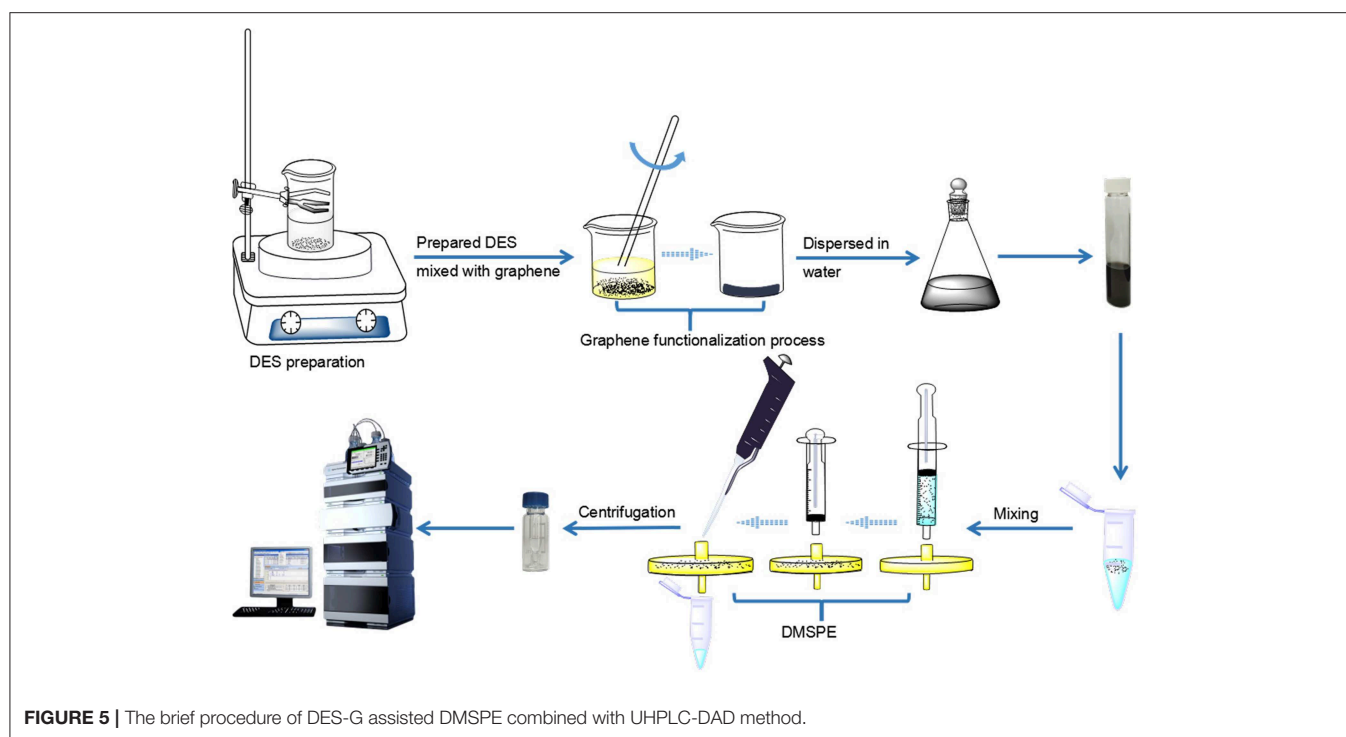
**TABLE 5** | Comparison of DES-G based DMSPE method with other methods for the analytes of pyrethroid insecticides.

Sample	Extraction method <sup>a</sup>	Analysis technique	Adsorbent <sup>b</sup>	Extraction solvent <sup>c</sup>	Extraction time	Linear range	Repeatability (RSD, %)	LOD	References
Vegetable oils	SPE	GC-MS-MS	C <sub>18</sub> (500 mg) and basic alumina (2 g)	acetonitrile (10 mL)	40 min	10–1000 µg/L	4–13%	0.3–1.4 ng/g	Tsai et al., 2009
Beebread	acetonitrile-based extraction	UHPLC-MS	PSA (150 mg)	heptane (5 mL)	–	0.1–10 ng/g	<20%	0.013–0.100 ng/g	Kocot et al., 2013
Fruit juices	SPI-SFO-HLLME	GC-MS	–	pivalic acid (260 µL)	5 min	0.023–500 ng/mL	4–7%	0.006–0.034 ng/mL	Carvalho, 2006
Vegetable oil	LLE-DLLME	GC-FID	–	DMF (1.0 mL) and 1,1,2-trichloroethane (75 µL)	10 min	55–6000 ng/g	5–13%	20–170 ng/g	Torbati et al., 2018
Water	MDSPE	HPLC	Ch-Si MNPs (50/100/200 mg)	acetonitrile/methanol (1:1, 5 mL)	20 min	0.0125–0.15 µg/mL	–	0.002–0.046 µg/mL	Zahrina et al., 2018
Beebread and apple	DMSPE	UHPLC-DAD	DES-G (1.5 µg/mL)	acetonitrile (100 µL)	1.5 min	0.01–1.0 µg/mL	0.04–2.41%	0.016–0.24 ng/mL	This work

<sup>a</sup>Extraction Method: SPE, solid-phases extraction; HLLME, homogeneous liquid–liquid microextraction; LLE-DLLME, liquid-liquid extraction-dispersive liquid-liquid microextraction; MDSPE, magnetic dispersive solid-phase extraction; DMSPE, dispersive micro solid-phase extraction.

<sup>b</sup>Adsorbent: PSA, primary and secondary amines; Ch-Si MNPs, chitosan-siloxane magnetic nanoparticles.

<sup>c</sup>Extraction Solvent: DEF, dimethylformamide.

**FIGURE 5** | The brief procedure of DES-G assisted DMSPE combined with UHPLC-DAD method.

at 210 nm. The mobile phases were (A) water and (B) acetonitrile with the gradient as follows: 70–90% (B) for 0–5 min, 90–100% (B) for 5–8 min and then a re-equilibration of 5 min. After being filtered through 0.22 µm filter, the sample solution of 2 µL was injected to UHPLC system and analyzed at 35°C with the flow rate at 0.4 mL/min. The SEM (Hitachi S4800, Tokyo, Japan), TEM (Hitachi HT-7700, Tokyo, Japan) and FT-IR (Thermo Scientific Nicolet iS5 spectrometer,

Madison, USA) were used for the characterization of DES, graphene and DES-G.

## DES Preparation

All DESs were synthesized by mixing different salts and HBD listed in **Table 1** according to previous works (Hayyan et al., 2015; Ruesgas-Ramón et al., 2017; Zahrina et al., 2018). The choline chloride and betaine were dried at 60°C for no more than 6 h

under vacuum before utilization due to the hygroscopic nature. Then the mixture was added to a jacketed vessel and heated at 70°C while stirring at 300 r. The final liquid was transferred to a well-sealed glass bottle until a uniform transparent liquid was obtained. The fresh DES samples were used through all the work in order to avoid any differences in DES properties caused by temperature and humidity changes.

## Graphene Functionalization Process

The treatment of graphene functionalization was based on previous research (Hayyan et al., 2015). Seven milliliter of DES and 200 mg of graphene were separately weighed and placed in a beaker. The mixture was stirred at room temperature until it was completely mixed. After sealing, it was sonicated at 60°C for 3 h and then dried under vacuum at 100°C for 3 h. The appropriate DES-G was weighed and diluted with water to prepare a 1,000 µg/mL stock solution for subsequent use.

## Sample Preparation

A sample processing method of fresh fruits and vegetables reported by Li et al. (2016) was adopted for the preparation of the beebeard with minor modifications. Briefly, 15 g of sample was weighed and 15 mL of acetonitrile were placed and mixed in a 50 mL centrifuge tube. Following full extraction, 1.50 g of NaCl and 6.00 g of anhydrous magnesium sulfate (MgSO<sub>4</sub>) were added and swirled for extraction and salting out until the solvent interacted sufficiently with the entire samples. The supernatant was transferred into a 15 mL centrifuge tube containing 2.4 g of C<sub>18</sub>, 1.16 g of MgSO<sub>4</sub> and 0.04 g of graphitized carbon black after centrifugation for 10 min at 4,000 r. The mixture was swirled to mix thoroughly and then centrifuged for 5 min (4,000 r). Finally, the supernatant was decanted and stored in a glass bottle (4°C).

The sample treatment procedure of *Curcuma wenyujin* and *D. officinale* was based on the Chinese Pharmacopeia (2015 edition). The specific steps are as follows: A precisely weighed 3 g of *Curcuma wenyujin* powder (40 mesh) was placed in a 50 mL centrifuge tube and 15 mL of 1% glacial acetic acid solution was added. The mixture was vortexed to completely infiltrate and left for 30 min, then 15 mL of acetonitrile was added into the centrifuge tube and swirled on a vortex mixer to homogenizing the sample. After the mixture was vigorously oscillated by vortex for 5 min (500 r), 6.00 g of MgSO<sub>4</sub> and 1.50 g of anhydrous sodium acetate were mixed with the sample, shook the mixture immediately and then oscillated (500 r, 3 min), cooled in ice

bath (10 min), centrifuged (4,000 r, 5 min). Next, the supernatant of 9 mL was transferred to a 50 mL centrifuge tube containing 900 mg of MgSO<sub>4</sub>, 300 mg of N-propylethylenediamine (PSA), 300 mg of C<sub>18</sub>, 300 mg of silica gel, and 90 mg of graphitized carbon black. The mixture was swirled to mix thoroughly and was oscillated vigorously (500 r, 5 min). After centrifugation for 5 min (4,000 r), 5 mL of the supernatant was accurately pipetted and stored in a glass bottle (4°C).

## Extraction and Analysis

The sample solution and graphene were placed in a 25 mL centrifuge tube at a concentration ratio of 1:2.5. The mixture was shaken to make the compounds fully bind with graphene at 500 r for 2 min. After adsorption, the graphene-bound analytes were filtered by a 0.22 µm nylon filter and left in the filter head. Finally, the target analytes were separated from graphene by 100 µL of eluent, and the eluate was further centrifuged at 13,000 r (5 min) for UHPLC analysis. The brief procedure of this work was shown in Figure 5.

## DATA AVAILABILITY

The authors declare that all relevant data supporting the findings of this study are available within the article and **Supplementary Information Files**.

## AUTHOR CONTRIBUTIONS

All authors listed have made a substantial, direct and intellectual contribution to the work, and approved it for publication.

## FUNDING

This study was supported by the Key projects of National Natural Science Foundation of China (81730108); Key Project of Zhejiang province Ministry of Science and Technology (2015C03055); Key Project of Hangzhou Ministry of Science and Technology (20162013A07).

## SUPPLEMENTARY MATERIAL

The Supplementary Material for this article can be found online at: <https://www.frontiersin.org/articles/10.3389/fchem.2019.00594/full#supplementary-material>

## REFERENCES

- Badawy, M. E. I., Marei, A. E. S. M., and El-Nouby, M. A. M. (2018). Preparation and characterization of chitosan-siloxane magnetic nanoparticles for the extraction of pesticides from water and determination by HPLC. *Sep. Sci. Plus* 1, 506–519. doi: 10.1002/sscp.201800084
- Beulens, A. J. M., Broens, D. F., Folstar, P., and Hofstede, G. J. (2005). Food safety and transparency in food chains and networks relationships and challenges. *Food Control* 16, 481–486. doi: 10.1016/j.foodcont.2003.10.010
- Camille, P., and Bandosz, T. J. (2009). Graphite oxide/polyoxometalate nanocomposites as adsorbents of ammonia. *J. Phys. Chem. C* 113, 3800–3809. doi: 10.1021/jp8097044
- Carvalho, F. P. (2006). Agriculture, pesticides, food security and food safety. *Environ. Sci. Policy* 9, 685–692. doi: 10.1016/j.envsci.2006.08.002
- Chandra, V., Park, J., Chun, J., Woo Lee, J., Hwang, I. C., and Kim, K. S. (2010). Water-dispersible magnetite-reduced graphene oxide composites for arsenic removal. *ACS Nano* 4, 3979–3986. doi: 10.1021/nn1008897
- Englert, J. M., Dotzer, C., Yang, G., Schmid, M., Papp, C., Gottfried, J. M., et al. (2011). Covalent bulk functionalization of graphene. *Nat. Chem.* 3, 279–286. doi: 10.1038/nchem.1010
- Esteve-Turrillas, F. A., Pastor, A., de la Guardia, M. (2005). Guardia, determination of pyrethroid insecticide residues in vegetable oils by using combined solid-phases extraction and tandem mass spectrometry detection. *Anal. Chim. Acta* 553, 50–57. doi: 10.1016/j.aca.2005.08.004

- Farajzadeh, M. A., Khoshmaram, L., and Nabil, A. A. A. (2014). Determination of pyrethroid pesticides residues in vegetable oils using liquid-liquid extraction and dispersive liquid-liquid microextraction followed by gas chromatography-flame ionization detection. *J. Food Compos. Anal.* 34, 128–135. doi: 10.1016/j.jfca.2014.03.004
- Farhadi, K., Matin, A. A., Amanzadeh, H., Biparva, P., Tajik, H., Farshid, A. A., et al. (2014). A novel dispersive micro solid phase extraction using zein nanoparticles as the sorbent combined with headspace solid phase micro-extraction to determine chlorophenols in water and honey samples by GC-ECD. *Talanta* 128, 493–499. doi: 10.1016/j.talanta.2014.06.002
- Feo, M. L., Eljarrat, E., and D., Barcelo' (2010). Determination of pyrethroid insecticides in environmental samples. TrAC-trend anal. *Green Anal. Chem.* 29, 692–705. doi: 10.1016/j.trac.2010.03.011
- Geim, A. K. (2009). Graphene\_status and prospects. *Science* 324, 1530–1534. doi: 10.1126/science.1158877
- Giroud, B., Vauchez, A., Vulliet, E., Wiest, L., and Buleté, A. (2013). Trace level determination of pyrethroid and neonicotinoid insecticides in beebread using acetonitrile-based extraction followed by analysis with ultra-high-performance liquid chromatography-tandem mass spectrometry. *J. Chromatogr. A* 1316, 53–61. doi: 10.1016/j.chroma.2013.09.088
- Hayyan, M., Abo-Hamad, A., AlSaadi, M. A., and Hashim, M. A. (2015). Functionalization of graphene using deep eutectic solvents. *Nanoscale Res. Lett.* 10:1004. doi: 10.1186/s11671-015-1004-2
- Hsiao, M. C., Liao, S. H., Yen, M. Y., Liu, P. I., Pu, N. W., Wang, C. A., et al. (2010). Preparation of covalently functionalized graphene using residual oxygen-containing functional groups, *ACS Appl. Mater. Inter.* 2, 3092–3099. doi: 10.1021/am100597d
- Karimi, M., Dadfarnia, S., and Shabani, A. M. H. (2017). Application of deep eutectic solvent modified cotton as a sorbent for online solid-phase extraction and determination of trace amounts of copper and nickel in water and biological samples. *Biol. Trace Element. Res.* 176, 207–215. doi: 10.1007/s12011-016-0814-0
- Karimi, M., Shabani, A. M., and H., Dadfarnia, S. (2016). Deep eutectic solvent-mediated extraction for ligand-less preconcentration of lead and cadmium from environmental samples using magnetic nanoparticles. *Microchim. Acta* 183, 563–571. doi: 10.1007/s00604-015-1671-9
- Kocot, K., Zawisza, B., Marguí, E., Queral, I., Hidalgo, M., and Sitko, R. (2013). Dispersive micro solid-phase extraction using multiwalled carbon nanotubes combined with portable total-reflection X-ray fluorescence spectrometry for the determination of trace amounts of Pb and Cd in water samples. *J. Anal. Atom. Spectrom.* 28:736. doi: 10.1039/c3ja50047k
- Li, B., Cao, H., and Yin, G. (2011). Mg(OH)2@reduced graphene oxide composite for removal of dyes from water. *J. Mater. Chem.* 21:13765. doi: 10.1039/c1jm13368c
- Li, W., Morgan, M. K., Graham, S. E., and Starr, J. M. (2016). Measurement of pyrethroids and their environmental degradation products in fresh fruits and vegetables using a modification of the quick easy cheap effective rugged safe (QuEChERS) method. *Talanta* 151, 42–50. doi: 10.1016/j.talanta.2016.01.009
- Liu, Q., Shi, J., and Jiang, G. (2012). Application of graphene in analytical sample preparation. TrAC-trend. *Anal. Chem.* 37, 1–11. doi: 10.1016/j.trac.2012.03.011
- Radosevic, K., Bubalo, M. C., Srcek, V. G., Grgas, D., Dragicevic, T. L., and Redovnikovic, I. R. (2015). Evaluation of toxicity and biodegradability of choline chloride based deep eutectic solvents. *Ecotox. Environ. Safe.* 112, 46–53. doi: 10.1016/j.ecoenv.2014.09.034
- Ruesgas-Ramón, M., Figueroa-Espinoza, M. C., and Durand, E. (2017). Application of Deep Eutectic Solvents (DES) for phenolic compounds extraction: overview, challenges, and opportunities. *J. Agric. Food Chem.* 65, 3591–3601. doi: 10.1021/acs.jafc.7b01054
- Seródio, P., and Nogueira, J. M. F. (2005). Development of a stir-bar-sorptive extraction-liquid desorption-large volume injection capillary gas chromatographic-mass spectrometric method for pyrethroid pesticides in water samples. *Anal. Bioanal. Chem.* 382, 1141–1151. doi: 10.1007/s00216-005-3210-8
- Shishov, A., Bulatov, A., Locatelli, M., Carradori, S., and Andruch, V. (2017). Application of deep eutectic solvents in analytical chemistry. A review. *Microchem. J.* 135, 33–38. doi: 10.1016/j.microc.2017.07.015
- Stankovich, S., Dikin, D. A., Dommett, G. H., Kohlhaas, K. M., Zimney, E. J., Stach, E. A., et al. (2006a). Graphene-based composite materials. *Nature* 442, 282–286. doi: 10.1038/nature04969
- Stankovich, S., Piner, R. D., Chen, X., Wu, N., Nguyen, S. T., and Ruoff, R. S. (2006b). Stable aqueous dispersions of graphitic nanoplatelets via the reduction of exfoliated graphite oxide in the presence of poly (sodium 4-styrenesulfonate). *J. Mater. Chem.* 16, 155–158. doi: 10.1039/B512799H
- Torbati, M., Farajzadeh, M. A., Torbati, M., A., Nabil, A. A., Mohebbi, A., Afshar Mogaddam, M. R., et al. (2018). Development of salt and pH-induced solidified floating organic droplets homogeneous liquid-liquid microextraction for extraction of ten pyrethroid insecticides in fresh fruits and fruit juices followed by gas chromatography-mass spectrometry. *Talanta* 176, 565–572. doi: 10.1016/j.talanta.2017.08.074
- Tsai, W. H., Chuang, H. Y., Chen, H. H., Huang, J. J., Chen, H. C., Cheng, S. H., et al. (2009). Application of dispersive liquid-liquid microextraction and dispersive micro-solid-phase extraction for the determination of quinolones in swine muscle by high-performance liquid chromatography with diode-array detection. *Anal. Chim. Acta* 656, 56–62. doi: 10.1016/j.aca.2009.10.008
- Wang, L., Wang, M., Yan, H., Yuan, Y., and Tian, J. (2014). A new graphene oxide/polypyrrole foam material with pipette-tip solid-phase extraction for determination of three auxins in papaya juice. *J. Chromatogr. A* 1368, 37–43. doi: 10.1016/j.chroma.2014.09.059
- Yilmaz, E., and Soylak, M. (2016). Ultrasound assisted-deep eutectic solvent based on emulsification liquid phase microextraction combined with microsample injection flame atomic absorption spectrometry for valence speciation of chromium(III/VI) in environmental samples, *Talanta* 160, 680–685. doi: 10.1016/j.talanta.2016.08.001
- Yilmaz, E., Ulusoy, H. I., Demir, O., and Soylak, M. (2018). A new magnetic nanodiamond/graphene oxide hybrid (Fe3O4@ND@GO) material for pre-concentration and sensitive determination of sildenafil in alleged herbal aphrodisiacs by HPLC-DAD system. *J. Chromatogr. B* 1084, 113–121. doi: 10.1016/j.jchromb.2018.03.030
- Zahrina, I., Nasikin, M., Krisanti, E., and Mulia, K. (2018). Deacidification of palm oil using betaine monohydrate-based natural deep eutectic solvents. *Food Chem.* 240, 490–495. doi: 10.1016/j.foodchem.2017.07.132
- Zhao, G., Jiang, L., He, Y., Li, J., Dong, H., Wang, X., et al. (2011). Sulfonated graphene for persistent aromatic pollutant management. *Adv. Mater.* 23, 3959–3963. doi: 10.1002/adma.201101007
- Zhao, L., Zhao, F., and Zeng, B. (2014). Preparation and application of sunset yellow imprinted ionic liquid polymer-ionic liquid functionalized graphene composite film coated glassy carbon electrodes. *Electrochim. Acta* 115, 247–254. doi: 10.1016/j.electacta.2013.10.181
- Zheng, H. B., Zhao, Q., Mo, J. Z., Huang, Y. Q., Luo, Y. B., Yu, Q. W., et al. (2013). Quick, easy, cheap, effective, rugged and safe method with magnetic graphitized carbon black and primary secondary amine as adsorbent and its application in pesticide residue analysis. *J. Chromatogr. A* 1300, 127–133. doi: 10.1016/j.chroma.2013.04.040
- Zhou, D., and Han, B. H. (2010). Graphene-based nanoporous materials assembled by mediation of polyoxometalate nanoparticles. *Adv. Funct. Mater.* 20, 2717–2722. doi: 10.1002/adfm.200902323

**Conflict of Interest Statement:** The authors declare that the research was conducted in the absence of any commercial or financial relationships that could be construed as a potential conflict of interest.

Copyright © 2019 Song, Zhang, Xie, Wang and Cao. This is an open-access article distributed under the terms of the Creative Commons Attribution License (CC BY). The use, distribution or reproduction in other forums is permitted, provided the original author(s) and the copyright owner(s) are credited and that the original publication in this journal is cited, in accordance with accepted academic practice. No use, distribution or reproduction is permitted which does not comply with these terms.





# Transformation Characteristics of Hydrogen-Donor Solvent Tetralin in the Process of Direct Coal Liquefaction

Hai-zhou Chang<sup>1</sup>, Jun-qi Li<sup>1</sup>, Shuai Du<sup>2\*</sup>, Kai-yuan Shen<sup>1</sup>, Qun Yang<sup>3</sup>, Han Yi<sup>1</sup> and Ji-wei Zhang<sup>1</sup>

<sup>1</sup> College of Science, University of Shanghai for Science and Technology, Shanghai, China, <sup>2</sup> SGS-CSTC Standards Technical Services Co., Ltd, Shenzhen, China, <sup>3</sup> School of Mechanical Engineering, University of Shanghai for Science and Technology, Shanghai, China

## OPEN ACCESS

### Edited by:

Mauricio A. Rostagno,  
Campinas State University, Brazil

### Reviewed by:

Halil Durak,  
Yüzüncü Yıl University, Turkey  
Zongqing Bai,  
Institute of Coal Chemistry  
(CAS), China

### \*Correspondence:

Shuai Du  
dushuai@foxmail.com

### Specialty section:

This article was submitted to  
Green and Sustainable Chemistry,  
a section of the journal  
Frontiers in Chemistry

Received: 14 June 2019

Accepted: 16 October 2019

Published: 01 November 2019

### Citation:

Chang H, Li J, Du S, Shen K, Yang Q,  
Yi H and Zhang J (2019)  
Transformation Characteristics of  
Hydrogen-Donor Solvent Tetralin in  
the Process of Direct Coal  
Liquefaction. *Front. Chem.* 7:737.  
doi: 10.3389/fchem.2019.00737

The aim of this study is to investigate the transformation of hydrogen-donor solvent tetralin in the direct liquefaction process of coal. Pure tetralin liquid as well as mixture of tetralin and Wucaiwan coal (WCW) were separately reacted under a liquefaction condition, and constituents of liquid product were analyzed by GC-MS. The results show that after the tetralin liquid reacts with high-pressure hydrogen, 90% of the reaction product is in liquid state, the gaseous products mainly include alkane gas and CO<sub>x</sub> gas. When the reaction temperatures were set at 380 and 420°C, respectively, the corresponding transformation rates of tetralin can be 34.72 and 52.74%. At 380°C, the tetralin mainly plays a role of passing active hydrogen, while at 420°C, it mainly occurs dehydrogenation transformation to provide active hydrogen, as well as generate naphthalene, methyl indan, and substituted benzene, etc. Taking tetralin as the hydrogen-donor solvent, the WCW was performed liquefaction reaction, and the obtained results show that the transformation rates of tetralin are 69.76 and 83.86% at liquefaction temperatures of 380 and 420°C, respectively. Tetralin mainly occur to dehydrogenation transformation to generate naphthalene, followed by methyl indan, where contents order of main constituents of the liquefaction products were: naphthalene > tetralin > methyl indan.

**Keywords:** coal liquefaction, tetralin, oil analysis, Gas analysis, transformation (of products)

## INTRODUCTION

Direct liquefaction of coal is an effective measure for clean utilization of coal, which converts solid coal (H/C ratio  $\approx$  0.8) to liquid fuels (H/C ratio  $\approx$  2) by adding hydrogen (Ren et al., 2010; Vasireddy et al., 2011). It is vital to provide enough hydrogen in a timely manner to stabilize free radicals from coal pyrolysis for getting more liquid fuels and inhibiting coke formation in the direct liquefaction process (Shui et al., 2010). It has been found solvent as a media plays a very important role in liquefaction process of coal (Mochida et al., 1990; Xue et al., 1999; Yan et al., 2001; Zhang et al., 2009), such as dissolving, providing, and passing active hydrogen as well as stabilizing free radicals, etc. Studies have revealed that tetralin is a kind of excellent hydrogen-donor solvent

**TABLE 1** | Proximate analysis and ultimate analysis of WCW coal.

Sample	Proximate		Analysis	Ultimate		Analysis		(wt.%, daf)
	M <sub>ad</sub>	A <sub>ad</sub>	V <sub>daf</sub>	C	H	N	S	O
WCW	12.28	6.11	31.13	79.75	3.55	0.63	0.59	15.48

(Neavel, 1976; Ishihara et al., 2002; Shu et al., 2003; Li and Ling, 2007; Zhang, 2011; Hou et al., 2018), where it can well dissolve and disperse coal particles, has strong ability to donate hydrogen as well as quickly stabilize free radicals, etc. Hydrogen transferred from tetralin affects oil yield and coal conversion significantly in the preheating stage of coal liquefaction (Hao et al., 2017). Approximately same total hydrogen consumption is observed under N<sub>2</sub> and H<sub>2</sub> with tetralin, and the hydrogen consumption from tetralin is higher than that from H<sub>2</sub> (Hao et al., 2018). It should be noted that tetralin is generally selected as hydrogen-donor solvent in direct liquefaction of coal conducted in laboratories. However, part of the tetralin tends to transform under the liquefaction conditions (Zhang et al., 2009). Since the specific transformation of tetralin is associated with the calculation of liquefaction product yield and understanding of liquefaction mechanism, knowing the transformation characteristics of tetralin during direct liquefaction process is a basic question that needs to be addressed. Yang et al. (1985a,b) studied the pyrolysis process of tetralin and found that the tetralin mainly leads to dehydrogenation reaction to generate naphthalene and isomerization reaction to generate methyl indan. Furthermore, they proposed the mechanism of radical reaction. Yang et al. (2011) summarized the reaction mechanism and reaction dynamics in tetralin hydrogenation pyrolysis. Ishihara et al. (2002) applied isotope labeling method to study the hydrogen transfer behaviors between coal and tetralin in direct liquefaction process, and they obtained the hydrogen donating pathways: I. Directly transferring active hydrogen; II. Transforming to naphthalene by dehydrogenation. Studies have reported the mechanism of tetralin pyrolysis as well as hydrogen donating behavior of tetralin in direct liquefaction process using isotope label method, but the transformation of tetralin itself in direct liquefaction process is still unknown. In this study, we obtained liquid products by separately performing reaction using pure tetralin as well as mixture of coal and tetralin under direct liquefaction condition. Then we utilized GC-MS to quantitatively analyze constituents of the liquid and changes of their contents, utilized GC to obtain the composition distribution in gas phase, hereby to study the transformation features of tetralin, so as to enrich the understanding of the mechanism of direct coal liquefaction.

## MATERIALS AND METHODS

### Materials

A Chinese WCW coal was used. Its ultimate and proximate analyses are listed in **Table 1**. The coal sample was ground to pass 200 mesh sieve and dried under a vacuum at 105°C for 4 h. Tetralin (AR) and Hexane (AR) provided

by Sinopharm Chemical Reagent Co., Ltd were used in the experiments.

## Direct Liquefaction Experiments

### Coal Direct Liquefaction Procedure

Two grams of WCW coal (200 mesh) and 4 g tetralin were weighted and transferred to the autoclave, added with catalyst (Fe<sub>2</sub>O<sub>3</sub>) (iron amount: 3 wt % of coal was transformed to Fe<sub>2</sub>O<sub>3</sub>) and co-catalyst S (0.4 times of Fe mass). The initial pressure of hydrogen was 5 MPa, and the temperature was set to be 380 and 420°C, respectively. The reaction was persisted for 60 min after obtaining the pre-set temperature, and then the experiment was terminated. Gas was collected after the autoclave cooled to room temperature. After the autoclave was opened, the oil and residue were fully transferred to paper-cylinder filtration and placed into an extraction tube, which was placed into a flask containing 200 g hexane, and refluxed in 107°C silicon oil bath pan for 48 h, hereby to obtain orange oil. Constituents of gas were analyzed using gas chromatograph and those of oil were analyzed using gas chromatograph-mass spectrometer.

### Tetralin Direct Liquefaction Procedure

Four grams of tetralin were weighted and transferred to the autoclave, added with catalyst (Fe<sub>2</sub>O<sub>3</sub>) [iron amount: 3 wt % of coal (2 g) was transformed to Fe<sub>2</sub>O<sub>3</sub>] and co-catalyst S (0.4 times of Fe mass). The initial pressure of hydrogen was 5 MPa, and the temperature was set to be 380 and 420°C, respectively. The reaction was persisted for 60 min after obtaining the pre-set temperature, and then the experiment was terminated. Gas was collected after the autoclave cooled to room temperature. After the autoclave was opened, the oil and residue were fully transferred to paper-cylinder filtration and placed into an extraction tube, which was placed into a flask containing 200 g hexane, and refluxed in a 107°C silicon oil bath pan for 48 h, hereby to obtain orange oil. Constituents of gas were analyzed using gas chromatograph and those of oil were analyzed using gas chromatograph-mass spectrometer.

## GC/MS Analysis

GC-MS Thermo Trace GC ISQ was used to analyze liquid phases in the experiments. Its key parameters include TR-5MS capillary column (length 30 m, inner diameter 0.25 mm, film thickness 0.25 μm); carrier gas: helium, flow rate 1.5 mL/min; split flow 20:1; temperature of injection port 280°C; EI source, ionization voltage 70 eV, temperature of ion source 275°C; mass scanning range 50–550 amu. The elevation of temperature was programed as follows: initial temperature of 50°C (1 min), and elevated to 90°C (5°C/min, 2 min) and elevated to 240°C (10°C/min, 1 min). The constituents of the obtained oil were analyzed, and the relative percentage of each constituent was calculated using area normalization method.

## RESULTS AND DISCUSSION

### Composition of Products of Tetralin and High-Pressure Hydrogen

Liquid, gas, and residue yield were calculated by equations shown as below,

**TABLE 2** | Contents of products obtained by tetralin and high-pressure hydrogen reaction.

Temperature	Yield/%		
	Liquid	Gas	Residue
380°C	92.14	4.93	2.93
420°C	85.76	8.39	5.85

**TABLE 3** | Composition of the raw material tetralin.

NO.	Compound	Molecular formula	Area%
1	Tetralin	C <sub>10</sub> H <sub>12</sub>	97.04
2	Naphthalene	C <sub>10</sub> H <sub>8</sub>	1.09
3	Methyl indan	C <sub>10</sub> H <sub>12</sub>	0.46
4	Butadiene styrene	C <sub>10</sub> H <sub>14</sub>	0.15
5	Ethylbenzene	C <sub>8</sub> H <sub>10</sub>	0.27
6	m-xylene	C <sub>8</sub> H <sub>10</sub>	0.22
7	Ethyltoluene	C <sub>9</sub> H <sub>12</sub>	0.28
8	n-decane	C <sub>10</sub> H <sub>22</sub>	0.15

Liquid yield:  $Y_l = M_l / (M_t + M_h)$

Residue yield:  $Y_r = (M_r - M_{cat.}) / (M_t + M_h)$

Gas yield:  $Y_g = 1 - Y_l - Y_r$

$Y_l$ ,  $Y_r$ ,  $Y_g$  are the yield of liquid, residue and gas.  $M_t$ ,  $M_h$ ,  $M_{cat.}$  are weight of tetralin, molecular hydrogen, and catalyst (Fe<sub>2</sub>O<sub>3</sub>).  $M_l$ ,  $M_r$  are weight of liquid and residue after the reaction.

**Table 2** lists the contents of gas, liquid, and solid obtained by tetralin under high-pressure hydrogen reaction at 380 and 420°C. At the designated temperature, contents of each constituent were ordered by: liquid > gas > solid, of which the contents of liquid constituent were 92.14 and 85.76%, respectively, which indicated that the tetralin is mainly in a liquid state during the reaction process, while part of it is transformed into gas and solid. Comparing products obtained at two temperatures revealed that with increasing temperature, content of liquid constituents was decreased and contents of gas and solid constituents were increased. Based on the above results, it indicated that an elevated temperature is prone to aggravate the liquid tetralin to transform to gas and solid products. Thus, it can be inferred that in direct coal liquefaction experiment using tetralin as hydrogen-donor solvent, part of tetralin will transform to gas and solid. Since the coal liquefaction requires a large amount of tetralin, effect of tetralin transformation on products of coal liquefaction is worthy of concern.

## GC-MS Analysis of Liquid Obtained by Tetralin and High-Pressure Hydrogen Reaction

### GC-MS Analysis of Pure Tetralin

In this paper, the transformation characteristics of tetralin were discussed on the basis of comparative analysis. In order to make the analysis results more reliable and accurate, the

**TABLE 4** | Relative content of hydrocarbons in liquid products.

No.	Compound	Molecular formula	Area%
<b>380°C</b>			
1	Tetralin	C <sub>10</sub> H <sub>12</sub>	65.28
2	Naphthalene	C <sub>10</sub> H <sub>8</sub>	13.71
3	Methyl indan	C <sub>10</sub> H <sub>12</sub>	12.48
4	Butylbenzene	C <sub>10</sub> H <sub>14</sub>	5.30
5	Ethylbenzene	C <sub>8</sub> H <sub>10</sub>	1.18
6	n-heneicosane	C <sub>21</sub> H <sub>44</sub>	0.48
7	Indane	C <sub>9</sub> H <sub>10</sub>	0.47
8	n-eicosane	C <sub>20</sub> H <sub>42</sub>	0.45
9	Hexadecane	C <sub>16</sub> H <sub>34</sub>	0.18
10	Methylnaphthalene	C <sub>11</sub> H <sub>10</sub>	0.17
11	Diethylbenzene	C <sub>10</sub> H <sub>14</sub>	0.16
12	m-xylene	C <sub>8</sub> H <sub>10</sub>	0.07
13	Ethyltoluene	C <sub>9</sub> H <sub>12</sub>	0.06
<b>420°C</b>			
1	Tetralin	C <sub>10</sub> H <sub>12</sub>	47.26
2	Naphthalene	C <sub>10</sub> H <sub>8</sub>	15.61
3	Methyl indan	C <sub>10</sub> H <sub>12</sub>	20.80
4	Butylbenzene	C <sub>10</sub> H <sub>14</sub>	5.68
5	Ethylbenzene	C <sub>8</sub> H <sub>10</sub>	4.95
6	Indane	C <sub>9</sub> H <sub>10</sub>	3.59
7	Methylnaphthalene	C <sub>11</sub> H <sub>10</sub>	0.57
8	n-eicosane	C <sub>20</sub> H <sub>42</sub>	0.42
9	Diethylbenzene	C <sub>10</sub> H <sub>14</sub>	0.30
10	Isopropyl benzene	C <sub>9</sub> H <sub>12</sub>	0.29
11	m-xylene	C <sub>8</sub> H <sub>10</sub>	0.28
12	Ethyltoluene	C <sub>9</sub> H <sub>12</sub>	0.12
13	Tridecane	C <sub>13</sub> H <sub>28</sub>	0.09

components of tetralin solvent were analyzed by GC-MS. Results (**Table 3**) show that 97.04% of the tetralin solvent exists in the form of tetralin, 2.62% in the form of non-tetralin, and 0.34% in the form of unknown components. The blank analysis of tetralin solvent is helpful to further study the transformation mechanism of tetralin in the liquefaction process of tetralin and coal liquefaction process using tetralin as hydrogen-donor solvent.

### GC-MS Analysis of Oil Products Obtained by Tetralin and High-Hydrogen Reaction

**Table 4** shows GC-MS analysis results of liquid obtained by tetralin and high-pressure hydrogen reaction, which demonstrated that at 380°C, contents of the main constituents of the liquid were ordered by: tetralin > naphthalene > methyl indan, of which the percentage of tetralin was 65.28%, which was significantly lower than the GC-MS analysis results of 97.04% of pure tetralin liquid. The reason is that the tetralin transforms to generate naphthalene (13.71%), methyl indan (12.48%), and substituted benzene (6.77%), as well as a small amount of straight-chain alkanes and methylnaphthalene, etc. At 420°C, contents of the main constituents of the liquid were



ordered by: tetralin > methyl indan > naphthalene, of which the content of tetralin was only 47.26%, while the contents of other constituents were increased. In details, the content of methyl indan was significantly increased to 20.80%, the content of naphthalene was increased to 15.05%. In addition, the content of substituted benzene was increased from 6.77 to 11.62%. These results indicated that an elevated temperature tends to enhance the transformation of tetralin, and tetralin is mainly transformed into methyl indan, followed by naphthalene at 420°C. In summary, analysis of constituents of the liquid showed that in the reaction process of tetralin and high-pressure hydrogen, tetralin could play a role of transferring hydrogen as illustrated in formula R-1 shown in **Scheme 1**, which was denoted as THN<sub>1</sub>, meanwhile it could also provide hydrogen through its own dehydrogenation transformation as illustrated in formula R-2 shown in **Scheme 1**, which was denoted as THN<sub>2</sub>. From **Table 2**, the transformation rates of tetralin were 34.72 and 52.74%, and the THN<sub>1</sub>/THN<sub>2</sub> was 1.88 and 0.90 at 380 and 420°C, respectively. These findings revealed that at a lower reaction temperature (such as 380°C), the hydrogen-donor solvent tetralin mainly plays a role of transferring active hydrogen. However, at a higher reaction temperature (such as 420°C), tetralin mainly provides active hydrogen through its own dehydrogenation transformation.

### GC-MS Analysis of Oil Products Obtained by Liquefaction of WCW

**Table 5** shows the GC-MS analysis of the oil products obtained by direct liquefaction of WCW, while taking tetralin as Exxon

donor solvent. As can be seen from the table, at a liquefaction temperature of 380°C, contents of the main constituents of oil were ordered by: naphthalene > tetralin > methyl indan, of which the content of naphthalene was highest, accounting for 58.67% of the total amount, while the content of tetralin was 26.42% (transformation rate of tetralin was 69.76%). At a liquefaction temperature of 420°C, contents of the main compositions of oil were still ordered by: naphthalene > tetralin > methyl indan, of which the content of naphthalene was as high as 65.96%, while the content of tetralin was only 14.86% (transformation rate of tetralin was 83.86%), which can be ascribed to the tetralin occurs dehydrogenation transformation to generate naphthalene, methyl indan, and other products.

As shown in **Table 6**, the oil yield of WCW at liquefaction temperature of 380 and 420°C were 29.30 and 17%, respectively. In liquefaction reaction, coal macromolecules can decompose to generate part of the naphthalene in the oil. Mass conservation proves that the naphthalene in the oil mainly derives from transformation of tetralin. Assuming the percentages of tetralin, naphthalene and methyl indan in oil product were denoted as

**TABLE 5 |** Relative content of hydrocarbons in oil.

No.	Compound	Molecular formula	Area%
<b>380°C</b>			
1	Naphthalene	C <sub>10</sub> H <sub>8</sub>	58.67
2	Tetralin	C <sub>10</sub> H <sub>12</sub>	26.42
3	Methyl indan	C <sub>10</sub> H <sub>12</sub>	5.49
4	Alkanes	C <sub>8</sub> -C <sub>20</sub>	3.56
5	Butylbenzene	C <sub>10</sub> H <sub>14</sub>	1.68
6	Methylnaphthalene	C <sub>11</sub> H <sub>10</sub>	1.15
7	Indane	C <sub>9</sub> H <sub>10</sub>	0.94
8	Ethylbenzene	C <sub>8</sub> H <sub>10</sub>	0.65
9	Pyrene	C <sub>16</sub> H <sub>10</sub>	0.36
10	Anthracene	C <sub>14</sub> H <sub>10</sub>	0.30
11	Fluorene	C <sub>13</sub> H <sub>10</sub>	0.20
12	Phenylpropane	C <sub>9</sub> H <sub>12</sub>	0.20
13	Acenaphthene	C <sub>12</sub> H <sub>8</sub>	0.18
14	2-methylbiphenyl	C <sub>13</sub> H <sub>12</sub>	0.18
<b>420°C</b>			
1	Naphthalene	C <sub>10</sub> H <sub>8</sub>	65.96
2	Tetralin	C <sub>10</sub> H <sub>12</sub>	14.86
3	Methyl indan	C <sub>10</sub> H <sub>12</sub>	7.12
4	Alkanes	C <sub>13</sub> -C <sub>20</sub>	4.04
5	Indane	C <sub>9</sub> H <sub>10</sub>	2.16
6	Methylnaphthalene	C <sub>11</sub> H <sub>10</sub>	1.77
7	Ethylbenzene	C <sub>8</sub> H <sub>10</sub>	1.40
8	Butylbenzene	C <sub>10</sub> H <sub>14</sub>	1.00
9	Pyrene	C <sub>16</sub> H <sub>10</sub>	0.36
10	Anthracene	C <sub>14</sub> H <sub>10</sub>	0.24
11	Fluorene	C <sub>13</sub> H <sub>10</sub>	0.21
12	Phenylpropane	C <sub>9</sub> H <sub>12</sub>	0.30
13	Acenaphthene	C <sub>12</sub> H <sub>8</sub>	0.14
14	2-methylbiphenyl	C <sub>13</sub> H <sub>12</sub>	0.43

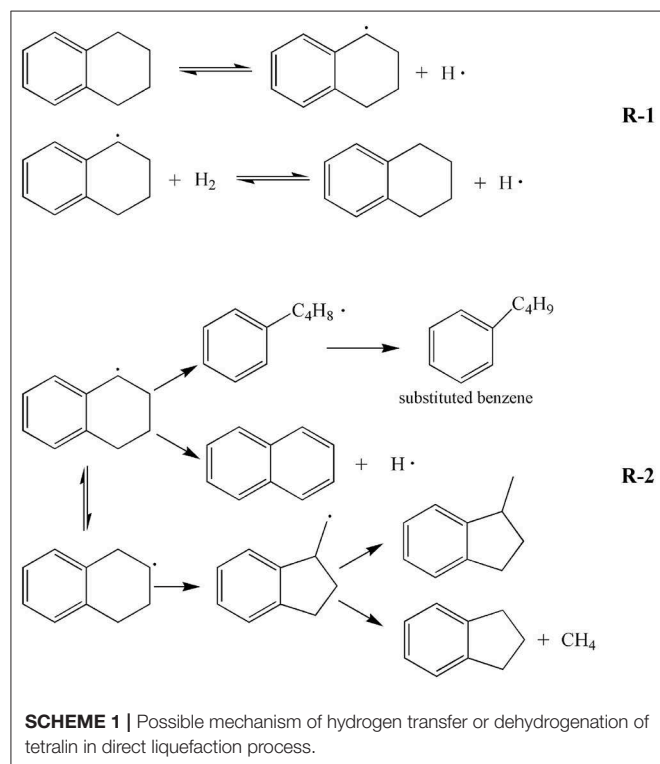


**TABLE 6** | Oil yield, transformation rate, and residue rate in liquefaction of WCW.

Temperature	$\eta_{oil}/\%$	$\eta_{conv}/\%$	$\eta_{char}/\%$
380°C	29.30	48.42	51.58
420°C	17.00	48.15	51.84

**TABLE 7** | Balancing results of mass of tetralin in oil product obtained by liquefaction (Assuming: under liquefaction conditions, the tetralin is completely in the liquid state and its mass is denoted as  $m_T$ , while the mass of oil product from coal transformation is denoted as  $m_o$ ).

Temperature	$m_T - (m_o + m_T) \cdot x$	$(m_o + m_T) \cdot y + (m_o + m_T) \cdot z$	$\Delta$
380°C	2.82	3.02	-0.20
420°C	3.32	3.23	0.090

$x$ ,  $y$ , and  $z$ , respectively, while the total mass of oil product obtained by liquefaction was  $m_o + m_T$ , we might obtain the masses of tetralin, naphthalene and methyl indan as  $(m_o + m_T) \cdot x$ ,  $(m_o + m_T) \cdot y$  and  $(m_o + m_T) \cdot z$ , respectively. **Table 7** shows the balancing results of tetralin in oil product obtained by liquefaction, from the  $\Delta$  value, reduction of tetralin is about the summation of masses of naphthalene and 2,3-indanyl, hereby proves that the naphthalene in oil product is mainly transformed from tetralin.

In addition, the main constituents of oil product obtained by liquefaction of WCW include tetralin, naphthalene, and methyl indan, and their contents were ordered by: naphthalene > tetralin > methyl indan. Therefore, it could be inferred that the tetralin was mainly transformed into naphthalene and methyl indan in liquefaction reaction of WCW, which was consistent with the constituents of oil obtained by reaction of tetralin and high-pressure hydrogen. In this study, liquefaction temperatures of 380 and 420°C were selected. Constituents of oil at these two temperatures were compared, and the results showed that the tetralin in the oil was significantly decreased with elevating temperature, which was reduced from 26.42 to 14.86%, and the content of naphthalene was increased from 58.67 to 65.96%, while the content of methyl indan was slightly increased from 6.43 to 9.28%. In addition, by comparison of the data in **Tables 3, 4**, the results revealed that the main constituents of oil presented a change of “two decrease, one increase,” i.e., contents of tetralin and methyl indan were decreased, while content of naphthalene was significantly increased. Therefore, it can be inferred that during the liquefaction of WCW, the hydrogen-donating paths for the tetralin are: (a) Mainly, it is a process for tetralin occurs dehydrogenation reaction to produce naphthalene; (b) C-C bond of tetralin molecules tends to break and reconstruct to generate isomer methyl indan, part of which occurs demethylation reaction to produce indan and methane gas; (c) C-C bond at  $\alpha$  site of tetralin molecules tends to cleavage into benzene butyl free radicals, and then transforms to substitute benzene and paraffin gas; (d) Tetralin molecules directly transfer active hydrogens as illustrated in formula (1). Overall, during the liquefaction process of WCW,

**TABLE 8** | Constituents of gas obtained by tetralin and high-pressure hydrogen reaction.

Tetralin	$CH_4$	$C_2H_6$	$C_3H_8$	$C_4H_{10}$	CO	$CO_2$
380°C	0.49	0.27	0.060	0.010	0.10	0.24
420°C	0.42	0.50	0.070	0.010	0.090	0.13

the hydrogen-donating path of hydrogen-donor solvent was similar to the reaction process of tetralin and high-pressure hydrogen. It is worth noting that the content of naphthalene was significantly higher than the contents of methyl indan and tetralin in oil obtained by liquefaction of WCW. The reason is that the path (a) is the main transformation process, and the naphthalene has a weaker hydrogen-donating ability and has a better thermal stability.

Compared with constituents of liquid obtained by reaction of tetralin and high-pressure hydrogen, the oil products obtained by coal liquefaction contain benzo pyrene, anthracene, fluorene, acenaphthene, and other polycyclic aromatic hydrocarbon structures. This part of aromatic constituents is mainly produced by coal macromolecule, i.e., at reaction temperature, weak bonds in coal macromolecule structure will break to produce aromatic free radicals, which bond to active hydrogen to produce aromatic compound.

## Constituents of Gas Obtained by Tetralin and High-Pressure Hydrogen Reaction

GC-9160 gas chromatograph was used to analyze the gas obtained by reaction of tetralin and high-pressure hydrogen, and the results (**Table 8**) showed low contents of alkane gas and  $CO_x$  gas. For  $CO_x$  gas, the distribution was characterized by  $CO_2 > CO$  at two reaction temperatures. For alkane gas, contents of gas were ordered by  $CH_4 > C_2H_6 > C_3H_8 > C_4H_{10}$  and  $C_2H_6 > CH_4 > C_3H_8 > C_4H_{10}$  at reaction temperature of 380 and 420°C, respectively. From the point of view of conservation of carbon atoms, both alkane and  $CO_x$  gases are transformed from tetralin. In summary, among the gas obtained by reaction of tetralin and high-pressure hydrogen, the content of alkane gas was greater than that of  $CO_x$  gas, where contents of the former were 2.4 and 4.5 times of those of the latter at 380 and 420°C, respectively, which in a whole presented distribution characteristics of rich alkanes, methane, and carbon dioxide.

## CONCLUSION

In conclusion, when the pure tetralin liquid reacts at liquefaction conditions, the tetralin mainly exists in a liquid state, while part of it may transform into gas and solid. In addition, the content of liquid constituent is decreased while the contents of gas and solid constituents are increased with elevating temperature.

In the reaction process of tetralin and high-pressure hydrogen, part of tetralin plays a role of transferring hydrogen, and the remaining part tends to provide hydrogen through

its own dehydrogenation transformation. At the lower temperature (such as 380°C), tetralin mainly plays a role of transferring active hydrogen with a transformation rate of 34.72%. Meanwhile, at a higher temperature (such as 420°C), tetralin mainly provides active hydrogen through dehydrogenation transformation and has a transformation rate of 52.74%, while it can transform into naphthalene, methyl indan, and substituted benzene, etc. In addition, gas phase produced from the reaction generally presents distribution of high concentration of alkanes, methane, and carbon dioxide, and both the alkane and CO<sub>x</sub> gases are transformed from tetralin.

As the hydrogen-donor solvent, the transformation rates of tetralin are 69.76 and 83.86% in liquefaction of WCW at temperatures of 380 and 420°C, respectively. The contents of main constituents of oil are ordered by: naphthalene>tetralin>methyl indan. In addition, compared with the oil product obtained by liquefaction of pure tetralin, content of tetralin in oil

product obtained by liquefaction of coal is significantly reduced. Meanwhile, the content of methyl indan is decreased. However, the content of naphthalene is significantly increased.

## DATA AVAILABILITY STATEMENT

All datasets generated for this study are included in the article/supplementary material.

## AUTHOR CONTRIBUTIONS

All authors listed have made a substantial, direct and intellectual contribution to the work, and approved it for publication.

## FUNDING

The authors are grateful to the financial supports from the National Natural Science Foundation of China (21276156).

## REFERENCES

- Hao, P., Bai, Z. Q., Hou, R. R., Xu, J. L., Bai, J., Guo, Z. X., et al. (2018). Effect of solvent and atmosphere on product distribution, hydrogen consumption and coal structural change during preheating stage in direct coal liquefaction. *Fuel* 211, 783–788. doi: 10.1016/j.fuel.2017.09.122
- Hao, P., Bai, Z. Q., Zhao, Z. T., Yan, J. C., Li, X., Guo, Z. X., et al. (2017). Study on the preheating stage of low rank coals liquefaction: product distribution, chemical structural change of coal and hydrogen transfer. *Fuel Process. Technol.* 159, 153–159. doi: 10.1016/j.fuproc.2017.01.028
- Hou, P. D., Zhou, Y. W., Guo, W. P., Ren, P. J., Qiang, G., Xiang, H. W., et al. (2018). Rational design of hydrogen-donor solvents for direct coal liquefaction. *Energy Fuels* 32, 4715–4723. doi: 10.1021/acs.energyfuels.7b03947
- Ishihara, A., Sutrisna, I. P., Miura, T., Saito, M., Qian, E. W., Kabe, T. J. E., et al. (2002). Elucidation of hydrogen transfer between coal and tritiated organic solvent. *Energy Fuels* 16, 1490–1498. doi: 10.1021/ef020074r
- Li, G., and Ling, K. C. (2007). Division of kinetic stages in coal direct liquefaction process and coal quick liquefaction at high temperature. *Clean Coal Technol.* 37, 22–25. doi: 10.3321/j.issn:0253-9993.2007.09.018
- Mochida, I., Takayama, A., Sakata, R., and Sakanishi, K. (1990). Hydrogen-transferring liquefaction of an Australian brown coal with polyhydrogenated condensed aromatics: roles of donor in the liquefaction. *Energy Fuels* 4, 81–84. doi: 10.1021/ef00019a015
- Neavel, R. C. (1976). Liquefaction of coal in hydrogen-donor and non-donor vehicles. *Fuel* 55, 237–242. doi: 10.1016/0016-2361(76)90095-8
- Ren, X. K., Fang, D. Y., Jin, J. L., and Gao, J. S. (2010). New proceed achieved in the direct coal liquefaction. *Chem. Ind. Eng. Prog.* 29, 198–204. doi: 10.16085/j.issn.1000-6613.2010.02.020
- Shu, G. P., Shi, S. D., and Li, K. J. (2003). *Coal Liquefaction Technology*. Beijing: Coal Industry Press.
- Shui, H. F., Cai, Z. Y., and Xu, C. B. (2010). Recent advances in direct coal liquefaction. *Energies* 3, 155–170. doi: 10.3390/en3020155
- Vasireddy, S., Morreale, B., Cugini, A., Song, C., and Spivey, J. J. (2011). Clean liquid fuels from direct coal liquefaction: chemistry, catalysis, technological status and challenges. *Energy Environ. Sci.* 4, 311–345. doi: 10.1039/C0EE00097C
- Xue, Y. B., Ling, K. C., and Zou, G. M. (1999). Functions and kinds of solvents in coal direct liquefaction. *Coal Convers.* 22, 1–4.
- Yan, R. P., Zhu, J. S., Yang, J. L., and Liu, Z. Y. (2001). Study on hydro-coprocessing of Yanzhou coal and catalytic cracking slurry oil: I. coal conversion and product distribution. *Acta Petrol. Sin.* 17, 1–7.
- Yang, P., Xin, J., Li, M. F., and Nie, H. (2011). Research advances in the hydroconversion of tetralin. *Pet. Process. Petroche.* 42, 1–6. doi: 10.3969/j.issn.1005-2399.2011.08.001
- Yang, X. L., Yang, H. X., and Han, D. G. (1985a). Kinetics and mechanism of thermolysis of tetralin. *Acta Phys. Chim. Sin.* 1, 249–257.
- Yang, X. L., Yang, H. X., and Han, D. G. (1985b). The Study of the intermediates reactions and the reaction mechanism in the thermolysis of tetralin. *Acta Phys. Chim. Sin.* 1, 571–574. doi: 10.3866/PKU.WHXB19850611
- Zhang, X. J. (2011). Study on solvents for direct coal liquefaction. *Clean Coal Technol.* 17, 25–28. doi: 10.3969/j.issn.1006-6772.2011.04.010
- Zhang, X. J., Wu, Y., Chen, Y., and Du, S. F. (2009). Discussion of n-d-M method for calculating aromatic carbon ratio of direct coal liquefaction solvent oil. *J. China Coal Soc.* 34, 1129–1132. doi: 10.13225/j.cnki.jccs.2009.08.001

**Conflict of Interest:** SD has been employed by company SGS-CSTC Standards Technical Services Co., Ltd.

The remaining authors declare that the research was conducted in the absence of any commercial or financial relationships that could be construed as a potential conflict of interest.

Copyright © 2019 Chang, Li, Du, Shen, Yang, Yi and Zhang. This is an open-access article distributed under the terms of the Creative Commons Attribution License (CC BY). The use, distribution or reproduction in other forums is permitted, provided the original author(s) and the copyright owner(s) are credited and that the original publication in this journal is cited, in accordance with accepted academic practice. No use, distribution or reproduction is permitted which does not comply with these terms.



# Highly Efficient Adsorption of Phenylethanoid Glycosides on Mesoporous Carbon

Helin Xu<sup>1</sup>, Wenjing Pei<sup>1</sup>, Xueqin Li<sup>1\*</sup> and Jinli Zhang<sup>1,2\*</sup>

<sup>1</sup> School of Chemistry and Chemical Engineering/Key Laboratory for Green Processing of Chemical Engineering of Xinjiang Bingtuan, Shihezi University, Shihezi, China, <sup>2</sup> Key Laboratory for Green Chemical Technology of Ministry of Education, School of Chemical Engineering and Technology, Tianjin University, Tianjin, China

## OPEN ACCESS

### Edited by:

Mauricio A. Rostagno,  
Campinas State University, Brazil

### Reviewed by:

Mohammad Boshir Ahmed,  
Gwangju Institute of Science and  
Technology, South Korea  
Miguel Angel Centeno,  
Instituto de Ciencia de Materiales de  
Sevilla (ICMS), Spain

### \*Correspondence:

Xueqin Li  
lixueqin861003@163.com  
Jinli Zhang  
zhangjinli@tju.edu.cn

### Specialty section:

This article was submitted to  
Green and Sustainable Chemistry,  
a section of the journal  
Frontiers in Chemistry

**Received:** 01 September 2019

**Accepted:** 30 October 2019

**Published:** 14 November 2019

### Citation:

Xu H, Pei W, Li X and Zhang J (2019)  
Highly Efficient Adsorption of  
Phenylethanoid Glycosides on  
Mesoporous Carbon.  
Front. Chem. 7:781.  
doi: 10.3389/fchem.2019.00781

PhGs are the major active compounds of *Cistanche tubulosa*, and it is extremely desirable for obtaining high purification of PhGs by adsorption from their extracts. To explore highly efficient adsorption of PhGs, a novel adsorption material for the efficient separation and purification of phenylethanoid glycosides (PhGs) from *Cistanche tubulosa* was explored. The three mesoporous carbons of ordered mesoporous carbon (CMK-3), disordered mesoporous carbon (DMC), and three-dimensional cubic mesoporous carbon (CMK-8) were compared for adsorption of PhGs. Meanwhile, adsorption isotherms, adsorption kinetics, and the optimization of adsorption conditions were investigated. The results indicated that CMK-3 showed the highest adsorption capacity of  $358.09 \pm 4.13$  mg/g due to its high specific surface area, large pore volume and oxygen-containing functional groups. The experimental data can be accurately described using the Langmuir model and pseudo-second-order model. The intra-particle diffusion model suggested that the rate-limiting steps of adsorption were intra-particle diffusion.

**Keywords:** *Cistanche tubulosa*, acteosides, echinacosides, phenylethanoid glycosides, mesoporous carbon, kinetic model, isothermal model

## INTRODUCTION

*Cistanche tubulosa* was an Orobanchaceae parasitic plant (Li et al., 2016; Wang X. et al., 2017), and it mainly grown on the roots of Tamarix plants and Calotropis species (Zhang W. et al., 2016; Yan et al., 2017). *Cistanche tubulosa* was originally recorded in Shen Nong's Chinese Materia Medica in ca. 100 B.C. The growth and cultivation of *Cistanche tubulosa* required severe environmental conditions, and it was widely planted in arid lands and deserts of the northern hemisphere, such as the provinces of Xinjiang, Inner Mongolia, Gansu, Qinghai, and the Ningxia Autonomous Region in China (You et al., 2016). *Cistanche tubulosa* was a precious Chinese tonic herb which had the functions of nourish the kidney, anti-aging, boosts the essence of blood, and moistens the large intestines to free stool (Gu et al., 2016; Shimada et al., 2017; Cui et al., 2018), and it has been reputation as "Ginseng of the Deserts" (Song et al., 2016; Wang et al., 2018). *Cistanche tubulosa* was officially recorded in the Chinese Pharmacopeia as the authentic source of *Cistanches Herba* (Chinese name: Roucon-grong) from 2005 edition (Wang T. et al., 2016; Pei et al., 2019).

Previous study had revealed several main chemical constituents of *Cistanche tubulosa*, including PhGs, iridoids, and polysaccharides (Li et al., 2018a). The structures of PhGs were mainly composed of cinnamic acid and phenylethyl alcohol that were attached to a  $\beta$ -glucopyranose through ester and glycosidic linkages (Luo et al., 2010), and PhGs have been regarded as the major active



components of *Cistanche tubulosa* possessing various pharmacological activities (Liao et al., 2018). The study shown that PhGs had a variety of medicinal properties, such as neuroprotection, immune regulation, anti-inflammatory, liver protection and antioxidant (Aiello et al., 2015; Shiao et al., 2017; Wu et al., 2018, 2019). According to phytochemical evaluations, PhGs such as echinacoside, acteoside were considered to be main active components and markers of *Cistanche tubulosa* (Li et al., 2017b), which were usually chosen as marker compounds for the quality evaluation of *Cistanche tubulosa* and the species of *Cistanche* were distinguished through these compounds. PhGs were naturally occurring water-soluble compounds because it had many hydroxyl groups and phenolic hydroxyl groups in the molecule. Thus, the PhGs can be separated from *Cistanche tubulosa* in an aqueous solution.

Many methods for the separation and purification of natural products have been developed including adsorption (Liu et al., 2016), membrane separation (Zhang et al., 2018b; Li et al., 2019) and solvent extraction, and so on (Li et al., 2015a,b; Wang S. et al., 2016; Zhang H. et al., 2016). However, membrane separation and solvent extraction were not suitable for large-scale preparation and they were difficult to achieve high recovery of the products (Zhang et al., 2018a). Adsorption was one of the most widely adopted methods for the separation natural products (Wang S. et al., 2016; Konggidinata et al., 2017). Owing to its unique and tunable pore structures, high surface areas and mechanical stability, mesoporous carbons (pore size between 2 and 50 nm) have been proven to be a kind of efficient adsorbents for adsorptive natural products. The study shown that mesoporous carbons were more suitable for adsorbing macromolecules, such as mesoporous carbons have been used by Qin et al. to enrichment of chlorogenic acid from eucommia ulmoides leaves (Qin et al., 2018). Li et al. synthesized two mesoporous carbons via a hydrothermal treatment approach, and evaluated adsorption performance of two mesoporous carbons for berberine hydrochloride and matrine from water (Li et al., 2018b). It was considered to be kind of promising material as a highly efficient adsorbent (Zhang et al., 2013; Tian et al., 2015; Zhou et al., 2016). Additionally, mesoporous carbons also have been applied on adsorptive removal of aromatic compounds, dyes, and heavy metals from wastewater (Kong et al., 2016). In previous published works, Liu et al. used a macroporous resin to adsorb PhGs from *Cistanche tubulosa*, and the purity of the PhGs increased but the adsorption capacity and desorption rate were low. Compared with macroporous resin, mesoporous carbons had the characteristics of large specific surface area, suitable pore size, and a high pore volume. Therefore, mesoporous carbon was considered to be a highly efficient adsorbent for PhGs. In this study, the three kinds of mesoporous carbon were selected as adsorbent for separation and purification of PhGs from *Cistanche tubulosa*.

This work main objective was to explore the adsorption performance of CMK-3 for separation and purification PhGs from *Cistanche tubulosa*. The effects of different concentrations, pH and temperature on the adsorption performance of CMK-3 were investigated and optimal adsorption conditions of PhGs were screened out. Mesoporous carbons were characterized by

FT-IR, BET, TEM, and TGA, adsorption isotherms and kinetics were performed and analyzed in detail.

## EXPERIMENTS

### Materials and Reagents

*Cistanche tubulosa* stem was purchased from Congrongtang Biological Technology Co., Ltd. (Xinjiang). The standards of echinacoside (purities  $\geq 98\%$ ) and acteoside (purities  $\geq 98\%$ ) were purchased from Sunny Biotech Co., Ltd. (Shanghai). Acetonitrile, methanol and acetic acid of HPLC were purchased from Thermo Fisher Scientific Co., Ltd. (Shanghai). The ethanol of analytical grade was purchased from Yongsheng Fine Chemical Co., Ltd. (Tianjin). Ordered mesoporous carbon (CMK-3), disordered mesoporous carbon (DMC) and three-dimensional cubic ordered mesoporous carbon (CMK-8) were purchased from Xianfeng Nano Material Technology Co., Ltd. (Nanjing).

### Characterization

The morphology and microstructures of the prepared samples were investigated using Transmission electron microscopy (TEM, Tecnai G2 F20) operated at 200 KV. The TEM samples were prepared under ambient conditions by depositing droplets of the ethanol solution with the mesoporous materials onto carbon films supported by Cu grids. Generally, a light source with a shorter wavelength was selected to increase the resolution of the microscope, and the structure of the mesoporous carbons can be clearly observed. The surface functional groups were qualitatively measured by Fourier transform infrared spectroscopy (FT-IR, AVATAR360) using the interaction between infrared radiation and matter molecules. FT-IR use attenuated total reflection method test, the conditions was step size of  $2\text{ cm}^{-1}$  and scanning range was  $4,000\text{--}400\text{ cm}^{-1}$ . The physical structure data such as the specific surface area, pore size and pore volume of the mesoporous carbons calculated by Brunauer-Emmett-Teller (BET, ASAP 2460). The procedure for the adsorbent was as follows: mesoporous carbons were degassed at  $60^\circ\text{C}$  for 12 h, and the  $\text{N}_2$  adsorption-desorption curves were tested at  $-196^\circ\text{C}$  to calculate the specific surface area, pore size and pore volume of the mesoporous carbon. Thermo gravimetric analyzer (TGA, STA 449 F3) is an instrument that it uses the thermo gravimetric to detect the temperature-mass relationship of a substance, and TGA measures the mass of a substance as a function of temperature under program temperature control. TGA data was obtained using a TGA in the temperature ranging from 30 to  $800^\circ\text{C}$  at a heating rate of  $10^\circ\text{C}/\text{min}$  under air atmosphere.

### HPLC Analysis

The content of echinacoside and acteoside was detection by high performance liquid chromatography (HPLC, Waters Co., USA). The system included an autosampler, high pressure pump and ultraviolet (UV) detector. The analysis was conducted on a symmetry C18 column ( $100\text{\AA}$ ,  $5\text{ }\mu\text{m}$ ,  $4.6 \times 250\text{ mm}$ ). HPLC used gradient elution method to separate and detect samples. The volume of injection loop was  $10\text{ }\mu\text{m}$ , the column temperature was  $30^\circ\text{C}$ , detection wavelength of UV spectrophotometer was

330 nm, the flow rate was 1 ml/min and the mobile phase was (A) acetonitrile and (B) acetic acid/water (1:44, v/v).

## Adsorption Equilibrium

The optimization experiment of adsorption condition for CMK-3 has been carried out using a mixture of acteoside and enchanoside and under the optimal conditions, the crude extract of *Cistanche tubulosa* was carried out on adsorption cycle experiment and all adsorption experiments were repeatedly carried out at least 3. In the same batch of experiments, mesoporous carbons of CMK-8 and DMC were run in parallel with the CMK-3. The three kinds of mesoporous carbon (CMK-3, DMC and CMK-8) each 10 mg were added to the three bottles, respectively. Then 15 mL sample solution with initial concentration of  $C_0$  (mg/mL) was added to bottle. The bottle was placed in constant temperature shaker of 30°C for 24 h until the adsorption equilibrium was reached. Then 1 mL of adsorption solution was filtered through a 0.22  $\mu$ m filter and the equilibrium concentration  $C_e$  (mg/mL) of the sample solution was determined by HPLC.

## Desorption Experiment

Then the desorption experiment of mesoporous carbon were carried out. The adsorbed mesoporous carbon under 15 mL of methanol/acetic acid (9:1, v/v) mixed solution, which was placed in the water bath of ultrasonic for 1 h at 30°C. The obtained desorption solution was filtered by a 0.22 filter before analyzing by HPLC.

The adsorption capacity  $q_e$  (mg/ml) was evaluated as follows:

$$q_e = (C_0 - C_e) \cdot v/w \quad (1)$$

where  $V$  is the volume of the solution (mL) and  $W$  is the weight of the mesoporous carbons (g).

## RESULTS AND DISCUSSION

### Characterization

**Figure 1** showed a TEM of the three kinds of mesoporous carbons. DMC was a disordered porous network, CMK-8 was a network structure of three-dimensional porous, and CMK-3 was a clearly striped structure with ordered one-dimensional pore, which was similar to the reported results (Wang et al., 2006; Luo et al., 2010).

**Figure 2** showed the FT-IR spectrum of the mesoporous carbons (CMK-3, DMC, and CMK-8) and FT-IR spectrum before and after CMK-3 adsorption. It can be seen from in **Figure 2A** that the functional groups on the surfaces of the mesoporous carbons were mainly oxygen-containing groups. The overall shapes of the spectra for the three kinds of mesoporous carbons were similar. The mesoporous carbons showed a peak band at 3,423  $\text{cm}^{-1}$  referring to stretching vibration band of O-H. The bands in the region of 1,580 and 1,629  $\text{cm}^{-1}$  correspond to stretching vibrations of the carbonyl and carboxyl C=O. Additionally, the peak occurring at 1,384  $\text{cm}^{-1}$  was found to be stretching vibrations of alcoholic C-O and the tensile vibration at

2,922 and 2,852  $\text{cm}^{-1}$  are correspond to the C-H on methylene and methyl groups, respectively. This indicated that the oxygen-containing groups existing on the surfaces of the mesoporous carbons might lead to a weak chemical interaction between PhGs molecules and the mesoporous carbons.

**Figure 2B** shows the FT-IR spectra of CMK-3 before and after adsorption, acteoside and enchanoside. The characteristic peak at 1,697  $\text{cm}^{-1}$  derived from the C=C of olefin in acteoside and enchanoside, while the bands in the region of 1,519–1,423  $\text{cm}^{-1}$  corresponded to stretching vibration peak of the aromatic ring C=C in acteoside and enchanoside. The tensile vibration at the 1,604  $\text{cm}^{-1}$  was the C=O bond and the peak at 1,157  $\text{cm}^{-1}$  caused by the stretching vibration of the ether bond in acteoside and enchanoside. Compared with the FT-IR spectrum of CMK-3 before adsorption, the FT-IR spectrum of CMK-3 after adsorption appeared the new peaks, which belonged to the characteristic peak of acteoside and enchanoside.

The  $\text{N}_2$  adsorption-desorption isotherms was an important parameter for adsorption of PhGs on CMK-3 and comparison of adsorbent structure. **Figure 3** showed the  $\text{N}_2$  adsorption-desorption isotherms of CMK-3, CMK-8, DMC, and CMK-3 after PhGs adsorption, respectively. As can be seen from the **Figure 3**, the isotherm of the mesoporous carbons were similar to type-IV isotherm that this type of isotherm was predominantly mesoporous, in which the range of pore size was between 2 and 50 nm (Sanz Pérez et al., 2019). The gap between adsorption and desorption isotherm was referred to hysteresis loop that caused by capillary condensation reaction. For capillary condensation reactions, capillary condensation occurs first in the smallest pores (Barsotti et al., 2016). This shows that CMK-3 had a smaller mesopore than does DMC and CMK-8, which was consistent with the results of **Table 1**. The isotherm of CMK-3 exhibits an  $H_1$  hysteresis loop that was indicative of the rapid pore filling associated with capillary condensation and the pore structure of CMK-3 was reasonably orderly. The isotherm of DMC exhibits  $H_3$  hysteresis loop, this type of hysteresis had disordered pores due to network of pores that caused an undefined structure of porous adsorbent. CMK-8 isotherms exhibit an  $H_2$  hysteresis loop, indicating that pore structure was complicated and pore size distribution was uneven.

The  $\text{N}_2$  adsorption-desorption isotherms of CMK-3 was compared before and after adsorption of PhGs. The isotherm of the CMK-3 after adsorption was also similar to type-IV isotherm in **Figure 3B**. It indicated that the CMK-3 maintained their mesoporous structure after the adsorption. As can be seen from **Table 1**, the specific surface and pore volume of CMK-3 after adsorption exhibited a marked decrease, the specific surface area of CMK-3 before and after adsorption decreased from 1,098.02 to 227.75  $\text{m}^2/\text{g}$ , and the pore volume of that reduced from 1.32 to 0.42  $\text{cm}^3/\text{g}$ . It indicated that PhGs molecules were adsorbed on CMK-3.

**Table 1** summarized the BET specific surface area, pore volume and pore size of the four samples. The BET surface areas of CMK-3, DMC and CMK-8 were 1,098.02, 430.42, and 596.00  $\text{m}^2/\text{g}$  and the pores volume were 1.32, 0.70, and 0.85  $\text{m}^3/\text{g}$ , respectively. The pore size of CMK-3 was 4.31 nm, lower than that of CMK-8 (9.58 nm) and DMC (5.18 nm). It can be seen

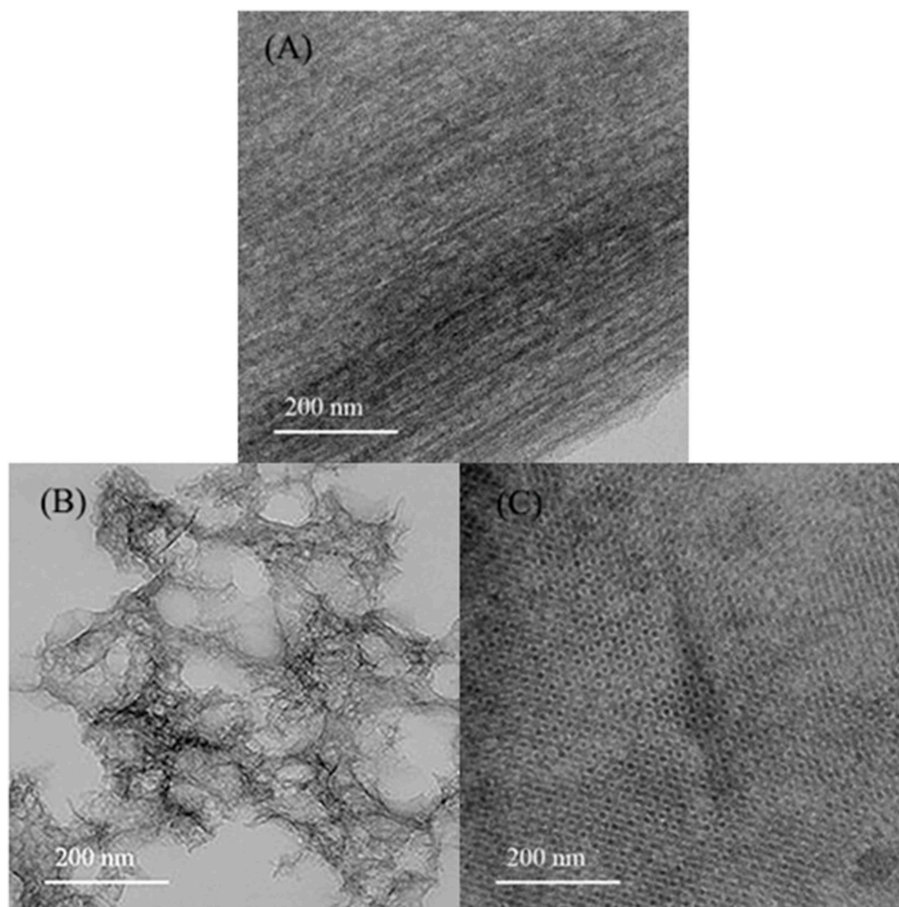


**FIGURE 1** | TEM of (A) CMK-3, (B) DMC, and (C) CMK-8.

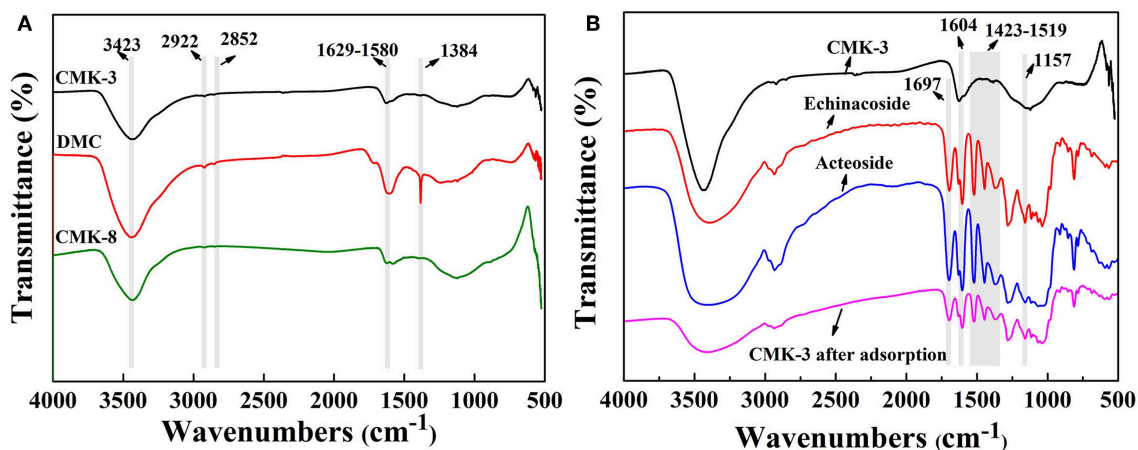


**FIGURE 2** | FT-IR spectra of (A) CMK-3, DMC, CMK-8, and (B) CMK-3 before and after adsorption, Echinacoside and Acteoside.

that the pore volume and specific surface area follows the order: CMK-3 > CMK-8 > DMC, while pore size follows the order: DMC > CMK-8 > CMK-3.

**Figure 4** shows the TGA curves of the three kinds of mesoporous carbons (CMK-3, CMK-8, and DMC). As can be seen from the **Figure 4**, the three kinds of mesoporous carbons

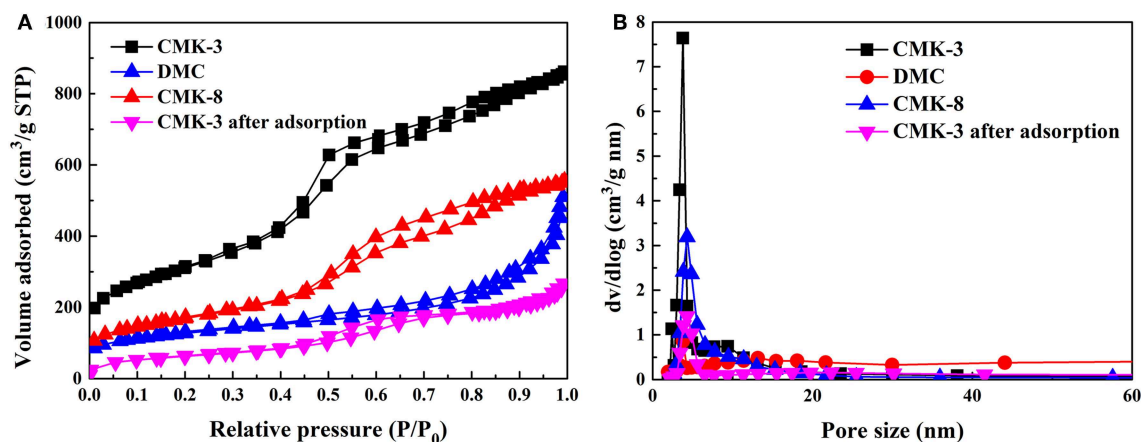


FIGURE 3 | (A)  $N_2$  adsorption-desorption isotherms and (B) Pore size distributions of the mesoporous carbons, and CMK-3 after adsorption.

TABLE 1 | BET characterization data of mesoporous carbons.

Mesoporous carbon	Hysteresis curve	Pore size (nm)	Pore volume (cm³/g)	Specific surface area (m²/g)
CMK-3	H <sub>1</sub>	4.31	1.32	1,098.02
DMC	H <sub>3</sub>	9.86	0.70	430.42
CMK-8	H <sub>2</sub>	5.18	0.85	596.00
CMK-3 after adsorption	H <sub>1</sub>	6.03	0.42	227.75

all have two distinct stages of mass loss: the first stage of mass loss was due to the evaporation of moisture in the mesoporous carbons before 100°C, the second mass loss stage of CMK-3, DMC and CMK-8 approximately occurs at 660, 427, and 615°C, respectively, which corresponds to the oxidative thermal decomposition of mesoporous carbons materials. It can be seen that the thermal decomposition temperature of CMK-3 was higher than CMK-3 and CMK-8, the thermal stability of CMK-3 was better than that of CMK-8 and DMC.

## Comparison of the Three Mesoporous Carbons Adsorption Performance

Because the three adsorbents are mainly composed of carbon, the adsorption interaction between PhGs and the mesoporous carbons was considered to be the same. Therefore, it was considered that the difference in adsorption performance was derived from the difference in the physical structure of mesoporous carbons. Table 2 shows the adsorption performance of the three kinds of mesoporous carbons. It can be seen from Table 2 that the three kinds of mesoporous carbons all can adsorb PhGs, and CMK-3 had the better adsorption performance than CMK-8 and DMC. This indicates that pore size of mesoporous carbons was larger than PhGs molecules, and pore size was not the main factor to affect the adsorption capacity for three mesoporous carbons. The adsorption capacity and desorption rates of CMK-3 were up to 189.37 mg/g and 94.96%, respectively. The adsorption capacity of CMK-3 was higher than that of

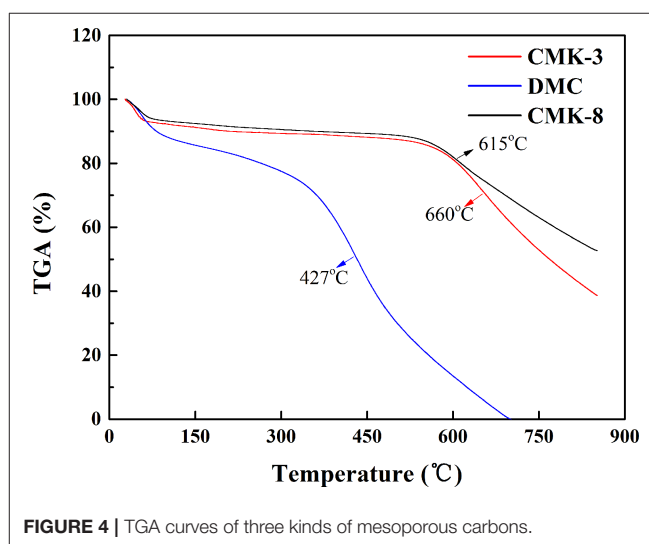


FIGURE 4 | TGA curves of three kinds of mesoporous carbons.

TABLE 2 | Adsorption performance of three kinds of mesoporous carbons.

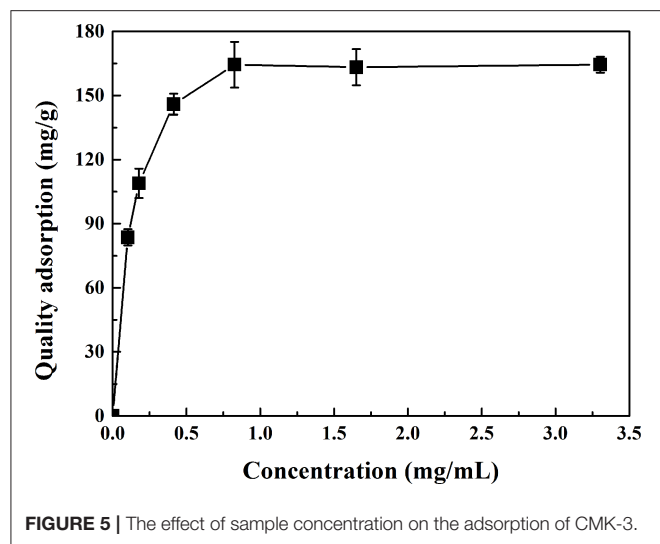
Mesoporous carbon	Adsorption quality (mg/g)	Desorption quality (mg/g)	Desorption rates (%)
CMK-3	189.37 ± 4.52	179.86 ± 3.36	94.98 ± 1.34
DMC	80.25 ± 2.60	74.05 ± 0.62	92.28 ± 0.77
CMK-8	135.75 ± 5.41	128.08 ± 3.18	94.35 ± 1.16

CMK-8. Because the pore volume and specific surface area of CMK-3 were larger than DMC and CMK-8, it indicated that the pore volume and specific surface area was main factor to affect the adsorption performance.

## Optimization of Adsorption Conditions

The optimization of adsorption experiment for CMK-3 has been carried out using a mix of both acteoside and enchanoside. Temperature, pH and concentration were the main influencing





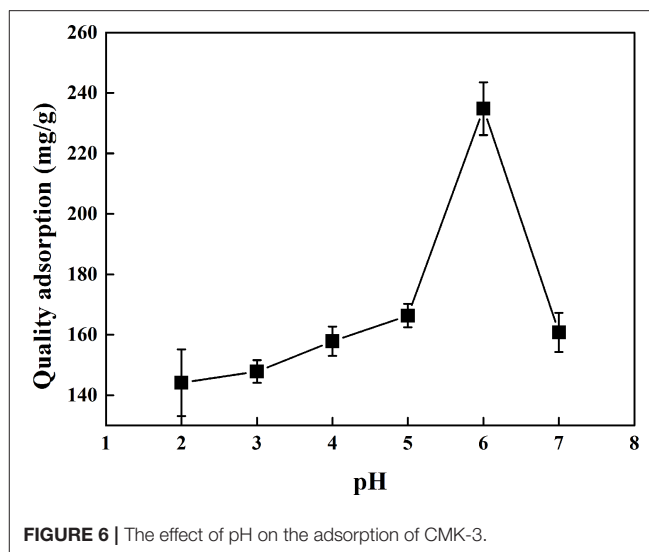
factors of CMK-3 adsorption performance. Thus, the effects of these three influencing factors on CMK-3 adsorption performance were investigated.

### Effect of Sample Concentration on Adsorption Performance of CMK-3

The effect of sample concentration on the adsorption performance of CMK-3 was shown in **Figure 5**. With the concentration increases, the capacity of adsorption increases. The adsorption capacity no longer increases with the increase of the sample concentration when the sample concentration was reached at 0.41 mg/g. At low initial concentration of sample, the adsorbent active sites were sufficient for adsorption of relatively small amount of PhGs molecules. In contrast, at high initial concentration of sample, the fixed amount of active sites on the adsorbents was not able to adsorption increasing amount of PhGs molecules. Thus, the adsorption capacity of CMK-3 for PhGs molecules tends to be balanced.

### Effect of pH on Adsorption Performance of CMK-3

**Figure 6** showed the effect of pH on the adsorption performance of CMK-3. It can be seen from **Figure 6** that the optimal pH value was 6 for adsorption of PhGs by CMK-3. The reasons as follows: PhGs had a large number of phenolic hydroxyl groups and belonged to the weak acidic molecules, the different pH values affected the ionization and stability of the PhGs molecules. The ionization of phenolic hydroxyl groups would be inhibited at low pH value, while the stability of phenolic hydroxyl groups on PhGs would decrease at high pH value. The inhibited ionization of phenolic hydroxyl groups on PhGs resulted in a decrease in the electrostatic interactions between PhGs and CMK-3, decreasing the adsorption performance of CMK-3 for PhGs. Thus, the optimum pH was 6 for CMK-3 adsorption.



### Effect of Temperature on Adsorption Performance of CMK-3

Temperature was an important parameter in the adsorption process. Temperature not only affects the diffusion of PhGs molecules at the external boundary layer interface, but also inside the adsorbent pores. **Figure 7** showed the effect of temperature on the adsorption capacity of CMK-3. The adsorption capacity of CMK-3 increase with temperature increased from 30 to 60°C. It has been reported the main reason was that the active site increases with increasing temperature due to endothermic nature of the process, and the intra-particle diffusion of the adsorbents increased with the increase of the adsorption temperature (Peng et al., 2015). In addition, the mobility of the PhGs molecules increased and their diffusion resistance decreased with increasing temperature. The adsorption capacity decreases with increasing temperature when the temperature was 60–80°C. It indicated that the adsorption temperature had an optimum value and PhGs molecules may be instability at high temperatures. Therefore, the optimum adsorption temperature was chosen to be 60°C.

The optimum adsorption conditions of CMK-3 were as follows: the sample concentration was 0.41 mg/g, solution pH was 6, and adsorption temperature was 60°C. Under optimal condition, the adsorption capacity of PhGs in crude extract on the CMK-3 was  $358.09 \pm 4.13$  mg/g, which was more than three times the adsorption capacity of PhGs on macroporous resins (HPD300, 94.93 mg/g) (Liu et al., 2013). Meanwhile, desorption rate of CMK-3 was 94.67% higher than that of macroporous resin.

### Adsorption Isotherms

The adsorption isotherms were shown in **Figure 8A**. With the increase of equilibrium concentration, the adsorption capacity for PhGs increased and reached saturation status. To further understand the adsorption performance of PhGs on CMK-3, the adsorption isotherms of CMK-3 were investigated using Langmuir and Freundlich models. The parameters of

adsorption was obtained from different models provide some useful information on the adsorption mechanisms. **Figures 8B,C** depicted the CMK-3 adsorption isotherms that modeled by Langmuir and Freundlich model.

The Langmuir model was based on the assumptions that adsorption takes place at specific homogeneous sites within the adsorbent, no significant interaction occurs among adsorbed species, and the adsorbent was saturated after one layer of

adsorbent molecules forms on the adsorbent surface. The linearized Langmuir isotherm equation can be written as follows:

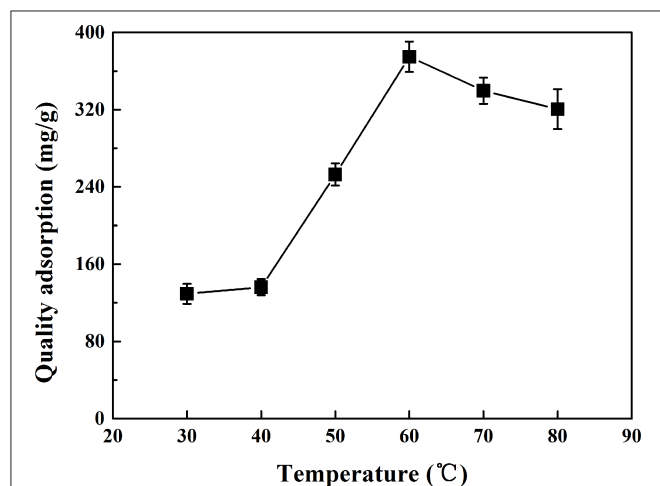
$$\frac{c_e}{q_e} = \frac{1}{K_L q_m} + \frac{c_e}{q_m} \quad (2)$$

The Freundlich model was commonly used to describe the adsorption characteristics of multilayer and heterogeneous surfaces (Wu et al., 2017). Its linearized form is given as follows:

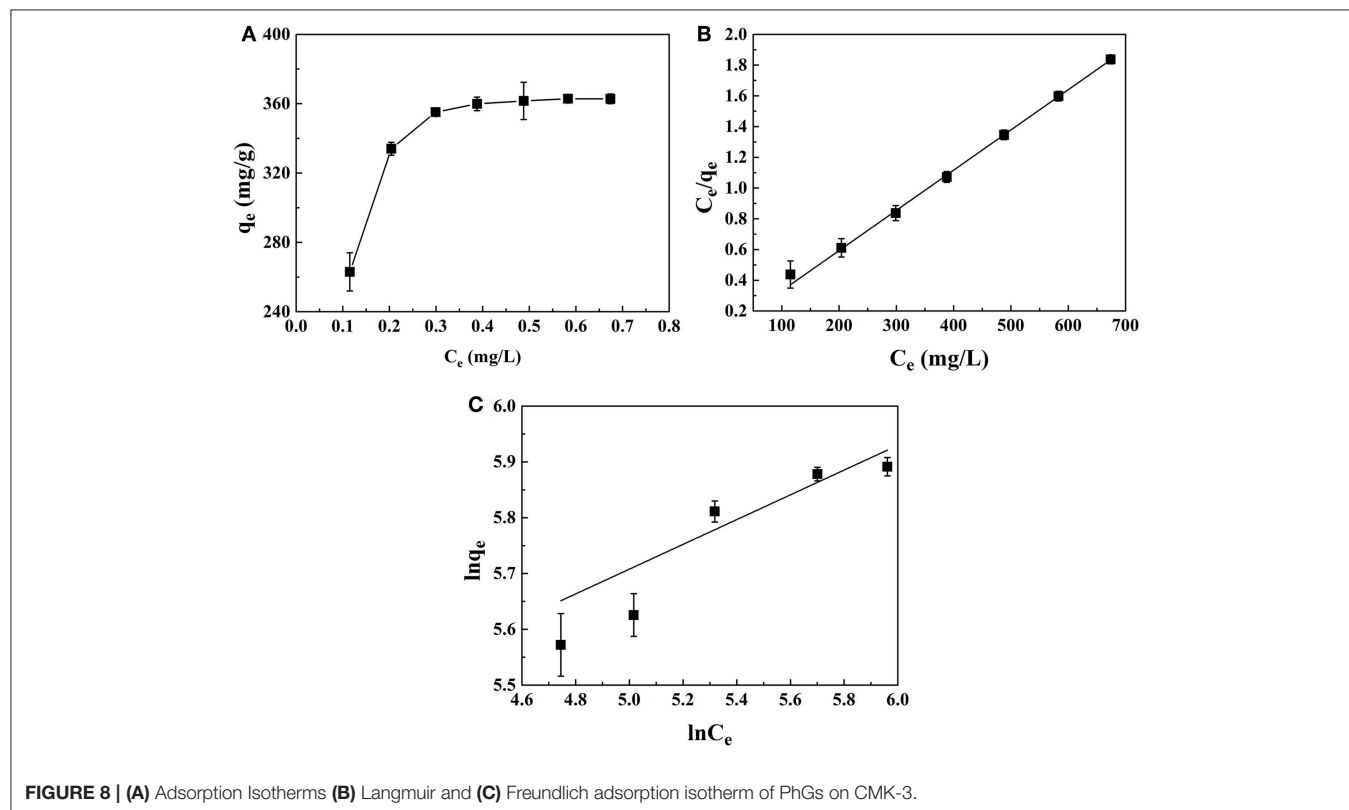
$$\ln q_e = \ln K_F + \frac{1}{n} \ln c_e \quad (3)$$

where  $q_m$  (mg/g) is the theoretical maximum monolayer adsorption capacity,  $K_L$  (mL/mg) is the Langmuir constant related to the adsorption energy reflecting the affinity between the adsorbate and adsorbent (Wu et al., 2017; He et al., 2019),  $K_F$  [(mg/g)•(mL/mg)<sup>1/n</sup>] and  $n$  are the Freundlich constants.  $K_F$  is an indicator of the relative adsorption capacity,  $n$  is related to the magnitude of the adsorption driving force and heterogeneity of the binding sites, and  $1/n$  indicates the favorability of the adsorption.

The parameters of the isotherm models were summarized in **Table 3**. The Langmuir model was more better than the Freundlich model for describing the adsorption data of PhGs on CMK-3, which indicated that the adsorption of the PhGs on the CMK-3 was a simple monolayer adsorption process (Wang F. et al., 2017). In addition, the presence of oxygen-containing



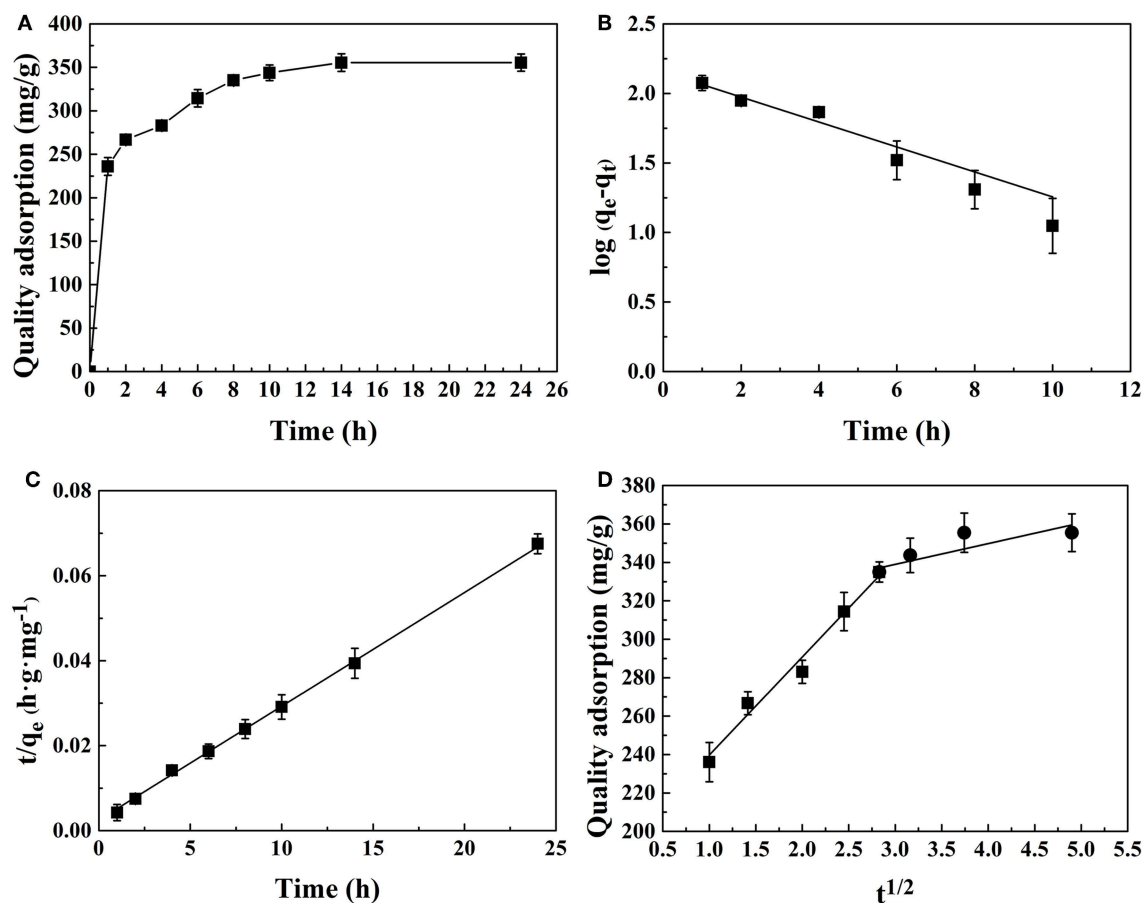
**FIGURE 7 |** The effect of temperature on the adsorption of CMK-3.



**FIGURE 8 |** (A) Adsorption Isotherms (B) Langmuir and (C) Freundlich adsorption isotherm of PhGs on CMK-3.

**TABLE 3** | Model parameters for adsorption of PhGs on CMK-3.

Langmuir adsorption isotherm ( $n = 5$ )			Freundlich adsorption isotherm ( $n = 5$ )		
$K_L$	$q_e(\text{mg/g})$	$R^2$	$K_F$	$1/n$	$R^2$
$0.038 \pm 0.025$	$380.70 \pm 16.23$	$0.999 \pm 0.005$	$99.32 \pm 20.46$	$0.22 \pm 0.074$	$0.737 \pm 0.086$

**FIGURE 9** | Adsorption kinetic models of PhGs onto CMK-3: (A) Adsorption kinetics of CMK-3 (B) pseudo-first-order, (C) pseudo-second-order, and (D) intra-particle diffusion model.

functional groups on the surface of CMK-3 enhanced the adsorption of PhGs. The maximum adsorption amount ( $q_m$ ) can reach 380.70 mg/g that was similar to the experimental value. In addition, the  $1/n$  value of PhGs was calculated to be 0.22, which was  $<0.5$ . It indicated that the adsorption of the PhGs on the CMK-3 could take place easily (Fu et al., 2007; Gan et al., 2018). This indicated that the adsorption of PhGs on CMK-3 was not completely a physical adsorption process. PhGs contain multiple hydroxyl groups which might form hydrogen bonds with the oxygen-containing functional groups on the CMK-3 and offer weak chemical adsorption for the adsorption. Therefore, CMK-3 adsorption of PhGs was a complex adsorption process combining physical adsorption with chemisorption.

## Adsorption Kinetics

CMK-3 adsorption capacities were investigated as a function of time to determine the adsorption equilibrium time in Figure 9A. The investigation shows that the equilibrium adsorption rate gradually decreases and gradually leveled off as the adsorption capacity approaches equilibrium. It was found that the adsorption equilibrium was reached after 14 h. The rapid initial adsorption rate could be due to the high concentration gradient between the PhGs and CMK-3 in the solution and the surface of CMK-3 had large availability of active sites.

Adsorption kinetics was evaluated by the application of the pseudo-first-order, pseudo-second-order and intra-particle diffusion models. The

**TABLE 4** | Parameters for the kinetic model of PhGs on CMK-3.

Pseudo-first-order model ( <i>n</i> = 5)			Pseudo-second-order model ( <i>n</i> = 5)		
<i>K</i> <sub>1</sub>	<i>q</i> <sub>m</sub> (mg/g)	<i>R</i> <sup>2</sup>	<i>K</i> <sub>2</sub>	<i>q</i> <sub>m</sub> (mg/g)	<i>R</i> <sup>2</sup>
0.090 ± 0.043	8.614 ± 3.62	0.84 ± 0.006	0.003 ± 0.001	373.13 ± 12.26	0.998 ± 0.005

plotted graphs of pseudo-first-order, pseudo-second-order models, and intra-particle diffusion model for adsorption PhGs onto CMK-3 were shown in **Figures 9B–D**, respectively.

The linear form of the kinetics models are expressed as follows:

Pseudo-first-order (Li et al., 2017a):

$$\log(q_e - q_t) = \log q_e - \frac{K_1}{2.303} t \quad (4)$$

Pseudo-second-order (Tang et al., 2018):

$$\frac{t}{q_t} = \frac{1}{K_2 q_e^2} + \frac{t}{q_t} \quad (5)$$

where *K*<sub>1</sub> (1/min) and *K*<sub>2</sub> (g/mg·min<sup>−1</sup>) are the rate constants of pseudo-first order rate equation and pseudo-second order rate equation, respectively. *q*<sub>e</sub> (mg/g) is the theoretical adsorption capacity at equilibrium.

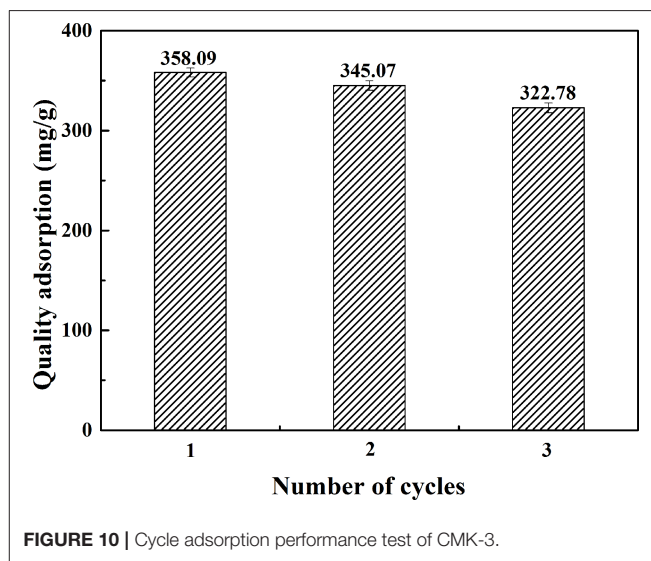
Intra-particle diffusion model:

$$q_t = K_p t^{\frac{1}{2}} + C \quad (6)$$

where *K*<sub>p</sub> is the intra-particle diffusion constant (mg/g min) and *C* is the reflection of boundary layer effect (mg/g).

The calculated values of *q*<sub>e</sub>, rate constants and correlation coefficient are shown in **Table 4**. The pseudo-second-order model gave an *R*<sup>2</sup> value of 0.998, while *R*<sup>2</sup> value of pseudo-first-order model was 0.84. It implies that the pseudo-second-order model exhibits better linear relationship than the pseudo-first-order model. **Figure 9C** shows that the linear plots of *t/q*<sub>e</sub> vs. *t* show good agreement with the experimental data from the pseudo-second-order model. The calculated *q*<sub>e</sub> of pseudo-second-order was quite similar to experimental data (**Table 4**). These results indicated that pseudo-second-order was more suitable kinetics model than pseudo-first-order.

However, the evaluation results of the pseudo-second-order model cannot determine the potential adsorption mechanism. It was generally accepted that adsorption kinetics was controlled by the diffusion mechanism, which consists external diffusion, boundary layer diffusion and intra-particle diffusion (Wong et al., 2019). The intra-particle diffusion model was used to determine if intra-particle diffusion were the rate-limiting steps.

**FIGURE 10** | Cycle adsorption performance test of CMK-3.

The intra-particle diffusion was said to be the rate limiting step when the *q*<sub>t</sub> vs. *t*<sup>1/2</sup> was linear. The intra-particle diffusion was only rate controlling step when the curve passes through the origin. It can be seen from **Figure 9D**, the intra-particle diffusion was governed by two different stages. The first stage of the curve represents surface adsorption. The second stage indicates intra-particle diffusion in the CMK-3 pores. As the intra-particle diffusion plot did not pass through the origin, the model indicated that the adsorption mechanism was more than one mechanism and intra-particle diffusion was not the only rate-limiting step. Thus, it can be concluded that the mechanism of PhGs adsorption on CMK-3 was complex that both the external surface adsorption and intra-particle diffusion occurred simultaneously.

## Repetitive Experiment

Reusability was an important factor for considering the use and value of adsorbents in practical applications. Therefore, the cyclic adsorption performance of CMK-3 for the crude extract was tested. **Figure 10** showed the results of cyclic adsorption of CMK-3 for crude extract of *Cistanche tubulosa*. It can be observed from the **Figure 10** that the adsorption capacity of CMK-3 changed from 358.09 ± 4.13 mg/g to 320.78 ± 5.62 mg/g after three cycles of adsorption, which indicated the CMK-3 had good repeatability, and CMK-3 can be repeatedly used to adsorb PhGs.

## CONCLUSIONS

The adsorption properties of PhGs on the three kinds of mesoporous carbons were investigated and the mesoporous carbon before and after adsorption were characterized. The results showed that CMK-3 had a largest specific surface area and pore volume among the three adsorbents (CMK-3, DMC, and CMK-8), and it can adsorb PhGs molecules more effective than DMC and CMK-8 from the extracts of *Cistanche tubulosa*. Because the oxygen-containing functional groups on the surface of CMK-3 can provide a large number of active adsorption sites for the PhGs molecules. In addition, hydrogen bonds were formed between hydroxyl groups of PhGs and the oxygen-containing functional groups of CMK-3. The adsorption capacity of crude extract for PhGs was  $358.09 \pm 4.13$  mg/g at the optimal conditions of 0.41 mg/L, pH = 6 and 60°C, and the corresponding desorption rate of CMK-3 was 95.02%. The adsorption data exhibited that adsorption of PhGs closely followed the Langmuir model and pseudo-second-order models, the intra-particle diffusion model suggested that the rate-limiting steps of adsorption were intra-particle diffusion model. The CMK-3 can be used as a potential adsorbent to highly efficient adsorb PhGs from *Cistanche tubulosa*.

## REFERENCES

- Aiello, N., Carlini, A., Scartezzini, F., Fusani, P., Berto, C., and Dall'Acqua, S. (2015). Harvest in different years of growth influences chemical composition of *Echinacea angustifolia* roots. *Ind. Crops Prod.* 76, 1164–1168. doi: 10.1016/j.indcrop.2015.08.029
- Barsotti, E., Tan, S. P., Saraji, S., Piri, M., and Chen, J. H. (2016). A review on capillary condensation in nanoporous media: implications for hydrocarbon recovery from tight reservoirs. *Fuel* 184, 344–361. doi: 10.1016/j.fuel.2016.06.123
- Cui, Q., Pan, Y., Zhang, W., Zhang, Y., Ren, S., Wang, D., et al. (2018). Metabolites of dietary acteoside: profiles, isolation, identification, and hepatoprotective capacities. *J. Agric. Food Chem.* 66, 2660–2668. doi: 10.1021/acs.jafc.7b04650
- Fu, Y., Zu, Y., Liu, W., Hou, C., Chen, L., Li, S., et al. (2007). Preparative separation of vitexin and isovitexin from pigeonpea extracts with macroporous resins. *J. Chromatogr. A* 1139, 206–213. doi: 10.1016/j.chroma.2006.11.015
- Gan, Q., Shi, W., Xing, Y., and Hou, Y. (2018). A polyoxoniobate/g-C<sub>3</sub>N<sub>4</sub> nanoporous material with high adsorption capacity of methylene blue from aqueous solution. *Front. Chem.* 6:7. doi: 10.3389/fchem.2018.00007
- Gu, C. M., Yang, X. Y., and Huang, L. F. (2016). Cistanches herba: a neuropharmacology review. *Front. Pharmacol.* 7:289. doi: 10.3389/fphar.2016.00289
- He, P. Y., Zhu, H. J., Ma, Y., Liu, N., Niu, X. H., Wei, M. B., et al. (2019). Rational design and fabrication of surface molecularly imprinted polymers based on multi-boronic acid sites for selective capture glycoproteins. *Chem. Eng. J.* 367, 55–63. doi: 10.1016/j.cej.2019.02.140
- Kong, D. B., Zheng, X. Y., Tao, Y., Lv, W., Gao, Y., Zhi, L., et al. (2016). Porous graphene oxide-based carbon artefact with high capacity for methylene blue adsorption. *Adsorption* 22, 1043–1050. doi: 10.1007/s10450-016-9798-5
- Konggidinata, M. I., Chao, B., Lian, Q., Subramaniam, R., Zappi, M., and Gang, D. D. (2017). Equilibrium, kinetic and thermodynamic studies for adsorption of BTEx onto ordered mesoporous carbon (OMC). *J. Hazard. Mater.* 336, 249–259. doi: 10.1016/j.jhazmat.2017.04.073
- Li, X., Cheng, Y., Zhang, H., Wang, S., Jiang, Z., Guo, R., et al. (2015a). Efficient CO<sub>2</sub> capture by functionalized graphene oxide nanosheets as fillers to fabricate

## DATA AVAILABILITY STATEMENT

All datasets generated for this study are included in the article/supplementary material.

## AUTHOR CONTRIBUTIONS

HX carried out all the experiments, did data collection, data analysis, and wrote the manuscript. WP helped to analyze the FT-IR data and did data collection. XL helped to explain some of the experimental results and revise the manuscript. JZ contributed to the scientific interpretation of results and revised the manuscript.

## FUNDING

We gratefully acknowledge the support from the National Natural Science Foundation for Young Scientists of China (Grant No. 21706166), the Program for Young Innovative Talents of Shihezi University (CXRC201802), the Program for Changjiang Scholars and Innovative Research Team in University (Grant No. IRT\_15R46), and Yangtze River scholar research project of Shihezi University (Grant No. CJXZ201601).

- multi-permselective mixed matrix membranes. *ACS Appl. Mater. Inter.* 7, 5528–5537. doi: 10.1021/acsami.5b00106
- Li, X., Hou, J., Guo, R., Wang, Z., and Zhang, J. (2019). Constructing unique cross-sectional structured mixed matrix membranes by incorporating ultrathin microporous nanosheets for efficient CO<sub>2</sub> separation. *ACS Appl. Mater. Inter.* 11, 24618–24626. doi: 10.1021/acsami.9b07815
- Li, X., Ma, L., Zhang, H., Wang, S., Jiang, Z., Guo, R., et al. (2015b). Synergistic effect of combining carbon nanotubes and graphene oxide in mixed matrix membranes for efficient CO<sub>2</sub> separation. *J. Membr. Sci.* 479, 1–10. doi: 10.1016/j.memsci.2015.01.014
- Li, Y., Peng, Y., Ma, P., Yang, H., Xiong, H., Wang, M., et al. (2018a). Antidepressant-like effects of Cistanche tubulosa extract on chronic unpredictable stress rats through restoration of gut microbiota homeostasis. *Front. Pharmacol.* 9:967. doi: 10.3389/fphar.2018.00967
- Li, Y., Peng, Y., Wang, M., Tu, P., and Li, X. (2017b). Human gastrointestinal metabolism of the Cistanches herba water extract *in vitro*: elucidation of the metabolic profile based on comprehensive metabolite identification in gastric juice, intestinal juice, human intestinal bacteria, and intestinal microsomes. *J. Agr. Food Chem.* 65, 7447–7456. doi: 10.1021/acs.jafc.7b02829
- Li, Y., Tang, S., Bao, Y., Shan, S., Yang, R., Mao, J., et al. (2017a). Adsorption of three flavonoids from aqueous solutions onto mesoporous carbon. *J. Chem. Eng. Data* 62, 3178–3186. doi: 10.1021/acs.jced.7b00268
- Li, Y., Xu, L., Bao, Y., Cheng, M., Wang, H., Shan, S., et al. (2018b). Hydrothermal synthesis of mesoporous carbons for adsorption of two alkaloids. *J. Porous Mat.* 25, 95–105. doi: 10.1007/s10934-017-0423-0
- Li, Z., Lin, H., Gu, L., Gao, J., and Tzeng, C. M. (2016). Herba Cistanche (Rou Cong-Rong): one of the best pharmaceutical gifts of traditional Chinese medicine. *Front. Pharmacol.* 7:41. doi: 10.3389/fphar.2016.00041
- Liao, P. L., Li, C. H., Tse, L. S., Kang, J. J., and Cheng, Y. W. (2018). Safety assessment of the Cistanche tubulosa health food product memoregain®: genotoxicity and 28-day repeated dose toxicity test. *Food Chem. Toxicol.* 118, 581–588. doi: 10.1016/j.fct.2018.06.012
- Liu, B., Dong, B., Yuan, X., Kuang, Q., Zhao, Q., Yang, M., et al. (2016). Enrichment and separation of chlorogenic acid from the extract of eupatorium adenophorum spreng by macroporous resin. *J. Chromatogr. B* 1008, 58–64. doi: 10.1016/j.jchromb.2015.10.026



- Liu, B., Ouyang, J., Yuan, X., Wang, L., and Zhao, B. (2013). Adsorption properties and preparative separation of phenylethanoid glycosides from *Cistanche deserticola* by use of macroporous resins. *J. Chromatogr. B* 937, 84–90. doi: 10.1016/j.jchromb.2013.08.018
- Luo, H., Peng, M., Ye, H., Chen, L., Peng, A., Tang, M., et al. (2010). Predictable and linear scale-up of four phenolic alkaloids separation from the roots of *menispermum dauricum* using high-performance counter-current chromatography. *J. Chromatogr. B* 878, 1929–1933. doi: 10.1016/j.jchromb.2010.05.002
- Pei, W., Guo, R., Zhang, J., and Li, X. (2019). Extraction of phenylethanoid glycosides from *Cistanche tubulosa* by high-speed shearing homogenization extraction. *J. AOAC Int.* 102, 63–68. doi: 10.5740/jaoacint.18-0039
- Peng, X., Hu, F., Lam, F. L. Y., Wang, Y., Liu, Z., and Dai, H. (2015). Adsorption behavior and mechanisms of ciprofloxacin from aqueous solution by ordered mesoporous carbon and bamboo-based carbon. *J. Colloid Interface Sci.* 460, 349–360. doi: 10.1016/j.jcis.2015.08.050
- Qin, G., Ma, J., Wei, W., Li, J., and Yue, F. (2018). The enrichment of chlorogenic acid from *eucommia ulmoides* leaves extract by mesoporous carbons. *J. Chromatogr. B* 1087–1088, 6–13. doi: 10.1016/j.jchromb.2018.04.036
- Sanz Pérez, E. S., Rodríguez Jardón, L., Arencibia, A., Sanz, R., Iglesias, M., and Maya, E. M. (2019). Bromine pre-functionalized porous polyphenylenes: new platforms for one-step grafting and applications in reversible CO<sub>2</sub> capture. *J. CO<sub>2</sub> Util.* 30, 183–192. doi: 10.1016/j.jcou.2019.02.005
- Shiao, Y. J., Su, M. H., Lin, H. C., and Wu, C. R. (2017). Echinacoside ameliorates the memory impairment and cholinergic deficit induced by amyloid beta peptides via the inhibition of amyloid deposition and toxicology. *Food Funct.* 8, 2283–2294. doi: 10.1039/C7FO00267J
- Shimada, H., Urabe, Y., Okamoto, Y., Li, Z., Kawase, A., Morikawa, T., et al. (2017). Major constituents of *Cistanche tubulosa*, echinacoside and acteoside, inhibit sodium-dependent glucose cotransporter 1-mediated glucose uptake by intestinal epithelial cells. *J. Funct. Foods* 39, 91–95. doi: 10.1016/j.jff.2017.10.013
- Song, Y., Song, Q., Li, J., Zhang, N., Zhao, Y., Liu, X., et al. (2016). An integrated strategy to quantitatively differentiate chemome between *Cistanche deserticola* and *C. tubulosa* using high performance liquid chromatography–hybrid triple quadrupole-linear ion trap mass spectrometry. *J. Chromatogr. A* 1429, 238–247. doi: 10.1016/j.chroma.2015.12.045
- Tang, Q., Duan, T., Li, P., Zhang, P., and Wu, D. (2018). Enhanced defluorination capacity from aqueous media via hydroxyapatite decorated with carbon nanotube. *Front. Chem.* 6:104. doi: 10.3389/fchem.2018.00104
- Tian, Y., Zhong, S., Zhu, X., Huang, A., Chen, Y., and Wang, X. (2015). Mesoporous carbon spheres: synthesis, surface modification and neutral red adsorption. *Mater. Lett.* 161, 656–660. doi: 10.1016/j.matlet.2015.09.055
- Wang, F., Zhu, Y., Wang, W., Zong, L., Lu, T., and Wang, A. (2017). Fabrication of CMC-g-PAM superporous polymer monoliths via eco-friendly pickering-MIPs for superior adsorption of methyl violet and methylene blue. *Front. Chem.* 5:33. doi: 10.3389/fchem.2017.00033
- Wang, H., Lam, F. L. Y., Hu, X., and Ng, K. M. (2006). Ordered mesoporous carbon as an efficient and reversible adsorbent for the adsorption of fullerenes. *Langmuir* 22, 4583–4588. doi: 10.1021/la052615l
- Wang, S., Li, X., Wu, H., Tian, Z., Xin, Q., He, G., et al. (2016). Advances in high permeability polymer-based membrane materials for CO<sub>2</sub> separations. *Energy Environ. Sci.* 9, 1863–1890. doi: 10.1039/C6EE00811A
- Wang, T., Chen, C., Yang, M., Deng, B., Kirby, G. M., and Zhang, X. (2016). *Cistanche tubulosa* ethanol extract mediates rat sex hormone levels by induction of testicular steroidogenic enzymes. *Pharm. Biol.* 54, 481–487. doi: 10.3109/13880209.2015.1050114
- Wang, X., Wang, X., and Guo, Y. (2017). Rapidly simultaneous determination of six effective components in *Cistanche tubulosa* by near infrared spectroscopy. *Molecules* 22:843. doi: 10.3390/molecules22050843
- Wang, X. Y., Xu, R., Chen, J., Song, J. Y., Newmaster, S. G., Han, J. P., et al. (2018). Detection of *Cistanche herba* (Rou Cong Rong) medicinal products using species-specific nucleotide signatures. *Front. Plant Sci.* 9:1643. doi: 10.3389/fpls.2018.01643
- Wong, S., Tumari, H. H., Ngadi, N., Mohamed, N. B., Hassan, O., Mat, R., et al. (2019). Adsorption of anionic dyes on spent tea leaves modified with polyethyleneimine (PEI-STL). *J. Clean. Prod.* 206, 394–406. doi: 10.1016/j.jclepro.2018.09.201
- Wu, C., Chien, M., Lin, N., Lin, Y., Chen, W., Chen, C., et al. (2019). Echinacoside isolated from *Cistanche tubulosa* putatively stimulates growth hormone secretion via activation of the ghrelin receptor. *Molecules* 24:E720. doi: 10.3390/molecules24040720
- Wu, M. R., Lin, C. H., Ho, J. D., Hsiao, G., and Cheng, Y. W. (2018). Novel protective effects of *Cistanche tubulosa* extract against low-luminance blue light-induced degenerative retinopathy. *Cell. Physiol. Biochem.* 51, 63–79. doi: 10.1159/000495162
- Wu, Y., Ma, Y., Pan, J., Gu, R., and Luo, J. (2017). Porous and magnetic molecularly imprinted polymers via pickering high internal phase emulsions polymerization for selective adsorption of  $\lambda$ -cyhalothrin. *Front. Chem.* 5:18. doi: 10.3389/fchem.2017.00018
- Yan, Y., Song, Q., Chen, X., Li, J., Li, P., Wang, Y., et al. (2017). Simultaneous determination of components with wide polarity and content ranges in *Cistanche tubulosa* using serially coupled reverse phase-hydrophilic interaction chromatography–tandem mass spectrometry. *J. Chromatogr. A* 1501, 39–50. doi: 10.1016/j.chroma.2017.04.034
- You, S. P., Ma, L., Zhao, J., Zhang, S. L., and Liu, T. (2016). Phenylethanoid glycosides from *Cistanche tubulosa* suppress hepatic stellate cell activation and block the conduction of signaling pathways in TGF- $\beta$ 1/smad as potential anti-hepatic fibrosis agents. *Molecules* 21:102. doi: 10.3390/molecules21010102
- Zhang, H., Dai, B., Wang, X., Li, W., Han, Y., Gu, J., et al. (2013). Non-mercury catalytic acetylene hydrochlorination over bimetallic Au–Co(III)/SAC catalysts for vinyl chloride monomer production. *Green Chem.* 15:829. doi: 10.1039/c3gc36840h
- Zhang, H., Guo, R., Hou, J., Wei, Z., and Li, X. (2016). Mixed-matrix membranes containing carbon nanotubes composite with hydrogel for efficient CO<sub>2</sub> separation. *ACS Appl. Mater. Inter.* 8, 29044–29051. doi: 10.1021/acsami.6b09786
- Zhang, H., Guo, R., Zhang, J., and Li, X. (2018a). Facilitating CO<sub>2</sub> transport across mixed matrix membranes containing multifunctional nanocapsules. *ACS Appl. Mater. Inter.* 10, 43031–43039. doi: 10.1021/acsami.8b15269
- Zhang, H., Tian, H., Zhang, J., Guo, R., and Li, X. (2018b). Facilitated transport membranes with an amino acid salt for highly efficient CO<sub>2</sub> separation. *Int. J. Greenh. Gas Con.* 78, 85–93. doi: 10.1016/j.ijggc.2018.07.014
- Zhang, W., Huang, J., Wang, W., Li, Q., Chen, Y., Feng, W., et al. (2016). Extraction, purification, characterization and antioxidant activities of polysaccharides from *Cistanche tubulosa*. *Int. J. Biol. Macromol.* 93, 448–458. doi: 10.1016/j.ijbiomac.2016.08.079
- Zhou, J. G., Wang, Y. F., Wang, J. T., Qiao, W. M., Long, D. H., and Ling, L. C. (2016). Effective removal of hexavalent chromium from aqueous solutions by adsorption on mesoporous carbon microspheres. *J. Colloid Interf. Sci.* 462, 200–207. doi: 10.1016/j.jcis.2015.10.001

**Conflict of Interest:** The authors declare that the research was conducted in the absence of any commercial or financial relationships that could be construed as a potential conflict of interest.

Copyright © 2019 Xu, Pei, Li and Zhang. This is an open-access article distributed under the terms of the Creative Commons Attribution License (CC BY). The use, distribution or reproduction in other forums is permitted, provided the original author(s) and the copyright owner(s) are credited and that the original publication in this journal is cited, in accordance with accepted academic practice. No use, distribution or reproduction is permitted which does not comply with these terms.



# Selective Adsorption and Purification of the Acteoside in *Cistanche tubulosa* by Molecularly Imprinted Polymers

Xiaobin Zhao, Wenjing Pei, Ruili Guo and Xueqin Li\*

Key Laboratory for Green Processing of Chemical Engineering of Xinjiang Bingtuan, School of Chemistry and Chemical Engineering, Shihezi University, Shihezi, China

## OPEN ACCESS

### Edited by:

Mauricio A. Rostagno,  
Campinas State University, Brazil

### Reviewed by:

Mohammad Boshir Ahmed,  
Gwangju Institute of Science and  
Technology, South Korea  
Piotr Lulinski,  
Medical University of Warsaw, Poland

### \*Correspondence:

Xueqin Li  
lixueqin861003@163.com

### Specialty section:

This article was submitted to  
Green and Sustainable Chemistry,  
a section of the journal  
Frontiers in Chemistry

**Received:** 02 September 2019

**Accepted:** 13 December 2019

**Published:** 23 January 2020

### Citation:

Zhao X, Pei W, Guo R and Li X (2020)  
Selective Adsorption and Purification  
of the Acteoside in *Cistanche tubulosa*  
by Molecularly Imprinted Polymers.  
Front. Chem. 7:903.  
doi: 10.3389/fchem.2019.00903

Acteoside (ACT) is the main component of phenylethanoid glycosides in *Cistanche tubulosa*, and it is extremely desirable for obtaining high purification of ACT by molecularly imprinted polymers (MIPs) from their extracts. In this study, MIPs were designed and synthesized to adsorb selectively the ACT in *C. tubulosa*. The effects of different functional monomers, cross-linkers, and solvents of MIPs were investigated. MIPs were studied in terms of static adsorption experiments, dynamic adsorption experiments, and selectivity experiments. The optimal functional monomer, cross-linking agent, and solvent are 4-vinylpyridine, ethylene glycol dimethylacrylate, and the mixed solvent (acetonitrile and *N,N*-dimethylformamide, 1:1.5, v/v), respectively. Under the optimal conditions, the synthesized MIP1 has a high adsorption performance for ACT. The adsorption capacity of MIP1 to ACT reached 112.60 mg/g, and the separation factor of ACT/echinacoside was 4.68. Because the molecularly imprinted cavities of MIP1 resulted from template molecules of ACT, it enables MIP1 to recognize selectively ACT. Moreover, the N–H groups on MIP1 can form hydrogen bonds with the hydroxyl groups on the ACT; this improves the separation factor of MIP1. The dynamic adsorption of ACT accorded with the quasi-second-order kinetics; it indicated that the adsorption process of MIP1 is the process of chemical adsorption to ACT. MIPs can be applied as a potential adsorption material to purify the active ingredients of herbal medicines.

**Keywords:** molecularly imprinted polymer, *Cistanche tubulosa*, acteoside, adsorption, hydrogen bond

## INTRODUCTION

*Cistanche tubulosa* is one of the valuable Chinese herbal remedies (Li et al., 2016; Morikawa et al., 2019). The crude extract of *C. tubulosa* mainly contains phenylethanoid glycosides, polysaccharides, oligosaccharides, flavonoids, polyphenols, and proteins, among which phenylethanoid glycosides are the most effective components of *C. tubulosa* (Wang et al., 2015, 2017; Yan et al., 2017). Studies have shown that phenylethanoid glycoside compounds have the effects of tonifying kidney Yang, anti-oxidation, anti-tumor, anti-aging, enhancing memory, etc. Phenylethanoid glycosides have a wide range of applications in medicine, health care, food, and so on (Yang et al., 2017; Fu et al., 2018; Wu et al., 2019; Xu et al., 2019). In order to obtain high-purity products, the highly selective separation of the target substance is the key to the problem. Therefore, it is of great significance to design and develop a purification method with good selectivity, high

efficiency, energy saving, and environmental friendliness for the development and utilization of *C. tubulosa*.

Phenylethanoid glycosides are the most important pharmacological active ingredients in *C. tubulosa*, including echinacoside (ECH), acteoside (ACT), isomeric, and 2-acetyl *C. tubulosa* glycosides. ECH and ACT are the main components of phenylethanoid glycosides, with content up to 90%. At present, the research of *C. tubulosa* mainly focuses on its pharmacological components. The separation and purification methods mainly include macroporous adsorption resin, high-speed countercurrent chromatography, membrane separation, and molecular imprinting (Han et al., 2012; Dong et al., 2015; Zhang et al., 2018a; Pei et al., 2019; Si et al., 2019). Macroporous adsorption resin is a mature technology, but there are some shortcomings such as a large amount of solvent, long time, low yield, and complex process. High-purity monomer compounds can be extracted from natural products by high-speed countercurrent chromatography. Membrane separation is a new kind of separation technology, which can make the effective components of natural products rich and with few impurities, but the separation process is complicated (Li et al., 2015a,b; Wang et al., 2016; Zhang et al., 2016, 2018b; Li X. et al., 2019). As a new separation technique, molecular imprinting can make the active components of natural products highly concentrated with few impurities and effectively improve the purity of products. Molecularly imprinted polymers (MIPs) have shown the important applications for the purification and preconcentration of biomolecules from complex human fluids such as urine or postmortem blood (Lulinski et al., 2015, 2016).

Molecular imprinting technology synthesizes highly cross-linked MIPs through template orientation, generating cavities that mimic binding sites of antibodies, enzymes, and other biological materials, and give priority to bind with template molecules, providing an effective method for molecular recognition (Hrobonova et al., 2018; Liang et al., 2018; Hong et al., 2019; Ma et al., 2019). MIPs have attracted wide attention in the fields of solid phase extraction, sensors, antibodies, enzyme simulation, receptors, and catalysts (Zhang et al., 2013; Ansari and Karimi, 2017; Dilemiz et al., 2017; Xiao et al., 2018; Yu et al., 2019). Recently, MIPs have potential applications in drug delivery devices or chiral resolution (Lulinski, 2017; Marc et al., 2018; BelBruno, 2019; Sobiech et al., 2019). The main advantages of MIPs are the ease of preparation and creation of “custom” possible binding sites, by adjusting the target molecule’s synthesis process needed as a template in the polymerization process, as well as the advantages of low production cost, stability, robustness, and acid and alkali resistance (Speltini et al., 2017; Wu et al., 2017; Xu et al., 2017; Li F. et al., 2019; Zhang et al., 2019). In particular, MIPs have been successfully used as a selective adsorbent for solid phase extraction to extract active ingredients from natural products (Huang et al., 2019; Li Z. et al., 2019; Wang Y. et al., 2019). Molecular imprinting is divided into covalent molecular imprinting and non-covalent molecular imprinting. Covalent molecular imprinting has the characteristics of strong adhesion and difficult elution of template molecules, while non-covalent molecular imprinting has the characteristics of strong adhesion and easy elution of template

molecules. Therefore, non-covalent molecular imprinting polymers are often used for the separation and purification of natural products. The binding mode of non-covalent molecular imprinting method and target components is generally weak covalent bond binding, such as hydrogen bond, van der Waals force, hydrophobic interaction,  $\pi$ - $\pi$  accumulation (Yoshikawa et al., 2016; Vicario et al., 2018), etc. The recent literatures have reported that the interaction between the components of prepolymerization complex can be discussed by the theoretical analysis for design of functional monomers, cross-linking agents, and solvents (Sobiech et al., 2014, 2017; Cowen et al., 2016; Giebultowicz et al., 2019). Precipitation polymerization is the most commonly used method in the synthesis of imprint materials, but the main disadvantage of this method is that the steps required for the preparation of imprint materials are complex and numerous (Phungpanya et al., 2018). Therefore, this study mainly obtained a kind of imprinted material with high selective adsorption capacity for ACT by bulk polymerization, which is a simple and rapid synthesis method (Cantarella et al., 2019; Wang H. et al., 2019).

The aim of this study is to obtain an imprinted material with high selective adsorption capacity for ACT by a simple and rapid synthesis method. A series of MIPs of different functional monomers and different solvents were synthesized by bulk polymerization. The synthetic materials were characterized by scanning electron microscopy (SEM) and Fourier transform infrared spectroscopy (FT-IR). The adsorption performance of phenylethanoid glycoside aqueous solution was evaluated, and its binding selectivity was studied in depth. The MIPs with optimal adsorption performance were used to adsorb and purify ACT from crude extract of *C. tubulosa*.

## MATERIALS AND METHODS

### Materials

Echinacoside (ECH,  $\geq 98\%$ ) and Acteoside (ACT,  $\geq 98\%$ ) were obtained from Sunny Biotech Co., Ltd. (Shanghai, China). *C. tubulosa* was obtained from Cistanche Rongtang Biotechnology Co., Ltd. (Xinjiang, China). 4-Vinylpyridine (4-VP, 98%), methacrylic acid (MAA, 98%), 2-hydroxyethyl methacrylate (HEMA, 98%), ethyleneglycol dimethacrylate (EGDMA, 98%), azodiisobutyronitrile (AIBN, 98%), divinylbenzeneare (DVB, 98%) and *N,N*-dimethylformamide (DMF, 99.5%) were obtained from Adamas Reagent Co., Ltd. (Shanghai, China). Acetonitrile (ACN,  $\geq 99.9\%$ ), methanol ( $\geq 99.9\%$ ), and acetic acid ( $\geq 99.9\%$ ) were obtained from ThermoFisher Scientific Co., Ltd. (Shanghai, China). Ethanol ( $\geq 99.7\%$ ) was obtained from Yong sheng Fine Chemical Co., Ltd. (Tianjin, China). Deionized water is prepared from laboratory pure water Smart-S15 system (Shanghai, China).

### Instruments

The surface morphology and microstructure were examined by scanning electron microscopy (SEM, SU8010, Hitachi, Japan). The chemical structure of MIPs (FT-IR, Nicolet AVATAR360, Nicolet, USA) was measured by FT-IR. FT-IR test conditions: the step length is  $2\text{ cm}^{-1}$  and the scanning range is  $4,000\text{--}500\text{ cm}^{-1}$ , and attenuated total reflection method is used to prepare the MIP.



**TABLE 1** | The gradient elution program of HPLC.

T (min)	A (%)	B (%)
0–8	13	87
8–20	13–20	87–80
20–23	20–50	80–50
23–25	50–13	50–87
25–28	13	87

**TABLE 2** | Calibration curves of ECH and ACT.

Component	Regression equation	R <sup>2</sup>	Linear range (μg/ml)
ECH	$Y = 1.32 \times 10^7 X - 1.50 \times 10^4$	0.999988	1.6–2,000
ACT	$Y = 1.71 \times 10^7 X - 1.57 \times 10^3$	0.999987	1.6–2,000

The pore size, distribution and specific surface area of MIPs are measured using a special physical adsorption device (Mike, ASAP 2460). Adsorbent test conditions: degassing at 60°C for 12 h, N<sub>2</sub> adsorption and desorption curves were measured at –196°C. <sup>1</sup>H nuclear magnetic resonance (<sup>1</sup>H NMR) spectra were recorded in DMSO-d<sub>6</sub> on an AV-300 spectrometer (Bruker, Switzerland) with TMS as internal standard and values are shown in ppm (δ).

High-performance liquid chromatography (HPLC) with ultraviolet (UV) ray detector was performed with a 2695 solution system (Waters, USA). A chromatography was performed on a reverse-phase C18 column (Symmetry, 250 × 4.6 mm, 5 μm). The analytical methods were as follows: the mobile phase was acetonitrile (A) and acetic acid/water (1:44, v/v) (B) at a flow rate of 1 ml/min with 10-μl injection volumes and the UV detector wavelength was set at 330 nm. The column temperature was maintained at 30°C (Yang et al., 2018). Gradient elution conditions are listed in **Table 1**.

HPLC analysis using ECH and ACT standard solutions (2 mg/ml, 1 mg/ml, 0.2 mg/ml, 0.04 mg/ml, 0.008 mg/ml, and 0.0016 mg/ml) gave ECH and ACT calibration. The linear regression equation is shown in **Table 2**.

The limits of detection for ACT and ECH were 0.528 and 0.528 μg/ml, respectively. The limits of quantification for ACT and ECH were 1.60 and 1.60 μg/ml, respectively. The accuracy of ACT and ECH were 1.40 and 1.89%, respectively. The same sample was injected five times to obtain ACT and ECH precision of 1.40 and 1.71%, respectively.

## Synthesis of MIPs

The preparation process of MIP1 as follows: firstly, the template molecule ACT (125.00 mg) and the functional monomer 4-VP (210.00 mg) were dissolved sufficiently in mixed solution (2.50 ml) of acetonitrile and *N,N*-dimethylformamide (1:1.5, v/v). Then, the prepolymerization reaction of the mixture was carried out at 25°C for 20 min. Subsequently, EGDMA (1.12 g) and AIBN (15.00 mg) were added and dissolved fully into the pre-polymerization mixture. The obtained prepolymer solution was evacuated and filled with argon gas. The process of

**TABLE 3** | Ratio of raw materials for molecularly imprinted polymerization.

Polymers	Template	Functional monomer	Cross-linker	Solvent
MIP1	ACT	4-VP	EGDMA	ACN:DMF (1.5:1, v/v)
MIP2	ACT	MAA	EGDMA	ACN:DMF (1.5:1, v/v)
MIP3	ACT	HEMA	EGDMA	ACN:DMF (1.5:1, v/v)
MIP4	ACT	4-VP	DVB	ACN:DMF (1.5:1, v/v)
MIP5	ACT	4-VP	EGDMA	Methanol
NIP1	-	4-VP	EGDMA	ACN:DMF (1.5:1, v/v)
NIP2	-	MAA	EGDMA	ACN:DMF (1.5:1, v/v)
NIP3	-	HEMA	EGDMA	ACN:DMF (1.5:1, v/v)
NIP4	-	4-VP	DVB	ACN:DMF (1.5:1, v/v)
NIP5	-	4-VP	EGDMA	Methanol

The molar ratio of template molecule to monomer in MIPs is 1:10, and the molar ratio of monomer to cross-linker of MIPs and NIPs is 1:3.

polymerization was carried out at 60°C for 24 h. Finally, the pale-yellow bulk polymers were obtained and grounded to powder, which was sieved through a 200-mesh screen.

The mixed solution of methanol and acetic acid (9:1, v/v) was used to elute template molecules of ACT. The ACT molecules were eluted and repeated to wash until no ACT molecules were found in MIP1. The residual acetic acid in MIP1 was washed with methanol, and then MIP1 were dried at 40°C.

ACT was used as the template molecule, and different functional monomers, cross-linkers, and solvents are listed in **Table 3** and used to synthesize MIPs and NIPs.

## Static Adsorption Experiments

Ten milligrams of ACT MIPs was accurately weighed and placed in a 10-ml black cap bottle. Ten milliliters of ACT standard solution with 0.50 mg/ml concentration was added. The black cap bottle was placed in a thermostatic shaker. The temperature was set at 30°C, the speed was 150 rpm, and the adsorption process was 24 h. One milliliter of the solution was used to determine the content of ACT in the filtrate by HPLC.

## Dynamic Adsorption Experiments

Fifty milliliters of sample solution (standard solution or *C. tubulosa* extract) was placed in a cap bottle, and 20.00 mg MIPs was added and placed in a shaker at 30°C for 24 h. The samples were sampled at a set time within 24 h. Compared with SPE, d-SPE was more valuable, because the process of d-SPE can avoid the problems on variations of pressure and flow rate. One milliliter of solution was taken from each sample and the concentration of ACT in the solution was determined by HPLC.

In order to investigate the adsorption process, the pseudo-first-order reaction model equation and pseudo-second-order reaction model equation were used to describe the adsorption process of ACT on adsorbents. The pseudo-first-order reaction model equation was as follows:

$$\log(q_e - q_t) = \log q_e - \frac{K_1}{2.303} t \quad (1)$$

where  $K_1$  is the adsorption rate constant of pseudo-first-order kinetic model;  $t$  (min) is time;  $q_t$  is the adsorption capacity of time  $t$ .

The quasi-second-order reaction model equation is as follows:

$$\frac{t}{q_t} = \frac{1}{K_2 q_e^2} + \frac{1}{q_e} \quad (2)$$

where  $K_2$  is the adsorption rate constant of the pseudo-second-order kinetic model.

## Selectivity Experiments

The standard solutions of ACT and ECH with a concentration of 0.50 mg/ml were put into the black cap bottle for adsorption experiments, such as the static adsorption conditions above. One milliliter was extracted from the adsorbed solution, and the ACT and ECH content in the filtrate were determined by HPLC.

The adsorption capacity  $Q$  (mg/g) for the template bound to MIPs was calculated according to the following equation (Zhao et al., 2017):

$$Q = \frac{(C_0 - C_1)V}{m} \quad (3)$$

where  $C_0$  (mg/ml) and  $C_1$  (mg/ml) are the initial concentration and equilibrium concentration of standard solutions (Wang H.B. et al., 2019),  $V$  (ml) is the volume of standard solution, and  $m$  (g) is the weight of the MIP.

The adsorption selectivity of MIPs was evaluated by two parameters such as the imprinting factor ( $IF$ ) and adsorption separation factor ( $\alpha$ ).

The calculation of the imprinting factor is as follows:

$$IF = \frac{Q_{MIP}}{Q_{NIP}} \quad (4)$$

where  $Q_{MIP}$  and  $Q_{NIP}$  are the adsorption capacity  $Q_e$  (mg/g) of the bound analyte at equilibrium on the MIP and the NIP, respectively.

The calculation of the adsorption separation factor is as follows:

$$\alpha = \frac{K_{D,template}}{K_{D,analog}} \quad (5)$$

$$K_D = \frac{(C_0 - C_e)V}{C_e m} \quad (6)$$

where  $C_e$  (mg/ml) is the concentration of the solution after absorbed,  $C_0$  (mg/ml) is the initial concentration of the solution,  $V$  (ml) is the volume of the solution in the absorbed process, and  $m$  (g) is the mass of the sorbent.  $K_{D,template}$  and  $K_{D,analog}$  are the static distribution coefficients toward the template molecules and analog, respectively (Singh et al., 2013).

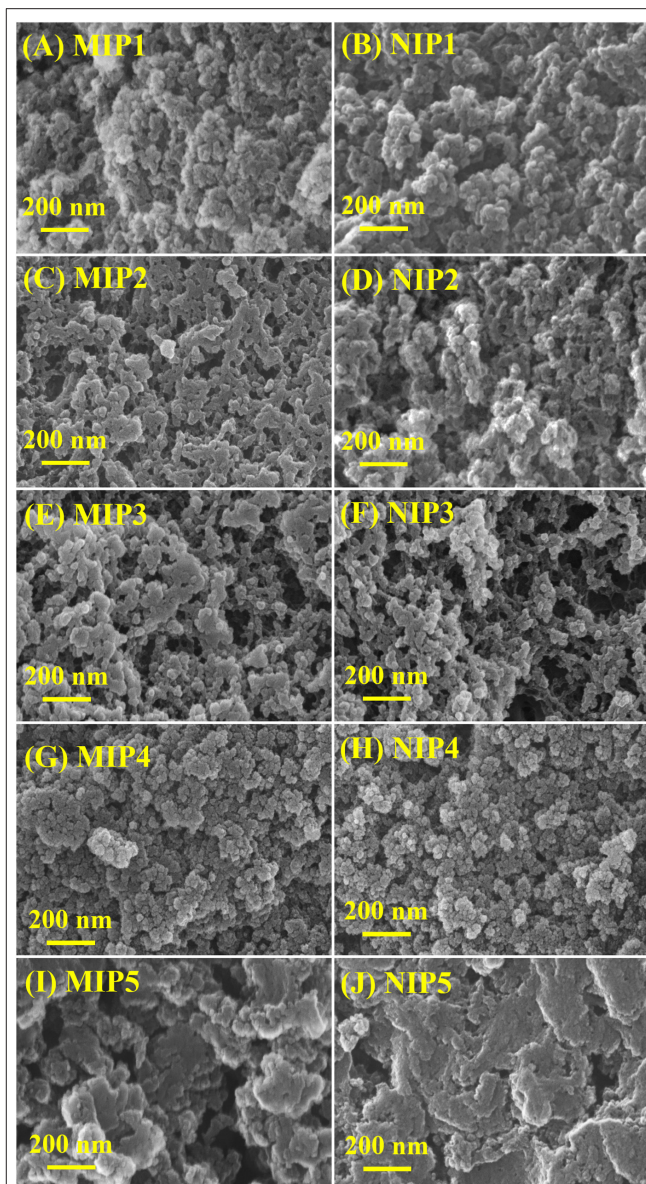


**FIGURE 1** | SEM of (A) MIP1, (B) NIP1, (C) MIP2, (D) NIP2, (E) MIP3, (F) NIP3, (G) MIP4, (H) NIP4, (I) MIP5, and (J) NIP5.

## RESULTS AND DISCUSSION

### Characterization of MIPs

The SEM images of MIPs and NIPs are shown in **Figure 1**. As can be seen from **Figure 1**, MIPs and NIPs show different loose structures in different monomers, cross-linking agents, and solvents. MIP1–MIP4 and NIP1–NIP4 are heterogeneous particles with irregular shape and different size. MIP5 and NIP5 are heterogeneous lamellar with irregular shape and different size. The structure of MIP1 prepared in EGDMA is looser than that MIP4 prepared in DVB (**Figures 1A,G**). The structure of MIP1 with ACN and DMF as solvent (1:1.5, v/v) is looser than that of MIP5 with methanol as solvent (**Figures 1A,I**). The loose

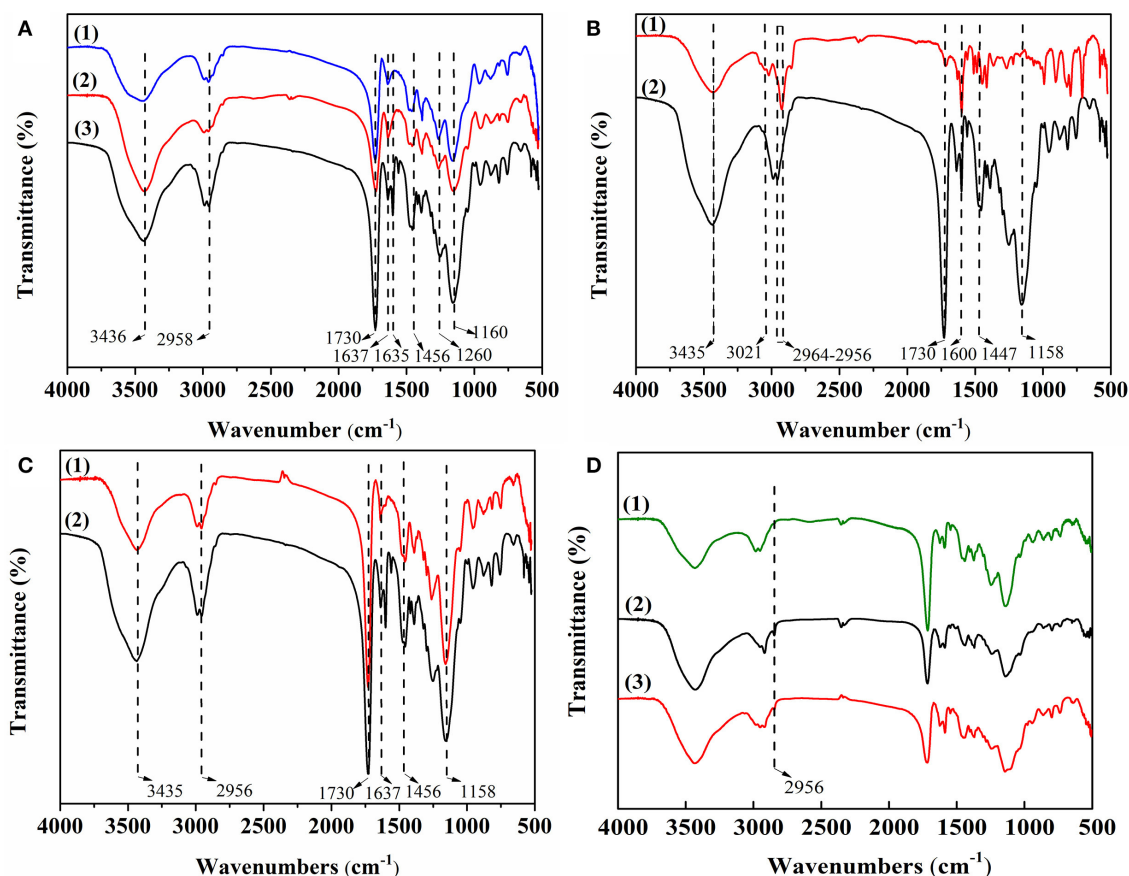


**FIGURE 2 | (A)** FT-IR spectra of MIPs with different functional monomers: (1) 4-VP of MIP1; (2) MAA of MIP2, and (3) HEMA of MIP3; **(B)** FT-IR spectra of MIPs with different cross-linkers: (1) DVB of MIP4 and (2) EGDMA of MIP1; **(C)** FT-IR spectra of MIPs with different solvents: (1) MIP5 and (2) MIP1; **(D)** FT-IR spectra of (1) NIP1, (2) MIP1-ACT, and (3) MIP1.

structure can speed up the molecular mass transfer and improve the binding speed of MIPs and ACT.

**Figure 2** shows FT-IR spectra of MIPs with different functional monomers (A), cross-linkers (B), and solvents (C). As shown in **Figure 2A**, the C=N stretching vibration peak and the C=C stretching vibration peak appeared in 4-VP at 1,637 cm<sup>-1</sup> and 1,456 cm<sup>-1</sup>, respectively (**Figure 2A**, trace1). The C=O stretching vibration peak and the C-O stretching vibration peak appeared in MAA at 1,730 and 1,260 cm<sup>-1</sup>, respectively (**Figure 2A**, trace2). The stretching vibration peak of  $\beta$ -hydroxy and the stretching vibration peak of methylene appeared in HEMA at 3,436 and 2,958 cm<sup>-1</sup>, respectively (**Figure 2A**, trace3). The results indicate that 4-VP, MAA, and HEMA were successfully polymerized into the MIPs. As shown in **Figure 2B**, the stretching vibration absorption peaks of unsaturated C-H bond and skeleton vibration absorption peaks of benzene ring appeared in DVB at 3,021 and 1,600 cm<sup>-1</sup>, respectively (**Figure 2B**, trace1). The stretching vibration absorption peaks of C=O and the stretching vibration absorption peaks of O-C-O appeared in EGDMA at 1,730 and 1,160 cm<sup>-1</sup>, respectively (**Figure 2B**, trace2). The results indicate that MIP4 and MIP1 were successfully polymerized. As shown in **Figure 2C**, it can be

seen that MIP1 and MIP5 had no peculiar characteristic peak, indicating its chemical structure is similar.

**Figure 2D** is the FT-IR spectra of NIP1, MIP1-ACT, and MIP1. The infrared spectrum of the NIP1 and the infrared spectrum of the MIP1 have the same characteristic peak, indicating that its chemical structure is similar (**Figure 2D**, trace1 and trace3). The infrared spectrum of the MIP1-ACT produced a new peak at 2,956 cm<sup>-1</sup> compared to the infrared spectrum of the MIP1 (**Figure 2D**, trace2 and trace3), due to the acyl group of ACT that interacts with 4-VP to form a hydrogen bond association on the MIP1, indicating that the template molecule has been adsorbed to the MIP1 through hydrogen bonding.

The hysteric curve and pore size distributions of MIPs and NIPs are shown in **Figure 3**. The hysteric curves of MIPs and NIPs exhibited "type IV" isotherm (**Figures 3A,B**). The pore size distributions of MIPs and NIPs were distributed in the range of 5–50 nm, which indicated that the pores of MIPs and NIPs belonged to mesopores (**Figures 3C,D**).

The data of specific surface area, pore volume, and pore size for MIPs and NIPs are listed in **Table 4**. The specific surface area of MIP1 was 593.91 m<sup>2</sup>/g with a pore size of 10.91 nm. The specific surface area of NIP1 was 427.12 m<sup>2</sup>/g with a pore size of



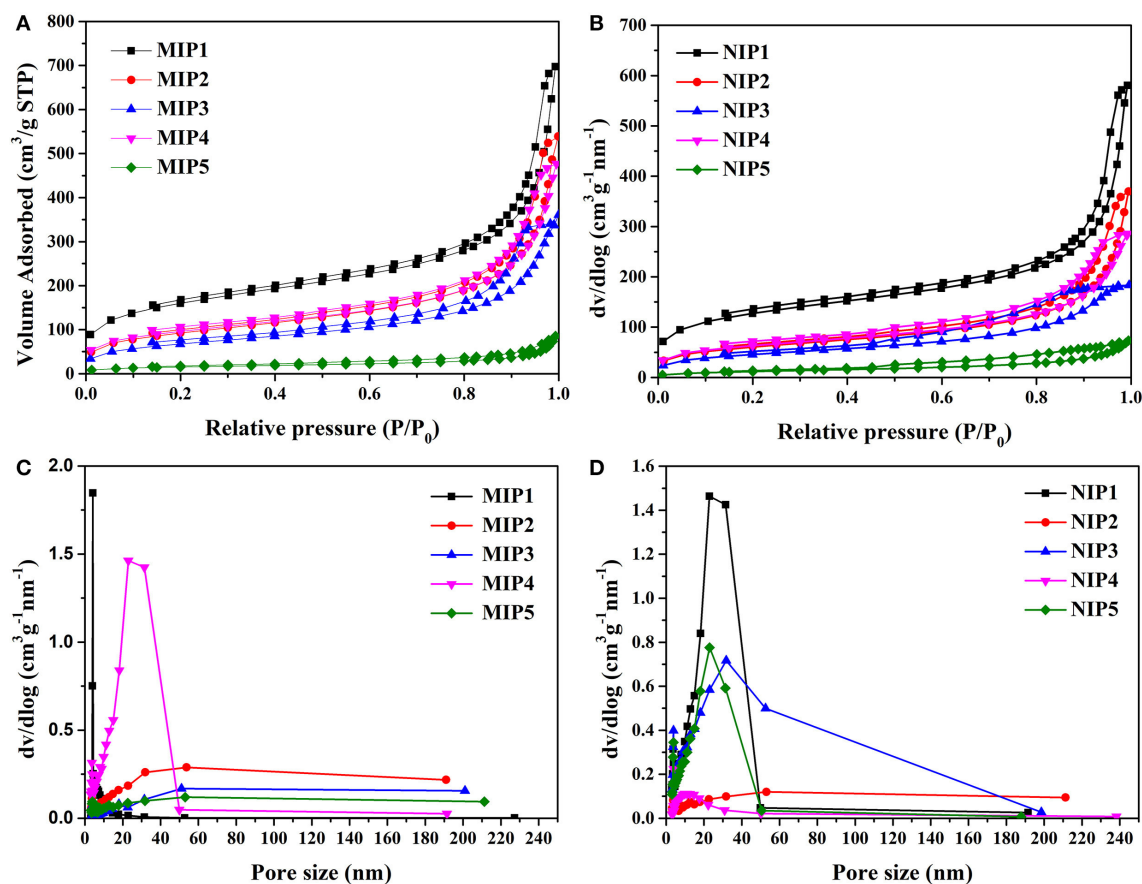


**FIGURE 3 |** BET data (A) hysteresis curve of MIPs, (B) hysteresis curve of NIPs, (C) pore distribution diagram of MIPs, and (D) pore distribution diagram of NIPs.

**TABLE 4 |** BET data for MIPs and NIPs.

Polymers	Hysteresis curve	Pore size (nm)	Pore volume (cm³/g)	Surface area (m²/g)
MIP1	H4	10.91	1.08	539.91
MIP2	H4	10.01	0.81	317.76
MIP3	H4	9.09	0.54	232.76
MIP4	H4	8.91	0.74	327.49
MIP5	H4	10.06	0.13	51.88
NIP1	H4	8.41	0.89	427.12
NIP2	H4	7.94	0.57	206.95
NIP3	H4	7.11	0.28	159.88
NIP4	H4	8.12	0.44	215.24
NIP5	H4	10.29	0.11	41.83

7.94 nm. Obviously, the specific surface area and pore size of the MIP1 were larger than that of the NIP1. This can be attributed to the presence of imprinted holes on the surface of MIP1. The high specific surface area and large pore size of MIP1 are favorable for increasing the adsorption capacity of MIP1 for ACT.

The  $^1\text{H}$  NMR spectra of ACT, monomers, and prepolymers are shown in **Figure 4**. The proton peaks of different phenolic hydroxyl groups on ACT appeared at 7.50, 6.75, 6.20, 5.02, 4.35, and 3.52 ppm (**Figures 4A–C**). As shown in **Figure 4A**, the proton peaks on the pyridine groups of 4-VP exhibited at 8.64, 7.45, 6.75, 6.17, and 5.54 ppm. Compared with the proton peaks of ACT and 4-VP, prepolymer of MIP1 appeared new proton peaks at 8.52, 8.01, 7.49, 6.67, 6.13, and 5.54 ppm, which resulted from the formed hydrogen bonds between ACT and 4-VP. As shown in **Figure 4B**, the proton peaks of MAA exhibited at 5.94, 5.53, and 1.47 ppm. Compared with the proton peaks of ACT and MAA, prepolymer of MIP2 presented new proton peaks at 7.95, 5.98, 5.67, and 1.03 ppm, which resulted from the formed hydrogen bonds between ACT and MAA. As shown in **Figure 4C**, the proton peaks of HEMA exhibited at 6.04, 5.56, 4.85, 4.11, and 3.75 ppm. Compared with the proton peaks of ACT and HEMA, prepolymer of MIP3 exhibited new proton peaks at 7.95, 6.15, 5.76, 4.32, and 3.66 ppm, which resulted from the formed hydrogen bonds between ACT and HEMA.

## Adsorption Experiment

In the process of MIPs preparation, the appropriate functional monomers determine whether molecularly imprinted polymers

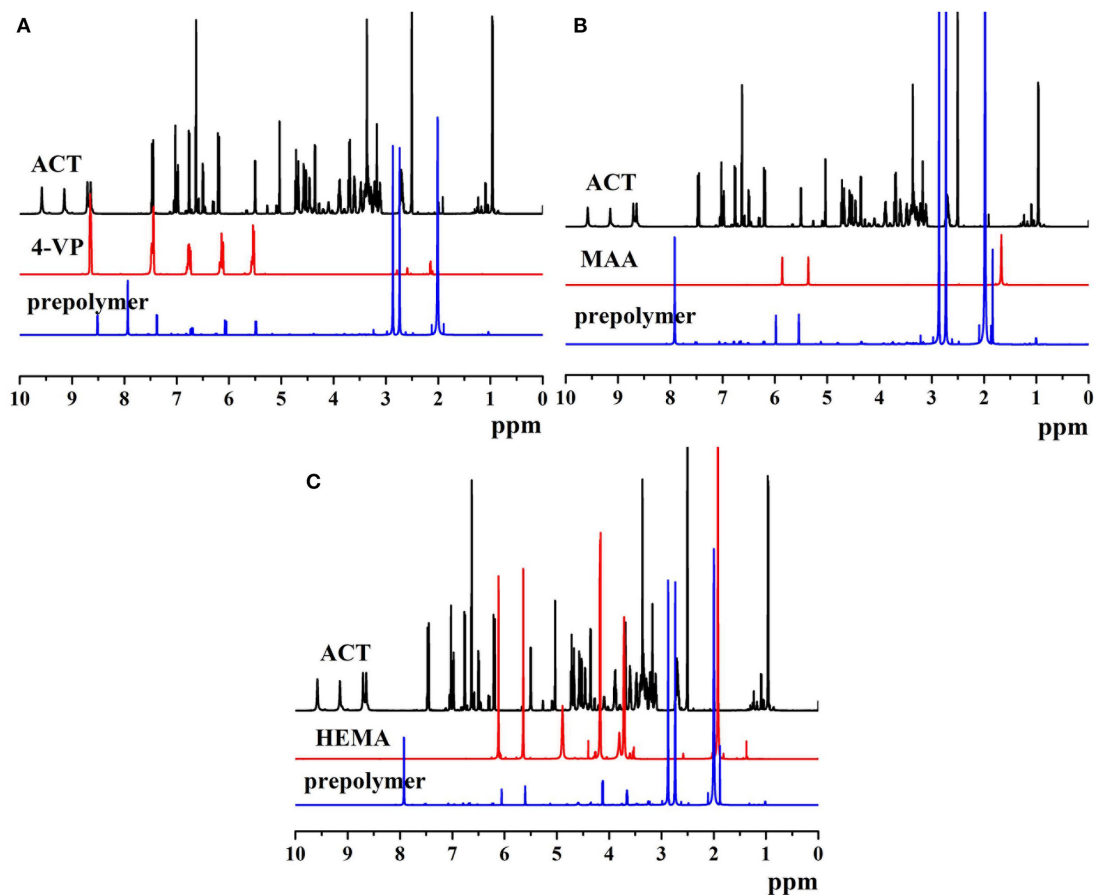


**FIGURE 4 |** The <sup>1</sup>H NMR spectra of (A) ACT, 4-VP, and ACT-4-VP prepolymer, (B) ACT, MAA, and ACT-MAA prepolymer, and (C) ACT, HEMA, and ACT-HEMA prepolymer.

**TABLE 5 |** Adsorption data of MIPs and NIPs.

Polymers	$Q_{\text{ACT}}$ (mg/g)	IF
MIP1	$168.05 \pm 4.65$	$2.69 \pm 0.13$
MIP2	$113.58 \pm 5.64$	$2.42 \pm 0.15$
MIP3	$124.01 \pm 4.39$	$0.87 \pm 0.008$
MIP4	$124.59 \pm 5.64$	$0.84 \pm 0.005$
MIP5	$5.79 \pm 6.34$	$0.32 \pm 0.21$
NIP1	$62.58 \pm 4.85$	-
NIP2	$46.91 \pm 5.76$	-
NIP3	$143.13 \pm 5.83$	-
NIP4	$147.77 \pm 6.32$	-
NIP5	$17.96 \pm 5.34$	-

-, not available for data ( $n = 3$ ).

have excellent recognition ability. This is because different functional monomers contain different functional groups and the interaction between template molecules is different. According to the acidity and alkalinity, functional monomers can be further divided into acidic functional monomers, basic functional monomers, and neutral functional monomers, and acidic template molecules should be selected as basic functional

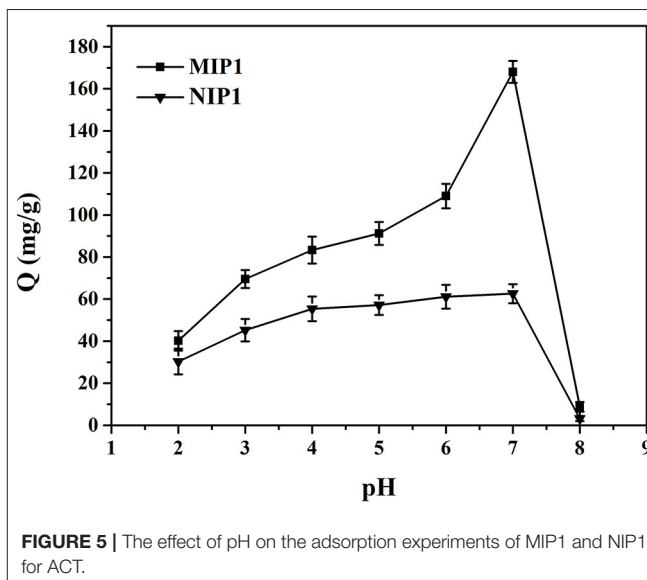


**FIGURE 5 |** The effect of pH on the adsorption experiments of MIP1 and NIP1 for ACT.

monomers. Hydrogen bonds can be formed between different functional groups of monomers and hydroxyl groups of the template molecules in MIPs (Hammam et al., 2018; Panjan et al.,



2018). 4-VP contains pyridine groups, and the pyridine groups can form hydrogen bonds with the hydroxyl groups in the template molecule of ACT. MAA contains carboxyl groups, and carboxyl groups can form hydrogen bonds with the hydroxyl groups in the template molecule of ACT. HEMA contains hydroxyl groups, and hydroxyl groups can form hydrogen bonds with template molecules of ACT (Yesilova et al., 2018; Haginaka et al., 2019; Luo et al., 2019). The static adsorption data of MIPs and NIPs are listed in Table 5. According to the data listed in Table 5, MIP1 has the highest adsorption capacity and the highest imprinting factor. The adsorption capacity of MIP1 was 168.05 mg/g, and the imprinting factor was 2.69. On one hand, MIP1 had large amounts of imprinted holes, which can match the spatial configuration of ACT, achieving selective adsorption for ACT. On the other hand, the hydroxyl groups on ACT contacted with the N-H groups of MIP1 in the adsorption process to form hydrogen bonds, which can increase adsorption capacity of ACT.

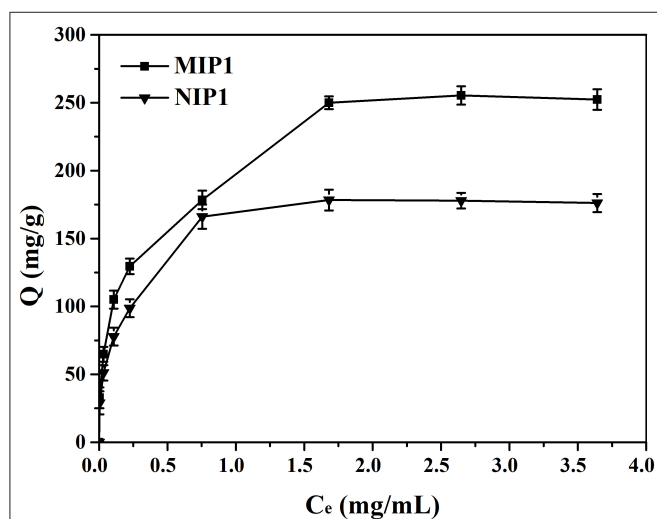


FIGURE 6 | Adsorption isotherms of MIP1 and NIP1 for ACT.

The effect of pH on the adsorption performance of MIP1 and NIP1 for ACT is shown in Figure 5. It can be seen from Figure 5 that the optimal pH value was 7 for adsorption of ACT by MIP1 and NIP1. The reasons are as follows: ACT had a large number of phenolic hydroxyl groups and belonged to the weak acidic molecules, and the different pH values affected the stability of ACT. The stability of phenolic hydroxyl groups on ACT molecules would decrease at  $\text{pH} > 7$  and  $\text{pH} < 7$ . This will reduce the amount of ACT adsorbed by MIP1 and NIP1. Thus, the optimum pH was 7 for MIP1 and NIP1 adsorption.

## Isothermal Adsorption Experiment

The isotherm adsorption curves of MIP1 and NIP1 for ACT were shown in Figure 6. It can be seen that the adsorption capacity of MIP1 for ACT increases with the increase of the initial ACT concentration, and this might be the reason that the amount of ACT was not enough to saturate the specific binding cavities. The adsorption curve reached the saturation and tended to be stable when the initial concentration exceeded 1.50 mg/ml, and the maximum adsorption capacity of MIP1 was 250.00 mg/g, which indicated that a great many ACT specific binding sites were produced during imprinting process. Figure 4 also shows that the amounts of ACT bound to the MIPs were in a high level compared with those of the NIPs under the same conditions.

## Scatchard Plot Analysis

The Scatchard plot of MIP1 and NIP1 for ACT is shown in Figure 7. The binding properties of MIPs were determined by Scatchard plot analysis, which was based on the following equation:

$$\frac{q_e}{c_e} = \frac{B_{\max} - q_e}{K_a} \quad (7)$$

where  $c_e$  is the equilibrium concentration of ACT in the solution,  $q_e$  is the amount of ACT bound to the MIPs at equilibrium,  $B_{\max}$  is the apparent maximum binding amount, and  $K_a$  is the dissociation constant.

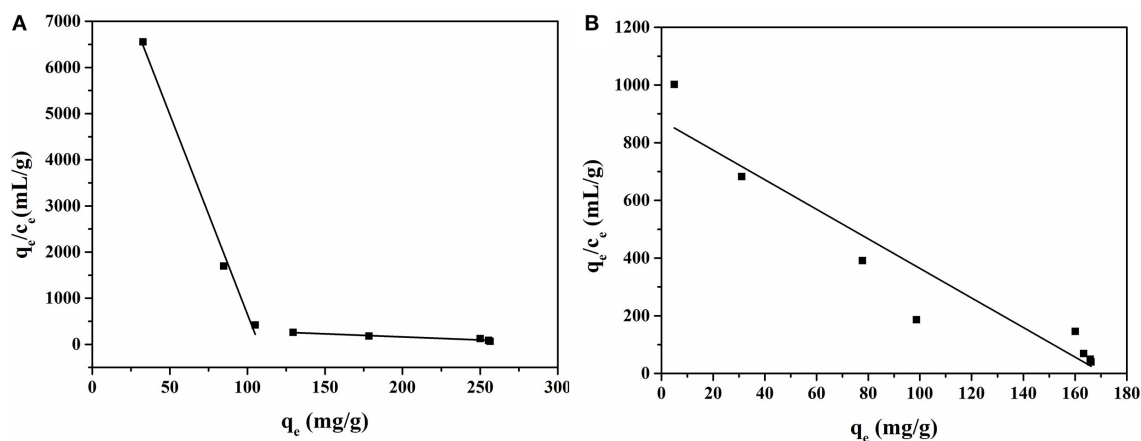
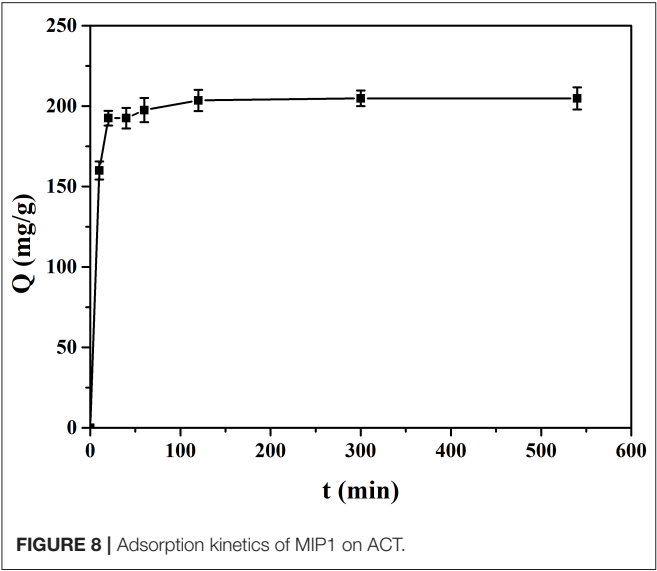


FIGURE 7 | Scatchard plot of MIP1 (A) and NIP1 (B) for ACT.

The Scatchard plot of MIP1 contained two different linear regression lines, suggesting two types of binding sites. As shown in **Figure 7A**, the left line suggested that the MIP1 had high binding affinity with ACT in the concentration range of 0.005–0.25 mg/ml. The  $K_a$  and  $B_{max}$  were found to be 1.94 mg/ml and 18,080.15 mg/g for dry polymer, respectively, and they were calculated from the intercept and slope of the regression equation  $q_e/c_e = -86.54q_e + 9310.66$  ( $R^2 = 0.98$ ). The right line indicated that MIP1 had low binding affinity in the concentration range of 0.25–4.00 mg/ml. The  $K_a$  and  $B_{max}$  were found to be 127.31 mg/ml and 54,316.81 mg/g for dry polymer, respectively, and they were calculated from the regression equation  $q_e/c_e = -1.32q_e + 426.65$  ( $R^2 = 0.91$ ). Meanwhile, it can be seen from the two equations that the slope of the straight line on the left side was small, and the slope of the straight line on the right side was large. The small slope had high binding affinity with ACT for MIP1.



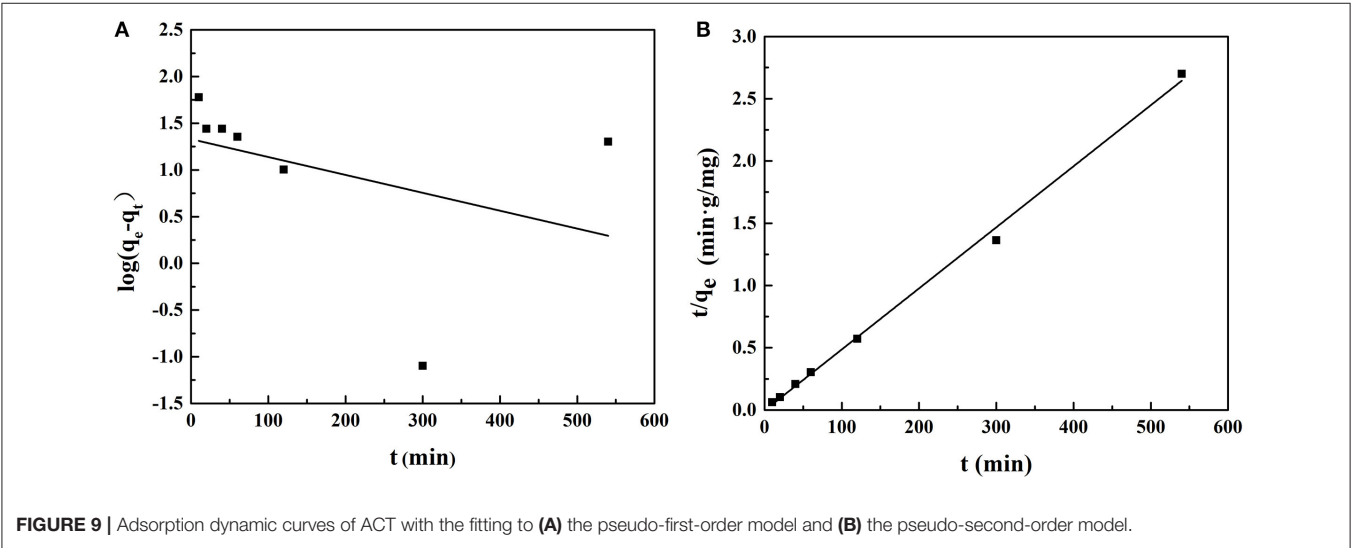
The Scatchard plot of NIP1 shows a straight line, indicating that there is only one type of binding site in NIP1. The  $K_a$  and  $B_{max}$  were found to be 12.19 mg/ml and 10,689.41 mg/g for dry polymer, respectively, and they were calculated from the regression equation  $q_e/c_e = -5.13q_e + 876.91$  ( $R^2 = 0.89$ ).

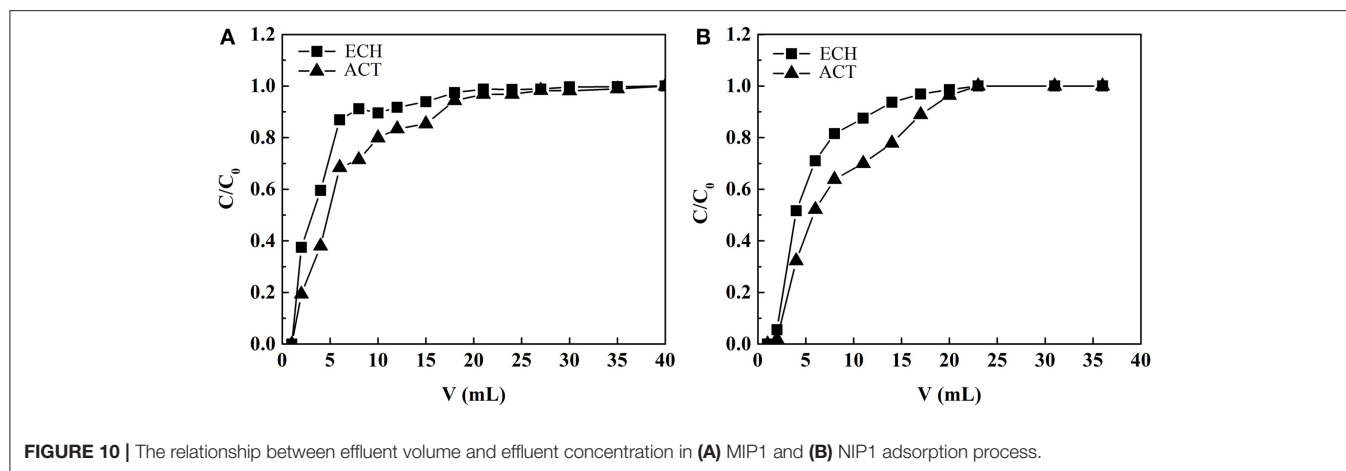
### Adsorption Kinetics Study

**Figure 8** shows the adsorption kinetics curve of MIP1 for ACT. The dynamic adsorption experiments were carried out in ACT solution with an initial concentration of 0.50 mg/ml; it can be seen that the adsorption capacity of MIP1 for ACT increases rapidly in 20 min and slowly in 100 min, but it does not change much after 150 min. Therefore, the equilibrium adsorption time of MIP1 is 150 min and the equilibrium adsorption capacity is 204.08 mg/g. At the beginning of dynamic adsorption, there are more free ACT molecules in ACT solution and more specific recognition sites in MIP1, so the hydrogen bonding rate between MIP1 and ACT is fast. After 20 min, the number of specific recognition sites of MIP1 and the number of free radicals in the ACT solution decreased, which reduced the binding rate of MIP1 and ACT, eventually reaching dynamic equilibrium.

**Figure 9** shows the quasi-first-order kinetic model and quasi-second-order kinetic model of ACT adsorption on MIP1, and **Table 6** shows the data fitted by the kinetic model. The equilibrium adsorption capacity in the dynamic adsorption equilibrium experiment of MIP1 was 204.08

TABLE 6   Fitting of quasi-first-order and quasi-second-order dynamic models.						
Adsorbent	Quasi-first-order kinetic fit curve			Quasi-second-order dynamic fitting curve		
	$K_1$	$Q_e$ (mg/g)	$R^2$	$K_2$	$Q_e$ (mg/g)	$R^2$
MIP1	0.0044	21.39	0.15	0.0052	204.08	0.99





mg/g. The experimental data are consistent with the pseudo-second-order kinetic fitting data, which proves that the adsorption behavior of MIP1 conforms to the pseudo-second-order kinetic model ( $R^2 > 0.99$ ). The dynamic adsorption equilibrium accords with the quasi-second-order kinetics; it indicates that chemical adsorption is a speed-control step in the adsorption process. Therefore, the adsorption behavior of ACT on MIP1 may be hydrogen bonding.

## Purification of ACT From *C. tubulosa*

### Preparation of the Extracts of *C. tubulosa*

Twenty grams of *C. tubulosa* powder was dispersed in a 50% ethanol solution at 70°C. The extraction was carried out for 2 min under a high shear homogenizer at 16,000 rpm. The extracts were filtered through a 0.22- $\mu$ m filter to obtain the extract of *C. tubulosa*.

### Preparation of Solid Phase Extraction Column and Solid Phase Extraction of ACT in the Extracts of *C. tubulosa*

One hundred milligrams of MIP1 was dispersed in the 50% ethanol solution and loaded into a solid phase extraction column, and the SPE column of MIP1 was then rinsed with a 50% ethanol solution at a flow rate of 2.00 ml/min for 10 min. The extracts of *C. tubulosa* were injected into the SPE column at a flow rate of 2.00 ml/min, and the sample concentration of the effluent was measured. The eluate was collected after the SPE column of MIP1 was eluted with 90% ethanol solutions and 10% ethanol solutions, respectively (Gao et al., 2016). The collected eluent was dried and dissolved in water for constant volume, and then the content of ACT was measured by HPLC.

Figure 10 shows the relationship between effluent volume and effluent concentration in the adsorption process of MIP1 and NIP1, respectively. The contents of ECH and ACT in the extract of *C. tubulosa* were 2.44 and 0.53 mg/ml, respectively. As can be seen from Figure 10, when the effluent volume is

40.00 ml, the concentrations of ACT and ECH in the effluent are the same as those in the extract of *C. tubulosa*, indicating that MIP1 reaches the adsorption equilibrium. When the effluent volume was 23.00 ml, the concentrations of ACT and ECH in the effluent were the same as those in the extract of *C. tubulosa*, indicating that NIP1 reached the adsorption equilibrium. The binding amount of ACT by MIP1 solid phase extraction column is larger than that by NIP1 solid phase extraction column; it indicated that MIP1 has excellent imprinting effect on ACT.

The content of ECH in the extract of *C. tubulosa* was 4.58 times that of ACT. The adsorption capacity of MIP1 on ACT and ECH was 36.86 and 88.67 mg/g, respectively. After the eluent is eluted, the recovery rate of ACT was 90.09%. The purity of ACT increased from 1.99 to 27.88%, and the increasing amplitude of purity is 1301.00%, which was higher than the increment of 960.00% by adsorption of microporous resins (HPD300) (Liu et al., 2013). The increase in purity of ACT results from the selective adsorption of ACT by molecularly imprinted cavity.

## CONCLUSIONS

An imprinting material with a high selective adsorption capacity is used for simple and rapid separation of ACT. MIPs were investigated in terms of static adsorption experiments, dynamic adsorption experiments, and selectivity experiments. The experimental results showed that MIP1 exhibited the optimal adsorption performance to ACT. MIP1 was prepared with ACT as template molecule, 4-VP as a functional monomer, EGDMA as a cross-linking agent, the volume ratio of ACN and DMF of 1:1.5 (v/v) as a solvent, and AIBN as initiator. The adsorption results displayed that the adsorption capacity of MIP1 to ACT reached 112.60 mg/g, and the separation factor of ACT/ECH was 4.68. The dynamic adsorption of ACT accorded with the quasi-second-order kinetics; it indicated that the adsorption process of MIP1 is the process of chemical adsorption to ACT. MIPs with

high selectivity make it a potential adsorption material for the purification of plant active ingredients.

## DATA AVAILABILITY STATEMENT

All datasets generated for this study are included in the article/supplementary material.

## AUTHOR CONTRIBUTIONS

XZ carried out experiments and wrote the manuscript. WP designed the experiments, provided useful suggestions, and solved the problems in the experiments. RG provided the

experiment tools. XL contributed to the study design, manuscript revision, and final version.

## ACKNOWLEDGMENTS

We gratefully acknowledge the support from the National Natural Science Foundation for Young Scientists of China (Grant No. 21706166), the Program for Young Innovative Talents of Shihezi University (CXRC201802), the Program for Changjiang Scholars and Innovative Research Team in University (Grant No. IRT\_15R46), and the Yangtze River scholar research project of Shihezi University (Grant No. CJXZ201601).

## REFERENCES

- Ansari, S., and Karimi, M. (2017). Novel developments and trends of analytical methods for drug analysis in biological and environmental samples by molecularly imprinted polymers. *Trends Anal. Chem.* 89, 146–162. doi: 10.1016/j.trac.2017.02.002
- BelBruno, J. J. (2019). Molecularly imprinted polymers. *Chem. Rev.* 119, 94–119. doi: 10.1021/acs.chemrev.8b00171
- Cantarella, M., Carroccio, S. C., Dattilo, S., Avolio, R., Castaldo, R., Puglisi, C., et al. (2019). Molecularly imprinted polymer for selective adsorption of diclofenac from contaminated water. *Chem. Eng. J.* 367, 180–188. doi: 10.1016/j.cej.2019.02.146
- Cowen, T., Karim, K., and Piletsky, S. (2016). Computational approaches in the design of synthetic receptors - A review. *Anal. Chim. Acta* 936, 62–74. doi: 10.1016/j.aca.2016.07.027
- Diltemiz, S. E., Kecili, R., Ersoez, A., and Say, R. (2017). Molecular imprinting technology in quartz crystal microbalance (QCM) sensors. *Sensors* 17, 454–454. doi: 10.3390/s17030454
- Dong, B., Yuan, X., Zhao, Q., Feng, Q., Liu, B., Guo, Y., et al. (2015). Ultrasound-assisted aqueous two-phase extraction of phenylethanoid glycosides from *Cistanche deserticola* Y. C. Ma stems. *J. Sep. Sci.* 38, 1194–1203. doi: 10.1002/jssc.201401410
- Fu, C., Li, J., Aipire, A., Xia, L., Yang, Y., Chen, Q., et al. (2018). *Cistanche tubulosa* phenylethanoid glycosides induce apoptosis in Eca-109 cells via the mitochondria-dependent pathway. *Oncol. Lett.* 17, 303–313. doi: 10.3892/ol.2018.9635
- Gao, D., Yang, F., Xia, Z., and Zhang, Q. (2016). Molecularly imprinted polymer for the selective extraction of luteolin from *Chrysanthemum morifolium* ramat. *J. Separation Science* 39, 3002–3010. doi: 10.1002/jssc.201600520
- Gieblutowicz, J., Sobiech, M., Ruzicka, M., and Lulinski, P. (2019). Theoretical and experimental approach to hydrophilic interaction dispersive solid-phase extraction of 2-aminothiazoline-4-carboxylic acid from human post-mortem blood. *J. Chromatogr. A* 1587, 61–72. doi: 10.1016/j.chroma.2018.12.028
- Haginaka, J., Nishimura, K., Kimachi, T., Inamoto, K., Takemoto, Y., and Kobayashi, Y. (2019). Retention and molecular-recognition mechanisms of molecularly imprinted polymers for promazine derivatives. *Talanta* 205:20149. doi: 10.1016/j.talanta.2019.120149
- Hammam, M. A., Wagdy, H. A., and El Nashar, R. M. (2018). Moxifloxacin hydrochloride electrochemical detection based on newly designed molecularly imprinted polymer. *Sens. Actua. B-Chem.* 275, 127–136. doi: 10.1016/j.snb.2018.08.041
- Han, L., Ji, L., Boakye-Yiadom, M., Li, W., Song, X., and Gao, X. (2012). Preparative isolation and purification of four compounds from *Cistanche deserticola* Y.C. Ma by high-speed counter-current chromatography. *Molecules* 17, 8276–8284. doi: 10.3390/molecules17078276
- Hong, S., She, Y., Cao, X., Wang, M., He, Y., Zheng, L., et al. (2019). A novel CdSe/ZnS quantum dots fluorescence assay based on molecularly imprinted sensitive membranes for determination of triazophos residues in cabbage and apple. *Front. Chem.* 7:130. doi: 10.3389/fchem.2019.00130
- Hrobonova, K., Machynakova, A., and Cizmarik, J. (2018). Determination of dicoumarol in *Melilotus officinalis* L. by using molecularly imprinted polymer solid-phase extraction coupled with high performance liquid chromatography. *J. Chromatogr. A* 1539, 93–102. doi: 10.1016/j.chroma.2018.01.043
- Huang, Y., Pan, J., Liu, Y., Wang, M., Deng, S., and Xia, Z. (2019). A SPE method with two MIPs in two steps for improving the selectivity of MIPs. *Anal. Chem.* 91, 8436–8442. doi: 10.1021/acs.analchem.9b01453
- Li, C., Ma, X., Zhang, X., Wang, R., Chen, Y., and Li, Z. (2016). Magnetic molecularly imprinted polymer nanoparticles-based solid-phase extraction coupled with gas chromatography-mass spectrometry for selective determination of trace di-(2-ethylhexyl) phthalate in water samples. *Anal. Bioanal. Chem.* 408, 7857–7864. doi: 10.1007/s00216-016-9889-x
- Li, F., Gao, J., Li, X., Li, Y., He, X., Chen, L., et al. (2019). Preparation of magnetic molecularly imprinted polymers functionalized carbon nanotubes for highly selective removal of aristolochic acid. *J. Chromatogr. A* 16, 168–177. doi: 10.1016/j.chroma.2019.06.043
- Li, X., Cheng, Y., Zhang, H., Wang, S., Jiang, Z., Guo, R., et al. (2015a). Efficient CO<sub>2</sub> capture by functionalized graphene oxide nanosheets as fillers to fabricate multi-permselective mixed matrix membranes. *ACS Appl. Mater. Interfaces* 7, 5528–5537. doi: 10.1021/acsami.5b00106
- Li, X., Hou, J., Guo, R., Wang, Z., and Zhang, J. (2019). Constructing unique cross-sectional structured mixed matrix membranes by incorporating ultrathin microporous nanosheets for efficient CO<sub>2</sub> separation. *ACS Appl. Mater. Interfaces* 11, 24618–24626. doi: 10.1021/acsami.9b07815
- Li, X., Ma, L., Zhang, H., Wang, S., Jiang, Z., Guo, R., et al. (2015b). Synergistic effect of combining carbon nanotubes and graphene oxide in mixed matrix membranes for efficient CO<sub>2</sub> separation. *J. Membr. Sci.* 479, 1–10. doi: 10.1016/j.memsci.2015.01.014
- Li, Z., Wang, J., Chen, X., Hu, S., Gong, T., and Xian, Q. (2019). A novel molecularly imprinted polymer-solid phase extraction method coupled with high performance liquid chromatography tandem mass spectrometry for the determination of nitrosamines in water and beverage samples. *Food Chem.* 292, 267–274. doi: 10.1016/j.foodchem.2019.04.036
- Liang, R., Wang, T., Zhang, H., Yao, R., and Qin, W. (2018). Soluble molecularly imprinted nanorods for homogeneous molecular recognition. *Front. Chem.* 6:81. doi: 10.3389/fchem.2018.00081
- Liu, B., Ouyang, J., Yuan, X., Wang, L., and Zhao, B. (2013). Adsorption properties and preparative separation of phenylethanoid glycosides from *Cistanche deserticola* by use of macroporous resins. *J. Chromatogr. B* 937, 84–90. doi: 10.1016/j.jchromb.2013.08.018
- Lulinski, P. (2017). Molecularly imprinted polymers based drug delivery devices: a way to application in modern pharmacotherapy. A review. *Mater. Sci. Eng.* 76, 1344–1353. doi: 10.1016/j.msec.2017.02.138
- Lulinski, P., Bamburowicz-Klimkowska, M., Dana, M., Szutowski, M., and Maciejewska, D. (2016). Efficient strategy for the selective determination of dopamine in human urine by molecularly imprinted solid-phase extraction. *J. Separ. Sci.* 39, 895–903. doi: 10.1002/jssc.201501159



- Lulinski, P., Giebulowicz, J., Wroczynski, P., and Maciejewska, D. (2015). A highly selective molecularly imprinted sorbent for extraction of 2-aminothiazoline-4-carboxylic acid - Synthesis, characterization and application in post-mortem whole blood analysis. *J. Chromatogr. A* 1420, 16–25. doi: 10.1016/j.chroma.2015.09.083
- Luo, Z., Xiao, A., Chen, G., Guo, Q., Chang, C., Zeng, A., et al. (2019). Preparation and application of molecularly imprinted polymers for the selective extraction of naringin and genistein from herbal medicines. *Analy. Methods* 11, 4890–4898. doi: 10.1039/C9AY01503E
- Ma, X., Lin, H., He, Y., She, Y., Wang, M., Abd El-Aty, A. M., et al. (2019). Magnetic molecularly imprinted polymers doped with graphene oxide for the selective recognition and extraction of four flavonoids from *Rhododendron* species. *J. Chromatogr. A* 1598, 39–48. doi: 10.1016/j.chroma.2019.03.053
- Marc, M., Kupka, T., Wiecek, P. P., and Namiesnik, J. (2018). Computational modeling of molecularly imprinted polymers as a green approach to the development of novel analytical sorbents. *Trends Anal. Chem.* 98, 64–78. doi: 10.1016/j.trac.2017.10.020
- Morikawa, T., Xie, H., Pan, Y., Ninomiya, K., Yuan, D., Jia, X., et al. (2019). A review of biologically active natural products from a desert plant *Cistanche tubulosa*. *Chem. Pharm. Bull.* 67, 675–689. doi: 10.1248/cpb.c19-00008
- Panjan, P., Monasterio, R. P., Carrasco-Pancorbo, A., Fernandez-Gutierrez, A., Sesay, A. M., and Fernandez-Sanchez, J. F. (2018). Development of a folic acid molecularly imprinted polymer and its evaluation as a sorbent for dispersive solid-phase extraction by liquid chromatography coupled to mass spectrometry. *J. Chromatogr. A* 1576, 26–33. doi: 10.1016/j.chroma.2018.09.037
- Pei, W., Guo, R., Zhang, J., and Li, X. (2019). Extraction of phenylethanoid glycosides from *Cistanche tubulosa* by high-speed shearing homogenization extraction. *J. AOAC. Int.* 102, 63–68. doi: 10.5740/jaoacint.18-0039
- Phungpanya, C., Chaipuang, A., Machan, T., Watla-ia, K., Thongpoon, C., and Suwanton, O. (2018). Synthesis of prednisolone molecularly imprinted polymer nanoparticles by precipitation polymerization. *Polym. Adv. Technol.* 29, 3075–3084. doi: 10.1002/pat.4428
- Si, Z., Yu, P., Dong, Y., Lu, Y., Ta, Z., Yu, X., et al. (2019). Thermo-responsive molecularly imprinted hydrogels for selective adsorption and controlled release of phenol from aqueous solution. *Front. Chem.* 6:674. doi: 10.3389/fchem.2018.00674
- Singh, M., Kumar, A., and Tarannum, N. (2013). Water-compatible 'aspartame'-imprinted polymer grafted on silica surface for selective recognition in aqueous solution. *Anal. Bioanal. Chem.* 405, 4245–4252. doi: 10.1007/s00216-013-6812-6
- Sobiech, M., Bujak, P., Lulinski, P., and Pron, A. (2019). Semiconductor nanocrystal-polymer hybrid nanomaterials and their application in molecular imprinting. *Nanoscale* 11, 12030–12074. doi: 10.1039/C9NR02585E
- Sobiech, M., Lulinski, P., Halik, P., and Maciejewska, D. (2017). The selective response of a templated polymer for the cationic drug pentamidine: implications from molecular simulations and experimental data. *RSC Adv.* 7, 46881–46893. doi: 10.1039/C7RA07590A
- Sobiech, M., Zolek, T., Lulinski, P., and Maciejewska, D. (2014). A computational exploration of imprinted polymer affinity based on voriconazole metabolites. *Analyst* 139, 1779–1788. doi: 10.1039/c3an01721d
- Speltini, A., Scalabrini, A., Maraschi, F., Sturini, M., and Profumo, A. (2017). Newest applications of molecularly imprinted polymers for extraction of contaminants from environmental and food matrices: a review. *Anal. Chim. Acta* 974, 1–26. doi: 10.1016/j.aca.2017.04.042
- Vicario, A., Solari, M., Felici, E., Aragon, L., Bertolino, F., and Gomez, M. R. (2018). Molecular imprinting on surface of silica particles for the selective extraction of benzylparaben in flow system applied to cosmetics and water samples. *Microchem. J.* 142, 329–334. doi: 10.1016/j.microc.2018.06.031
- Wang, H., Yuan, L., Zhu, H., Jin, R., and Xing, J. (2019). Comparative study of capsaicin molecularly imprinted polymers prepared by different polymerization methods. *J. Polym. Sci. Pol. Chem.* 57, 157–164. doi: 10.1002/pola.29281
- Wang, H. B., Ma, F., Zhou, L., Qian, Y., Sun, Y. S., Xu, Y. K., et al. (2019). Polar surface dominated octagonal Sn doped ZnO nanowires and their room-temperature photoluminance properties. *Appl. Surf. Sci.* 476, 265–270. doi: 10.1016/j.apsusc.2018.12.282
- Wang, S., Li, X., Wu, H., Tian, Z., Xin, Q., He, G., et al. (2016). Advances in high permeability polymer-based membrane materials for CO<sub>2</sub> separations. *Energy Environ. Sci.* 9, 1863–1890. doi: 10.1039/C6EE00811A
- Wang, X., Wang, X., and Guo, Y. (2017). Rapidly simultaneous determination of six effective components in *Cistanche tubulosa* by near infrared spectroscopy. *Molecules* 22, 843–843. doi: 10.3390/molecules22050843
- Wang, Y., Wang, Y., and Liu, H. (2019). A novel fluorescence and SPE adsorption nanomaterials of molecularly imprinted polymers based on quantum dot-grafted covalent organic frameworks for the high selectivity and sensitivity detection of ferulic acid. *Nanomaterials* 9:305. doi: 10.3390/nano9020305
- Wang, Y. J., Zhou, S. M., Xu, G., and Gao, Y. Q. (2015). Interference of phenylethanoid glycosides from *Cistanche tubulosa* with the MTT assay. *Molecules* 20, 8060–8071. doi: 10.3390/molecules20058060
- Wu, C. J., Chien, M. Y., Lin, N. H., Lin, Y. C., Chen, W. Y., Chen, C. H., et al. (2019). Echinacoside isolated from *Cistanche tubulosa* putatively stimulates growth hormone secretion via activation of the ghrelin receptor. *Molecules* 24, 720–720. doi: 10.3390/molecules24040720
- Wu, Y., Ma, Y., Pan, J., Gu, R., and Luo, J. (2017). Porous and magnetic molecularly imprinted polymers via pickering high internal phase emulsions polymerization for selective adsorption of lambda-cyhalothrin. *Front. Chem.* 5:18. doi: 10.3389/fchem.2017.00018
- Xiao, D., Jiang, Y., and Bi, Y. (2018). Molecularly imprinted polymers for the detection of illegal drugs and additives: a review. *Microchim. Acta.* 185:247. doi: 10.1007/s00604-018-2735-4
- Xu, H. T., Zhang, C. G., He, Y. Q., Shi, S. S., Wang, Y. L., and Chou, G. X. (2019). Phenylethanoid glycosides from the *Schnabelia nepetifolia* (Benth.) PDCantino promote the proliferation of osteoblasts. *Phytochemistry* 164, 111–121. doi: 10.1016/j.phytochem.2019.05.003
- Xu, J., Medina-Rangel, P. X., Haupt, K., and Tse Sum Bui, B. (2017). Guide to the preparation of molecularly imprinted polymer nanoparticles for protein recognition by solid-phase synthesis. *Method Enzymol.* 590, 115–141. doi: 10.1016/bs.mie.2017.02.004
- Yan, Y., Song, Q., Chen, X., Li, J., Li, P., Wang, Y., et al. (2017). Simultaneous determination of components with wide polarity and content ranges in *Cistanche tubulosa* using serially coupled reverse phase-hydrophilic interaction chromatography-tandem mass spectrometry. *J. Chromatogr. A* 1501, 39–50. doi: 10.1016/j.chroma.2017.04.034
- Yang, J., Li, Y., Huang, C., Jiao, Y., and Chen, J. (2018). A phenolphthalein-dummy template molecularly imprinted polymer for highly selective extraction and clean-up of bisphenol a in complex biological, environmental and food samples. *Polymers* 10:1150. doi: 10.3390/polym10101150
- Yang, J., Xu, H., Wu, S., Ju, B., Zhu, D., Yan, Y., et al. (2017). Preparation and evaluation of microemulsion-based transdermal delivery of *Cistanche tubulosa* phenylethanoid glycosides. *Mol. Med. Rep.* 15, 1109–1116. doi: 10.3892/mmr.2017.6147
- Yesilova, E., Osman, B., Kara, A., and Ozer, E. T. (2018). Molecularly imprinted particle embedded composite cryogel for selective tetracycline adsorption. *Separ. Purif. Technol.* 200, 155–163. doi: 10.1016/j.seppur.2018.02.002
- Yoshikawa, M., Tharpa, K., and Dima, S. O. (2016). Molecularly imprinted membranes: past, present, and future. *Chem. Rev.* 116, 11500–11528. doi: 10.1021/acs.chemrev.6b00098
- Yu, M., Wu, L., Miao, J., Wei, W., Liu, A., and Liu, S. (2019). Titanium dioxide and polypyrrole molecularly imprinted polymer nanocomposites based electrochemical sensor for highly selective detection of p-nonylphenol. *Anal. Chim. Acta* 1080, 84–94. doi: 10.1016/j.aca.2019.06.053
- Zhang, H., Dai, B., Wang, X., Li, W., Han, Y., Gu, J., et al. (2013). Non-mercury catalytic acetylene hydrochlorination over bimetallic Au-Co(III)/SAC catalysts for vinyl chloride monomer production. *Green Chem.* 15, 829–836. doi: 10.1039/c3gc36840h
- Zhang, H., Guo, R., Hou, J., Wei, Z., and Li, X. (2016). Mixed-matrix membranes containing carbon nanotubes composite with hydrogel for efficient CO<sub>2</sub> separation. *ACS Appl. Mater. Interfaces* 8, 29044–29051. doi: 10.1021/acsami.6b09786
- Zhang, H., Guo, R., Zhang, J., and Li, X. (2018a). Facilitating CO<sub>2</sub> transport across mixed matrix membranes containing multifunctional nanocapsules. *ACS Appl. Mater. Interfaces* 10, 43031–43039. doi: 10.1021/acsami.8b15269



- Zhang, H., Tian, H., Zhang, J., Guo, R., and Li, X. (2018b). Facilitated transport membranes with an amino acid salt for highly efficient CO<sub>2</sub> separation. *Int. J. Greenh. Gas Con.* 78, 85–93. doi: 10.1016/j.ijggc.2018.07.014
- Zhang, Y., Lu, Y., Zhong, J., Li, W., Wei, Q., and Wang, K. (2019). Molecularly imprinted polymer microspheres prepared via the two-step swelling polymerization for the separation of lincomycin. *J. Appl. Polym. Sci.* 136:47938. doi: 10.1002/app.47938
- Zhao, F., Wang, S., She, Y., Zhang, C., Zheng, L., Jin, M., et al. (2017). Subcritical water extraction combined with molecular imprinting technology for sample preparation in the detection of triazine herbicides. *J. Chromatogr. A* 1515, 17–22. doi: 10.1016/j.chroma.2017.06.011

**Conflict of Interest:** The authors declare that the research was conducted in the absence of any commercial or financial relationships that could be construed as a potential conflict of interest.

Copyright © 2020 Zhao, Pei, Guo and Li. This is an open-access article distributed under the terms of the Creative Commons Attribution License (CC BY). The use, distribution or reproduction in other forums is permitted, provided the original author(s) and the copyright owner(s) are credited and that the original publication in this journal is cited, in accordance with accepted academic practice. No use, distribution or reproduction is permitted which does not comply with these terms.



# Fungi as a Potential Source of Pigments: Harnessing Filamentous Fungi

Rishu Kalra<sup>1</sup>, Xavier A. Conlan<sup>2</sup> and Mayurika Goel<sup>1\*</sup>

<sup>1</sup> Division of Sustainable Agriculture, TERI-Deakin Nanobiotechnology Centre, The Energy and Resources Institute, Gurugram, India, <sup>2</sup> School of Life and Environmental Sciences, Deakin University, Geelong, VIC, Australia

## OPEN ACCESS

### Edited by:

Ana Carolina De Aguiar,  
Campinas State University, Brazil

### Reviewed by:

Matthew Shawkey,  
Ghent University, Belgium  
Yanis Caro,  
Université de la Réunion, France  
Mireille Fouillaud,  
Université de la Réunion, France

### \*Correspondence:

Mayurika Goel  
mayurikagoel@gmail.com;  
mayurika.goel@teri.res.in

### Specialty section:

This article was submitted to  
Green and Sustainable Chemistry,  
a section of the journal  
Frontiers in Chemistry

Received: 15 January 2020

Accepted: 08 April 2020

Published: 08 May 2020

### Citation:

Kalra R, Conlan XA and Goel M (2020)  
Fungi as a Potential Source of  
Pigments: Harnessing Filamentous  
Fungi. *Front. Chem.* 8:369.  
doi: 10.3389/fchem.2020.00369

The growing concern over the harmful effects of synthetic colorants on both the consumer and the environment has raised a strong interest in natural coloring alternatives. As a result the worldwide demand for colorants of natural origin is rapidly increasing in the food, cosmetic and textile sectors. Natural colorants have the capacity to be used for a variety of industrial applications, for instance, as dyes for textile and non-textile substrates such as leather, paper, within paints and coatings, in cosmetics, and in food additives. Currently, pigments and colorants produced through plants and microbes are the primary source exploited by modern industries. Among the other non-conventional sources, filamentous fungi particularly ascomycetous and basidiomycetous fungi (mushrooms), and lichens (symbiotic association of a fungus with a green alga or cyanobacterium) are known to produce an extraordinary range of colors including several chemical classes of pigments such as melanins, azaphilones, flavins, phenazines, and quinines. This review seeks to emphasize the opportunity afforded by pigments naturally found in fungi as a viable green alternative to current sources. This review presents a comprehensive discussion on the capacity of fungal resources such as endophytes, halophytes, and fungi obtained from a range of sources such as soil, sediments, mangroves, and marine environments. A key driver of the interest in fungi as a source of pigments stems from environmental factors and discussion here will extend on the advancement of greener extraction techniques used for the extraction of intracellular and extracellular pigments. The search for compounds of interest requires a multidisciplinary approach and techniques such as metabolomics, metabolic engineering and biotechnological approaches that have potential to deal with various challenges faced by pigment industry.

**Keywords:** fungi, pigments, endophytes, lichen, halophytes

## INTRODUCTION

Color is both the first and most pleasing feature an individual notices when approaching food and this feature is known to be associated with the flavor, safety, and nutritional value of the food item in question (Pathare et al., 2013; Spence, 2015). This has been a consistent theme throughout history with the ancient Egyptians and Romans around 1500 B.C describing the concept food colors and how they relate to bioactivity (Adam Burrows, 2009). Initially nature was the only source of food colors (Rohrig, 2016; Yusuf et al., 2017), however, the high cost of extraction and instability

of the traditionally natural colors drove the development of synthetic colors during the 1800s. Perkin's mauve pigment was the first synthetic color discovered by English chemist Sir William Henry Perkin in 1856 (Garfield, 2002). This discovery led to the foundation of new era of synthetic dyes commonly known as "coal-tar colors," derived from aniline and other organic compounds. These synthetic colors were widely used in industries having an impact in textiles, cosmetics and pharmaceuticals (Morris and Travis, 1992; Adam Burrows, 2009). More, serious apprehensions against synthetic colors were raised in 2007 after a study at University of Southampton highlighted the link between some artificial colors and hyperactivity in children (McCann et al., 2007; Arnold et al., 2012). These colors known as "the Southampton six" including sunset yellow FCF (E110), quinolone yellow (E104), carmoisine (E122), allura red (E129), tartrazine (E102), and ponceau 4R (E124) became the focus of the impact of colorants on humans.

In 2010, European Union (EU) regulators directed compulsory warnings on children's food labeling and recommended the limited acceptable daily consumption levels of some colourings. Similarly, organizations like the United States Food and Drug Administration (US-FDA) and World Health Organization (WHO) also regulated the usage of these colors in food, drugs, and cosmetic items. With the advent of the various issues associated with the over use of synthetic pigments, intense research in natural color dyes has been initiated in recent years (Mapari et al., 2010; Aberoumand, 2011; FDA, 2011; Harasym and Bogacz-Radomska, 2016; Mehrad et al., 2018; Duarte et al., 2019).

Natural food coloring is a major focus of the modern food manufacture industry and is an ever growing market allowing an increase in research in this space (Faustino et al., 2019). This has been led by growing customer awareness and demand for products without synthetic colorants and has fueled the growth of natural color industry. Natural food color not only gives an appealing and appetizing look but might also possesses nutritional and health benefits (Delgado-Vargas and Paredes-Lopez, 2003; Bora et al., 2019). Nature has always been considered a treasure trove of organisms comprising plants, animals, and microorganisms with a capacity to produce pigments. Some of the established natural pigments that are frequently employed to provide color to food and are considered safe include anthocyanins, carotenoids, betalains, chlorophylls, and curcumin (Mortensen, 2006; Socaciu, 2007; Gengatharan et al., 2015; Janiszewska-Turak et al., 2016; Corrêa et al., 2019). These components not only provide the coloring property to the food industry but also enhance the nutritious and pharmacological potential of the food product through primarily acting as antioxidants. Detailed studies on the characteristics and properties of these natural pigments has been conducted and discussed by research groups, however the potential of these pigments as a source of new commercial pigments is limited by a number of factors. Some of the challenges which the natural color industry is facing include raw material availability and the

stability and sensitivity of these natural pigments toward various external parameters (Scotter, 1995; Mercadante, 2007; Galaffu et al., 2015). To better understand the opportunity for colors from natural sources what is known about the well-studied plants and animal sources needs to be extended into microorganisms which have the potential as a source for biopigments production (Sen et al., 2019).

Pigments produced from microbial origin have several advantages over those obtained from plant or animal including supply sustainability; yield; cost efficiency; stability; labor cost and ease of downstream processing (Joshi et al., 2003; Tuli et al., 2015). Innumerable reports are available on the application of various biotechnological tools for the isolation of a plethora of new colors from microbial origin (Joshi and Attri, 2005; Rymbai et al., 2011; Gharibzahedi et al., 2012). Among various microbial alternatives, microalgae and fungi produce a remarkable range of water soluble biopigments that have a range of ecological functions (Gmoser et al., 2017; Heer and Sharma, 2017), however, lower harvest yields of the algal cultures is the major bottleneck to exploit its potential for commercial production (Hejazi and Wijffels, 2004). In efforts to utilize fungi for biopigment production, basidiomycetous fungi which have been utilized by ancient cultures for dyeing silk and wool (Hernández et al., 2019) have been studied. However, bulk production of these fungi for commercial purpose is not feasible. Thus, the industry is more focussed on filamentous fungi which can be easily grown in lab and allowed for the opportunity for large scale production. This include fungi from a broad range of environments of marine origin, soil endophytic fungi from terrestrial and marine flora and endolichenic fungus (Mapari et al., 2010; Gao et al., 2013; Dufosse et al., 2014).

Many colors produced by the filamentous fungi for example ankaflavin and canthaxanthin from *Monascus* sp. and Arpink red™ pigment (Natural red™) from the strain *Penicillium oxalicum* var. *armeniaca* are already in the market (Mapari et al., 2009). Though natural colors have taken a lead in comparison to the synthetic ones in a rapidly changing industry, the exploration of fungal based pigments still needs attention toward their potential as future industrial pigment. This review will highlight the potential filamentous fungi sources that have the capacity to be explored in order to produce these pigments, their application as commercial natural colorants and challenges faced by the industry for the commercial application of these pigments. Focus will be given to the advanced analytical techniques that are currently used to identify novel pigment components and how these techniques can be applied to study the biosynthetic pathway. In addition to these, metabolic engineering approaches that have the potential to enable the mass production of the fungal resources of colorants for a broad range of industries will also be studied. Further newer greener and sustainable extraction techniques used for the isolation of the pigments for industrial application will be explored highlighting the emerging green economy.

## FUNGI AS A SOURCE OF PIGMENTS

Increasing demand, limited resources and various disadvantages associated with the currently authorized natural pigments such as limited availability throughout the year, instability against light, heat and adverse pH, variation in pigment extraction and low water solubility, demands new research into the sustainable sources of natural colorants. Recently, fungi have attracted special attention for the production of natural pigments based on the fact that they contain compounds with high light and chemical stability, a spectrum of colors, high yield and a sustainable supply (Durán et al., 2002; Fouillaud et al., 2016; Chen et al., 2017).

Pigments production by fungal colonies has kindled interest among mycologist since the 19th century and can be considered a microbial reserve for the production of food grade pigments. Fungi are known to produce a wide array of pigments which includes metabolites from several classes such as melanins, anthraquinones, hydroxyanthraquinones, azaphilones, carotenoids, oxopolyene, quinones and naphthoquinone (Figure 1) (Mapari et al., 2005; Osmanova et al., 2010; Xie et al., 2016; Chuyen and Eun, 2017; Pombeiro-Sponchiado et al., 2017). In Figure 1 some of the shades and colors hues produced by different class of metabolites and their basic chemical structures can be observed. Arpink red™ pigment (Natural red™) which is the first commercial red color from a fungus has been produced from the strain *Penicillium oxalicum* var. *armeniaca* CCM 8242 isolated from soil (Caro et al.,

2017). Biosynthetically, many of these pigments are polyketides derivatives which are produced abundantly in the majority of the ascomycetous fungi. g *Neurospora* spp. and *Monascus* spp. are such examples of ascomycetes fungi highlighting a key area for further development. Besides, polyketide based molecules; other classes of pigmented metabolites present in various filamentous fungi are terpenoids, polyphenols, and carotenoids. To gain an understanding of the breadth of color afforded by these molecules some of the common pigments produced by these species are displayed in Table 1.

Many of these natural pigments are found to have a range of pharmacological activities and help fungi in various biological roles such as compounds acting as enzyme cofactors (flavins) (Rao et al., 2017); prevention against the harmful effects of photo-oxidation (carotenoids) (Gmoser et al., 2017) and the protection against environmental stress (melanins) (Dufosse et al., 2014). Though these fungal pigments have been found to be associated with diverse biological activities, the physiological role and factors regulating their production are largely unstudied (Sen et al., 2019). Recent advances in analytical and biotechnological tools employing computational and molecular means helps in deciphering the components responsible for color production, their *de novo* pathway and genome responsible for its production. Concurrently, alternative routes for mass production of these metabolites may be achieved using heterologous expression. Manipulation of culture conditions and co-culturing can also help to enhance the expression and yield of a particular pigment.

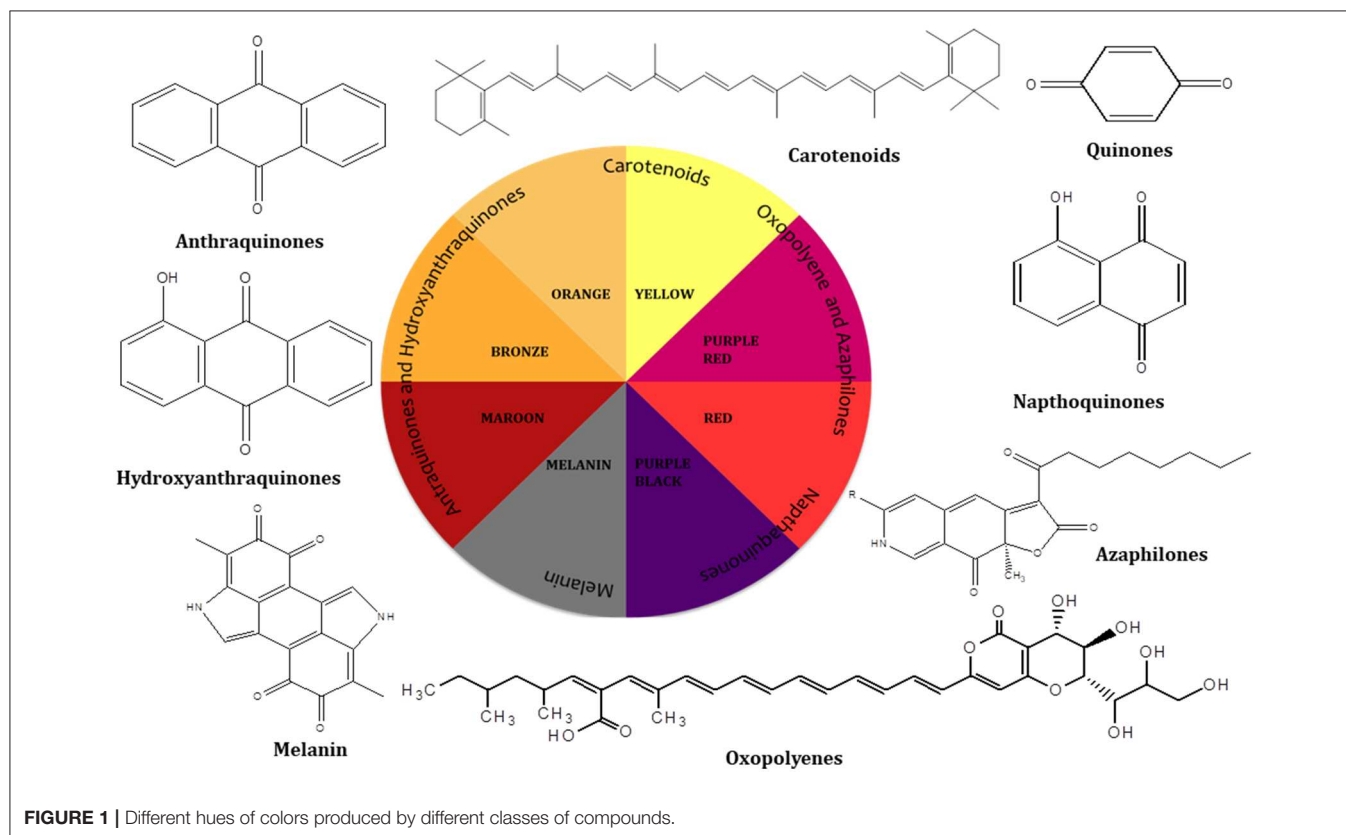


**FIGURE 1** | Different hues of colors produced by different classes of compounds.

**TABLE 1** | Examples of selected pigments produced by different fungal species grouped with respect to genus producing them.

S.no.	Fungal/lichen species	Pigment	Class of compound	Pigments color	Molecular formula and weight	References
1.	<i>Alternaria solani</i> , <i>Alternaria porri</i> , <i>Alternaria tomatophila</i>	Altersolanol A	Hydroxyanthraquinone	Yellow	C <sub>16</sub> H <sub>16</sub> O <sub>8</sub> ; 336.3	Andersen et al., 2008
2.	<i>Alternaria</i> sp. ZJ9-6B	Alterporriol K	Anthraquinone	Red	C <sub>32</sub> H <sub>26</sub> O <sub>10</sub> ; 586.14	Huang et al., 2011
3.	<i>Alternaria</i> sp. ZJ9-6B	Alterporriol L	Anthraquinone	Red	C <sub>32</sub> H <sub>26</sub> O <sub>12</sub> ; 602.54	Huang et al., 2011
4.	<i>Alternaria</i> sp. ZJ9-6B	Alterporriol M	Anthraquinone	Red	C <sub>32</sub> H <sub>25</sub> O <sub>12</sub> ; 601.13	Huang et al., 2011
5.	<i>Alternaria</i> sp. ZJ9-6B	Macrosporin	Hydroxyanthraquinone	Yellow	C <sub>16</sub> H <sub>12</sub> O <sub>5</sub> ; 284.2	Huang et al., 2011
6.	<i>Alternaria</i> sp. ZJ9-6B	Dactylariol	Hydroxyanthraquinone	Not mentioned	C <sub>16</sub> H <sub>16</sub> O <sub>7</sub> ; 320.2	Huang et al., 2011
7.	<i>Alternaria</i> sp. ZJ9-6B	Tetrahydroaltersolanol B	Hydroxyanthraquinone	Not mentioned	C <sub>16</sub> H <sub>20</sub> O <sub>6</sub> ; 308.3	Huang et al., 2011
8.	<i>Alternaria</i> sp. (SK11)	Alterporriols C	Hydroxyanthraquinone	Orange	C <sub>32</sub> H <sub>26</sub> O <sub>13</sub> ; 618.5	Xia et al., 2014
9.	<i>Amygdalaria panaeola</i>	Panaefluorolines A	Isoquinoline	Yellowish green	C <sub>19</sub> H <sub>24</sub> NO <sub>4</sub> <sup>+</sup> ; 330.4	Kinoshita et al., 2003
10.	<i>Amygdalaria panaeola</i>	Panaefluorolines B	Isoquinoline	Yellowish green	C <sub>17</sub> H <sub>20</sub> NO <sub>4</sub> <sup>+</sup> ; 302.34	Kinoshita et al., 2003
11.	<i>Amygdalaria panaeola</i>	Panaefluorolines C	Isoquinoline	Yellowish green	C <sub>18</sub> H <sub>22</sub> NO <sub>4</sub> <sup>+</sup> ; 316.4	Kinoshita et al., 2003
12.	<i>Aspergillus sulphureus</i>	Viopurpurin	Naphtoquinones	Purple	C <sub>29</sub> H <sub>20</sub> O <sub>11</sub> ; 544.5	Durley et al., 1975
13.	<i>Aspergillus sulphureus</i>	Rubrosulfin	Naphtoquinones	Red	C <sub>29</sub> H <sub>20</sub> O <sub>10</sub> ; 528.5	Durley et al., 1975; Stack et al., 1977
14.	<i>Aspergillus ochraceus</i>	Viomellein	Quinone	Reddish-brown	C <sub>30</sub> H <sub>24</sub> O <sub>11</sub> ; 560.50	Stack and Mislivec, 1978
15.	<i>Aspergillus ochraceus</i>	Xanthomegnin	Dihydroisocoumarin	Orange	C <sub>30</sub> H <sub>22</sub> O <sub>12</sub> ; 574.48	Stack and Mislivec, 1978; Frisvad et al., 2004,
16.	<i>Aspergillus glaucus</i>	Catenarin	Hydroxyanthraquinone	Red	C <sub>15</sub> H <sub>10</sub> O <sub>6</sub> ; 286.2	Anke et al., 1980
17.	<i>Aspergillus glaucus</i>	Rubrocristin	Hydroxyanthraquinone	Red	C <sub>16</sub> H <sub>12</sub> O <sub>6</sub> ; 300.3	Anke et al., 1980
18.	<i>Aspergillus glaucus</i> , <i>Aspergillus cristatus</i> , <i>Aspergillus repens</i>	Erythroglauclin	Hydroxyanthraquinone	Red	C <sub>16</sub> H <sub>12</sub> O <sub>6</sub> ; 300.26	Durán et al., 2002
19.	<i>Aspergillus glaucus</i>	Aspergiolide B	Hydroxyanthraquinone	Red	C <sub>26</sub> H <sub>17</sub> O <sub>9</sub> ; 473.08	Du et al., 2008
20.	<i>Aspergillus variegator</i>	Variegatorquinone A	Quinone	Yellow	C <sub>20</sub> H <sub>17</sub> O <sub>9</sub> ; 401.08	Wang et al., 2007
21.	<i>Aspergillus variegator</i>	Variegatorquinone A	Quinone	Yellow	C <sub>17</sub> H <sub>15</sub> O <sub>6</sub> ; 315.08	Wang et al., 2007
22.	<i>Aspergillus</i> sp. strain 05F16	Bostrycin	Anthraquinone	Red	C <sub>16</sub> H <sub>16</sub> O <sub>8</sub> ; 336.29	Xu et al., 2008
23.	<i>Aspergillus</i> sp. strain 05F16	Tetrahydrobostrycin	Anthraquinone	Yellow	C <sub>16</sub> H <sub>21</sub> O <sub>8</sub> ; 341.12	Xu et al., 2008
24.	<i>Aspergillus</i> sp. strain 05F16	1-deoxytetrahydrobostrycin	Anthraquinone	Yellow	C <sub>16</sub> H <sub>21</sub> O <sub>7</sub> ; 325.12	Xu et al., 2008
25.	<i>Aspergillus fumigatus</i>	Melanin	1,8-dihydroxynaphthalene	Dark-brown	C <sub>18</sub> H <sub>10</sub> N <sub>2</sub> O <sub>4</sub> ; 318.28	Gonçalves et al., 2012
26.	<i>Aspergillus niger</i>	Azanigerones B	Azaphilones	Yellow	C <sub>21</sub> H <sub>28</sub> O <sub>6</sub> ; 376.44	Zabala et al., 2012

(Continued)



TABLE 1 | Continued

S.no.	Fungal/lichen species	Pigment	Class of compound	Pigments color	Molecular formula and weight	References
27.	<i>Aspergillus niger</i>	Azanigerones C	Azaphilones	Yellow	C <sub>21</sub> H <sub>26</sub> O <sub>7</sub> ; 390.43	Zabala et al., 2012
28.	<i>Aspergillus glaucus</i>	Physcion	Hydroxyanthraquinone	Yellow	C <sub>16</sub> H <sub>12</sub> O <sub>5</sub> ; 284.3	Gessler et al., 2013
29.	<i>Aspergillus nidulans</i>	Emodin	Hydroxyanthraquinone	Yellow	C <sub>15</sub> H <sub>10</sub> O <sub>5</sub> ; 270.2	Gessler et al., 2013
30.	<i>Blakeslea trispora</i>	Lycopene	Carotenoids	Red	C <sub>40</sub> H <sub>56</sub> ; 536.87	Wang et al., 2012
31.	<i>Blakeslea trispora</i>	β-carotene	Carotenoids	Yellow-orange	C <sub>40</sub> H <sub>56</sub> ; 536.87	Yan et al., 2013
32.	<i>Curvularia lunata</i>	Chrysophanol	Hydroxyanthraquinone	Orange-red	C <sub>15</sub> H <sub>10</sub> O <sub>4</sub> ; 254.2	Durán et al., 2002
33.	<i>Curvularia lunata</i>	Cynodontin	Hydroxyanthraquinone	Bronze	C <sub>15</sub> H <sub>10</sub> O <sub>6</sub> ; 286.2	Durán et al., 2002
34.	<i>Curvularia lunata</i>	Erythroglauclin	Hydroxyanthraquinon	Red	C <sub>16</sub> H <sub>12</sub> O <sub>6</sub> ; 300.26	Caro et al., 2017
35.	<i>Dreschlera teres</i> , <i>Dreschlera dictyoides</i> , <i>Dreschlera avenae</i> .	Helminthosporin	Hydroxyanthraquinone	Maroon	C <sub>15</sub> H <sub>10</sub> O <sub>5</sub> ; 270.2	Durán et al., 2002
36.	<i>Dreschlera teres</i> , <i>Dreschlera dictyoides</i> , <i>Dreschlera avenae</i> .	Catenarin	Hydroxyanthraquinon	Red	C <sub>15</sub> H <sub>10</sub> O <sub>6</sub> ; 286.2	Durán et al., 2002
37.	<i>Dreschlera teres</i> , <i>Dreschlera dictyoides</i> , <i>Dreschlera avenae</i> .	Tritisporin	Hydroxyanthraquinon	Brownish-red	C <sub>15</sub> H <sub>10</sub> O <sub>4</sub> ; 254.2	Durán et al., 2002
38.	<i>Daldinia concentrica</i>	Daldinin A	Azaphilones	Yellow	C <sub>15</sub> H <sub>18</sub> O <sub>5</sub> Na; 301.1	Shao et al., 2008
39.	<i>Daldinia concentrica</i>	Daldinin B	Azaphilones	Yellow	C <sub>15</sub> H <sub>18</sub> O <sub>4</sub> ; 285.1	Shao et al., 2008
40.	<i>Daldinia concentrica</i>	Daldinin C	Azaphilones	Yellow	C <sub>15</sub> H <sub>21</sub> O <sub>4</sub> ; 265.1	Shao et al., 2008
41.	<i>Emericella purpurea</i>	Epurpurins A	Dicyanide derivatives	Greenish-yellow	C <sub>28</sub> H <sub>28</sub> N <sub>2</sub> O <sub>2</sub> ; 424	Takahashi et al., 1996
42.	<i>Emericella purpurea</i>	Epurpurins B	Dicyanide derivatives	Greenish-yellow	C <sub>23</sub> H <sub>20</sub> N <sub>2</sub> O <sub>2</sub> ; 356.19	Takahashi et al., 1996
43.	<i>Emericella purpurea</i>	Epurpurins C	Dicyanide derivatives	Greenish-yellow	C <sub>18</sub> H <sub>12</sub> N <sub>2</sub> O <sub>2</sub> ; 288.08	Takahashi et al., 1996
44.	<i>Emericella falconensis</i> and <i>Emericella fructiculosa</i>	Falconensin A	Azaphilones	Yellow	C <sub>23</sub> H <sub>23</sub> O <sub>6</sub> Cl <sub>2</sub> ; 466.33	Ogasawara et al., 1997
45.	<i>Emericella falconensis</i> and <i>Emericella fructiculosa</i>	Falconensin E	Azaphilones	Yellow	C <sub>23</sub> H <sub>25</sub> O <sub>7</sub> Cl; 448.9	Ogasawara et al., 1997
46.	<i>Eurotium amstelodami</i>	Erythroglauclin	Hydroxyanthraquinone	Red	C <sub>16</sub> H <sub>12</sub> O <sub>6</sub> ; 300.26	Podojil et al., 1978
47.	<i>Eurotium repens</i>	Auroglauclin	Hydroquinones	Orange-red	C <sub>19</sub> H <sub>22</sub> O <sub>3</sub> ; 304.4	Podojil et al., 1978
48.	<i>Eurotium repens</i>	Physcion	Hydroxyanthraquinone	Yellow	C <sub>16</sub> H <sub>12</sub> O <sub>5</sub> ; 284.3	Podojil et al., 1978
49.	<i>Eurotium rubrum</i> and <i>Eurotium cristatum</i>	Rubrocristin	Hydroxyanthraquinone	Red	C <sub>16</sub> H <sub>12</sub> O <sub>6</sub> ; 300.3	Anke et al., 1980
50.	<i>Eurotium chevalieri</i>	Flavoglaucin	Hydroquinones	Yellow	C <sub>19</sub> H <sub>28</sub> O <sub>3</sub> ; 304.4	Ishikawa et al., 1984
51.	<i>Eurotium rubrum</i> and <i>Eurotium cristatum</i>	Catenarin	Hydroxyanthraquinone	Red	C <sub>15</sub> H <sub>10</sub> O <sub>6</sub> ; 286.2	Durán et al., 2002
52.	<i>Eurotium sp</i>	Isodihydroauroglauclin	Hydroquinones	Orange	C <sub>19</sub> H <sub>24</sub> O <sub>3</sub> ; 300.4	Gawas et al., 2002

(Continued)

TABLE 1 | Continued

S.no.	Fungal/lichen species	Pigment	Class of compound	Pigments color	Molecular formula and weight	References
53.	<i>Eurotium sp.</i>	Tetrahydroauroglauclin	Hydroquinones	Yellow	C <sub>19</sub> H <sub>26</sub> O <sub>3</sub> ; 302.4	Gawas et al., 2002
54.	<i>Eurotium rubrum</i>	3-O-( $\alpha$ -D-ribofuranosyl)-questin	Hydroxyanthraquinone	Orange	C <sub>21</sub> H <sub>19</sub> O <sub>9</sub> ; 415.10	Li et al., 2009
55.	<i>Eurotium rubrum</i>	Asperflavin	Hydroxyanthraquinone	Greenish	C <sub>16</sub> H <sub>16</sub> O <sub>5</sub> ; 288.29	Li et al., 2009
56.	<i>Eurotium rubrum</i>	2-O-methyleurotinone	Eurotinone analogs	Not mentioned	C <sub>16</sub> H <sub>14</sub> O <sub>6</sub> ; 302.27	Li et al., 2009
57.	<i>Fusarium fujikuroi</i>	Norbikaverin	Benzoxanthentrione	Red	C <sub>19</sub> H <sub>12</sub> O <sub>8</sub> ; 368.29	Kjær et al., 1971; Medentsev and Akimenko, 1998
58.	<i>Fusarium fujikuroi</i>	Bikaverin	Benzoxanthentrione	Red	C <sub>20</sub> H <sub>14</sub> O <sub>8</sub> ; 382.32	Kjær et al., 1971; Wiemann et al., 2009
59.	<i>Fusarium fujikuroi</i>	$\beta$ -carotene	Carotenoids	Red	C <sub>40</sub> H <sub>56</sub> ; 536.87	Avalos et al., 2017
60.	<i>Fusarium oxysporum</i>	13-hydroxynorjavanicin	Naphthoquinone	Red	C <sub>14</sub> H <sub>12</sub> O <sub>7</sub> ; 292.06	Tatum et al., 1985
61.	<i>Fusarium oxysporum</i>	1,4-naphthalenedione-3,8-dihydroxy-5,7-dimethoxy-2-(2-oxopropyl)	Naphthoquinone	Red	C <sub>15</sub> H <sub>14</sub> O <sub>7</sub> ; 306.08	Tatum et al., 1985
62.	<i>Fusarium oxysporum</i>	5-O-methyljavanicin	Naphthoquinone	Red	C <sub>16</sub> H <sub>16</sub> O <sub>6</sub> ; 304.09	Tatum et al., 1985
63.	<i>Fusarium oxysporum</i>	9-O-methylanhydrofusarubin	Naphthoquinone	Purple	C <sub>16</sub> H <sub>14</sub> O <sub>6</sub> ; 302.79	Tatum et al., 1985
64.	<i>Fusarium oxysporum</i>	5-O-methylsolaniol	Naphthoquinone	Red	C <sub>16</sub> H <sub>18</sub> O <sub>6</sub> ; 306.31	Tatum et al., 1985
65.	<i>Fusarium oxysporum</i>	8-O-methylbostrycoidin	Naphthoquinone	Red	C <sub>16</sub> H <sub>13</sub> NO <sup>5</sup> ; 299.08	Tatum et al., 1985
66.	<i>Fusarium oxysporum</i>	8-O-methylanhydrofusarubinlactol	Naphthoquinone	Red	C <sub>16</sub> H <sub>14</sub> O <sub>7</sub> ; 318.07	Tatum et al., 1985
67.	<i>Fusarium culmorum</i>	Aurofusarin	Naphthoquinone	Red	C <sub>30</sub> H <sub>18</sub> O <sub>12</sub> ; 570.46	Medentsev et al., 2005
68.	<i>Fusarium culmorum</i>	Bostrycoidin	Naphthoquinone	Red	C <sub>15</sub> H <sub>11</sub> NO <sub>5</sub> ; 285.26	Medentsev et al., 2005
69.	<i>Fusarium fujikuroi</i>	8-O-methylfusarubin	Naphthoquinone	Red	C <sub>16</sub> H <sub>16</sub> O <sub>7</sub> ; 320.29	Studt et al., 2012
70.	<i>Graphis desquamescens</i>	Graphisquinone	Quinone	Red	C <sub>11</sub> H <sub>10</sub> O <sub>5</sub> ; 222.19	Miyagawa et al., 1994
71.	<i>Graphis scripta</i>	Graphenone	Furandione	Yellow-orange	C <sub>14</sub> H <sub>14</sub> O <sub>4</sub> ; 246.26	Miyagawa et al., 1994
72.	<i>Monascus sp.</i>	Monascin	Azaphilone	Yellow	C <sub>21</sub> H <sub>26</sub> O <sub>5</sub> ; 358.43	Karrer and Helfenstein, 1932; Feng et al., 2012; Wang C. et al., 2017
73.	<i>Monascus rubropunctatus</i>	Rubropunctatin	Azaphilone	Orange	C <sub>21</sub> H <sub>22</sub> O <sub>5</sub> ; 354.39	Haws et al., 1959
74.	<i>Monascus purpureus</i>	Monascorubramine	Azaphilone	Red	C <sub>23</sub> H <sub>27</sub> NO <sub>4</sub> ; 381.46	Fielding et al., 1960
75.	<i>Monascus rubropunctatus</i>	Rubropunctamine	Azaphilone	Red	C <sub>23</sub> H <sub>30</sub> O <sub>5</sub> ; 386.48	Fielding et al., 1960
76.	<i>Monascus purpureus</i>	Monascorubrin	Azaphilone	Orange	C <sub>23</sub> H <sub>26</sub> O <sub>5</sub> ; 382.45	Fielding et al., 1960
77.	<i>Monascus sp.</i>	Ankaflavine	Azaphilone	Yellow	C <sub>23</sub> H <sub>30</sub> O <sub>5</sub> ; 386.48	Mapari et al., 2006

(Continued)

TABLE 1 | Continued

S.no.	Fungal/lichen species	Pigment	Class of compound	Pigments color	Molecular formula and weight	References
78.	<i>Monascus purpureus</i>	Monapilol A	Azaphilone	Orange	C <sub>23</sub> H <sub>29</sub> O <sub>5</sub> ; 385.20	Hsu et al., 2011
79.	<i>Monascus purpureus</i>	Monapilol B	Azaphilone	Orange	C <sub>21</sub> H <sub>25</sub> O <sub>5</sub> ; 357.17	Hsu et al., 2011
80.	<i>Monascus purpureus</i>	Monapilol C	Azaphilone	Orange	C <sub>26</sub> H <sub>33</sub> O <sub>6</sub> ; 441.22	Hsu et al., 2011
81.	<i>Monascus purpureus</i>	Monapilol D	Azaphilone	Orange	C <sub>24</sub> H <sub>29</sub> O <sub>6</sub> ; 413.19	Hsu et al., 2011
82.	<i>Penicillium multicolor</i>	Pencolide	Maleimide	Yellow to orange	C <sub>9</sub> H <sub>9</sub> NO <sub>4</sub> ; 195.174	Birkinshaw et al., 1963
83.	<i>Penicillium frequentans</i>	Questin	Hydroxyanthraquinone	Yellow to orange-brown	C <sub>16</sub> H <sub>12</sub> O <sub>5</sub> ; 284.26	Mahmoodian and Stickings, 1964
84.	<i>Penicillium rubrum</i>	Mitorubrin	Azaphilone	Yellow	C <sub>21</sub> H <sub>18</sub> O <sub>7</sub> ; 382.4	Büchi et al., 1965
85.	<i>Penicillium purpurogenum</i>	Purpurogenone	Quinone	Yellow-orange	C <sub>29</sub> H <sub>20</sub> O <sub>11</sub> ; 544.10	Roberts and Thompson, 1971
86.	<i>Penicillium phoeniceum</i>	Phoenicin	Toluquinone	Yellow	C <sub>14</sub> H <sub>10</sub> O <sub>6</sub> ; 274.23	Steiner et al., 1974
87.	<i>Penicillium cyclopium</i> , <i>Penicillium viridicatum</i>	Xanthomegnin	Dihydroisocoumarin	Orange	C <sub>30</sub> H <sub>22</sub> O <sub>12</sub> ; 574.48	Stack and Mislivec, 1978; Frisvad et al., 2004,
88.	<i>Penicillium cyclopium</i> , <i>Penicillium viridicatum</i>	Viomellein	Quinone	Reddish-brown	C <sub>30</sub> H <sub>24</sub> O <sub>11</sub> ; 560.50	Stack and Mislivec, 1978; Frisvad et al., 2004
89.	<i>Penicillium paraherquei</i>	Atrovenetin	Furanone	Yellow	C <sub>19</sub> H <sub>18</sub> O <sub>6</sub> ; 342.34	Ishikawa et al., 1991
90.	<i>Penicillium</i> sp. AZ.	PP-V, 12-carboxylmonascorubramine	Azaphilone	Purple-red	C <sub>23</sub> H <sub>25</sub> NO <sub>6</sub> ; 412.17	Ogihara et al., 2000
91.	<i>Penicillium</i> sp. AZ.	PP-R, 7-(2-hydroxyethyl)-monascorubramine	Azaphilone	Purple-red	C <sub>25</sub> H <sub>31</sub> N; 426.22	Ogihara et al., 2000
92.	<i>Penicillium oxalicum</i>	Arpink red <sup>TM</sup>	Anthraquinone	Red	C <sub>25</sub> H <sub>26</sub> O <sub>14</sub>	Sardaryan, 2002; Dufossé et al., 2005; Caro et al., 2017
93.	<i>Penicillium bilaii</i>	Citromycetin	Chromene	Yellow	C <sub>14</sub> H <sub>10</sub> O <sub>7</sub> ; 290.22	Capon et al., 2007
94.	<i>Penicillium bilaii</i>	Citromycin	Chromene	Yellow	C <sub>13</sub> H <sub>10</sub> O <sub>5</sub> ; 246.21	Capon et al., 2007
95.	<i>Penicillium bilaii</i>	(-)-2,3-dihydrocitromycetin	Chromene	Yellow	C <sub>14</sub> H <sub>12</sub> O <sub>7</sub> ; 292.24	Capon et al., 2007
96.	<i>Penicillium bilaii</i>	(-)-2,3-dihydrocitromycin	Chromene	Yellow	C <sub>13</sub> H <sub>12</sub> O <sub>5</sub> ; 248.07	Capon et al., 2007
97.	<i>Penicillium purpurogenum</i>	N-glutarylmonascorubramine	Azaphilone	Purple-red	C <sub>28</sub> H <sub>33</sub> NO <sub>8</sub> ; 511.23	Mapari et al., 2009
98.	<i>Penicillium purpurogenum</i>	N-glutarylubropunctamine	Azaphilone	Purple-red	C <sub>26</sub> H <sub>29</sub> NO <sub>8</sub> ; 483.20	Mapari et al., 2009
99.	<i>Penicillium mameffei</i>	Monascorubrin	Azaphilone	Orange	C <sub>23</sub> H <sub>26</sub> O <sub>5</sub> ; 382.45	Woo et al., 2014
100.	<i>Penicillium aculeatum</i>	Ankaflavine	Azaphilone	Yellow	C <sub>23</sub> H <sub>30</sub> O <sub>5</sub> ; 386.48	Krishnamurthy et al., 2018
101.	<i>Phycomyces blakesleeana</i>	β-carotene	Carotenoids	Yellow-orange	C <sub>40</sub> H <sub>56</sub> ; 536.87	Garton et al., 1950
102.	<i>Talaromyces funiculosus</i>	Ravenelin	Xanthone	Yellow	C <sub>14</sub> H <sub>11</sub> O <sub>5</sub> ; 259.06	Padhi et al., 2019

(Continued)

TABLE 1 | Continued

S.no.	Fungal/lichen species	Pigment	Class of compound	Pigments color	Molecular formula and weight	References
103.	<i>Trichoderma aureoviride</i>	Chrysophanol	Hydroxyanthraquinone	Orange-red	C <sub>15</sub> H <sub>10</sub> O <sub>4</sub> ; 254.2	De Stefano and Nicoletti, 1999
104.	<i>Trichoderma harzianum</i>	Emodin	Hydroxyanthraquinone	Yellow	C <sub>15</sub> H <sub>10</sub> O <sub>5</sub> ; 270.2	Lin et al., 2012
105.	<i>Trichoderma harzianum</i>	Pachybasin	Hydroxyanthraquinone	Yellow	C <sub>15</sub> H <sub>10</sub> O <sub>3</sub> ; 238.3	Lin et al., 2012
106.	<i>Trypethelium eluteriae</i>	Trypethelonamide A	Naphthoquinone	Yellow	C <sub>23</sub> H <sub>29</sub> NO <sub>5</sub> ; 400.21	Basnet et al., 2019
107.	<i>Trypethelium eluteriae</i>	5'-hydroxytrypethelone	Naphthoquinone	Violet red	C <sub>16</sub> H <sub>16</sub> O <sub>5</sub> ; 289.10	Basnet et al., 2019
108.	<i>Trypethelium eluteriae</i>	(-)-trypethelone	Naphthoquinone	Violet red	C <sub>16</sub> H <sub>16</sub> O <sub>4</sub> ; 372.29	Basnet et al., 2019
109.	<i>Trypethelium eluteriae</i>	(+)-trypethelone	Naphthoquinone	Violet red	C <sub>16</sub> H <sub>16</sub> O <sub>4</sub> ; 372.29	Basnet et al., 2019
110.	<i>Trypethelium eluteriae</i>	(+)-8-hydroxy-7-methoxytrypethelone	Naphthoquinone	Violet red	C <sub>17</sub> H <sub>19</sub> O <sub>5</sub> ; 303.12	Basnet et al., 2019

Fungi capable of producing pigments can be sourced from diverse environmental conditions and lend them to be explored as a source of commercial pigments (Figure 2).

## DIFFERENT SOURCES OF FUNGI PRODUCING PIGMENTS

### Marine Ecosystems

Fungi derived from marine environments have higher diversity and a unique scaffold of secondary metabolites which helps in their survival and their presence in extreme environmental circumstances such as absence of light, high salinity, high pressure, and low temperature. These circumstances lead to the development of extremophile microorganisms with the capacity to produce some unique molecules (Coker, 2016; Duarte et al., 2019). Fungal isolates from differential marine environment represent a major source of undiscovered pigment potential and should be target areas for commercial investigation.

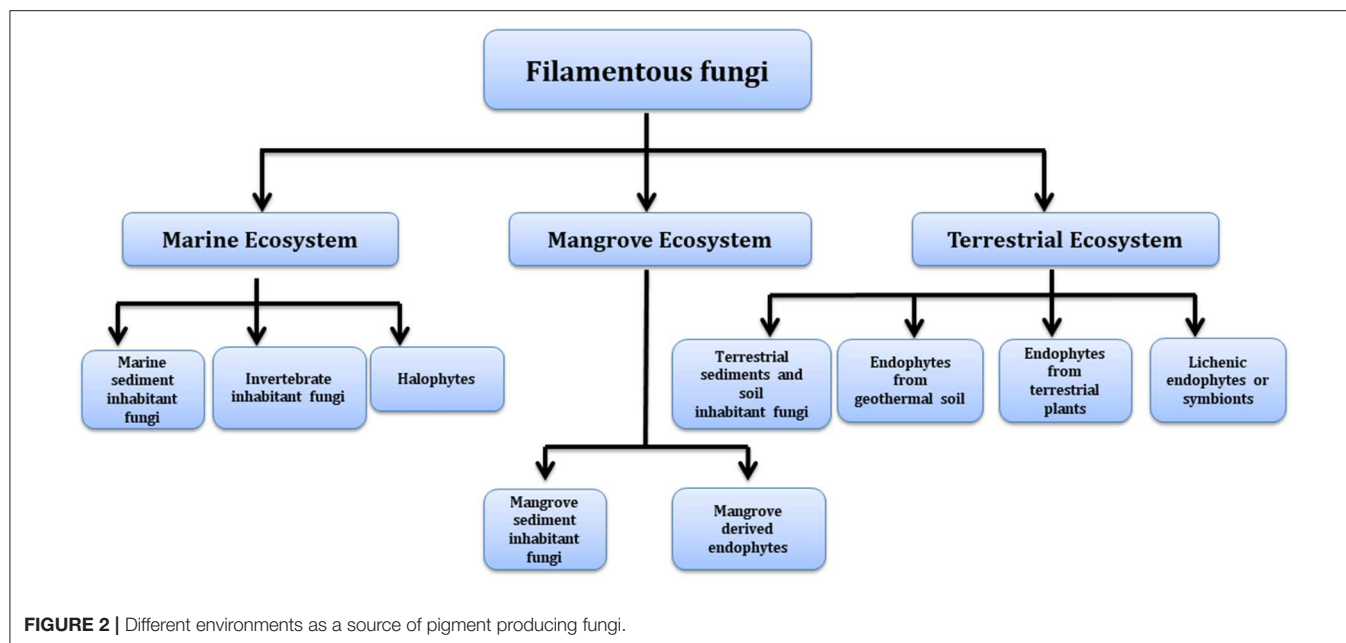
### Marine Sediment

*Penicillium bilaii* is a marine derived fungi isolated from the Huon estuary (Port Huon, Tasmania, Australia) yielding a yellow colored fungal pigment known as citromycetin and citromycin together with two dihydro analogs, (-)-2,3-dihydrocitromycetin and (-)-2,3-dihydrocitromycin (Capon et al., 2007). Similarly, *Microsporium* sp., isolated from the sample collected from Golmae Village (Ulsan City, Korea) was found to produce yellow compound flavoglaucin (Li et al., 2006). Aspergiolide B and (+)-Variecolorquinones A metabolites having red and yellow color, respectively, have been isolated from *Aspergillus glaucus* collected from marine sediment surrounding mangrove roots of Fujian Province (China) (Du et al., 2008). A water soluble red color pigments was also reported from a fungus isolated from the marine sediment sample collected from Miramar

(India). The sample was identified as *Penicillium* sp NIOM-02. Release of red pigment around the colony on malt extract agar (MEA) plate indicated its hydrophilic behavior (Dhale and Vijay-Raj, 2009). In a recent study, *Talaromyces* spp., and *Trichoderma atroviride* strains obtained from marine sediment were identified as potential red pigment producers (Lebeau et al., 2017). *Talaromyces albobiverticillius* 30548, a red pigment producer strain was also isolated from sediment obtained from Reunion Island (Indian Ocean). Most of the compounds identified from this strain have been characterized as azaphilones (Venkatachalam et al., 2019). With the interest in both red and yellow hues for food colouration marine sediments are an area that could be targeted for the identification of further pigments.

### Invertebrate Inhabitant Fungi

Sessile and non-sessile invertebrates such as corals, sponges and squirts, present in marine environment are often brilliantly colored. This bright color present in these invertebrates may be derived from photosynthetic pigments of symbiotic microorganism present in these organisms. Xu et al. (2008) has investigated fungi isolated from tropical coral reefs in order to study the extent of the bioactive molecules they contain. The team was able to isolate two novel yellow colored hexahydroanthrones named tetrahydrobostrycin and 1-deoxytetrahydrobostrycin together with red pigment bostrycin from the *Aspergillus* sp. strain of fungus isolated from coral reef off Manado, Indonesia (Xu et al., 2008). Similarly, ethyl acetate extract of the fungus *Eurotium cristatum* (ECE), isolated from the marine sponge *Mycale* sp., furnished a yellow colored compounds 2-(2', 3-epoxy-1',3'-heptadienyl)-6-hydroxy-5-(3-methyl-2-butenyl) benzaldehyde and 1,8-dihydroxy-6-methoxy-3-methyl-9,10-anthracenedione (physcion) (Almeida et al., 2010). In a recent study, Fouillaud and her team collected coral rubble and living coral from underwater volcano slopes, hard substrates, open water and sediments from different



marine environments around Reunion Island in the Indian Ocean (Fouillaud et al., 2017). *Talaromyces albobiverticillius* (B and C) strains isolated from these samples were explored for pigment production and were found to generate an array of pigments unveiling specific orange/red hues under submerged fermentation in potato dextrose broth (PDB) (Venkatachalam et al., 2018). The team has isolated 42 colored compounds highlighting a range of promising hues and molecules. These isolates belong mainly to the *Aspergillus*, *Penicillium* and *Talaromyces* genera in the family of *Trichocomaceae* (Fouillaud et al., 2017) and as such are key species for industrial scale production. *Alternaria* is also known for its bioactive metabolites, most of which are anthraquinone derivatives which are mostly pigmented molecules having wide range of biological activities. Zheng et al., has isolated several hydroanthraquinones and anthraquinone dimers from the *Alternaria* sp. ZJ-2008003, a fungi found in soft coral of South China Sea. Some of these are bright pigmented molecules having red, pink and yellow hues (Zheng et al., 2012) which are further evidence of the broad range of colors available from invertebrate inhabiting fungus.

### Halophytes

Microorganisms that can survive and grow well in areas of high salt (NaCl) concentration are known as halophilic extremophiles. Halophilic fungi possess great significance in biotechnological applications due to their ability to produce ample amounts of extracellular metabolites (Oren, 2010; Singha, 2012; Ali et al., 2014). Melanins are one such class of pigmented molecules and hold an important position in various cosmetic and pharmaceutical applications. The halophilic fungal strain *Trimmatostroma salinum* and *Phaeotheca triangularis* isolated from the halophiles of eastern coast of the Adriatic Sea, produce melanin pigments in solutions of saturated concentrations of

sodium chloride (Kogej et al., 2004). Similarly, it was also found that a diffusible dark pigment is released on potato dextrose agar by the black yeast named *Hortaea werneckii*. This pigment holds great importance as medicinal value owing to its activity against *Salmonella typhi* and *Vibrio parahaemolyticus* (Rani et al., 2013). Further a distinctive isolate collected from a hypersaline water sample from Puerto Rico was identified as new species of *Periconia* genus and found to produce an unusual blue pigment (Cantrell et al., 2006). Halotolerant fungi have also been reported to contain some bright colored quinone compounds. Variecolorquinones A and B are two yellow colored quinone compounds that have been obtained from a halotolerant fungal strain *Aspergillus variecolor* B-17 (Wang et al., 2007). With the capacity to produces colors into the blue range the halophytes are of interest to the food industry in order to extend the color spectrum available to them.

### Mangrove Ecosystem

Mangrove ecosystems afford a remarkably diverse habitat presenting unique properties of both marine and terrestrial environment in a single ecosystem. However, the fluctuating saline and tidal habitat, extreme stress conditions and high temperature of the mangrove allows only a limited number of species that can survive in such hostile environment (Kathiresan and Bingham, 2001). Thus, the species inhabiting this intimidating environment offers an extremely affluent reserve for significant novel and biologically active compounds. However, only a small amount of mangrove fungi have been studied so far in spite of their potential for production of array of natural pigments (Das et al., 2002; Zhang et al., 2012). Some of the key findings from these reports are described in the following sections.



## Mangrove Sediment

Chintapenta et al. (2014) has isolated ~100 mangrove fungi from the Godavari mangroves of India. Most of the strains were found to be pigment producers however special interest toward a red color directed further study on *Penicillium*, which was then interogated for optimization of its media conditions and the effect of metals and salts on pigment yield. The main purpose of the study was to optimize the effect of various bioelements (Chintapenta et al., 2014) and it was shown that a higher concentration of salt has a negative effect on pigment yield. This is due to the fact that the presence of these electrolytes alter the pH of the medium and prevent diffusion of pigment. On the other hand, calcium, iron, zinc enhanced the pigment yield and those correlates well with typically beneficial elements that form part of plant growth.

## Mangrove Derived Endophytes

Mangrove endophytic fungi encompasses the second largest assemblage of marine fungi and support the host plants by releasing some unprecedented metabolites which protect them from various harsh geoclimatic conditions. These endophytic fungi have been known for their various prospective applications in biotechnological and pharmaceutical field owing to the presence of structurally unique bioactive and diverse biomolecules including pigments. In an attempt to study the diversity of endophytic fungi from the tropical mangrove species, *Rhizophora mucronata*, 78 fungal isolates harboring inside the leaf tissues have been identified. Some of these isolates displayed distinctive pigmentation and are also reported to deliver a range of biological activities. These isolates produce an array of color such as green, gray/black, brown, orange, yellow, purple, and violet (Hamzah et al., 2018). Similarly, an endophytic fungus of the *Alternaria* sp., isolated from fruit of the mangrove tree *Aegiceras corniculatum* (South China Sea) is able to produce bright colored anthraquinone based compounds having hues of yellow to red. These compounds were identified as altersolanol A, alterporriols C–M, macrosporin, dactylariol, tetrahydroaltersolanol B and physcion (Huang et al., 2011). In an attempt to isolate potent radical scavenging compounds from endophytic fungi an isolate of *Eurotium rubrum* has been cultured from the inner tissue of the stem of the mangrove plant *Hibiscus tiliaceus* from Hainan Island (China). Several new pigmented components has been isolated from this fungi including questin and 3-O-( $\alpha$ -D-ribofuranosyl)-questin having an orange shade, asperflavin having a yellow shade, and the 2-O-methyleurotinone having a brown shade (Li et al., 2009). Similarly the *Eurotium* Sp. has also been obtained from leaves of a mangrove plant *Porteresia coarctata* (Roxb) and led to the isolation of two colored compounds identified as tetrahydroauroglauclin (yellow) and isodihydroauroglauclin (orange) (Gawas et al., 2002).

## Terrestrial Ecosystem

Terrestrial systems are a rich source of filamentous fungi and the presence of the fungi in a particular system such as sediments, soil, and decaying matter and as endophytes are mostly correlated with the production of some unique

metabolites. Terrestrial microbes are also good sources of pigment producing fungi and have been relatively more explored than the aforementioned systems.

## Terrestrial Sediments and Soil

Terrestrial sediments and soil supports the growth of filamentous fungi because of a lower level of mechanical disturbances and sheer forces that may disrupt fungal mycelia. Several studies revealed the production of pigmented components from fungi collected from soil sediments. In a study, soil sample collected from a volcanic ash from Japan yielded four bianthraquinones and two monoanthraquinones compounds having orange-red hues. These compounds were found predominantly in various soils samples collected from Japan and Nepal (Fujitake et al., 1998). An Australian terrestrial isolate of *Penicillium striatisporum* collected near Shalvey, New South Wales yielded yellow pigments. These pigments were identified as citromycetin, citromycin, dihydro analog (–)-2,3-dihydrocitromycetin (Capon et al., 2007). *Fusarium verticillioides* isolated from soil (Chiang Mai, Thailand) was found to be a potential producer of naphthoquinone pigment (Boonyapranai et al., 2008). In a study conducted to investigate and optimize the production of pigments in submerged culture of *Penicillium purpurogenum* DPUA 1275, a strain isolated from soil samples was found to release yellow, orange, and red color (Santos-Ebinuma et al., 2013). Similarly, bioprospecting of fungi collected from an Amazon soil for the possibility of pigment production yielded five strains *Penicillium sclerotiorum* 2AV2, *Aspergillus calidoustus* 4BV13, *Penicillium sclerotiorum* 2AV6, *Penicillium citrinum* 2AV18, and *Penicillium purpurogenum* 2BV41. All of these strain were able to produce pigmented molecules however, *P. sclerotiorum* 2AV2 produced intensely colored pigments (Dos Reis Celestino et al., 2014). With the intention to evaluate the capacity of ascomycetous fungi as a promising source for the production of various components including color, Lebeau et al. (2017) has analyzed 15 ascomycetous fungal strains, out of which 11 fungal strains were of terrestrial origin. Out of all of these two terrestrial strains *Penicillium purpurogenum rubisclerotium* and *Fusarium oxysporum*, and two marine strains identified as *Talaromyces* spp., and *Trichoderma atroviride* were identified as potential red pigment producers (Lebeau et al., 2017). Recently, a cold adapted fungal strain of *Penicillium* sp. (GBPI\_P155) isolated from the high altitude soil of Indian Himalayan region was reported to produce dark orange pigment. This extracted pigment was also found to be active against actinobacteria and several Gram-positive and Gram-negative bacteria (Pandey et al., 2018).

## Endophyte Fungi From Terrestrial Plants

Endophytic fungi isolated from higher plants are a lucrative source of bioactive molecules and as such are gaining considerable attention from industries and various natural product chemists. Consequently, the numbers of scientific investigations have focussed on the isolation and identification of novel endophytes from these plants in order to obtain various bioactive molecules. These endophytic fungi are also known to produce various pigmented molecules which are mostly

associated with certain specific biological activity of plants (Kaul et al., 2012). An endophytic fungus *Phyllosticta capitalensis* harbor as a foliar endophyte in a number of geographic regions tending to be hosted mostly in woody trees. To investigate the production of melanin production in this endophytic fungus, Suryanarayanan and co-workers have isolated this strains from diverse locations such as dry deciduous forests, moist deciduous forests and semi-evergreen forests. The production of melanin in the hyphae of *P. capitalensis* found to be liable for the fitness and survival of this fungus as a cosmopolitan endophyte, was shown to produce the melanin in order to help in sustaining the of fungi in stressful environments (Suryanarayanan et al., 2004). Similarly, a strain SX01, obtained from the twigs of *Ginkgo biloba*, was found to be a strong producer of red pigment which can be used as a producer of natural food additive (Qiu et al., 2010). In a similar study, *Aegle marmelos* which is a medicinal tree acclaimed for curing a range of disorders was investigated for the isolation of endophytic fungi. This experiment led to isolation of 169 endophytic fungal strains and importantly 67 among those were found to be pigmented (Mani et al., 2015).

### Endophytes From Plants Inhabiting Geothermal Soil

Geothermal ecosystems are an exclusive combination of scarce microclimatic and edaphic environments which provides distinctive habitats enabling the survival of unique vegetation. The environmental stresses of these areas includes elevated soil temperatures, elevated air temperatures, humidity, excess alkalinity, acidity and the presence of higher concentrations of some metals such as aluminum which eliminates most vascular plant species from surviving in these conditions. Species which can survive such circumstances are mostly unique to these specific regions or have some unique features which enable them to survive in such adverse conditions (Smale et al., 2018). Redman et al. (2002) proved that the presence of mutualistic fungi particularly endophytic fungi in *Dichanthelium lanuginosum* assist in the survival of plant in geothermal soil and is the basis for the thermo-tolerance to the plant. The author also inferred that thermal protection in plants could be due to the production of the fungal pigment melanin which aids in the dissipation of heat along the hyphae (Redman et al., 2002).

### Lichens and Endolichenic Fungi

Among the broad range of microbial resources, lichens are the ones which are gaining importance and have become the focus of significant pharmaceutical companies due to the presence of unique metabolites (Stocker-Wörgötter et al., 2013; Calcott et al., 2018). Lichens are microbial assemblages having a close symbiotic relationship between the fungal partner known as mycobiont and a photosynthetic algal partner known as photobionts (Culbertson and Culbertson, 1970; DePriest, 2004). In this association the fungal partner protects the algal partner from adverse geoclimatic influences. One way this protection is provided is the production of pigmented molecules by the fungal partner which are known to be effective in shielding algal partner from ultraviolet radiation (Nybakken et al., 2004; Nguyen et al., 2013).

However, the slow growth rate of lichen in nature is a major hurdle to obtain these pigments for commercial exploitation. Considering this, recent reports have described obtaining pigments from cultured mycobionts opening new pathways for commercialization of these compounds from lichens (Stocker-Wörgötter, 2008; Calcott et al., 2018). Miyagawa et al. (1994), isolated two novel pigments, identified as graphisquinone and graphenone from the cultured mycobionts of the lichens *Graphis desquamescens* and *Graphis scripta* and these are red quinone and a yellow-orange furandione, respectively (Miyagawa et al., 1994).

It has also been observed that some of the isolated lichen mycobionts produce new metabolites under laboratory driven stressed conditions such as osmotic stress, which are otherwise not produced by the natural lichen thallus (Miyagawa et al., 1993). Moriyasu et al.'s team (2001) found a bright yellow pigment yielded by the spore-derived mycobiont culture from a lichen of the *Haematomma* sp. (Moriyasu et al., 2001). Importantly this pigment could not be found in natural sample with the aid of traditional chemical analysis. It was also observed that some mycobionts release fluorescent pigments which were otherwise not present in lichen thallus growing naturally. A cultured mycobiont from the lichen *Amygdalaria panaeola* released three new fluorescent pigments namely panaefluorolines A–C (Kinoshita et al., 2003) extending the color range and utility of these types of sources to industrial applications. A wide range of hues and shades have been reported from the mycobiont of lichen *Trypethelium eluteriae* which includes a yellow pigment, trypethelonamide A and a novel dark violet red pigment 5'-hydroxytrypethelone along with three known dark violet-red pigments (–)-trypethelone, (+)-trypethelone and (+)-8-hydroxy-7-methoxytrypethelone (Basnet et al., 2019). Isolation of endolichenic fungi from the lichen thallus has also attracted attention for their potential to produce a range of bioactive molecules including pigments. A recent study on the isolation of bioactive molecules from the endolichenic fungus *Talaromyces funiculosus* yielded three compounds including ravenelin which is a yellow colored homogeneous powder that also possess good antimicrobial activity thus making it advantageous to the pharmaceutical and food sectors (Padhi et al., 2019).

## CURRENT CHALLENGES IN HARNESSING THE POTENTIAL OF FUNGI

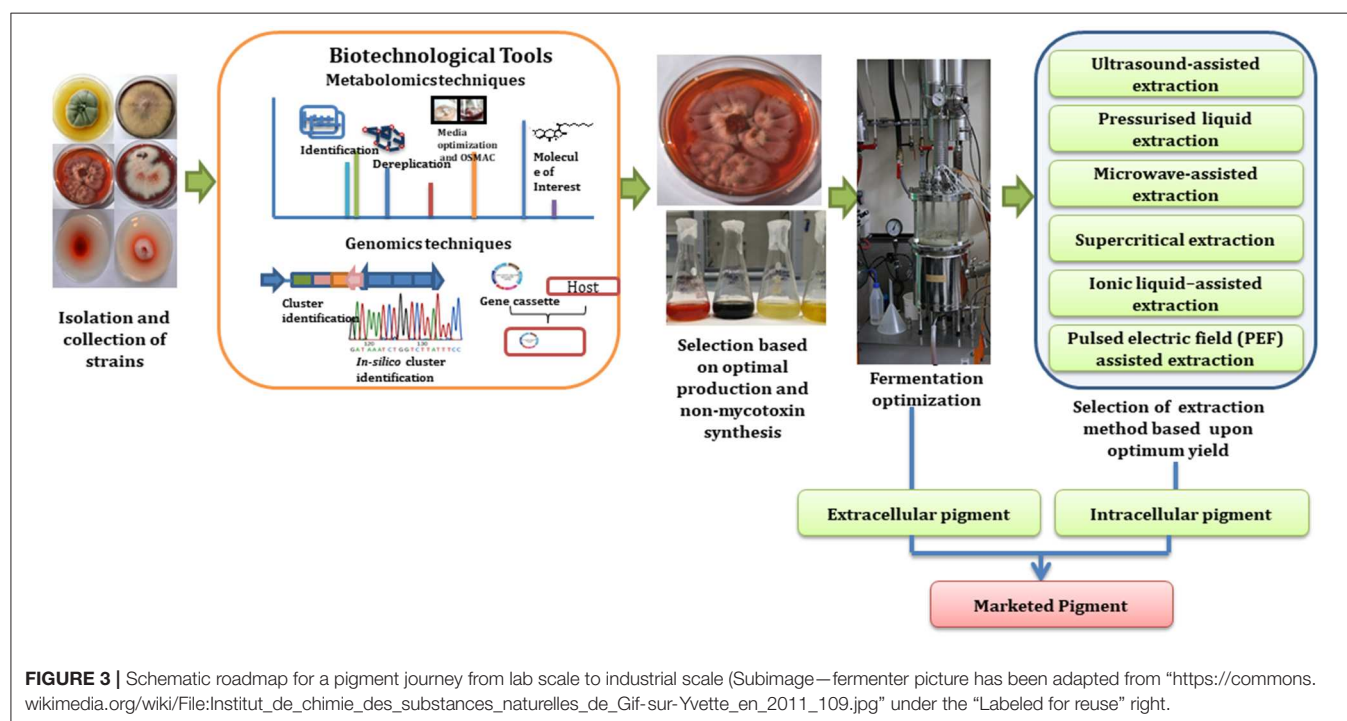
Although, there are a plethora of fungal resources which can serve as a source of potential pigments it is important to note that there are several challenges faced by industry which curtail the process of commercialization. Sustainability and progression of the fungal based pigment industry is mainly reliant upon three important factors (a) absence of mycotoxin in fungal pigments (b) pigment yield (c) pigment stability and purity (Lebeau et al., 2017).

Food grade pigments need approval through regulatory agencies and the most important precondition in their consideration is toxicological safety of the product (Food

Administration Drug, 2015; Sigurdson et al., 2017). Most of the fungi producing pigments are known to synthesize some toxic metabolites known as mycotoxins along with the pigments. The production of these mycotoxins irrefutably restricts the application of these pigments either directly in food or as an additive owing to its own safety issue (Dufossé et al., 2005). A well-known example is the production of toxin citrinin along with *Monascus* pigments which posed a challenge over its safe use and thus was prohibited in the European Union and the United States (Carvalho et al., 2005). Another major challenge in fungal pigments is the pigment yield. The range of chemical entities and the range of properties limit its profitable yield with targeted isolation methodologies (Chadni et al., 2017). Pigment yield in a culture can be enhanced by increasing the biomass growth or by enhancing the accumulation of intracellular pigments (Das et al., 2007; Dufosse et al., 2014). Medium optimization which includes monitoring of operating conditions such as media composition, temperature, agitation, aeration and pH are critical parameters to regulate in order to reach optimum pigment production (Mondal et al., 2015). The cost effectiveness of the selected media is also an important parameter to consider and at scale is particularly important for industrial processing. Another important challenge is the stability of natural pigments against environmental factors such as pH, light, moisture, temperature and food matrices (Ogbonna, 2016) where a shorter shelf life due to instability of molecule at varied conditions may limit its application as commercial pigments. However, such stability issues can be addressed with the help of novel approaches such as microencapsulation (Ersus and Yurdagel, 2007; Özkan and Bilek, 2014) and nanoformulation (Mehrad et al., 2018). These formulations can help to improve

the physical properties and stability which have been routinely used for other purposes in the food industry including milk processing.

Technology that use shell materials as the basis for the microencapsulation of pigments include freeze-drying, spray-drying, emulsion and coacervation. Spray-drying is the most widely used technique in food industry for pigment stabilization and increases the shelf life of the product significantly. Several studies have discussed the food applications of microencapsulated natural colorants (Azeredo et al., 2007; Ersus and Yurdagel, 2007) which have been broadly accepted by the industry. However, there is another technique called as nanoencapsulation, the application of this technique is limited in industries till date. Nanoencapsulation can be employed to enhance the stability and solubility issues associated with natural pigments. The considerably small size of nanoemulsions and nanocapsules make them a useful vehicle for the distribution of non-polar pigments in aqueous solutions of those from fungal sources. Matsuo and his co-workers in a recent study prepared two types of nanoparticles encapsulating *Monascus* pigments employing a hydroxypropyl cellulose (HPC) and poly (lactic-co-glycolic) acid (PLGA) copolymer. These formulations were found to enhance the photostability of the *Monascus* based pigment and drew the attention of researchers in this field. It is important to note however that the PLGA based nanoparticle were effective toward improving the stability upon photobleaching of the pigments as compared to the HPC nanoparticles (Matsuo et al., 2018). Application of these approaches to enhance the solubility and stability of natural pigments as per the requirement based on food commodity could be a promising area of research for further advancement.





## BIOTECHNOLOGICAL ADVANCES IN PIGMENT PRODUCTION

### Metabolomics

A number of technologies to overcome issues associated within the pigment industry are already in place and many are in the process of implementation. The recent advent of biotechnological based approaches have been established toward intelligent screening methods for the selection of appropriate strains and exploit the traditionally overlooked potential of pigment production by various fungal strains. A step stage in the use of biotechnological approaches has been observed within the industry in the past decade with a focus on the execution of different ways for intelligent screening (excluding toxic producing strains) which has been shown to increase the yield of pigment production (Mapari et al., 2005). Screening of possible pigment-producing fungal strains with the help of metabolomic tools helps in clustering strains on the basis of their characteristic metabolites including functional groups associated with color and also allows for some control over the selection of the strains with known toxic metabolites (Hajjaj et al., 1999; Archer, 2000). Approaches involving the latest data handling methods and chemoinformatics tools for the identification of metabolites help to perform a systematic study of these molecules in target species. These studies not only assist in dereplication of already known molecules but also help in targeting novel pigments with a chromophore similar to already established pigments (Elyashberg et al., 2002). An example of using automated techniques for the targeted screening of molecules of interest has been performed with the aid of computerized screening which has led to the novel production of monascus like pigments. An approach using X-hitting algorithm was shown to be useful when applied to the UV-vis spectra of metabolites (cross hits). The tool has been used as a quick way to screen ascomycetous filamentous fungi belonging to *Penicillium* subgenus *Biverticillium* which is not reported to produce citrinin or any other mycotoxin (Mapari et al., 2008).

### Metabolic Engineering

Besides the identification of metabolites with these mass-metabolomics techniques, genome knowledge also helps in identification of desired secondary metabolites (Arora, 2003). Recent advances in molecular biology and metabolic engineering has helped in streamlining the process of pigment industrialization as described in **Figure 3**. For instance, tools involved in molecular biology helps in sequencing of fungal genomes and thus assist in identification of genes involved in production of pigmented metabolite (Sankari et al., 2018). The use of genome mining strategies for the discovery of new pigmented molecules is one of the most constructive techniques as it not only allows studying the complete metabolic capacity of fungal strain but also allows studying the gene clusters that are not expressed in standard laboratory culture conditions (Nielsen and Nielsen, 2017). These gene clusters can then be engineered in controlled ways for the overproduction of a desired pigment or expressed in a heterologous host for the large scale production of selected pigments (Pfeifer and Khosla, 2001; Jiang et al.,

2010). Cloning the genes and encoding for a selected pigments biosynthesis into microbial vectors such as *Bacillus subtilis*, *E. coli*, *Corynebacterium glutamicum*, *Pseudomonas putida*, and *Pichia pastoris* has been considered as a more reliable and cost effective approach for industrial production process. Production of carotenoids mainly  $\beta$ -carotene and torularhodin has been enhanced in *Rhodotorula mucilaginosa* KC8 by using metabolic engineering and a mutagenesis approach (Wang Q. et al., 2017). Further, novel betalain derivative production has been shown to be induced in *Saccharomyces cerevisiae* as a heterologous microbial host by using glucose as a substrate and by using different amines in the culture (Grewal et al., 2018). This is particularly important as it leads to control of the biological process in an industrial setting and could be the key to realizing the potential of this field.

In a recent study conducted by Chen and co-workers, production of monascin and ankaflavin pigments have been studied by knockout of the *mrPigF* gene and elucidation of the MonAzPs biosynthesis in *Monascus ruber* M7. The findings in this study provided a roadmap toward the selective and controlled biosynthesis of the desired MonAzPs constituents (Chen et al., 2017). Similarly, Balakrishnan et al. (2013) studied the azaphilone pigment biosynthetic gene cluster using the T-DNA random mutagenesis in *Monascus purpureus*. It was found that transcription of transcriptional regulator gene (*mppR1*) and the polyketide synthase gene (*MpPKS5*) was significantly repressed in the W13 albino mutant. Additionally, targeted inactivation of *MpPKS5* gave rise to an albino mutant, validating the role of *mppR1* and *MpPKS5* toward azaphilone pigment biosynthesis. Importantly the *MpPKS5* gene cluster includes SAT/KS/AT/PT/ACP/MT/R domains, which is also preserved in other azaphilone polyketide synthases. Likewise, six azaphilone compounds, azanigerones A–F have also been linked with aza gene cluster in *Aspergillus niger* ATCC 1015. This was confirmed with the help of transcriptional analysis and deletion of a key polyketide synthase (PKS) gene (Zabala et al., 2012) where whole genome expression analysis together with existing knowledge of polyketide synthase (PKS) genes helped in identification of three novel clusters of co-expressed genes in *F. verticillioides*. With the help of functional analysis of PKS genes linked to these clusters, a violet pigment in sexual fruiting bodies (perithecia) and the mycotoxins fusarin C and fusaric acid were identified (Brown et al., 2012). In another study, attempt was made to identify the gene responsible for the production of 1,8-dihydroxynaphthalene-melanin pigment (DHN-melanin) in *Ascochyta rabiei*. Degenerate PCR primers were used to obtain an *ArPKS1* which is encoding for a polypeptide with high similarity to polyketide synthase (PKS) involved in biosynthesis of DHN-melanin in other ascomycetous fungi through site-directed mutagenesis of *ArPKS1* in *A. rabiei* generated melanin-deficient pycnidial mutants confirming the linkage of *ArPKS1* with melanin production (Akamatsu et al., 2010). Two strains of *Streptomyces galilaeus* ATCC 31133 and ATCC 31671 known to produce anthracyclines namely aclacinomycin A and 2-hydroxyaklavinone, anthraquinones, aloesaponarin II after transformation with DNA from *Streptomyces coelicolor* containing four genetic loci, *actI*, *actIII*, *actIV*, and *actVII* (Bartel

et al., 1990). Identification of gene cluster and elucidation of the promoters regulator using various molecular biology tools such as sequencing of fungal genomes would help in studying the molecular aspects of pigment generation. These advances will also assist in understanding the complexity associated with the biosynthetic pathways of pigment metabolites which can be exploited for industrial application.

## Culture Optimization

The culture environment presents a range of critical parameters than can be studied in order to control the composition and yield of fungal secondary metabolites. One Strain Many Compounds (OSMAC) is a well-known model which has highlighted the concept of changes in the fungal secondary metabolism with respect to growth conditions (Romano et al., 2018). Thus, media optimization is also a prerequisite parameter to be considered for maximizing the yield of the fermentative product. This strategy involves the abiotic modifications to the culture environment by modifying the culture medium composition such as altering the source of carbon and nitrogen and controlling the operating parameters like the redox status, temperature, light intensity, wavelength, culture configuration (aeration, agitation, static, liquid, or solid) and pH. In an attempt to identify the effect of media composition on pigment yield the effects of glutamic acid on the production of monacolin K pigment and expression of the monacolin K biosynthetic gene cluster has been studied. The presence of glutamic acid medium in spite of the original medium increased the monacolin K production from 48.4 to 215.4 mg l<sup>-1</sup> which is equivalent to 3.5 times. Upregulation of the expression of *mokB-mokI*; on day 8 in the presence of glutamic acid was the driver behind this upsurge (Zhang et al., 2017). Beyond the substrate and culture conditions, bioreactor design also plays a significant role in optimizing the process of pigment production and this is an area that the process industry will be able to add their expertise for the realization of efficient controlled natural pigment manufacture (Zhong et al., 1992; Spier et al., 2011).

## PROCESSING AND EXTRACTION OF NATURAL PIGMENTS

Filamentous fungi are a great source of wide range of metabolites such as polyphenols, polyketides, carotenoids and terpenoids (Rao et al., 2017). Selection of extraction techniques is one of the crucial step for the efficient recovery of these metabolites and mostly reliant upon the nature of metabolites of interest and localization of these metabolites in the fungal culture (Chadni et al., 2017). Some of the pigments are extracellular and released in the fermentation broth which makes their extraction downstream less trivial than the intracellular pigments that requires specialized extraction techniques for their removal from biomass (Morales-Oyervides et al., 2017). Introduction of cheap, efficient and safe extraction methodology for the recovery of natural pigments is one of the major challenges to be overcome in order to enable production at a large scale. A series of conventional techniques which includes organic solvent extraction (soxhlet, homogenization,

and shaking), hydrodistillation, centrifugation extraction, and steam distillation have been worked upon in order to extract pigments from various fungi although the upscaling of these processes is a non-trivial exercise. Nevertheless, the quest of biotech industries for unearthing the safer extraction technologies over the last two decades fuelled a tremendous amount of research toward the development of newer greener extraction and separation methods. Once these major issues have been addressed by the industry, focus can be placed on the challenge of keeping the process cheap, efficient and fast.

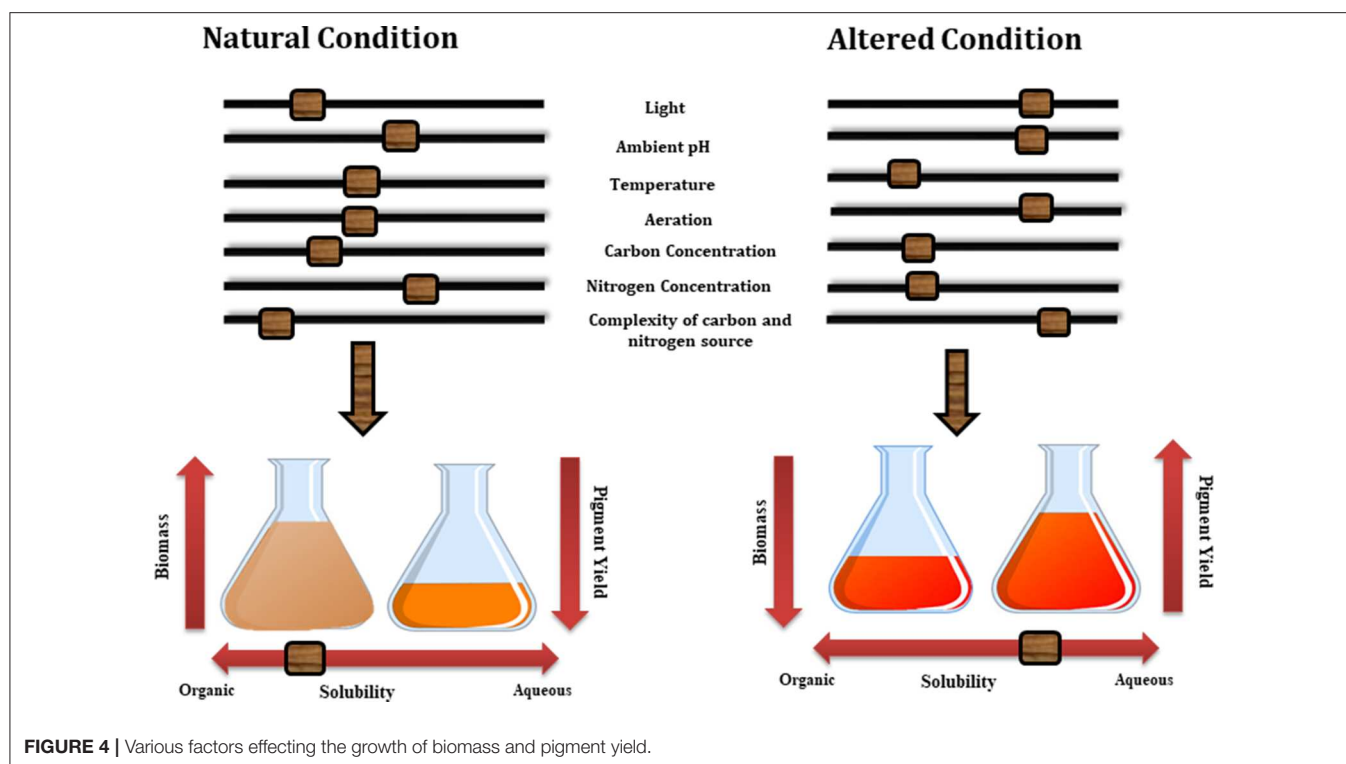
## Extraction of Extracellular Pigments

For the purpose of easy and feasible downstream processing, extracellular and water soluble pigments obtained from the submerged culture are preferred (Velmurugan et al., 2010). Water soluble pigments do not require any organic solvents for their extraction thus are considered safe and also can be used directly in different food commodities without further modification or engaging any carriers/stabilizers. Conversely, intracellular and water insoluble compounds requires conventional extraction processes with organic solvents, which are not only complicated (due to safety and environmental impact) and time-consuming processes but also bring the need for more costly and rigorous regulatory controls. Therefore, removing these tedious extraction processes would help in alleviating the use of large amount of solvents, which not only reduce the production time but also eliminates the cost of an extraction process and assists in making the pigment production more economical and safer and environmentally friendly (Hu et al., 2012). Extraction of extracellular pigments through submerged culture is mainly controlled by two parameters fermentation optimization and fermentation processing which we shall focus on in the next two sections.

## Fermentation Optimization

Although the cellular mechanism behind the secretion of these metabolites are still not known a number of studies have highlighted the effect of various growth conditions, such as medium composition and process parameters on the nature and yield of these metabolites. Thus by altering various growth conditions in submerged culture such as pH, aeration, light exposure, concentration of carbon and nitrogen in the medium and their ratio, production of extracellular and water soluble pigments can be altered (**Figure 4**) (Hajjaj et al., 1998). For example, changes in the pH of culture medium of *Monascus* sp. alter the concentration of extracellular pigments in particular (Mukherjee and Singh, 2011). Similarly, Lebeau et al. (2017) emphasized the fact that medium composition plays a very important role for the selection of extracellular pigments. In their study the effect of simple and complex forms of carbon sources on the mycelium biomass and extracellular pigment production has been discussed and it was concluded that simple form of carbon such as defined minimal dextrose broth (DMD) favors the production of higher biomass but low pigment production. Additionally the complex form of carbon and nitrogen sources present in potato dextrose broth (PDB) along with essential cofactors including magnesium, calcium, iron, phosphorus, zinc,





manganese and copper (all present in PDB broth) encourages the production of extracellular pigments over biomass production.

A successful industrial bioprocess development relies on the optimization step which includes optimization of biomass yield and its bioactive production with stimulating metabolic precision. On industrial scale, two major submerged fermentation techniques are mostly applied in order to discover metabolites of interest by amplifying their production from a laboratory to large scale. First is fed-batch approach (Caro et al., 2017) which primarily works like batch fermentation until the exhaustion of one or more substrates which are then renewed by addition of fresh medium through a targeted feeding regime. A fixed volume or variable volume of substrate or medium is then used accordingly (Li et al., 2000; Amanullah et al., 2010). Krairak et al. (2000) and Chen et al. (2015) have used the fed-batch fermentation technique and optimized the condition required for the maximizing yellow pigment yield from different *Monascus* sp. Their studies provided an appropriate fermentation strategy to produce high proportion of yellow pigments in high cell density culture (Krairak et al., 2000; Chen et al., 2015). On the other hand the continuous mode approach works on the delaying of the exponential phase by feeding the microbial cells with fresh nutrients and the cells are routinely collected from the bioreactor at the defined rate and reaction time point (Vogel et al., 2012). Both of these techniques are also popular among pigment industry with the implication that together with suitable optimization process would result in production of large amount of extracellular pigments which can be easily collected or processed without solvent extraction.

### Fermentation Processing

Aqueous two-phase system (ATPS) is one of the most popular methods used for the extraction of pigmented compounds from the fermented broth (Iqbal et al., 2016). This approach uses liquid-liquid fractionation and is based upon the use of green ionic liquids for extraction of pigmented molecules. Separation of different hydrophilic solutes into two immiscible aqueous phases is mainly based upon their differential selectivity toward different polymer-polymer, polymer-salt, or salt-salt and solute combinations formed in these two phases. Aqueous two-phase systems offers several advantages for downstream control of biomolecules (1) both the phases are composed of water compared to organic solvents in conventional extraction thus provides favorable environment to molecules and supports the stability of their structure and bioactivity, (2) an environmental friendly process, (3) are economically favorable (McQueen and Lai, 2019).

Several researchers have implemented ATPS extraction approaches for the isolation of pigments from submerged culture broths. Ventura and co-workers implemented ATPS based on quaternary ammonium and imidazolium system for the recovery of red pigment from the fermented broth of *Penicillium purpurogenum* DPUA 1275. The purpose of the study was to separate red pigment molecule from the remaining colorants and contaminant proteins present in the fermented broth. They have concluded that the optimal extraction system based upon tetraethylammonium bromide ionic liquid assisted in the high partition coefficients of the red pigment ( $K_{\text{red}} = 24.4 \pm 2.3$ ) and protein removal ( $EE_{\text{Total}} = 60.7 \pm 2.8 \%$ ) from the fermentation broth (Ventura et al., 2013).

## Extraction of Intracellular Pigments

For the extraction of hydrophobic compounds and intracellular compounds, green extraction methods are more preferable as they are either free from organic solvents or need fewer amounts of solvents and thus are considered more safe and environment friendly. Some of these extraction techniques also work on low temperature which also helps in the extraction of thermolabile pigments without their degradation. These extraction techniques include ultrasound-assisted extraction (UAE) (Vilkhu et al., 2008; Cheung et al., 2013), pulsed electric field (PEF) assisted extraction (Goettel et al., 2013; Fincan, 2017), pressurized liquid extraction (Lebeau et al., 2017, 2019), microwave-assisted extraction (MAE) (Vázquez et al., 2014), ionic liquid-assisted extraction (Ventura et al., 2013; Grosso et al., 2015; Lebeau et al., 2016) and supercritical CO<sub>2</sub> extraction (Cocks et al., 1995; Chaudhari, 2013). Most of these techniques have been tested for the extraction of bioactive compounds from numerous natural resources. Only few reports are available for the extraction of carotenoids pigments using green extraction methods from raw plant materials, microalgae and seaweeds (Poojary et al., 2016). The implication of all these novel extraction techniques in extraction of fungal based pigments with or without involvement of GRAS (generally regarded as safe) solvents could be an interesting avenue to be explored further by research teams and industry.

### Ultrasound-Assisted Extraction (UAE)

Ultrasound-assisted extraction (UAE) has been well-acknowledged as an efficient and environmentally safe extraction methods in number of phyto-pharmaceutical industries (Chemat et al., 2017). Owing to the thermolabile nature of most of the natural metabolites, possibility of their degradation during thermal extraction is very high. In contrast, ultrasound-assisted extraction resulted in increased extraction efficiency at lower temperature. This method of extraction is mainly based upon the employment of high-intensity ultrasound pressure waves to accelerate the extraction of a solid material in a liquid solvent. These waves work by generating localized pressure which ultimately cause the tissue to rupture and assist in release of intracellular substances into the solvent. It is mainly working on acoustic energy which is not absorbed by molecule but is transmitted through the medium. Ultrasound waves are transmitted through medium by means of pressure waves induced vibrational motion of the molecules (Tiwari, 2015).

The major advantage of using ultrasound-assisted extraction is its faster kinetics which further contributes toward enhanced extraction yield. The other benefit of using UAE is that its apparatus is simple and cheap and is quite easy to use compared to other novel extraction techniques. Further, UAE can be done with a smaller amount of solvent which helps in extracting a wide variety of bioactive compounds including those that are water soluble (Vilkhu et al., 2008).

### Pressurized Liquid Extraction (PLE)

Pressurized liquid extraction (PLE) also known as accelerated solvent extraction (ASE), is a very recent extraction technique and has emerged as an advanced technique to conventional

solvent extraction methods such as reflux, Soxhlet extraction, percolation or maceration in terms of solvent consumption, extraction time, extraction yields and reproducibility (Mustafa and Turner, 2011). It is an automated technique used for the exhaustive extraction from solid matrices with the help of elevated pressure and temperature and diminishing solvent consumption. Both the parameters work together for the complete removal of metabolites from matrix and the high pressure assists in the penetration of solvents in the sample while with the help of higher temperature the solubility and diffusion rate of the metabolites is enhanced by breaking the interactions between matrix and analytes (Richter et al., 1996). Application of the elevated conditions in PLE helps in the reduction of total extraction time and consumption of extraction solvents. Recently, PLE has been shown to be the most popular technique for extraction of bioactive molecules from plants and fungi owing to its advantage to preserve the closest possible compositions of the molecule (Camel, 2001). In a recent study performed by Lebeau et al. (2017), extraction of intracellular pigments from the fungal biomass was performed using six-stage pressurized liquid extraction (PLE). Extraction of red pigments in optimum yield from *Talaromyces* species proved PLE as a faster and greener extraction technique as compared to conventional extraction techniques (Lebeau et al., 2017).

### Microwave-Assisted Extraction (MAE)

Microwave (MW) radiation falls between frequencies ranging from 300 MHz (radio radiation) to 300 GHz in the electromagnetic spectrum. Microwave-assisted extraction (MAE) employs microwave radiation as the source of energy to heat the sample and solvent mixture based on the dipole moments (Li et al., 2012; Xiong et al., 2016). Microwave-assisted extraction is one of the advanced extraction techniques known for its efficient extraction efficiency with minimum solvent consumption and lower extraction time. This technique is mostly used for the extraction of high-value bioactive compounds present in various biological matrices and helps in producing high quality extracts (Pare et al., 1991). Factors which are considered to demonstrate an important role in the extraction and separation efficacy and selectivity of MAE are the substrate material, solvents, solid-liquid ratio, temperature, pressure, and particle size (Chupin et al., 2015).

The relevance and potential of water as the only solvent or in solvent free microwave assisted processes for the extraction of bioactive metabolites has been critically discussed by a number of reviews (Filly et al., 2016; Seoane et al., 2017). Water being the most safe, nontoxic, non-flammable, non-corrosive, and environmentally benign falls under the category of green solvent and in combination with microwave assisted water extraction helps in the extraction of wide range of metabolites from fungal and plant matrices (Flórez et al., 2015). Pasquet et al. (2011) identified MAE as the best extraction technique for the isolation of pigments from microalgal sources owing to its reproducibility, rapidity, uniform heating, and high extraction yields (Pasquet et al., 2011). Similarly, some other studies have also reported potential of MAE in the extraction of pigments from plant

sources and what has been learnt by these experiment can be exploited in this field (Kiss et al., 2000; Liazid et al., 2011).

### Supercritical Extraction (SFE)

A surge in the application of supercritical extraction (with CO<sub>2</sub>) as a greener extraction technique in natural product chemistry was observed during the last decade (Da Silva et al., 2016). Supercritical extraction is an innovative extraction technique based upon the employment of liquefied carbon dioxide gas as the supercritical fluid for the extraction of bioactive molecules from solid matrices (Khaw et al., 2017). This technique is working on the principle of augmented solvating power of specific gases above their critical limit and thus the gas behave like a supercritical fluid having properties of liquid together with gas as extracting fluid. Combining the transport properties of a gaseous phase with density like a liquid phase provides the supercritical fluid, a cutting edge feature as a novel extracting medium. Dissolving power of these supercritical fluids is determined by the pressure and temperature employed during the extraction process which can be adjusted by manipulating these parameters (Zabot et al., 2012). One of the major advantages of using SFE for the extraction of natural metabolites is the extraction of thermolabile compounds as extraction can be performed at low temperatures. It has also been acknowledged as a green sustainable technique for the selective isolation of molecules.

However, supercritical CO<sub>2</sub> is mainly used for the extraction of non-polar compounds due to its hydrophobic nature but its polarity can be tailored in combination with different co-solvent such as ethanol for the extraction of relatively polar compounds as xanthophylls and ethylene for extraction of carotenoids. Several examples of employment of SFE for carotenoids extraction from several substrates from laboratory to the commercial scale have been reported (Nobre et al., 2006; Kitada et al., 2009). Several parameters such as temperature, time, pressure, flowrate, choice of co-solvent can considerably modify the extraction yield and efficiency along with selectivity for compounds of interest. Accordingly, selection of these parameters must be judiciously taken into account for an efficient and selective recovery of target analytes.

### Ionic Liquid-Assisted Extraction

Ionic liquids (ILs) have emerged as tailor-made solvents for the extensive extraction and purification of natural-derived bioactive compounds. It has been recognized as tuneable designer solvent owing to its diverse array of salt combination fabricated for particular range of compounds and helps to overcome the drawback of limited selectivity associated with the usage of organic solvent (Passos et al., 2014). Moreover, implementation of ILs helps to make the process more economical and also helps to diminish the environmental footprint.

These ILs in combination with water or organic solvents can be implemented directly in extraction of bioactive molecules from biomass known as simple ILs assisted SLE (Solid liquid extraction). However owing to its ionic behaviors, these ILs can interact with electromagnetic fields and therefore can be used in combination with MAE known as IL-based microwave-assisted

extraction or UAE known as IL-based ultrasonic-assisted extraction (Ventura et al., 2017).

A very recent study has discussed the application of protic ionic liquids (PILs) as cell lytic agents to extract and improve the extractive yield of intracellular carotenoids from yeast *Rhodotorula glutinis* biomass (Mussagy et al., 2019).

### Pulsed Electric Field (PEF) Assisted Extraction

Pulsed electric field (PEF) processing is a non-thermal extraction technique working on the principle of electroporation or electro-permeabilization. It is a process of exposing the sample matrix to short impulses of high intensity electric field which eventually result in cell membrane disintegration and increased its permeability. This effect can be of reversible or irreversible nature depending on process parameters which includes amplitude, intensity, number, duration and frequency of the external electric waves. Most of the secondary metabolites are positioned inside the plant cells and increased permeability of the cell membrane helps in the rapid diffusion of the solvent inside the cell and removal of these metabolites in external environment. Unipolar or bipolar pulses with square-wave shaped or exponential frequencies are mostly used in this treatment. Pulsed electric field assisted extraction can be used for the selective extraction of metabolites by manipulating the intensity of treatment which is mainly controlled by pulse duration, electric field strength, treatment time or energy input. Numbers of studies have discussed the potential of using PEF in pigments extraction from algal cells and different matrices (Grimi et al., 2014; Luengo et al., 2015). Parniakov et al. (2015) has also discussed the effect of the combination of PEF and solvent extractions containing biphasic mixture of organic solvents at different pH for the recovery of hydrophobic carotenoids and other pigments in an efficient manner. Result of their study highlighted the effect of two step extraction as high levels of extracted non-degraded proteins was recovered at the first step during PEF extraction and substantial enhancement of pigments yield at the second step. Also, this two stage PEF-assisted procedure allowed also effective extraction using lower amount of organic solvents (Parniakov et al., 2015).

## CONCLUSION

The major aim for the pigment industry, especially for food grade pigments is to look for a sustainable and potential source of pigments which is relatively safe for human health and the environment. The modern inclination in society for “natural” ingredients and consumer concern toward the deleterious effects of synthetic pigments on health and environment rekindled the interest toward the use of natural colorants. Progressive growth involving various biotechnological tools for the supply of nutritive, attractive healthy and high sensorial quality products has been observed in last decades which has made this process more economical and suitable for mass applications. Nature may be excellent source of safe colors, however, key limitations such as raw material availability and variation in pigment profile associated with colors obtained from plant source, navigate color industry toward the potential of colors obtained from microbial sources particularly fungal resources.

Keeping the advantages afforded by fungal diversity in mind, fungi are considered as cell factories for pigment production, where researchers can play with functionality. Fungal species obtained from various sources are known to produce and yield wide array of pigments which are usually associated with multifaceted biological activities together with extraordinary range of colors. Although the number of traditional technologies for the production of pigments such as monascin (from a fungus) are already well-advanced a lot of research on new alternatives, exploring novel means and sources for the biotechnological production of these pigments in profitable yield are in progression. Thus, further research is necessary to find optimize pigment properties such as yield and composition by optimized growth parameter, using metabolic engineering tools, introduction of low cost organic substrates for value addition, presence of different elicitors for pigment production, stabilizing

methods for improving pigment application and suitable greener and environmentally safer extraction methods for the extraction at large scale.

## AUTHOR CONTRIBUTIONS

RK contributed toward drafting and editing of the article. MG and XC contributed toward the critical revisions and final approval of the article.

## ACKNOWLEDGMENTS

The authors thank The Energy and Resources Institute, India and Deakin University, Australia to carry out the research work. RK is supported by Deakin University HDR scholarship (Candidate ID—218121642).

## REFERENCES

- Aberoumand, A. (2011). A review article on edible pigments properties and sources as natural biocolorants in foodstuff and food industry. *World J. Dairy Food Sci.* 6, 71–78.
- Adam Burrows, J. D. (2009). Palette of our palates: a brief history of food coloring and its regulation. *Compr. Rev. Food Sci.* 8, 394–408. doi: 10.1111/j.1541-4337.2009.00089.x
- Akamatsu, H. O., Chilvers, M. I., Stewart, J. E., and Peever, T. L. (2010). Identification and function of a polyketide synthase gene responsible for 1, 8-dihydroxynaphthalene-melanin pigment biosynthesis in *Ascochyta rabiei*. *Curr. Genet.* 56, 349–360. doi: 10.1007/s00294-010-0306-2
- Ali, I., Siwarungson, N., Punnapayak, H., Lotrakul, P., Prasongsuk, S., Bankeeree, W., et al. (2014). Screening of potential biotechnological applications from obligate halophilic fungi, isolated from a man-made solar saltern located in Phetchaburi province, Thailand. *Pak. J. Bot.* 46, 983–988.
- Almeida, A. P., Dethoup, T., Singburaudom, N., Lima, R., Vasconcelos, M. H., Pinto, M., et al. (2010). The *in vitro* anticancer activity of the crude extract of the sponge-associated fungus *Eurotium cristatum* and its secondary metabolites. *J. Nat. Pharm.* 1, 25–29. doi: 10.4103/2229-5119.73583
- Amanullah, A., Otero, J. M., Mikola, M., Hsu, A., Zhang, J., and Aunins, J. (2010). Novel micro-bioreactor high throughput technology for cell culture process development: reproducibility and scalability assessment of fed-batch CHO cultures. *Biotechnol. Bioeng.* 106, 57–67. doi: 10.1002/bit.22664
- Andersen B., Dongo, A., and Pryor, B. M., (2008). Secondary metabolite profiling of *alternaria dauci*, *A. porri*, *A. solani*, and *A. tomatophila*. *Mycol. Res.* 112, 241–250. doi: 10.1016/j.mycres.2007.09.004
- Anke, H., Kolthoum, I., Zähner, H., and Laatsch, H., (1980). Metabolic products of microorganisms. 185. The anthraquinones of the *Aspergillus glaucus* group. I. Occurrence, isolation, identification and antimicrobial activity. *Arch. Microbiol.* 126, 223–230. doi: 10.1007/BF00409924
- Archar D. B., (2000). Filamentous fungi as microbial cell factories for food use. *Curr. Opin. Biotech.* 11, 478–483. doi: 10.1016/S0958-1669(00)00129-4
- Arnold, L. E., Lofthouse, N., and Hurt, E., (2012). Artificial food colors and attention-deficit/hyperactivity symptoms: conclusions to dye for. *Neurotherapeutics* 9, 599–609. doi: 10.1007/s13311-012-0133-x
- Arora, D. K. (2003). “Chemical identification of fungi: metabolite profiling and metabolomics,” in *Fungal Biotechnology in Agricultural, Food, and Environmental Applications* (Bosa Roca, FL: CRC Press), 29–45.
- Avalos, J., Pardo-Medina, J., Parra-Rivero, O., Ruger-Herreros, M., Rodríguez-Ortiz, R., Hornero-Méndez, D., et al. (2017). Carotenoid biosynthesis in *Fusarium*. *J. Fungi (Basel)*. 3:39. doi: 10.3390/jof3030039
- Azeredo, H. M., Santos, A. N., Souza, A. C., Mendes, K. C., and Andrade, M. I. R. (2007). Betacyanin stability during processing and storage of a microencapsulated red beetroot extract. *Am. J. Food Technol.* 2, 307–312. doi: 10.3923/ajft.2007.307.312
- Balakrishnan, B., Karki, S., Chiu, S. H., Kim, H. J., Suh, J. W., Nam, B., et al. (2013). Genetic localization and *in vivo* characterization of a *Monascus azaphilone* pigment biosynthetic gene cluster. *Appl. Microbiol. Biotechnol.* 97, 6337–6345. doi: 10.1007/s00253-013-4745-9
- Bartel, P. L., Zhu, C. B., Lampel, J. S., Dosch, D. C., Connors, N. C., and Strohl, W. R. (1990). Biosynthesis of anthraquinones by interspecies cloning of actinorhodin biosynthesis genes in streptomycetes: clarification of actinorhodin gene functions. *J. Bacteriol.* 172, 4816–4826. doi: 10.1128/JB.172.9.4816-4826.1990
- Basnet, B.B., Liu, L., Zhao, W., Liu, R., Ma, K., and Bao, L. (2019). New 1, 2-naphthoquinone-derived pigments from the mycobiont of lichen *Trypethelium eluteriae* Sprengel. *Nat. Prod. Res.* 33, 2044–2050. doi: 10.1080/14786419.2018.1484458
- Birkinshaw, J., Kalyanpur, M., and Stickings, C. (1963). Studies in the biochemistry of micro-organisms. pencolide, a nitrogen-containing metabolite of *Penicillium multicolor* grigorieva-manilova and poradielova. *Biochem. J.* 86, 237–243. doi: 10.1042/bj0860237
- Boonyapranai, K., Tungpradit, R., Lhieochaiphant, S., and Phutrakul, S. (2008). Optimization of submerged culture for the production of naphthoquinones pigment by *Fusarium verticillioides*. *Chiang Mai. J. Sci.* 35, 457–466.
- Bora, P., Das, P., Bhattacharyya, R., and Saikia, M. (2019). Biocolour: the natural way of colouring food. *J. Pharmacogn. Phytochem.* 8, 3663–3668.
- Brown, D. W., Butchko, R. A., Busman, M., and Proctor, R. H. (2012). Identification of gene clusters associated with fusaric acid, fusarin, and perithecial pigment production in *Fusarium verticillioides*. *Fungal Genet. Biol.* 49, 521–532. doi: 10.1016/j.fgb.2012.05.010
- Büchi, G., White, J., and Wogan, G. (1965). The structures of mitorubrin and mitorubrinol. *J. Am. Chem. Soc.* 87, 3484–3489. doi: 10.1021/ja01093a036
- Calcott, M. J., Ackerley, D. F., Knight, A., Keyzers, R. A., and Owen, J. G. (2018). Secondary metabolism in the lichen symbiosis. *Chem. Soc. Rev.* 47, 1730–1760. doi: 10.1039/C7CS00431A
- Camel, V. (2001). Recent extraction techniques for solid matrices—supercritical fluid extraction, pressurized fluid extraction and microwave-assisted extraction: their potential and pitfalls. *Analyst* 126, 1182–1193. doi: 10.1039/b008243k
- Cantrell, S. A., Casillas-Martinez, L., and Molina, M. (2006). Characterization of fungi from hypersaline environments of solar salterns using morphological and molecular techniques. *Mycol. Res.* 110, 962–970. doi: 10.1016/j.mycres.2006.06.005
- Capon, R. J., Stewart, M., Ratnayake, R., Lacey, E., and Gill, J. H. (2007). Citromycetins and bilains A–C: new aromatic polyketides and diketopiperazines from Australian marine-derived and terrestrial *Penicillium* spp. *J. Nat. Prod.* 70, 1746–1752. doi: 10.1021/np0702483
- Caro, Y., Venkatachalam, M., Lebeau, J., Fouillaud, M., and Dufossé, L. (2017). “Pigments and colorants from filamentous fungi,” in *Fungal Metabolites*, eds J.-M. Mérillon and K. G. Ramawat (Springer International Publishing), 499–568. doi: 10.1007/978-3-319-25001-4\_26



- Carvalho, J. C. D., Oishi, B. O., Pandey, A., and Soccol, C. R. (2005). Biopigments from *Monascus*: strains selection, citrinin production and color stability. *Braz. Arch. Biol. Technol.* 48, 885–894. doi: 10.1590/S1516-89132005000800004
- Chadni, Z., Rahaman, M. H., Jerin, I., Hoque, K., and Reza, M. A. (2017). Extraction and optimisation of red pigment production as secondary metabolites from *Talaromyces verruculosus* and its potential use in textile industries. *Mycology* 8, 48–57. doi: 10.1080/21501203.2017.1302013
- Chaudhari, V. M. (2013). Optimization of the extraction parameters for the production of biopigment from the new isolate of distillery effluent. *J. Sci. Innov. Res.* 2, 1044–1051.
- Chemat, F., Rombaut, N., Sicaire, A. G., Meullemiestre, A., Fabiano-Tixier, A. S., and Abert-Vian, M. (2017). Ultrasound assisted extraction of food and natural products. Mechanisms, techniques, combinations, protocols and applications. A review. *Ultrason. Sonochem.* 34, 540–560. doi: 10.1016/j.ultsonch.2016.06.035
- Chen, G., Shi, K., Song, D., Quan, L., and Wu, Z. (2015). The pigment characteristics and productivity shifting in high cell density culture of *Monascus anka* mycelia. *BMC Biotechnol.* 15:72. doi: 10.1186/s12896-015-0183-3
- Chen, W., Chen, R., Liu, Q., He, Y., He, K., Ding, X., et al. (2017). Orange, red, yellow: biosynthesis of azaphilone pigments in *Monascus* fungi. *Chem. Sci.* 8, 4917–4925. doi: 10.1039/C7SC00475C
- Cheung, Y.-C., Siu, K.-C., and Wu, J.-Y. (2013). Kinetic models for ultrasound-assisted extraction of water-soluble components and polysaccharides from medicinal fungi. *Food Bioproc. Tech.* 6, 2659–2665. doi: 10.1007/s11947-012-0929-z
- Chintapenta, L. K., Rath, C. C., Maringinti, B., and Ozbay, G. (2014). Pigment production from a mangrove *Penicillium*. *Afr. J. Biotechnol.* 13, 2668–2674. doi: 10.5897/AJB2014.13838
- Chupin, L., Maunu, S. L., Reynaud, S., Pizzi, A., Charrier, B., and Bouhtoury, F. C. E. (2015). Microwave assisted extraction of maritime pine (*Pinus pinaster*) bark: impact of particle size and characterization. *Ind. Crop Prod.* 65, 142–149. doi: 10.1016/j.indcrop.2014.11.052
- Chuyen, H. V., and Eun, J.-B. (2017). Marine carotenoids: Bioactivities and potential benefits to human health. *Crit. Rev. Food Sci.* 57, 2600–2610. doi: 10.1080/10408398.2015.1063477
- Cocks, S., Wrigley, S. K., Chicarelli-Robinson, M. I. S., and Smith, R. M. (1995). High-performance liquid chromatography comparison of supercritical-fluid extraction and solvent extraction of microbial fermentation products. *J. Chromatogr. A* 697, 115–122. doi: 10.1016/0021-9673(94)00817-S
- Coker, J. A. (2016). Extremophiles and biotechnology: current uses and prospects. *F1000Res.* 5:396. doi: 10.12688/f1000research.7432.1
- Corrêa, R. C. G., Garcia, J. A. A., Correa, V. G., Vieira, T. F., Bracht, A., and Peralta, R.M. (2019). Pigments and vitamins from plants as functional ingredients: current trends and perspectives. *Adv. Food Nutr. Res.* 90, 259–303. doi: 10.1016/b.sfnr.2019.02.003
- Culberson, W. L., Culberson, C. F. (1970). A phylogenetic view of chemical evolution in the lichens. *Bryologist.* 73:1. doi: 10.1639/0007-2745(1970)73[1:APVOCE]2.0.CO;2
- Da Silva, R. P., Rocha-Santos, T. A., and Duarte, A. C. (2016). Supercritical fluid extraction of bioactive compounds. *Trend Anal. Chem.* 76, 40–51. doi: 10.1016/j.trac.2015.11.013
- Das, A., Parida, A., Basak, U., and Das, P. (2002). Studies on pigments, proteins and photosynthetic rates in some mangroves and mangrove associates from Bhitarkanika, Orissa. *Mar. Biol.* 141, 415–422. doi: 10.1007/s00227-002-0847-0
- Das, A., Yoon, S.-H., Lee, S.-H., Kim, J.-Y., Oh, D.-K., and Kim, S.-W. (2007). An update on microbial carotenoid production: application of recent metabolic engineering tools. *Appl. Microbiol. Biotechnol.* 77, 505–512. doi: 10.1007/s00253-007-1206-3
- De Stefano, S., and Nicoletti, R. (1999). Pachybasin and chrysophanol, two anthraquinones produced by the fungus *Trichoderma aureoviride*. *Tabacco* 7, 21–24.
- Delgado-Vargas, F., and Paredes-Lopez, O. (2003). *Natural Colorants for Food and Nutraceutical Uses*. Boca Raton, FL: CRC press. doi: 10.1201/9781420031713
- DePriest, P. T. (2004). Early molecular investigations of lichen-forming symbionts: 1986–2001. *Annu. Rev. Microbiol.* 58, 273–301. doi: 10.1146/annurev.micro.58.030603.123730
- Dhale, M. A., and Vijay-Raj, A. S. (2009). Pigment and amylase production in *Penicillium* sp NIOM-02 and its radical scavenging activity. *Int. J. Food Sci. Tech.* 44, 2424–2430. doi: 10.1111/j.1365-2621.2009.01983.x
- Dos Reis Celestino, J., De Carvalho, L. E., Da Paz Lima, M., Lima, A. M., Ogusku, M. M., and De Souza, J. V. B. (2014). Bioprospecting of amazon soil fungi with the potential for pigment production. *Process Biochem.* 49, 569–575. doi: 10.1016/j.procbio.2014.01.018
- Du, L., Zhu, T., Liu, H., Fang, Y., Zhu, W., and Gu, Q. (2008). Cytotoxic polyketides from a marine-derived fungus *Aspergillus glaucus*. *J. Nat. Prod.* 71, 1837–1842. doi: 10.1021/np800303t
- Duarte, A. W. F., De Menezes, G. C. A. E., Silva, T. R., Bicas, J. L., Oliveira, V. M., and Rosa, L. H. (2019). “Antarctic fungi as producers of pigments,” in *Fungi of Antarctica*, ed. L. Rosa (Springer: Cham), 305–318. doi: 10.1007/978-3-030-18367-7\_14
- Dufosse, L., Fouillaud, M., Caro, Y., Mapari, S. A., and Sutthiwong, N. (2014). Filamentous fungi are large-scale producers of pigments and colorants for the food industry. *Curr. Opin. Biotech.* 26, 56–61. doi: 10.1016/j.copbio.2013.09.007
- Dufossé, L., Galaup, P., Yaron, A., Arad, S. M., Blanc, P., Murthy, K. N. C., et al. (2005). Microorganisms and microalgae as sources of pigments for food use: a scientific oddity or an industrial reality? *Trends Food Sci. Technol.* 16, 389–406. doi: 10.1016/j.tifs.2005.02.006
- Durán, N., Teixeira, M. F., De Conti, R., and Esposito, E. (2002). Ecological-friendly pigments from fungi. *Crit. Rev. Food Sci.* 42, 53–66. doi: 10.1080/10408690290825457
- Durley, R. C., Macmillan, J., Simpson, T. J., Glen, A. T., and Turner, W. B. (1975). Fungal products. part XIII. xanthomegnin, viomellin, rubrosulphin, and viopurpurin, pigments from *Aspergillus sulphureus* and *Aspergillus melleus*. *J. Chem. Soc. [Perkin 1]* 1, 163–169. doi: 10.1039/p19750000163
- Elyashberg, M. E., Blinov, K. A., Williams, A. J., Martirosian, E. R., and Molodtsov, S. G. (2002). Application of a new expert system for the structure elucidation of natural products from their 1D and 2D NMR data. *J. Nat. Prod.* 65, 693–703. doi: 10.1021/np0103315
- Ersus, S., and Yurdagel, U. (2007). Microencapsulation of anthocyanin pigments of black carrot (*Daucus carota* L.) by spray drier. *J. Food Eng.* 80, 805–812. doi: 10.1016/j.jfoodeng.2006.07.009
- Faustino, M., Veiga, M., Sousa, P., Costa, E. M., Silva, S., and Pintado, M. (2019). Agro-food byproducts as a new source of natural food additives. *Molecules* 24:1056. doi: 10.3390/molecules24061056
- FDA (2011). *21CFR73.85 (caramel) in Code of Federal Regulation Title 21 – Food and Drugs 511 Revised As of April 1, 2011*. Federal Register vol. 78, no. 156, Tuesday, August 13, 2013, 512 Rules and Regulations, p. 49117.
- Feng, Y., Shao, Y., and Chen, F. (2012). *Monascus* pigments. *Appl. Microbiol.* 96, 1421–1440. doi: 10.1007/s00253-012-4504-3
- Fielding, B., Haws, E., Holker, J., Powell, A., Robertson, A., Stanway, D., et al. (1960). Monascorubrin. *Tetrahedron Lett.* 1, 24–27. doi: 10.1016/S0040-4039(01)82691-5
- Filly, A., Fabiano-Tixier, A. S., Louis, C., Fernandez, X., and Chemat, F. (2016). Water as a green solvent combined with different techniques for extraction of essential oil from lavender flowers. *Cr. Chim.* 19, 707–717. doi: 10.1016/j.crci.2016.01.018
- Fincan, M. (2017). “Potential application of pulsed electric fields for improving extraction of plant pigments,” in *Handbook of Electroporation*, ed D. Miklavcic (Cham: Springer), 1–22. doi: 10.1007/978-3-319-26779-1\_34-1
- Flórez, N., Conde, E., and Domínguez, H. (2015). Microwave assisted water extraction of plant compounds. *J. Chem. Technol.* 90, 590–607. doi: 10.1002/jctb.4519
- Food and Administration Drug (2015). *Direct Food Substances Affirmed as Generally Recognized as Safe*. Food and Drug Administration, 417–418.
- Fouillaud, M., Venkatachalam, M., Girard-Valenciennes, E., Caro, Y., and Dufossé, L. (2016). “Marine-derived fungi producing red anthraquinones: new resources for natural colors,” in *8th International Conference of Pigments in Food, “Coloured foods for health benefits,”* (Cluj-Napoca, Romania).
- Fouillaud, M., Venkatachalam, M., Llorente, M., Magalon, H., Cuét, P., and Dufossé, L. (2017). Biodiversity of pigmented fungi isolated from marine environment in La Réunion island, Indian ocean: new resources for colored metabolites. *J. Fungi* 3:36. doi: 10.3390/jof3030036
- Frisvad, J. C., Smedsgaard, J., Larsen, T. O., and Samson, R. A. (2004). Mycotoxins, drugs and other extrolites produced by species in *Penicillium* subgenus *Penicillium*. *Stud. Mycol.* 49:e41.
- Fujitake, N., Suzuki, T., Fukumoto, M., and Oji, Y. (1998). Predominance of dimers over naturally occurring anthraquinones in soil. *J. Nat. Prod.* 61, 189–192. doi: 10.1021/np9703050



- Galafu, N., Bortlik, K., and Michel, M. (2015). "An industry perspective on natural food colour stability," in *Colour Additives for Foods and Beverages* (Cambridge, UK: Woodhead Publishing), 91–130. doi: 10.1016/B978-1-78242-011-8.00005-2
- Gao, J.-M., Yang, S.-X., and Qin, J.-C. (2013). Azaphilones: chemistry and biology. *Chem. Rev.* 113, 4755–4811. doi: 10.1021/cr300402y
- Garfield, S. (2002). *Mauve: How One Man Invented a Color That Changed the World*. New York, NY: WW Norton and Company.
- Garton, G., Goodwin, T., and Lijinsky, W. (1950). The biogenesis of beta-carotene in the fungus *Phycomyces blakesleeanus*. *Biochem. J.* 2:35.
- Gawas, D., Tilvi, S., Naik, C., and Parameswaran, P. (2002). "Fungal metabolites: tetrahydroauroglaucon and isodihydroauroglaucon from the marine fungus, *Eurotium* sp.," in *Proceedings of the National Conference on Utilization of Bioresources - NATCUB-2002, October 24-25, 2002*, eds A. Sree, Y.R. Rao, B. Nanda, V.N. Misra (Bhubaneswar: Regional Research Laboratory), 453–457.
- Gengatharan, A., Dykes, G. A., and Choo, W. S. (2015). Betalains: natural plant pigments with potential application in functional foods. *LWT-Food Sci. Technol.* 64, 645–649. doi: 10.1016/j.lwt.2015.06.052
- Gessler, N., Egorova, A., and Belozerskaya, T. (2013). Fungal anthraquinones. *Appl. Biochem. Microbiol.* 49, 85–99. doi: 10.1134/S000368381302004X
- Gharibzadeh, S. M. T., Razavi, S. H., Mousavi, S. M., and Moayedi, V. (2012). High efficiency canthaxanthin production by a novel mutant isolated from *Dietzia natronolimnaea* HS-1 using central composite design analysis. *Ind. Crops Prod.* 40, 345–354. doi: 10.1016/j.indcrop.2012.03.030
- Gmoser, R., Ferreira, J. A., Lennartsson, P. R., and Taherzadeh, M. J. (2017). Filamentous ascomycetes fungi as a source of natural pigments. *Fungal Biol. Biotechnol.* 4:4. doi: 10.1186/s40694-017-0033-2
- Goettl, M., Eing, C., Gusbeth, C., Straessner, R., and Frey, W. (2013). Pulsed electric field assisted extraction of intracellular valuables from microalgae. *Algal Res.* 2, 401–408. doi: 10.1016/j.algal.2013.07.004
- Gonçalves, R., Lisboa, H., and Pombeiro-Sponchiado, S. (2012). Characterization of melanin pigment produced by *Aspergillus nidulans*. *World J. Microb. Biot.* 28, 1467–1474. doi: 10.1007/s11274-011-0948-3
- Grewal, P. S., Modavi, C., Russ, Z. N., Harris, N. C., and Dueber, J. E. (2018). Bioproduction of a betalain color palette in *Saccharomyces cerevisiae*. *Metab. Eng.* 45, 180–188. doi: 10.1016/j.ymben.2017.12.008
- Grimi, N., Dubois, A., Marchal, L., Jubeau, S., Lebovka, N. I., and Vorobiev, E. (2014). Selective extraction from microalgae *Nannochloropsis* sp. using different methods of cell disruption. *Bioresour. Technol.* 153, 254–259. doi: 10.1016/j.biortech.2013.12.011
- Grosso, C., Valentão, P., Ferreres, F., and Andrade, P. B. (2015). Alternative and efficient extraction methods for marine-derived compounds. *Mar. Drugs* 13, 3182–3230. doi: 10.3390/md13053182
- Hajjaj, H., Blanc, P., Goma, G., and Francois, J. (1998). Sampling techniques and comparative extraction procedures for quantitative determination of intra- and extracellular metabolites in filamentous fungi. *FEMS Microbiol. Lett.* 164, 195–200. doi: 10.1111/j.1574-6968.1998.tb13085.x
- Hajjaj, H., Klaebe, A., Lore, M. O., Goma, G., Blanc, P. J., and François, J. (1999). Biosynthetic pathway of citrinin in the filamentous fungus *Monascus ruber* as revealed by <sup>13</sup>C nuclear magnetic resonance. *Appl. Environ. Microbiol.* 65, 311–314. doi: 10.1128/AEM.65.1.311-314.1999
- Hamzah, T. N. T., Lee, S. Y., Hidayat, A., Terhem, R., Faridah-Hanum, I., and Mohamed, R. (2018). Diversity and characterization of endophytic fungi isolated from the tropical mangrove species, rhizophora mucronata, and identification of potential antagonists against the soil-borne fungus, fusarium solani. *Front. Microbiol.* 9:1707. doi: 10.3389/fmicb.2018.01707
- Harasym, J., and Bogacz-Radomska, L. (2016). Colorants in foods-from past to present. *Nauki Inz. Technol.* 3, 21–35. doi: 10.15611/nit.2016.3.02
- Haws, E., Holker, J., Kelly, A., Powell, A., and Robertson, A. (1959). 722. The chemistry of fungi. Part XXXVII. The structure of rubropunctatin. *J. Chem. Soc. (Resumed)*. 3598–3610. doi: 10.1039/jr9590003598
- Heer, K., and Sharma, S. (2017). Microbial pigments as a natural color: a review. *Int. J. Pharm. Sci. Res.* 8, 1913–1922. doi: 10.13040/IJPSR.0975-8232.8(5).1913-22
- Hejazi, M. A., and Wijffels, R. H. (2004). Milking of microalgae. *Trends Biotechnol.* 22, 189–194. doi: 10.1016/j.tibtech.2004.02.009
- Hernández, V. A., Galleguillos, F., Thibaut, R., and Müller, A. (2019). Fungal dyes for textile applications: testing of industrial conditions for wool fabrics dyeing. *J. Text. Inst.* 110, 61–66. doi: 10.1080/00405000.2018.1460037
- Hsu, Y.-W., Hsu, L.-C., Liang, Y.-H., Kuo, Y.-H., and Pan, T.-M. (2011). New bioactive orange pigments with yellow fluorescence from *Monascus*-fermented dioscorea. *J. Agr. Food Chem.* 59, 4512–4518. doi: 10.1021/jf1045987
- Hu, Z., Zhang, X., Wu, Z., Qi, H., and Wang, Z. (2012). Perstraction of intracellular pigments by submerged cultivation of monascus in nonionic surfactant micelle aqueous solution. *Appl. Microbiol.* 94, 81–89. doi: 10.1007/s00253-011-3851-9
- Huang, C.-H., Pan, J.-H., Chen, B., Yu, M., Huang, H.-B., Zhu, X. et al. (2011). Three bianthraquinone derivatives from the mangrove endophytic fungus *Alternaria* sp. ZJ9-6B from the South China Sea. *Mar. Drugs* 9, 832–843. doi: 10.3390/md9050832
- Iqbal, M., Tao, Y., Xie, S., Zhu, Y., Chen, D., Wang, X. et al. (2016). Aqueous two-phase system (ATPS): an overview and advances in its applications. *Biol. Proced. Online* 18:18. doi: 10.1186/s12575-016-0048-8
- Ishikawa, Y., Morimoto, K., and Hamasaki, T. (1984). Flavoglaucon, a metabolite of *Eurotium chevalieri*, its antioxidation and synergism with tocopherol. *J. Am. Oil Chem. Soc.* 61, 1864–1868. doi: 10.1007/BF02540819
- Ishikawa, Y., Morimoto, K., and Iseki, S. (1991). Atrovetin as a potent antioxidant compound from *Penicillium* species. *J. Am. Oil Chem. Soc.* 68, 666–668. doi: 10.1007/BF02662291
- Janiszewska-Turak, E., Pisarska, A., and Królczyk, J. B. (2016). Natural food pigments application in food products. *Nauka. Przyroda. Technol.* 10:51. doi: 10.17306/J.NPT.2016.4.51
- Jiang, P.-X., Wang, H.-S., Zhang, C., Lou, K., and Xing, X.-H. (2010). Reconstruction of the violacein biosynthetic pathway from *Duganella* sp. B2 in different heterologous hosts. *Appl. Microbiol.* 86, 1077–1088. doi: 10.1007/s00253-009-2375-z
- Joshi, V., and Attri, D. (2005). Solid state fermentation of apple pomace for the production of value added products. in *Poll. Urban Ind. Environ.*, eds S. N. Das, Y. V. Swamy, K. K. Rao, and V. N. Misra (New Delhi: Allied Publisher Private Limited), 180–186.
- Joshi, V., Attri, D., Bala, A., and Bhushan, S. (2003). Microbial pigments. *Indian J. Biotechnol.* 2, 362–369.
- Karrer, P., and Helfenstein, A. (1932). Plant pigments. *Annu. Rev. Biochem.* 1, 551–580. doi: 10.1146/annurev.bi.01.070132.003003
- Kathiresan, K., and Bingham, B. L. (2001). Biology of mangroves and mangrove ecosystems. *Adv. Mar. Biol.* 40, 84–254. doi: 10.1016/S0065-2881(01)40003-4
- Kaul, S., Gupta, S., Ahmed, M., and Dhar, M. K. (2012). Endophytic fungi from medicinal plants: a treasure hunt for bioactive metabolites. *Phytochem. Rev.* 11, 487–505. doi: 10.1007/s11101-012-9260-6
- Khaw, K. Y., Parat, M. O., Shaw, P. N., and Falconer, J. R. (2017). Solvent supercritical fluid technologies to extract bioactive compounds from natural sources: a review. *Molecules* 22:1186. doi: 10.3390/molecules22071186
- Kinoshita, K., Yamamoto, Y., Koyama, K., Takahashi, K., and Yoshimura, I. (2003). Novel fluorescent isoquinoline pigments, panaefluorolines A–C from the cultured mycobiont of a lichen, *Amygdalaria panaeola*. *Tetrahedron. Lett.* 44, 8009–8011. doi: 10.1016/j.tetlet.2003.08.109
- Kiss, G. A. C., Forgacs, E., Cserhati, T., Mota, T., Morais, H., and Ramos, A. (2000). Optimisation of the microwave-assisted extraction of pigments from paprika (*Capsicum annuum* L.) powders. *J. Chromatogr. A* 889, 41–49. doi: 10.1016/S0021-9673(00)00440-4
- Kitada, K., Machmudah, S., Sasaki, M., Goto, M., Nakashima, Y., Kumamoto, S., et al. (2009). Supercritical CO<sub>2</sub> extraction of pigment components with pharmaceutical importance from *Chlorella vulgaris*. *J. Chem. Technol. Biotechnol.* 84, 657–661. doi: 10.1002/jctb.2096
- Kjær, D., Kjær, A., Pedersen, C., Bu'lock, J., and Smith, J. (1971). Bikaverin and norbikaverin, benzoxanthentriene pigments of *Gibberella fujikuroi*. *J. Chem. Soc. C Organic* 2792–2797. doi: 10.1039/J39710002792
- Kogej, T., Wheeler, M. H., Lanišnik Rižner, T., and Gunde-Cimerman, N. (2004). Evidence for 1, 8-dihydroxynaphthalene melanin in three halophilic black yeasts grown under saline and non-saline conditions. *FEMS Microbiol. Lett.* 232, 203–209. doi: 10.1016/S0378-1097(04)00073-4
- Krairak, S., Yamamura, K., Irie, R., Nakajima, M., Shimizu, H., Chim-Anage, P., et al. (2000). Maximizing yellow pigment production in fed-batch culture of *Monascus* sp. *J. Biosci. Bioeng.* 90, 363–367. doi: 10.1016/S1389-1723(01)80002-5
- Krishnamurthy, S., Narasimha Murthy, K., and Thirumale, S. (2018). Characterization of ankaflavin from *Penicillium aculeatum* and its cytotoxic properties. *Nat. Prod. Res.* 1–6. doi: 10.1080/14786419.2018.1522633

- Lebeau, J., Petit, T., Clerc, P., Dufossé, L., and Caro, Y. (2019). Isolation of two novel purple naphthoquinone pigments concomitant with the bioactive red bikaverin and derivatives thereof produced by *Fusarium oxysporum*. *Biotechnol. Prog.* 35:e2738. doi: 10.1002/btpr.2738
- Lebeau, J., Venkatachalam, M., Fouillaud, M., Dufossé, L., and Caro, Y. (2016). "Extraction of fungal polyketide pigments using ionic liquids," *8th International Conference of Pigments in Food*, "Coloured foods for health benefits," (Cluj-Napoca, Romania), 2405–2426.
- Lebeau, J., Venkatachalam, M., Fouillaud, M., Petit, T., Vinale, F., Dufossé, L., et al. (2017). Production and new extraction method of polyketide red pigments produced by ascomycetous fungi from terrestrial and marine habitats. *J. Fungi*. 3:34. doi: 10.3390/jof3030034
- Li, D.-L., Li, X.-M., and Wang, B.-G. (2009). Natural anthraquinone derivatives from a marine mangrove plant-derived endophytic fungus *Euotium rubrum*: structural elucidation and DPPH radical scavenging activity. *J. Microbiol. Biotechnol.* 19, 675–680.
- Li, Y., Fabiano-Tixier, A. S., Abert-Vian, M., and Chemat, F. (2012). "Microwave-assisted extraction of antioxidants and food colors," in *Microwave-assisted Extraction for Bioactive Compounds* (Boston, MA: Springer), 103–125. doi: 10.1007/978-1-4614-4830-3\_5
- Li, Y., Li, X., Lee, U., Kang, J. S., Choi, H. D., and Sona, B. W. (2006). A new radical scavenging anthracene glycoside, asperflavin ribofuranoside, and polyketides from a marine isolate of the fungus *Microsporium*. *Chem. Pharm. Bull.* 54, 882–883. doi: 10.1248/cpb.54.882
- Li, Z. J., Shukla, V., Fordyce, A. P., Pedersen, A. G., Wenger, K. S., and Marten, M. R. (2000). Fungal morphology and fragmentation behavior in a fed-batch *Aspergillus oryzae* fermentation at the production scale. *Biotechnol. Bioeng.* 70, 300–312. doi: 10.1002/1097-0290(20001105)70:3<300::AID-BIT7>3.0.CO;2-3
- Liaid, A., Guerrero, R. F., Cantos, E., Palma, M., and Barroso, C. G. (2011). Microwave assisted extraction of anthocyanins from grape skins. *Food Chem.* 124, 1238–1243. doi: 10.1016/j.foodchem.2010.07.053
- Lin, Y.-R., Lo, C.-T., Liu, S.-Y., and Peng, K.-C. (2012). Involvement of pachybasin and emodin in self-regulation of trichoderma harzianum mycoparasitic coiling. *J. Agr. Food Chem.* 60, 2123–2128. doi: 10.1021/jf202773y
- Luengo, E., Martínez, J. M., Bordetas, A., Álvarez, I., and Raso, J. (2015). Influence of the treatment medium temperature on lutein extraction assisted by pulsed electric fields from *Chlorella vulgaris*. *Innov. Food Sci. Emerg. Technol.* 29, 15–22. doi: 10.1016/j.ifset.2015.02.012
- Mahmoodian, A., and Stickings, C. (1964). Studies in the biochemistry of micro-organisms. 115. Metabolites of *Penicillium frequentans* Westling: isolation of sulochrin, asteric acid, (+)-bisdechlorogedonin and two new substituted anthraquinones, questin and questinol. *Biochem. J.* 92, 369–378. doi: 10.1042/bj0920369
- Mani, V. M., Gnana Soundari, A. P., Karthiyaini, D., and Preethi, K. (2015). Bioprospecting endophytic fungi and their metabolites from medicinal tree *Aegle marmelos* in Western Ghats, India. *Mycobiology* 43, 303–310. doi: 10.5941/MYCO.2015.43.3.303
- Mapari, S. A., Hansen, M. E., Meyer, A. S., and Thrane, U. (2008). Computerized screening for novel producers of *Monascus*-like food pigments in *Penicillium* species. *J. Agr. Food Chem.* 56, 9981–9989. doi: 10.1021/jf801817q
- Mapari, S. A., Meyer, A. S., and Thrane, U. (2006). Colorimetric characterization for comparative analysis of fungal pigments and natural food colorants. *J. Agr. Food Chem.* 54, 7027–7035. doi: 10.1021/jf062094n
- Mapari, S. A., Meyer, A. S., Thrane, U., and Frisvad, J. C. (2009). Identification of potentially safe promising fungal cell factories for the production of polyketide natural food colorants using chemotaxonomic rationale. *Microb. Cell Fact.* 8:24. doi: 10.1186/1475-2859-8-24
- Mapari, S. A., Nielsen, K. F., Larsen, T. O., Frisvad, J. C., Meyer, A. S., and Thrane, U. (2005). Exploring fungal biodiversity for the production of water-soluble pigments as potential natural food colorants. *Curr. Opin. Biotech.* 16, 231–238. doi: 10.1016/j.copbio.2005.03.004
- Mapari, S. A., Thrane, U., and Meyer, A. S. (2010). Fungal polyketide azaphilone pigments as future natural food colorants? *Trends Biotechnol.* 28, 300–307. doi: 10.1016/j.tibtech.2010.03.004
- Matsuo, T., Hara, T., Ikemoto, H., Jacques, K., Kasai, S., Kinjo, A., et al. (2018). Improvement of photobleaching of *Monascus* pigments using novel nanoencapsulation technology. *Sci. Bull. Facul. Agric. Univ. Ryukyus.* 65, 83–89. Available online at: <http://hdl.handle.net/20.500.12000/44608>
- McCann, D., Barrett, A., Cooper, A., Crumpler, D., Dalen, L., Grimshaw, K., et al. (2007). Food additives and hyperactive behaviour in 3-year-old and 8/9-year-old children in the community: a randomised, double-blinded, placebo-controlled trial. *Lancet* 370, 1560–1567. doi: 10.1016/S0140-6736(07)61306-3
- McQueen, L., and Lai, D. (2019). Ionic liquid aqueous two-phase systems from a pharmaceutical perspective. *Front. Chem.* 7:135. doi: 10.3389/fchem.2019.00135
- Medentsev, A., and Akimenko, V. (1998). Naphthoquinone metabolites of the fungi. *Phytochem.* 47, 935–959. doi: 10.1016/S0031-9422(98)80053-8
- Medentsev, A., Arinbasarova, A. Y., and Akimenko, V. (2005). Biosynthesis of naphthoquinone pigments by fungi of the genus *Fusarium*. *Appl. Biochem. Microbiol.* 41, 503–507. doi: 10.1007/s10438-005-0091-8
- Mehrad, B., Ravanfar, R., Licker, J., Regenstein, J. M., and Abbaspourrad, A. (2018). Enhancing the physicochemical stability of  $\beta$ -carotene solid lipid nanoparticle (SLNP) using whey protein isolate. *Food Res. Int.* 105, 962–969. doi: 10.1016/j.foodres.2017.12.036
- Mercadante, A. Z. (2007). "Carotenoids in foods: sources and stability during processing and storage," in *Food colorants: Chemical and Functional Properties*. ed. C. Socaciu (Boca Raton, FL: CRC press), 213–240.
- Miyagawa, H., Hamada, N., Sato, M., and Eeno, T. (1994). Pigments from the cultured lichen mycobionts of *graphis scripta* and *G. desquamescens*. *Phytochem.* 36, 1319–1322. doi: 10.1016/S0031-9422(00)89659-4
- Miyagawa, H., Hamada, N., Sato, M., and Ueno, T. (1993). Hypostrepsilic acid, a new dibenzofuran from the culture lichen mycobiont of *Evernia esorediosa*. *Phytochem.* 34, 589–591. doi: 10.1016/0031-9422(93)80057-Y
- Mondal, S., Samantaray, D., and Mishra, B. (2015). Optimization of pigment production by a novel *Bacillus* sp. BMRH isolated from cow dung. *J. Pure Appl. Microbiol.* 9, 2321–2326.
- Morales-Oyervides, L., Oliveira, J., Sousa-Gallagher, M., Méndez-Zavala, A., and Montañez, J. C. (2017). Perstraction of intracellular pigments through submerged fermentation of *talaromyces* spp. in a surfactant rich media: a novel approach for enhanced pigment recovery. *J. Fungi*. 3:33. doi: 10.3390/jof3030033
- Moriyasu, Y., Miyagawa, H., Hamada, N., Miyawaki, H., and Ueno, T. (2001). 5-Deoxy-7-methylbostrycoidin from cultured mycobionts from *Haematomma* sp. *Phytochem.* 58, 239–241. doi: 10.1016/S0031-9422(01)00167-4
- Morris, P. J., and Travis, A. S. (1992). A history of the international dyestuff industry. *Amer. Dyestuff Rep.* 81, 59–59.
- Mortensen, A. (2006). Carotenoids and other pigments as natural colorants. *Pure Appl. Chem.* 78, 1477–1491. doi: 10.1351/pac200678081477
- Mukherjee, G., and Singh, S. K. (2011). Purification and characterization of a new red pigment from *Monascus purpureus* in submerged fermentation. *Process Biochem.* 46, 188–192. doi: 10.1016/j.procbio.2010.08.006
- Mussagy, C. U., Santos-Ebinuma, V. C., Gonzalez-Miquel, M., Coutinho, J. A., and Pereira, J. F. (2019). Protic ionic liquids as cell-disrupting agents for the recovery of intracellular carotenoids from yeast *rhodotorula glutinis* CCT-2186. *ACS Sustain. Chem. Eng.* 7, 16765–16776. doi: 10.1021/acssuschemeng.9b04247
- Mustafa, A., and Turner, C. (2011). Pressurized liquid extraction as a green approach in food and herbal plants extraction: a review. *Anal. Chim. Acta* 703, 8–18. doi: 10.1016/j.jaca.2011.07.018
- Nguyen, K. H., Chollet-Krugler, M., Gouault, N., and Tomasi, S. (2013). UV-protectant metabolites from lichens and their symbiotic partners. *Nat. Prod. Rep.* 30, 1490–1508. doi: 10.1039/c3np70064j
- Nielsen, J. C., and Nielsen, J. (2017). Development of fungal cell factories for the production of secondary metabolites: linking genomics and metabolism. *Synth. Syst. Biotechnol.* 2, 5–12. doi: 10.1016/j.synbio.2017.02.002
- Nobre, B. P., Mendes, R. L., Queiroz, E. M., Pessoa, F. L. P., Coelho, J. P., and Palavra, A. F. (2006). Supercritical carbon dioxide extraction of pigments from *Bixa orellana* seeds (experiments and modeling). *Braz. J. Chem. Eng.* 23, 251–258. doi: 10.1590/S0104-66322006000200013
- Nybakken, L., Solhaug, K. A., Bilger, W., and Gauslaa, Y. (2004). The lichens *Xanthoria elegans* and *cetraria islandica* maintain a high protection against UV-B radiation in Arctic habitats. *Oecologia* 140, 211–216. doi: 10.1007/s00442-004-1583-6
- Ogasawara, N., Mizuno, R., and Kawai, K.-I. (1997). Structures of a new type of yellow pigments, falconenones A and B, from *Emericella falconensis*. *J. Chem. Soc. [Perkin 1]* 1, 2527–2530. doi: 10.1039/a701277b
- Ogbonna, C. N. (2016). Production of food colourants by filamentous fungi. *Afr. J. Microbiol. Res.* 10, 960–971. doi: 10.5897/AJMR2016.7904

- Ogihara, J., Kato, J., Oishi, K., Fujimoto, Y., and Eguchi, T. (2000). Production and structural analysis of PP-V, a homologue of monascorubramine, produced by a new isolate of *Penicillium* sp. *J. Biosci. Bioeng.* 90, 549–554. doi: 10.1016/S1389-1723(01)80039-6
- Oren, A. (2010). Industrial and environmental applications of halophilic microorganisms. *Environ. Technol.* 31, 825–834. doi: 10.1080/09593330903370026
- Osmanova, N., Schultze, W., and Ayoub, N. (2010). Azaphilones: a class of fungal metabolites with diverse biological activities. *Phytochem. Rev.* 9, 315–342. doi: 10.1007/s11101-010-9171-3
- Özkan, G., and Bilek, S.E. (2014). Microencapsulation of natural food colourants. *Int. J. Food Sci. Nutr.* 3, 145–156. doi: 10.11648/j.ijnfs.20140303.13
- Padhi, S., Masi, M., Cimmino, A., Tuzi, A., Jena, S., Tayung, K., et al. (2019). Funiculosone, a substituted dihydroxanthene-1,9-dione with two of its analogues produced by an endolichenic fungus *Talaromyces funiculosus* and their antimicrobial activity. *Phytochem.* 157, 175–183. doi: 10.1016/j.phytochem.2018.10.031
- Pandey, N., Jain, R., Pandey, A., and Tamta, S. (2018). Optimisation and characterisation of the orange pigment produced by a cold adapted strain of *Penicillium* sp. (GBPI\_P155) isolated from mountain ecosystem. *Mycol.* 9, 81–92. doi: 10.1080/21501203.2017.1423127
- Pare, J. J., Sigouin, M., and Lapointe, J. (1991). *Canada Minister of Environment Microwave-Assisted Natural Products Extraction*. Washington, DC: U.S. Patent and Trademark Office.
- Parniakov, O., Barba, F. J., Grimi, N., Marchal, L., Jubeau, S., Lebovka, N., et al. (2015). Pulsed electric field assisted extraction of nutritionally valuable compounds from microalgae *Nannochloropsis* spp. using the binary mixture of organic solvents and water. *Innov. Food Sci. Emerg.* 27, 79–85. doi: 10.1016/j.ifset.2014.11.002
- Pasquet, V., Chérouvrier, J.R., Farhat, F., Thiéry, V., Piot, J.M., Bérard, J.B., et al. (2011). Study on the microalgal pigments extraction process: performance of microwave assisted extraction. *Process Biochem.* 46, 59–67. doi: 10.1016/j.procbio.2010.07.009
- Passos, H., Freire, M. G., and Coutinho, J. A. (2014). Ionic liquid solutions as extractive solvents for value-added compounds from biomass. *Green Chem.* 16, 4786–4815. doi: 10.1039/C4GC00236A
- Pathare, P. B., Opara, U. L., and Al-Said, F. A. -J. (2013). Colour measurement and analysis in fresh and processed foods: a review. *Food Bioproc. Tech.* 6, 36–60. doi: 10.1007/s11947-012-0867-9
- Pfeifer, B. A., and Khosla, C. (2001). Biosynthesis of polyketides in heterologous hosts. *Microbiol. Mol. Biol. Rev.* 65, 106–118. doi: 10.1128/MMBR.65.1.106-118.2001
- Podojil, M., Sedmera, P., Vokoun, J., Betina, V., Barathova, H., Duračková, Z., et al. (1978). *Eurotium* (*Aspergillus*) *repens* metabolites and their biological activity. *Folia Microbiol.* 23, 438–443. doi: 10.1007/BF02885572
- Pombeiro-Sponchiado, S. R., Sousa, G. S., Andrade, J. C., Lisboa, H. F., and Gonçalves, R. C. (2017). “Production of melanin pigment by fungi and its biotechnological applications,” in *Melanin*, ed M. Blumenberg (London, UK: InTech), 47–74. doi: 10.5772/67375
- Poojary, M. M., Barba, F. J., Aliakbarian, B., Donsi, F., Pataro, G., Dias, D. A., et al. (2016). Innovative alternative technologies to extract carotenoids from microalgae and seaweeds. *Mar. drugs.* 14:214. doi: 10.3390/md14110214
- Qiu, M., Xie, R., Shi, Y., Chen, H., Wen, Y., Gao, Y., et al. (2010). Isolation and identification of endophytic fungus SX01, a red pigment producer from *Ginkgo biloba* L. *World J. Microb. Biot.* 26, 993–998. doi: 10.1007/s11274-009-0261-6
- Rani, M. H. S., Ramesh, T., Subramanian, J., and Kalaiselvam, M. (2013). Production and characterization of melanin pigment from halophilic black yeast *Hortaea werneckii*. *Int. J. Pharm. Res. Rev.* 2, 9–17.
- Rao, N., Prabhu, M., Xiao, M., and Li, W. J. (2017). Fungal and bacterial pigments: secondary metabolites with wide applications. *Front. Microbiol.* 8:1113. doi: 10.3389/fmicb.2017.01113
- Redman, R. S., Sheehan, K. B., Stout, R. G., Rodriguez, R. J., and Henson, J. M. (2002). Thermotolerance generated by plant/fungal symbiosis. *Science* 298, 1581–1581. doi: 10.1126/science.1072191
- Richter, B. E., Jones, B. A., Ezzell, J. L., Porter, N. L., Avdalovic, N., and Pohl, C. (1996). Accelerated solvent extraction: a technique for sample preparation. *Anal. Chem.* 68, 1033–1039. doi: 10.1021/ac9508199
- Roberts, J. C., and Thompson, D. (1971). Studies in mycological chemistry. Part XXVII. Reinvestigation of the structure of purpurogenone, a metabolite of *Penicillium purpurogenum* Stoll. *J. Chem. Soc. C Organic* 3488–3492. doi: 10.1039/j39710003488
- Rohrig, B. (2016). Eating with your eyes: the chemistry of food colorings. *Chemistry* 2015:2015.
- Romano, S., Jackson, S. A., Patry, S., and Dobson, A. D. (2018). Extending the “one strain many compounds” (OSMAC) principle to marine microorganisms. *Mar. Drugs* 16:244. doi: 10.3390/md16070244
- Rymbai, H., Sharma, R., and Srivastav, M. (2011). Bio-colorants and its implications in health and food industry—a review. *Int. J. Pharm. Tech. Res.* 3, 2228–2244.
- Sankari, M., Rao, P.R., Hemachandran, H., Pullela, P.K., Tayubi, I.A., Subramanian, B., et al. (2018). Prospects and progress in the production of valuable carotenoids: insights from metabolic engineering, synthetic biology, and computational approaches. *J. Biotech.* 266, 89–101. doi: 10.1016/j.jbiotec.2017.12.010
- Santos-Ebinuma, V. C., Teixeira, M. F. S., and Pessoa, A. (2013). Submerged culture conditions for the production of alternative natural colorants by a new isolated *Penicillium purpurogenum* DPUA 1275. *J. Microbiol. Biotechnol.* 23, 802–810. doi: 10.4014/jmb.1211.11057
- Sardaryan, E. (2002). Strain of the microorganism *Penicillium oxalicum* var. *Armeniaca* and its application. *Google Pat.* 6, 340–586.
- Scotter, M. J. (1995). Characterisation of the coloured thermal degradation products of bixin from annatto and a revised mechanism for their formation. *Food Chem.* 53, 177–185. doi: 10.1016/0308-8146(95)90785-6
- Sen, T., Barrow, C. J., and Deshmukh, S. K. (2019). Microbial pigments in the food industry—challenges and the way forward. *Front. Nutr.* 6:7. doi: 10.3389/fnut.2019.00007
- Seoane, P. R., Flórez-Fernández, N., Piñeiro, E. C., and González, H. D. (2017). “Microwave-assisted water extraction,” in *Water Extraction of Bioactive Compounds*, eds H. D. González and M. J. G. Muñoz (Amsterdam: Elsevier), 163–198. doi: 10.1016/B978-0-12-809380-1.00006-1
- Shao, H.-J., Qin, X.-D., Dong, Z.-J., Zhang, H.-B., and Liu, J.-K. (2008). Induced daldinin A, B, C with a new skeleton from cultures of the ascomycete *Daldinia concentrica*. *J. Antibiot. Res.* 61, 115–119. doi: 10.1038/ja.2008.119
- Sigurdson, G. T., Tang, P., and Giusti, M. M. (2017). Natural colorants: food colorants from natural sources. *Annu. Rev. Food Sci.* 8, 261–280. doi: 10.1146/annurev-food-030216-025923
- Singha, T. K. (2012). Microbial extracellular polymeric substances: production, isolation and applications. *IOSR J. Pharm.* 2, 271–281. doi: 10.9790/3013-0220276281
- Smale, M. C., Wiser, S. K., Bergin, M. J., and Fitzgerald, N. B. (2018). A classification of the geothermal vegetation of the Taupo Volcanic Zone, New Zealand. *J. Roy. Soc. New Zeal.* 48, 21–38. doi: 10.1080/03036758.2017.1322619
- Socaciu, C. (ed.). (2007). “Updated technologies for extracting and formulating food colorants,” in *Food Colorants: Chemical and Functional Properties* (Boca Raton, FL: CRC press), 303–328. doi: 10.1201/9781420009286
- Spence, C. (2015). On the psychological impact of food colour. *Flavour.* 4:21. doi: 10.1186/s13411-015-0031-3
- Spier, M. R., Vandenbergh, L., Medeiros, A. B. P., and Soccol, C. R. (2011). Application of different types of bioreactors in bioprocesses,” in *Bioreactors: Design, Properties and Applications*, eds P. G. Antolli and Z. Liu (Hauppauge, NY: Nova Science Publishers), 53–87.
- Stack, M. E., Eppley, R. M., Dreifuss, P. A., and Pohland, A. E. (1977). Isolation and identification of xanthomegnin, viomellein, rubrosulphin, and viopurpurin as metabolites of *penicillium viridicatum*. *Appl. Environ. Microbiol.* 33, 351–355. doi: 10.1128/AEM.33.2.351-355.1977
- Stack, M. E., and Mislivec, P. B. (1978). Production of xanthomegnin and viomellein by isolates of *Aspergillus ochraceus*, *Penicillium cyclopium*, and *Penicillium viridicatum*. *Appl. Environ. Microbiol.* 36, 552–554. doi: 10.1128/AEM.36.4.552-554.1978
- Steiner, E., Kalamar, J., Charollais, E., and Posternak, T. (1974). Recherches sur la biochimie des champignons inférieurs IX. Synthèse de précurseurs marques et biosynthèse de la phoenicine et de l’oosporeine. *Helv. Chim. Acta* 57, 2377–2387. doi: 10.1002/hlca.19740570810
- Stocker-Worgotter, E. (2008). Metabolic diversity of lichen-forming ascomycetous fungi: culturing, polyketide and shikimate metabolite production, and PKS genes. *Nat. Prod. Rep.* 25, 188–200. doi: 10.1039/B606983P
- Stocker-Wörgötter, E., Cordeiro, L. M. C., and Iacomini, M. (2013). “Accumulation of potential pharmaceutically relevant lichen metabolites



- in lichens and cultured lichen symbionts,” in *Studies in Natural Products Chemistry*, Vol. 39. (Great Britain, UK: Elsevier), 337–380. doi: 10.1016/B978-0-444-62615-8.00010-2
- Studt, L., Wiemann, P., Kleigrewe, K., Humpf, H.-U., and Tudzynski, B. (2012). Biosynthesis of fusarubins accounts for pigmentation of *Fusarium fujikuroi* perithecia. *Appl. Environ. Microbiol.* 78, 4468–4480. doi: 10.1128/AEM.00823-12
- Suryanarayanan, T. S., Ravishankar, J. P., Venkatesan, G., and Murali, T. S. (2004). Characterization of the melanin pigment of a cosmopolitan fungal endophyte. *Mycol. Res.* 108, 974–978. doi: 10.1017/S0953756204000619
- Takahashi, H., Nozawa, K., and Kawai, K.-I. (1996). Isolation and structures of dicyanide derivatives, epurpurins A to C, from *Emericella purpurea*. *Chem. Pharm. Bull.* 44, 2227–2230. doi: 10.1248/cpb.44.2227
- Tatum, J., Baker, R., and Berry, R. (1985). Naphthoquinones produced by *Fusarium oxysporum* isolated from citrus. *Phytochem.* 24, 457–459. doi: 10.1016/S0031-9422(00)80746-3
- Tiwari, B. K. (2015). Ultrasound: a clean, green extraction technology. *TRAC-Trend. Anal. Chem.* 71, 100–109. doi: 10.1016/j.trac.2015.04.013
- Tuli, H. S., Chaudhary, P., Beniwal, V., and Sharma, A. K. (2015). Microbial pigments as natural color sources: current trends and future perspectives. *Int. J. Food Sci. Tech.* 52, 4669–4678. doi: 10.1007/s13197-014-1601-6
- Vázquez, M. B., Comini, L. R., Martini, R. E., Montoya, S. N., Bottini, S., and Cabrera, J. L. (2014). Comparisons between conventional, ultrasound-assisted and microwave-assisted methods for extraction of anthraquinones from *Heterophyllaea pustulata* Hook f. (Rubiaceae). *Ultrason. Sonochem.* 21, 478–484. doi: 10.1016/j.ultrsonch.2013.08.023
- Velmurugan, P., Kim, M.-J., Park, J.-S., Karthikeyan, K., Lakshmanaperumalsamy, P., Lee, K.-J., et al. (2010). Dyeing of cotton yarn with five water soluble fungal pigments obtained from five fungi. *Fiber Polym.* 11, 598–605. doi: 10.1007/s12221-010-0598-5
- Venkatachalam, M., Gérard, L., Milhau, C., Vinale, F., Dufossé, L., and Fouillaud, M. (2019). Salinity and temperature influence growth and pigment production in the marine-derived fungal strain *Talaromyces albobiverticillius* 30548. *Microorganisms* 7:10. doi: 10.3390/microorganisms7010010
- Venkatachalam, M., Zelena, M., Cacciola, F., Ceslova, L., Girard-Valenciennes, E., Clerc, P., et al. (2018). Partial characterization of the pigments produced by the marine-derived fungus *Talaromyces albobiverticillius* 30548. Towards a new fungal red colorant for the food industry. *J. Food Compos. Anal.* 67, 38–47. doi: 10.1016/j.jfca.2017.12.036
- Ventura, S. P., Santos-Ebinuma, V. C., Pereira, J. F., Teixeira, M. F., Pessoa, A., and Coutinho, J. A. (2013). Isolation of natural red colorants from fermented broth using ionic liquid-based aqueous two-phase systems. *J. Ind. Microbiol. Biot.* 40, 507–516. doi: 10.1007/s10295-013-1237-y
- Ventura, S. P., Silva, F. E. A., Quental, M. V., Mondal, D., Freire, M. G., and Coutinho, J. A. (2017). Ionic-liquid-mediated extraction and separation processes for bioactive compounds: past, present, and future trends. *Chem. Rev.* 117, 6984–7052. doi: 10.1021/acs.chemrev.6b00550
- Vilkhu, K., Mawson, R., Simons, L., and Bates, D. (2008). Applications and opportunities for ultrasound assisted extraction in the food industry—A review. *Innov. Food Sci. Emerg.* 9, 161–169. doi: 10.1016/j.ifset.2007.04.014
- Vogel, J. H., Nguyen, H., Giovannini, R., Ignowski, J., Garger, S., Salgotra, A., and Tom, J. (2012). A new large-scale manufacturing platform for complex biopharmaceuticals. *Biotechnol. Bioeng.* 109, 3049–3058. doi: 10.1002/bit.24578
- Wang, C., Chen, D., and Qi, J. (2017). “Biochemistry and molecular mechanisms of *Monascus* pigments” in *Bio-pigmentation and Biotechnological Implementations*, ed O. V. Singh (Hoboken, NJ: Wiley-Blackwell), 173–191. doi: 10.1002/9781119166191.ch8
- Wang, J.-F., Liu, X.-J., Liu, R.-S., Li, H.-M., and Tang, Y.-J. (2012). Optimization of the mated fermentation process for the production of lycopene by *Blakeslea trispora* NRRL 2895 (+) and NRRL 2896 (–). *Bioproc. Biosyst. Eng.* 35, 553–564. doi: 10.1007/s00449-011-0628-6
- Wang, Q., Liu, D., Yang, Q., and Wang, P. (2017). Enhancing carotenoid production in *Rhodotorula mucilaginosa* KC8 by combining mutation and metabolic engineering. *Ann. Microbiol.* 67, 425–431. doi: 10.1007/s13213-017-1274-2
- Wang, W.-L., Lu, Z.-Y., Tao, H.-W., Zhu, T.-J., Fang, Y.-C., Gu, Q.-Q., et al. (2007). Isoechinulin-type alkaloids, varicolorins A–L, from halotolerant *Aspergillus varicolor*. *J. Nat. Prod.* 70, 1558–1564. doi: 10.1021/np070208z
- Wiemann, P., Willmann, A., Straeten, M., Kleigrewe, K., Beyer, M., Humpf, H.U., et al. (2009). Biosynthesis of the red pigment bikaverin in *Fusarium fujikuroi*: genes, their function and regulation. *Mol. Micro.* 72, 931–946. doi: 10.1111/j.1365-2958.2009.06695.x
- Woo, P.C., Lam, C.-W., Tam, E.W., Lee, K.-C., Yung, K.K., Leung, C.K., et al. (2014). The biosynthetic pathway for a thousand-year-old natural food colorant and citrinin in *Penicillium marneffei*. *Sci. Rep.* 4, 6728. doi: 10.1038/srep06728
- Xia, G., Li, J., Li, H., Long, Y., Lin, S.E., Lu, Y., et al. (2014). Alterporriol-type dimers from the mangrove endophytic fungus, *Alternaria* sp. (SK11), and their *MptpB* inhibitions. *Mar. Drugs* 12, 2953–2969. doi: 10.3390/md12052953
- Xie, F., Chang, W., Zhang, M., Li, Y., Li, W., Shi, H., et al. (2016). Quinone derivatives isolated from the endolichenic fungus *Phialocephala fortinii* are Mdr1 modulators that combat azole resistance in *Candida albicans*. *Sci. Rep.* 6:33687. doi: 10.1038/srep33687
- Xiong, W., Chen, X., Lv, G., Hu, D., Zhao, J., and Li, S. (2016). Optimization of microwave-assisted extraction of bioactive alkaloids from lotus plumule using response surface methodology. *J. Pharm. Anal.* 6, 382–388. doi: 10.1016/j.jpba.2016.05.007
- Xu, J., Nakazawa, T., Ukai, K., Kobayashi, H., Mangindaan, R.E., Wewengkang, D.S., et al. (2008). Tetrahydrobostrycin and 1-deoxytetrahydrobostrycin, two new hexahydroanthrone derivatives, from a marine-derived fungus *Aspergillus* sp. *J. Antibiot. Res.* 61, 415–419. doi: 10.1038/ja.2008.57
- Yan, Z., Wang, C., Lin, J., and Cai, J. (2013). Medium optimization using mathematical statistics for production of  $\beta$ -Carotene by *Blakeslea trispora* and fermenting process regulation. *Food Sci. Biotechnol.* 22, 1667–1673. doi: 10.1007/s10068-013-0265-8
- Yusuf, M., Shabbir, M., and Mohammad, F. (2017). Natural colorants: historical, processing and sustainable prospects. *Nat. Products Bioprospect.* 7, 123–145. doi: 10.1007/s13659-017-0119-9
- Zabala, A. O., Xu, W., Chooi, Y.-H., and Tang, Y. (2012). Discovery and characterization of a silent gene cluster that produces azaphilones from *Aspergillus niger* ATCC 1015 reveal a hydroxylation-mediated pyran-ring formation. *Chem Biol* 19, 1049–1059. doi: 10.1016/j.chembiol.2012.07.004
- Zabot, L. G., Moraes, M. N., and Meireles, M. A. A. (2012). Supercritical fluid extraction of bioactive compounds from botanic matrices: experimental data, process parameters and economic evaluation. *Recent Pat. Eng.* 6, 182–206. doi: 10.2174/187221212804583204
- Zhang, C., Chen, K., Liu, Y., Kovacs, J. M., Flores-Verdugo, F., and De Santiago, F. J. F. (2012). Spectral response to varying levels of leaf pigments collected from a degraded mangrove forest. *J. Appl. Remote Sens.* 6:063501. doi: 10.1117/1.JRS.6.063501
- Zhang, C., Liang, J., Yang, L., Chai, S., Zhang, C., Sun, B., et al. (2017). Glutamic acid promotes monacolin K production and monacolin K biosynthetic gene cluster expression in *Monascus*. *AMB Exp.* 7, 1–9. doi: 10.1186/s13568-016-0311-z
- Zheng, C.-J., Shao, C.-L., Guo, Z.-Y., Chen, J.-F., Deng, D.-S., Yang, K.-L., et al. (2012). Bioactive hydroanthraquinones and anthraquinone dimers from a soft coral-derived *Alternaria* sp. fungus. *J. Nat. Prod.* 75, 189–197. doi: 10.1021/np200766d
- Zhong, J.-J., Tatsuiji, S., Kinoshita, S.-I., and Toshiomi, Y. (1992). “Production of red pigments by *Perilla frutescens* cells in bioreactors,” in *Biochemical Engineering for 2001*, eds S. Furusaki, I. Endo, and R. Matsuno (Tokyo: Springer), 262–265. doi: 10.1007/978-4-431-68180-9\_70

**Conflict of Interest:** The authors declare that the research was conducted in the absence of any commercial or financial relationships that could be construed as a potential conflict of interest.

Copyright © 2020 Kalra, Conlan and Goel. This is an open-access article distributed under the terms of the Creative Commons Attribution License (CC BY). The use, distribution or reproduction in other forums is permitted, provided the original author(s) and the copyright owner(s) are credited and that the original publication in this journal is cited, in accordance with accepted academic practice. No use, distribution or reproduction is permitted which does not comply with these terms.



# Extraction of Flavonoids From Natural Sources Using Modern Techniques

Jaísa Oliveira Chaves<sup>1</sup>, Mariana Corrêa de Souza<sup>1</sup>, Laise Capelasso da Silva<sup>1</sup>, Daniel Lachos-Perez<sup>2</sup>, Paulo César Torres-Mayanga<sup>3,4</sup>, Ana Paula da Fonseca Machado<sup>3</sup>, Tânia Forster-Carneiro<sup>3</sup>, Mercedes Vázquez-Espinosa<sup>5</sup>, Ana Velasco González-de-Peredo<sup>5</sup>, Gerardo Fernández Barbero<sup>5</sup> and Mauricio Ariel Rostagno<sup>1\*</sup>

<sup>1</sup> Multidisciplinary Laboratory in Food and Health, School of Applied Sciences, University of Campinas, Limeira, Brazil,

<sup>2</sup> Laboratory of Optimization, Design and Advanced Control - Bioenergy Research Program, School of Chemical Engineering, University of Campinas, Campinas, Brazil, <sup>3</sup> School of Food Engineering, University of Campinas, Campinas, Brazil, <sup>4</sup> Facultad de Ingeniería, Universidad Nacional Micaela Bastidas de Apurímac, Abancay, Peru, <sup>5</sup> Department of Analytical Chemistry, Faculty of Sciences, University of Cadiz, Cadiz, Spain

## OPEN ACCESS

### Edited by:

Florent Allais,  
AgroParisTech Institut des Sciences et  
Industries du Vivant et de  
L'environnement, France

### Reviewed by:

Paul-Henri Ducrot,  
INRA UMR1318 Institut Jean Pierre  
Bourgin, France  
Diana Garcia-Bemet,  
Laboratoire de Biotechnologie de  
l'Environnement (INRA), France

### \*Correspondence:

Mauricio Ariel Rostagno  
mauricio.rostagno@fca.unicamp.br

### Specialty section:

This article was submitted to  
Green and Sustainable Chemistry,  
a section of the journal  
Frontiers in Chemistry

Received: 28 October 2019

Accepted: 18 August 2020

Published: 25 September 2020

### Citation:

Chaves JO, de Souza MC, da  
Silva LC, Lachos-Perez D,  
Torres-Mayanga PC, Machado APdF,  
Forster-Carneiro T,  
Vázquez-Espinosa M,  
González-de-Peredo AV, Barbero GF  
and Rostagno MA (2020) Extraction of  
Flavonoids From Natural Sources  
Using Modern Techniques.  
Front. Chem. 8:507887.  
doi: 10.3389/fchem.2020.507887

Flavonoids are one of the main groups of polyphenols found in natural products. Traditional flavonoid extraction techniques are being replaced by advanced techniques to reduce energy and solvent consumption, increase efficiency and selectivity, to meet increased market demand and environmental regulations. Advanced technologies, such as microwaves, ultrasound, pressurized liquids, supercritical fluids, and electric fields, are alternatives currently being used. These modern techniques are generally faster, more environmentally friendly, and with higher automation levels compared to conventional extraction techniques. This review will discuss the different methods available for flavonoid extraction from natural sources and the main parameters involved (temperature, solvent, sample quantity, extraction time, among others). Recent trends and their industrial importance are also discussed in detail, providing insight into their potential. Thus, this paper seeks to review the innovations of compound extraction techniques, presenting in each of them their advantages and disadvantages, trying to offer a broader scope in the understanding of flavonoid extraction from different plant matrices.

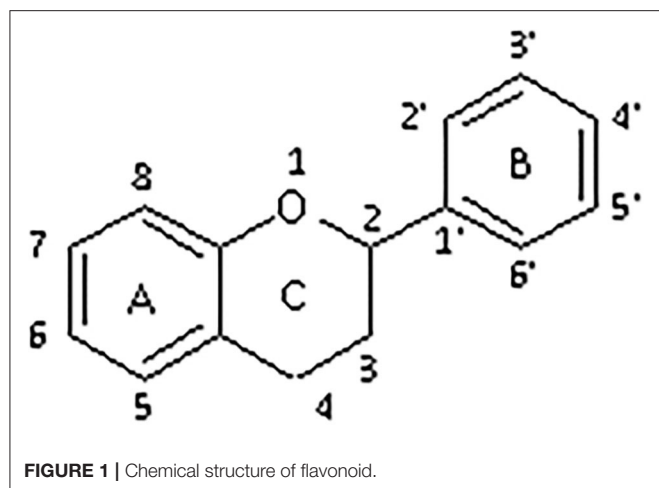
**Keywords:** flavonoids, natural products, extraction, sample preparation, modern techniques

## INTRODUCTION

Flavonoids are a class of natural phenolic compounds synthesized in plants as bioactive secondary metabolites (Nabavi et al., 2018) that are responsible for the characteristics of flavor, color, and pharmacological activities (Scarano et al., 2018). They are potent antioxidants protecting plants from unfavorable environmental conditions (Nabavi et al., 2018). Studies have shown that flavonoids have immunomodulatory, anti-inflammatory (Yahfoufi et al., 2018) and anticancer activities (Abotaleb et al., 2018; Chirumbolo et al., 2018; Rodriguez-Garcia and Sanchez-Quesada, 2019).

All flavonoids are based on a fifteen-carbon flavone skeleton C6 (A ring)-C3 (C ring)-C6 (B ring), composed by two benzene rings (A and B) connected by a heterocyclic pyrene ring (C) containing oxygen, as shown in **Figure 1**. They can be grouped into different classes (flavonols, isoflavones, flavones, chalcones, flavanones, and anthocyanidins) (**Table 1**), depending on the





carbon of the C-ring in which the B-ring is bound and the degree of saturation and oxidation of the C-ring (Panche et al., 2016; Abotaleb et al., 2018; Durazzo et al., 2019). The various classes of flavonoids differ in the oxidation level and substitution pattern of the C ring, while individual compounds within a class differ in the substitution pattern of the A and B rings (Kumar and Pandey, 2013; Panche et al., 2016). A chromane ring (A and C) is attached to a B ring (**Figure 1**) at C2 in flavonoids or C3 in isoflavonoids (Panche et al., 2016) (**Figure 2**).

Based on their potential and the importance of foreseen applications, researchers have been extensively studying techniques and conditions specifically for the extraction of flavonoids from natural products and foods either for analytical, preparative, or industrial purposes. Therefore, several techniques for extracting flavonoids to increase the extraction yields of these major bioactive compounds have been implemented. Various techniques have been proposed, including maceration, percolation, hydro-distillation, boiling, reflux, soaking, and soxhlet (Alara et al., 2018a). However, these techniques are characterized by the use of large amounts of organic solvents with high purity, lower extraction yields, low selectivity, long extraction times, thermal degradation of target compounds, associated environmental concerns and costs, compared to other techniques (Rostagno et al., 2010; Galanakis, 2012; Farzaneth and Carvalho, 2017).

Advanced techniques and strategies are continually being developed to overcome the limitations of conventional methods for the extraction of these compounds. These techniques include ultrasound-assisted extraction (UAE), supercritical fluid extraction (SFE), microwave-assisted extraction (MAE), solid-phase extraction (SPE), enzyme-assisted extraction, pressurized liquid extraction (PLE or accelerated solvent extraction—ASE), extraction assisted by pulsed electric field (PEF), and a combination of different techniques. These modern techniques are very effective in the removal of flavonoids from the most diverse types of natural matrices. More importantly, they also allow reducing the use of organic solvents and replacing them with alternative “green” solvents while achieving high yields

in short extraction times. Therefore, these techniques can be categorized as “green extraction” techniques (Chemat et al., 2012; Khoddami et al., 2013; Galván et al., 2018; Alexandre et al., 2020; Dzah et al., 2020; Pashazadeh et al., 2020; Sarfarazi et al., 2020; Sengar et al., 2020; Tungmunthum et al., 2020).

There are several reviews available in the literature focusing on one or more extraction techniques, compounds and compound classes and tissue type or plant (Rostagno et al., 2009; Chan et al., 2011; Mustafa and Turner, 2011; Miljevic et al., 2014; Barba et al., 2016; Kala et al., 2016; Roohinejad et al., 2016; Sookjitsumran et al., 2016; Vinatoru et al., 2017; Galván et al., 2018; Dzah et al., 2020).

Due to the complex nature of sample matrix and diverse chemical characteristics of flavonoids, it is consensual among scholars in this field that there is no single and standard method to be used for every material or flavonoids to be extracted at this time.

Thus, this article seeks to revise the innovations of the techniques available, offering a broader scope in the understanding of the extraction of flavonoids from different matrices to be explored by researchers working in this field.

## ADVANCED EXTRACTIONS TECHNIQUES

### Ultrasound-Assisted Extraction (UAE)

#### Fundamentals

Ultrasound is an intensification technique which is widely used for the extraction of bioactive compounds from natural products with applications in industries such as food and pharmaceuticals (Akbari, 2019). The intensification process is based on the acoustic cavitation phenomena, which consists of the formation of stable or transient gas bubbles by the compression and expansion cycles caused by the passage of ultrasonic waves through the liquid (Leong et al., 2011) and the subsequent rupture, which causes the release of bioactive compounds, and this rupture depends on the extraction conditions (Chen X. J. et al., 2007; Um et al., 2018). As bubbles accumulate energy, they reach a critical point where they implode and release this energy instantaneously, breaking intermolecular interactions between target compounds and the matrix of the sample as well as causing mechanical effects in the extraction medium and the structure of the sample matrix. The mechanical effects include the reduction of particle size and damage of cells, allowing more significant interaction between the solvent and the sample, and consequently, improving mass transfer, which in turn will return higher yields in shorter times (Um et al., 2018). Increased solubilization of the mixture formed in the extraction is also one of the effects of cavitation since the ultrasonic waves allow movement of the liquid from shear forces and turbulence caused by bubbles imploding (Vilkhu et al., 2011; Meullemiestre et al., 2016).

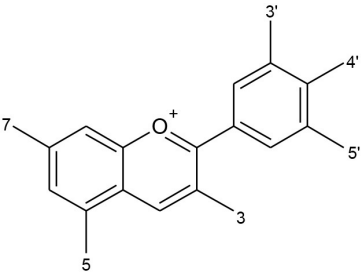
In general, UAE can be explored in more sustainable processes due to the high efficiency associated with its use, allowing lower consumption of solvents and energy. UAE also provides faster extractions, with high reproducibility, rapid return on investment, simplification of manipulation and processing, and higher purity of the final product when compared to

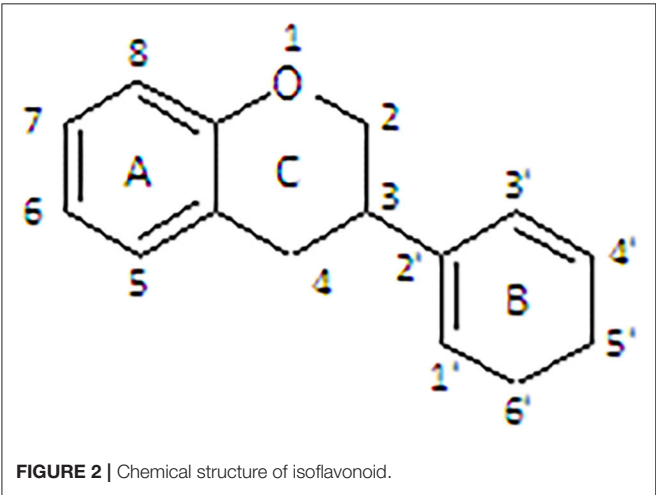
**TABLE 1** | Classification of flavonoids and their classes according to their skeletal structure.

Flavonoid group	Compound	Skeletal structure	3'	4'	5'	3	5	7
Flavonol	Quercetin		OH	OH	–	OH	–	–
	Isorhamnetin		O-CH <sub>3</sub>	OH	–	OH	–	–
	Kaempferol		H	OH	–	OH	–	–
	Spiraeoside		OH	O-glucose	–	OH	–	–
	Quercitrin		OH	OH	–	O-rhamnose	–	–
	Isoquercitrin		OH	OH	–	O-glucose	–	–
Isoflavone	Genistein		–	OH	–	–	OH	OH
	Genistin		–	OH	–	–	OH	O-glucose
	Daidzein		–	OH	–	–	–	OH
	Daidzin		–	OH	–	–	–	O-glucose
	Biochanin A		–	O-CH <sub>3</sub>	–	–	OH	OH
	Formononetin		–	O-CH <sub>3</sub>	–	–	–	OH
Flavone	Apigenin		H	–	–	–	–	–
	Luteolin		OH	–	–	–	–	–
Chalcones	Phloretin		OH	–	OH	–	–	–
	Chalconarigenin		–	–	OH	–	–	–
Flavanone	Narigenin		H	OH	–	–	–	OH
	Hesperitin		OH	O-CH <sub>3</sub>	–	–	–	OH
	Narirutin		H	OH	–	–	–	O-rutinoside
	Naringin		H	OH	–	–	–	O-neohesperidose
	Hesperidin		OH	O-CH <sub>3</sub>	–	–	–	O-rutinoside

(Continued)

TABLE 1 | Continued

Flavonoid group	Compound	Skeletal structure	3'	4'	5'	3	5	7
Anthocyanins	Cyanidin		OH	OH	–	OH	OH	OH
	Cyanin		OH	OH	–	O-glucose	OH	OH
	Delphinidin		OH	OH	OH	OH	OH	OH
	Pelargonidin		–	OH	OH	OH	OH	OH



conventional extraction methods (Palma et al., 2013; Chemat et al., 2017). UAE can be used in many types of matrices, such as fruits, teas, seeds, vegetables, or flowers, which are sources of many bioactive compounds of different classes (Shirsath et al., 2012; Tabaraki et al., 2012). However, the conditions and the combinations of the variables of the process must be cautiously defined according to the type of sample and compound to be extracted, including factors such as the frequency used and usually between 20 kHz and 100 MHz, ultrasound power, time, temperature, quantity and preparation of the sample, and selection, volume, and concentration of solvent (Rostagno et al., 2010; Da Porto et al., 2013).

Parameters Influencing UAE Processes

The extraction of natural products is a complex process, where each variable, individually or combined with others, can affect the results. It is of the utmost importance to evaluate each component of the process and their interactions, such as solvent, sample, power, frequency, and intensity, temperature, time, and make of the equipment.

Extraction solvent

Without a doubt, the choice of solvent is the primary variable in any extraction method. The extraction solvent should be chosen based mainly on the solubility and intensity of the interactions with the matrix. The characteristics of the solvent to be observed are, among others, polarity, pH, viscosity, surface tension, vapor pressure, melting point, boiling point, density, specific gravity, as well as the effect on purity, and activity of the extracted compound (Mason, and Lorimer, 2002). These factors should be thoroughly thought out, mainly because they decrease the cavitation threshold, disfavoring the removal of the compounds from the matrix (Mason, and Lorimer, 2002).

Consideration should also be given to the extraction parameters and their suitability for the solvent, the intermediate and final products to be used, and how the solvent can react with the target compounds under extraction conditions. An important factor is the biochemical and physicochemical properties of the solvents because they define the nature of the medium in addition to interacting with the treated material and extracted compounds. The possible changes that can occur in the solvents during the extraction process can have significant effects on the stability of the flavonoids and the efficiency of the treatments (Dzah et al., 2020).

A solvent with low vapor pressure, at the adjusted temperature, facilitates cavitation increasing the effects of ultrasound in the process. In contrast, viscous solutions, such as oils, increases the amplitude of the waves, hindering the propagation of ultrasound, and mechanical effects on the sample caused by the cavitation (Santos et al., 2009; Flannigan and Suslick, 2010).

In general, organic solvents (methanol, ethanol, acetonitrile, petroleum ether, acetone), water, and mixtures of these solvents are used for the removal of flavonoids from plant matrices, such as herbs, industrial residues, stems or plant seeds. Organic solvents such as ethanol, methanol, acetone, and isopropanol, mixed with varying proportions of water, have been widely used to extract flavonoids from plant sources using UAE. There are extractions with 100% of either organic solvent or water used for extraction. In some studies, extraction solvents can be acidified to preserve sensitive flavonoids from oxidative degradation (Dzah, 2014). The acids produce hydrogen ions

(H<sup>+</sup>) that stabilize free radicals that may be produced during ultrasonication (Dzah et al., 2020). Several studies have shown that due to the polarity of flavonoids, organic solvents, such as methanol, are more efficient for their extraction. Non-toxic and biodegradable alternatives, such as ethanol, are being explored to some extent in extraction methods to reduce the impact of organic solvents on the environment while providing similar, or even superior performance (Fu et al., 2019). Ionic or eutectic solvents containing acids citric and lactic acid and multiphasic systems, such as cloud point extraction, are also new alternatives to toxic solvents (Vankar and Srivastava, 2010; Ekezie et al., 2017; Cunha and Fernandes, 2018; Biata et al., 2019).

The extraction performance can also be affected by the solvent pH by altering the ionic strength, which affects the solubility of the compounds and their interactions with the sample matrix. Several studies have evaluated the optimum pH to extract flavonoids from plant matrices. A recent report (Mai et al., 2020) investigated the influence of the pH of the solvent on the recovery of *Euonymus alatus* flavonoids and suggested that recoveries increased in acidic pH (2.5–3.5) and decreased at higher pH. Another report, which in this case evaluated polyphenols, indicated that its extraction from pomegranate peel is affected by the solvent's pH, with the best results being observed in acidic medium (Motikar et al., 2020). On pH above 7.0, lower extraction yields were recorded.

For the ultrasound-assisted extraction of bioactive compounds from the *Citrus reticulata* bark, slightly acidic electrolyzed water (pH 6.20) produced the best results for the extraction of total phenolic compounds. Still, higher yields of flavonoids were reported with acid electrolyzed water pH 3.24 (Soquetta et al., 2019).

Another example of the influence of the pH was reported for the ultrasound-assisted extraction of polyphenols from Satsuma mandarin leaves, where a higher yield of total flavonoids was observed at pH 2 in water. The highest amounts of total phenolic compounds and total flavonoids were achieved in acidic media (Cigeroglu et al., 2017).

The reports available in the literature suggest that higher flavonoids yields are usually produced in acidic medium. For polyphenols, this trend can be explained by the fact that an acidic pH supports the cleavage of phenolics bound to proteins and carbohydrate polymers (Ilbay et al., 2014). With a low pH value, phenols are protonated that take the hydrophobic nature to molecules that interact more strongly with the hydrophobic micellar surfactant and, therefore, readily penetrate the micelles (El-Abbassi et al., 2014). At a higher pH, phenols are deprotonated, and their ionic characteristics increase, leading to a decrease in the solubility of hydrophobic phenolic compounds in micelles due to the higher activity of protons. Thus, the amount of phenols extracted increases with the reduction of the pH (Gortzi et al., 2008; El-Abbassi et al., 2014).

### Sample

Depending on the target compounds, the sample may be fresh or dry (plants, oleaginous, seeds, yeast, algae, among others), and the structure, moisture, plasticity, and composition of the material will entail the recovery of compounds from the sample

matrix. Thus, the preparation of the sample matrix before extraction is of paramount importance, especially because some compounds are sensitive to the processes of preparation, such as drying, homogenization, and sifting. In addition to preserving the matrix compounds, the sample preparation also ensures the extraction efficiency as it can eliminate interferences, increase the concentration of the analyte in the mixture and provide the optimum particle size (Rostagno et al., 2009).

The ratios between sample quantity and solvent, as well as particle size, are also factors that should be taken into consideration to maximize extraction yield because they influence the cavitation phenomena and final concentration of the extracts (Vilkhu et al., 2011). It has been suggested that a proportion between 1:5 and 1:10 sample/solvent (solid vegetal material) for ultrasonic bath extraction is suitable for the recovery of bioactive compounds from plants (Vinatoru et al., 2017). Such high ratios may be adequate when considering the production of a concentrated extract. Still, when the objective of the extraction is sample preparation for quantitative analysis of flavonoids, a higher solvent amount (1:50, 1:100, or even higher) may be required to ensure that target compounds were removed entirely from the sample matrix. The ranges of the solid / solvent ratio are reported in the literature and it is often not indicated whether it is on a dry or wet basis. It is understood that it usually refers to fresh and not dry material. In the case of material that has been dried, it is necessary to hydrate the matrix to allow the solubilization of the compounds of interest and consequently it may be necessary to increase the ratio.

Higher efficiency can be achieved using sequential extraction processes as in each extraction, as the fresh solvent will be available and will improve solubility. Still, additional steps will be required between extractions, such as centrifugation or filtration.

Particle size is also a factor that influences the efficiency of the UAE. It should be evaluated according to the matrix, and as a function of the compounds to be extracted. In general, small particles remain on the solvent surface and are not affected by cavitation bubbles, while large particles decrease the permeability or diffusion of solvent in the sample (Khan et al., 2010). A study developed for *Areca nut* polyphenol extraction tested particle sizes between 841, 425, 250, and 180  $\mu\text{m}$ , and the highest recoveries were obtained with a particle size of 250  $\mu\text{m}$  (Chavan and Singhal, 2013). Another study using UAE for orange peel flavone extraction tested particle sizes between 0.5, 1.0, 1.5, 2.0, and 2.5  $\text{cm}^2$ , with the best yielding particle size being 2  $\text{cm}^2$ .

### Ultrasound power, frequency, and intensity

Ultrasound power directly affects the cavitation and shear forces in the extraction medium. As ultrasound power increases, so does the cavitation and its mechanical effects as well as mass transfer of compounds from the sample matrix to the solvent. However, excessive power can negatively affect the extraction process due to the degradation of target compounds, reducing yields. To fully explore UAE as an intensification technique, it is required to adjust power considering sample moisture, the temperature of the medium, and solvent used (Wei et al., 2010).

Another critical parameter in UAE is frequency. The frequency used for the extraction of bioactive compounds from

natural products usually ranges between 20 and 120 kHz. There are some reports that frequency can modulate the removal of different compounds from the sample matrix (Machado et al., 2019). In the case of phenolics from grapes lower frequency of 40 kHz provided higher yields than 120 kHz (González-Centeno et al., 2014). On another recent report, a higher yield of phenolics from pomegranate peels was also achieved with lower frequency (37 kHz). Still, higher antioxidant capacity was observed in the extracts obtained with higher frequency (80 kHz), indicating that frequency can affect the composition of the extract.

High frequencies do not allow the process of cavitation to happen fully, because they decrease the time of expansion of the bubbles, thus reducing the size and impact of these in the sample (Mason, and Lorimer, 2002). On the other hand, in low frequencies, the bubbles are in smaller quantities, but with larger diameters, which assists the physical effects generated in the sample, such as the transfer of masses between the sample and the solvent (Escalpez et al., 2011).

It is also essential to consider ultrasound intensity, which is the energy emitted per second per area of the emitting surface, being directly connected with the amplitude of the transducer and the sound wave. Thus, the higher the ultrasonic intensity, the greater the amplitude, and the better the extraction efficiency. Higher amplitudes are associated with the more significant collision between the bubbles originating from the cavitation and the sample. However, very large amplitudes can also lead to the rapid deterioration of the ultrasonic transducer, leading to liquid agitation and not to the cavitation phenomenon. Thus, attention should be paid to the amplitude, especially considering the solvent, where high amplitudes are suitable in more viscous solvents such as the oils (Tiwari, 2015; Machado et al., 2019).

### *Temperature and extraction time*

The temperature of the medium should be closely related to the properties of the solvent since the temperature increase causes a decrease of the viscosity and surface tension of the solvent but increases the vapor pressure. Increased vapor pressure decreases the effectiveness of the cavitation process and leads to lower extraction efficiency.

The vapor pressure of the liquid influences the cavitation process, and lower vapor pressure solvents are more advisable in UAE extractions because they induce a more significant collapse between cavitation bubbles. Thus, solvents with high vapor pressure and, consequently, high boiling temperatures, do not fully explore the potential of UAE due to reduced cavitation (Flannigan and Suslick, 2010).

High temperature, however, also facilitates the increase of cavitation bubbles, increasing the contact area and diffusion between solid and solvent. Thus, for better effects of ultrasound associated with cavitation, medium to low temperatures are indicated (between 20 and 70°C), depending on the sample, and especially for thermosensitive ones (Palma et al., 2013; Pasrija and Anand haramakrishnan, 2015).

Maran et al. (2017) studied the effect of extraction temperature, among other parameters, on the recovery of anthocyanin, flavonoids, and total phenolics of *Nephelium lappaceum* bark extracts obtained through the UAE. It was

observed that the yield was increased due to the increase in porosity of the material, more significant solvation, and mass transfer when the extraction temperature increased.

On the other hand, the required extraction time of the process will depend on several factors. The overall extraction kinetic curve can be divided into three stages: constant extraction rate (CER), where compound are more easily extracted from the sample matrix; falling extraction rate (FER), where compounds being extracted present some interactions with the matrix, hindering their removal; and diffusional controlled (DC), where compounds depend on diffusion to be removed (Palma et al., 2013).

When considering the production of extracts, the extraction time is usually determined by the conditions that are most favorable to the mass transfer from the matrix to the medium, generally between CER and FER part of the extraction curve. However, the exact extraction time will depend on several economic factors and manufacturing costs, but especially the raw material cost (Palma et al., 2013). In contrast, for analytical purposes, it is necessary to ensure that target compounds were completely removed from the sample, which is usually done by overextending the extraction time.

Applications for obtaining concentrated extracts of flavonoids, which usually exploit the first stages of the extraction process (CER and FER), can also explore the benefits of the use of ultrasound. There is a more significant potential of this technique in the preparation of samples for quantitative analysis since ultrasound has a substantial effect on diffusion and can accelerate the final phase of the diffusion-controlled extraction process (CD).

There are other important aspects associated with extraction time, including the amount and type of solvent used, the amount and characteristics of the sample (protein content for example), temperature, flow rate (in dynamic extractions), ultrasound intensity and frequency, potential degradation of target compounds, among others, making this one of the most challenging techniques to be optimized. Usually, extraction time is determined experimentally on a case by case basis.

### **Applications of UAE to Flavonoids From Natural Products**

During the last decade, several UAE methods have been developed, and a significant number of applications for the recovery of flavonoids can be found in the literature. Some of these applications are shown in **Table 2**. The use of ultrasound has grown in recent years. In most cases, the produced results indicate that it accelerates the extraction process and decreases the amount of solvents used (Zhang L. et al., 2009; Oniszczyk and Podgórski, 2015). The most used solvents for the extraction of flavonoids are ethanol, mixtures with water at different proportions, and natural deep eutectic solvents (NADES), which are based on their ability to solubilize moderately polar flavonoids with a relatively low cost and environmental impact. Regarding ultrasound, the most used type of equipment is the ultrasonic bath operating at 40 kHz with fixed power. Specific conditions, such as temperature and extraction time, vary significantly due to the particularity of the composition of each raw material.



**TABLE 2 |** Experimental conditions used for extraction ultrasound flavonoids from natural products.

Sample	Solvent (%)	Power (W)	Frequency (kHz)	Temperature (°C)	Time (min)	Sample/ volume (g:mL)	Equipment	Target compounds	Yield or recovery	Reference
Cocoa Shells ( <i>Theobroma cacao</i> )	70–90 ethanol	296	40	45–65	30–60	1:50	Bath	Total flavonoids	7.47 mg/g	Mid Yusof et al., 2019
Basil leaves ( <i>Ocimum tenuiflor</i> )	30–70 Ethanol	50	30	40	5–15	1:40	Ultrasonic processor	Total flavonoids	6.69 QE mg/g	Upadhyay et al., 2015
Eucommia leaves ( <i>Folium eucommie</i> )	30–50 ethanol	850	59	5	5–75	1:50	Bath	Total flavonoids	41%	Huang et al., 2009
Guava leaves ( <i>Psidium guajava</i> )	Water	250–450	–	0–80	5–45	5:200	Bath	Total flavonoids	Not mentioned	Li et al., 2019
Sophora leaves ( <i>Sophora flavescen</i> )	40–80 methanol	120	40	20–80	20–80	1:26	Bath	Trifolirhizin Formononetin Isoxanthohumol Maackiain Kurarinone	2.570 mg/g 0.213 mg/g 0.534 mg/g 0.797 mg/g 3.091 mg/g	Zhou et al., 2019
Rugosa rose fruit ( <i>Rosa rugosa</i> Thunb.)	50–95% ethanol	200	40	30–50	30–50	1:20	Bath	Individual flavonoids	54.32–75.23 mg/g	Um et al., 2018
Hawthorn seed	55–85% ethanol	40	40	55–75	30–50	1:22	Bath	Total flavonoids	16.45 mg/g	Pan et al., 2012
Flower ( <i>Citrus aurantium</i> L. var. amara Engl)	40–80% ethanol	200	–	30–80	10–80	1:20	Bath	Total flavonoids	1.87%	Yang et al., 2010
Grapefruit ( <i>Citrus paradisi</i> L.)	20–100% ethanol	100	40	4–70	5–48	1:8	Bath	Total flavonoids	50%	Garcia-Castello et al., 2015
Curry leaf ( <i>Murraya koenigii</i> L.)	40–80% methanol	880–150	–	40–80	20	1:20	Bath	Naringin Epicatequin Catequin Quercetin Myricetin	0.203 mg/g 0.678 mg/g 0.325 mg/g 0.350 mg/g 0.703 mg/g	Ghasemzadeh et al., 2014
<i>Canna indica</i>	Methanol. ethanol. ethyl- acetate. acetone and water	100–500	20	25–30	5–20	20:50	Bath	Total flavonoids	0.3409 g/g	Srivastava and Vankar, 2010
Wine less	NADES	380	37	35	5–45	0.1:1	Bath	Anthocyanins	Not mentioned	Bosiljkov et al., 2017
Dittany ( <i>Origanum dictamnus</i> ), fennel ( <i>Foeniculum vulgare</i> ), manjorom ( <i>Origanum majorana</i> ), sage ( <i>Salvia officinalis</i> ) and mint ( <i>Mentha spicata</i> )	NADES	140	37	80	90	0.1:15	Bath	Total flavonoids	109.67 mg GAE g–1 dw	Bakirtzi et al., 2016

## Microwave-Assisted Extraction (MAE) Fundamentals

Currently, novel green extraction techniques with efficient and rapid process have appeared to correct the limitations of conventional extraction methods, such as the vast quantities of solvents used, the high temperatures applied, or the long extraction times needed (Dahmoune et al., 2014).

Microwaves are non-ionizing electromagnetic (EM) waves located between the radio-frequency range at the lower frequency and infrared at the higher frequency in the electromagnetic spectrum within the frequency band of 300 MHz to 300 GHz. In this extraction technique, the microwave energy is delivered through polar components interactions to generate heat by conversions of electromagnetic into thermal energies (Pimentel-Moral et al., 2018b). This conversion occurs via two mechanisms: by dipole rotation, i.e., through reversals of dipoles and by ionic conduction, i.e., by displacement of charged ions present in the solute as well as the solvent (Dean et al., 1995). When microwave energy absorption occurs, the conversion of electromagnetic energy into heat depends on the relation between the dielectric loss factor ( $\epsilon''$ ) and the dielectric constant ( $\epsilon'$ ) for a given material (Mello et al., 2014). This relation is known as the dissipation factor (or loss tangent,  $\tan \delta$ ). MAE heats all the sample fluid, allowing the extraction solution (solvent and sample) to reach the desired temperature more rapidly. It avoids the thermal gradient caused by conventional heating (Biesaga, 2011), which increases the risk of degradation of thermolabile bioactive compounds (Wu et al., 2001). Therefore, the improvement in extraction yields is not only produced by the increase in temperature within

the extraction medium, but also by the effect of microwave electromagnetic radiation on vibrations of both types of bonds (extraction solvents and the analytes to extract) (Ameer et al., 2017). Concerning the release of the compounds from the matrix, during microwave heating, a considerable amount of pressure builds up inside the biomaterial, improving the porosity of the matrix, which allows better penetration of extracting solvent through it (Kratchanova et al., 2004). **Figure 3** represents a microwave extraction system, both in a closed system and in an open system, in addition to diagramming the difference between conventional heating and microwave heating (Camel, 2001; Destandau et al., 2013; Rosa et al., 2018).

## Influential Parameters in the Extraction Process

The degradation of flavonoids can be caused by several factors such as light, air, time, and temperature. Furthermore, the efficiency of MAE depends to a great extent on the selection of the operating conditions and the parameters that affect the extraction mechanisms and performance. The choice of an extraction method is based on the highest recovery of the targeted compound, retention of the required properties of the compound ease of application of the extraction method with available resources, and the properties of the targeted flavonoid compound. Various factors influence the performance of the MAE, such as the nature of the solvent, the ratio sample amount: solvent volume, the extraction time, the microwave power, the temperature, among others (Chan et al., 2011).

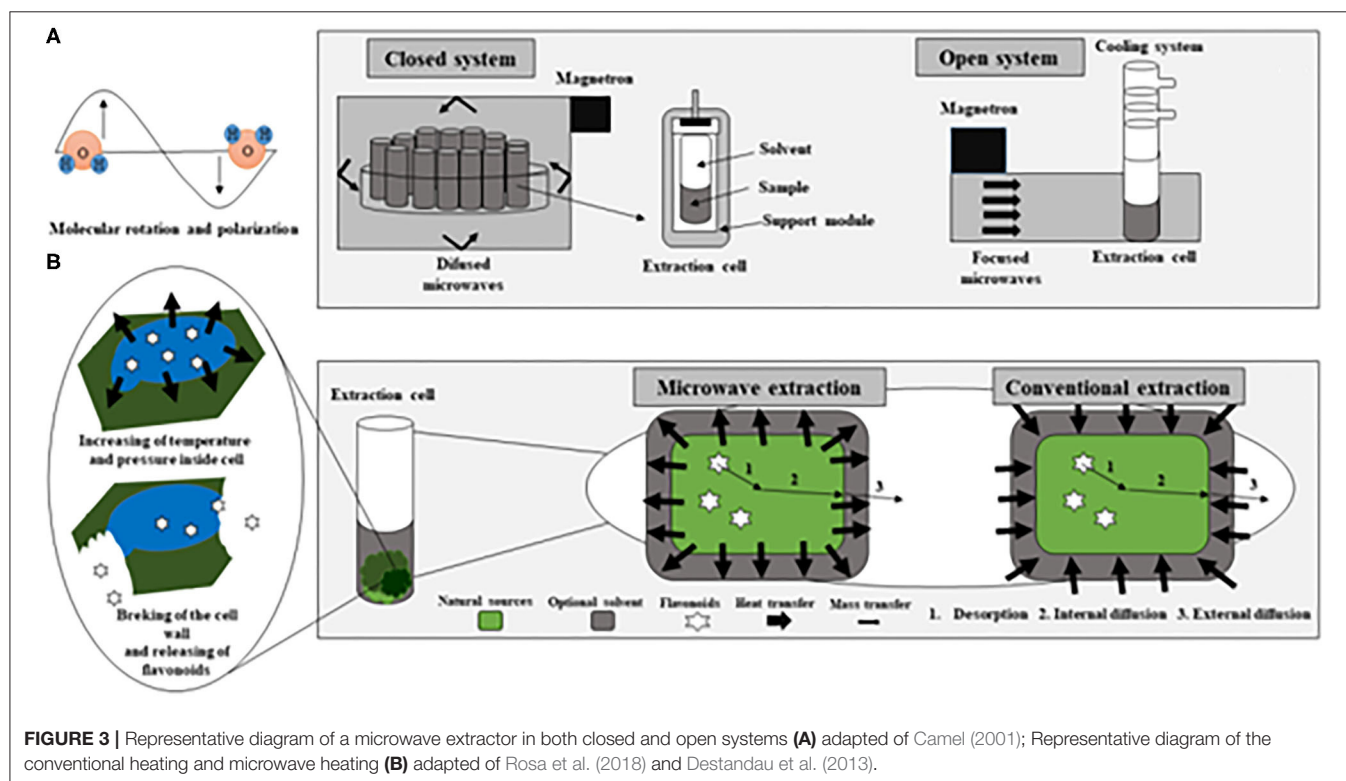


**FIGURE 3 |** Representative diagram of a microwave extractor in both closed and open systems (A) adapted of Camel (2001); Representative diagram of the conventional heating and microwave heating (B) adapted of Rosa et al. (2018) and Destandau et al. (2013).

### Extraction solvent

As mentioned above, the dielectric constant and the dissipation factor are two critical parameters involved in MAE. Therefore, it is essential to choose solvent mixtures to modify the dielectric constant until obtained suitable characteristics for the extracted sample. On the one hand, solvents like ethanol, methanol, or water can absorb microwave energy due to their high dielectric constant and dielectric loss, which can lead to a faster rate of heating of the solvent concerning the plant material (Zhang F. et al., 2009). On the other hand, for the extraction of thermolabile compounds, a solvent combination with relatively lower dielectric properties can be used to ensure that the solvent temperature will remain lower to cool-off the solutes once they are liberated into the solvent (Routray and Orsat, 2012).

The polarity of the solvent and the solubility of the targeted compound in the solvent must also be considered. There is no standardized solvent composition for all since it is difficult to establish general rules, so the best solvent varies with each targeted compound (Xiang and Wu, 2017). In general, the solvent most used for polar flavonoids extraction is a mixture of water and organic solvents. Within these, methanol is highly toxic and is not practical for use in the processing of food and pharmaceutical products. It is generally used in analytical applications in different proportions depending on the compounds to be extracted (Chen et al., 2008). The most commonly used is ethanol, as it is a green solvent with low toxicity. As mentioned above, adding a certain amount of water to the ethanol solvent has been shown to improve extraction efficiency. However, as can be seen in **Table 3**, the best extraction yields are obtained with different concentrations of ethanol (35–90%) in aqueous solution, according to the literature consulted. The presence of water would improve the mass transfer between the solid and the liquid by increasing the permeability of the matrix of the plant, thus improving heating efficiency (Zhang et al., 2007; Zhong et al., 2016). However, the optimal percentage of water-ethanol will depend on the characteristics of the matrix, the extraction conditions (power, temperature, time, among others), and the compounds to be extracted. For less polar flavonoids, such as aglycones of isoflavones, flavanones, methylated flavones, and flavonols, solvents used also include chloroform, acetone, dichloromethane, diethyl ether, hexane or ethyl acetate (Grigonis et al., 2005). Some specific examples for diverse matrices using the mentioned above solvent are shown in **Table 3**.

The pH of the solvent can also significantly affect the efficiency of the extraction steps. The effect of pH on the flavonoids extraction is closely related to their structure. Given the broad class of existing flavonoids, authors have reported different optimal pHs for its extraction. Some authors (Xin et al., 2008; Xiangnan et al., 2014; Bouras et al., 2015) have shown that alkaline extraction was more efficient in recovering flavonoids than acidic solvent extraction ( $\text{pH } 12 > \text{pH } 7 > \text{pH } 2$ ). Specifically, Bouras et al. (2015), founded that flavonoid compounds [naringenin, (+)-catechin, (–)-epicatechin, (–)-epigallocatechin] increased  $\sim 1.25$  times with the presence of 0.01 M sodium hydroxide compared to pure water, when extracting flavonoids from *Quercus* bark using MAE. This

behavior is linked to the fact that basic pHs remove tannins, phenolic acids, and other polyphenols linked by ester bonds, reduces bark extract viscosity, and increases the reactivity of the extract, increases the accessibility of solid residue by removing the lignin physical barrier, and damages the cell structure. Other authors showed better extractions with acidic solvents. It happens when anthocyanins are studied, a class of flavonoid which have a stable conformation, the cation flavilium, at pH from 1.0 to 3.0. In cases where the use of acid is necessary, low concentrated acids and mainly hydrochloric acid can be used until a pH between 1 and 4.5 is achieved (Yang and Zhai, 2010; Teng et al., 2013).

In addition to common solvents, ionic liquids (ILs) have been reported as eco-friendly solvents for the MAE of several flavonoids. Room-temperature ILs, resulting from the combination of organic cations and various anions that may be liquids at room temperature, are salts with melting points of below ca.  $100^{\circ}\text{C}$ . The main ILs used in the literature are: 1-butyl-3-methylimidazolium chloride [[bmim]Cl], 1-butyl-3-methylimidazolium bromide [[bmim]Br], and 1-butyl-3-methylimidazolium tetrafluoroborate [[bmim]BF<sub>4</sub>] between others. For the synthesis of [bmim]Cl and [bmim]Br, a mixture between 1-methylimidazole and the corresponding halogenoalkane in a 1:1.2 molar ratio is employed. [bmim][BF<sub>4</sub>] is prepared by the reaction of [bmim]Cl and NaBF<sub>4</sub> at the same molar ratio. All the solutions are prepared at different concentrations with deionized water (Liu et al., 2005). Specifically, ILs have extended into areas of analytical chemistry and liquid-liquid extraction, and show excellent solvent properties: negligible vapor pressure, a wide liquid range, good thermal stability, tunable viscosity, miscibility with water and organic solvent, and good solubility and capacity of extraction for several organic compounds (Deng et al., 2006). The ionic liquids employed and their concentrations (usually between 1.5 and 3 mol L<sup>–1</sup>) have great influence in the MAE extractions of the flavonoids. Concerning the type of IL employed, the extraction yields of flavonoids are largely dependent on the anions for the same class of ILs, highlighting Br<sup>–</sup>, Cl<sup>–</sup>, BF<sub>4</sub><sup>–</sup>, SO<sub>4</sub><sup>2–</sup>, N(CN)<sub>2</sub><sup>–</sup>, H<sub>2</sub>PO<sub>4</sub><sup>–</sup>, PF<sub>6</sub><sup>–</sup>, CF<sub>3</sub>SO<sub>3</sub><sup>–</sup>, and CF<sub>3</sub>CO<sub>2</sub><sup>–</sup>, due to the anion-dependency of the solubilities of analytes in ILs (Du et al., 2009). Furthermore, ILs which have cationic moieties with an electron-rich aromatic  $\pi$ -system produced stronger interactions with solute molecules capable of undergoing polarity,  $\pi$ - $\pi$  and  $n$ - $\pi$  interactions (Du et al., 2007). Concerning the ILs concentration, Du showed that the yields of the extraction of polyphenolic compounds from *P. guajava* leaves and *S. china* tubers increased with the increase in the concentration of [bmim]Br. This behavior is due to the solvation power and multiple interactions of [bmim]Br and its capacity to change the dissipation factor of the solution and improved the transfer efficiency of microwave energy.

### Sample: volume ratio

Another factor that affects MAE is the relationship between the amount of sample and the solvent volume. The objective should be to minimize the use of solvent and maximize the yields. On the one hand, high volumes of solvent require more microwave energy due to microwave radiation would be absorbed

**TABLE 3 |** Some representative applications involving the use of MAE for the recovery of flavonoids from natural sources.

Sample	Solvent (%)	Power (W)	Extraction volume (mL)	Temperature (°C)	Time (min)	Sample/volumen (g:mL)	Target compounds	Quantification method	Yield or recovery	Reference
Grapes skin (Tintilla de Rota)	40:60% methanol:water	500	25	100	5	2:25 g DW:mL solvent	Individual Anthocyanins	HPLC-DAD, using malvidin-3-glucoside as standard	1.86 mg standard/g DW	Liaizid et al., 2011
<i>Morus alba</i> L. leaves	60:40% ethanol:water	560	250	100	5	1:15 g FW:mL solvent	Total flavonoids	NaNO <sub>2</sub> -Al(NO <sub>3</sub> ) <sub>3</sub> -NaOH colorimetric assay, using rutin as standard	2.5%	Li et al., 2009
<i>Platycladus orientalis</i> L. leaves	80:20% methanol:water	80	5	–	5	1:5 g DW:mL solvent	Total flavonoids	Dynamic MAE coupled with on-line derivatization and UV-vis detection, using quercitrin as standard	98.5% (w/w)	Chen L. et al., 2007
<i>Gordonia axillaris</i>	36.89:63.11% ethanol:water	400	15	40	71.04	1:29.56 g DW:mL solvent	Total flavonoids	Method described by Lamaison and Carnet (1990) with some modifications, using as standard solution	3.11 mg standard/g DW	Li et al., 2017
Tomato (Round tomato)	100% water	200	20	60	20	45:1,000 g DW:mL solvent	Individual flavonoids	HPLC, using external standards for each flavonoid	6.78–11.7 mg standard/g DW	Pinela et al., 2016
<i>Morus nigra</i> L.	70:30% ethanol:water	500	125	35	10	1:50 g DW:mL solvent	Total flavonoids	Aluminum chloride method, using quercetin as standard	2.35–2.83 mg standard/g DW	Koyu et al., 2018
<i>Radix Astragal</i> roots	90:10% ethanol:water	1,000	50	110	25	1:25 g DW:mL solvent	Individual flavonoids	HPLC-UV, using external standards for each flavonoid	1.190 mg standard/g DW	Xiao et al., 2008
Apple ( <i>Malus domestica</i> ) roots	60:40% ethanol:water	1,500	20	100	20	0.1:20 g DW:mL solvent	Individual flavonoids	HPLC, using external standards for each flavonoid	17.1 mg standard/g DW	Moreira et al., 2017
Black rice ( <i>Oryza sativa</i> cv. Poiréton) husk	67.34:32.66% ethanol:water	640	–	49.5	0.5	1:40.79 g DW:mL solvent	Total flavonoids	Aluminum chloride method, using catechin as standard	0.0304 mg standard/g DW	Jha et al., 2017
Green tea ( <i>Camellia sinensis</i> L.)	100% water	100	200	50	15	1:20 g DW:mL solvent	Total and individual catechin	Folin-Ciocalteu (Total) and various spectroscopic analysis along with their respective catechins (individual)	8.80%	Kalai and Ignasimuthu, 2018



by the solvent. This additional power could cause the solvent heating rate to increase drastically, which results in the thermal degradation of the bioactive compounds (Spigno and De Faveri, 2009; Alara et al., 2018a). On the other hand, low volumes of solvent promote the mass transfer barrier, since the distribution of the active compounds is concentrated in certain regions, which limits the movement of the compounds outside the matrix of the cell (Hao et al., 2002). An optimum ratio sample amount: solvent volume assurance uniform and effective heating (Zhou and Liu, 2006). Some authors indicate that the ratio most used for the extraction of this type of compound is around 1:30 g/mL (Zhao et al., 2018). For much of the matrices shown in **Table 3**, ratios around this value were used.

### *Microwave power*

The plant cell walls tend to absorb microwave energy and cause an increase in internal superheating resulting in cell disruption that facilitates leaching out of flavonoids from the samples and so that the analytes can diffuse and dissolve in the solvent (Bouras et al., 2015). In general, the extraction performance increases with higher microwave power, up to 500 W (1 g of leaf powder) (Mandal and Mandal, 2010). For many of the matrices shown in **Table 3**, microwave powers up to this value were used. In any case, it is necessary to take into account not only the applied power but also its relation to the sample mass (power density). However, very high power can lead to lower yields, which can be attributed to the heat generated by the microwave energy causing the disintegration and thermal degradation of the total flavonoid content in the sample (Dahmoune et al., 2014; Alara et al., 2018b). Alara et al. (2018a) obtained an improvement in the yields of the total flavonoids as the level of microwave power increased from 400 to 500 W (10 g of leaf powder). However, the yields declined with power above 500 W, with the lowest values observed at 600 W.

### *Extraction temperature*

Concerning the extraction temperature, it is an essential factor to be considered both in open system extraction and in closed system extraction. High temperatures cause a decrease in viscosity and surface tension, which allows better penetration of the solvent into the sample matrix. Also, it increases the molecular movement by accelerating the mass transfer of intracellular bioactive compounds from the plant matrix (Zhao et al., 2017). However, above 100°C, the extraction yield decreases by breaking down the molecular structure of the bioactive compounds (Pimentel-Moral et al., 2018b). However, this temperature limit varies with the type of compounds to be extracted, since the degradation temperature of each compound is different. The number and type of substituents present in the aromatic ring, as well as the position, influence stability. A smaller number of substituents increase flavonoid stability.

Additionally, when the compounds have several substituents on the ring, the hydroxylates are more readily degradable than the methoxylated ones (Routray and Orsat, 2012). Also, the sugar portion stabilized the flavonoids during the extraction process. Several researchers use temperatures around 60°C since it is sufficient to extract the compounds of interest without causing

their degradation (Jin et al., 2017; Xiang and Wu, 2017). However, there are other authors that for certain compounds use higher temperatures, even higher than 100°C (Pinela et al., 2016).

Finally, it is also essential to have in mind the relationship between temperature and extraction time. With increasing extraction time, the extraction yields will firstly increase and then will decrease, probably because over-exposure to microwave temperature may lead to thermal degradation of bioactive compounds. So, it is necessary to reach equilibrium between the applied extraction time and temperature.

### *Extraction time*

The yields of extracts tend to increase when the extraction time increases. However, at prolonged time of exposure to microwave radiation, even at low temperatures or low operating power, the risk of thermal degradation of polyphenols chemical structures is inevitable (Wang et al., 2010). Therefore, there will be an irradiation time limit for each of the bioactive compounds present in the matrix in which quality yields can be obtained (Yedhu and Rajan, 2016). For this reason, the extraction time of the MAE can vary from a few minutes (Carniel et al., 2017; Liang et al., 2017) to more than half an hour in some cases (Bouras et al., 2015; Zhao et al., 2018). If a longer extraction time is required, extraction cycles can be used, which consists of the extraction of the sample in several successive stages in order not to use severe conditions (Zhao et al., 2018).

### *Plant matrix characteristic*

Besides the operating conditions discussed in the previous sections, the characteristics of the sample also affect the performance of MAE. A critical factor in the recovery of flavonoids is the particle size of the sample. Fine powders can improve the extraction process by providing a large surface contact area between the solvent and sample. Sample diameter reduction also ruptures cell walls, which increase the penetration of the microwave radiation. Thus, they are directly exposed to extraction solvent as well as a shorter distance for the transfer of target compounds through cell walls to solvent, thus increasing the extraction yields (Kong et al., 2010). For the production of fine powders, the sample preparation steps are essential and include drying, milling, grinding, and homogenization of the sample before the extraction for optimum extraction yield. The only problem associated with the use of fine particles is that it would cause difficulty in separating the extract from the residue, and probably, additional clean up steps may have to be employed (Chan et al., 2011).

Furthermore, to this essential step, other pretreatments can be applied to the sampled. For example, samples treated by solvent for 90 min before extraction can enhance the heating efficiency of MAE, promote the diffusion and improve the mass transfer of active compounds to the solution (Pan et al., 2003). Also, the dried sample matrix pretreated with water helps localized heating of microwave. In this sense, apart from the particle size, the solvent pretreatment has considerable effects on the sample matrix for efficient extraction.

## Applications of MAE to Flavonoids From Natural Products

MAE has been applied successfully in the development of methods for the extraction of bioactive compounds of interest, both polar and non-polar, in multiple matrices. Specifically, MAE has been increasingly recommended in the last few years as an excellent method for the lab-scale, precision, and quantification studies of flavonoid samples. However, scale-up based on microwave extraction for the large-scale production of flavonoids is still under research and development (Orsat and Routray, 2017). Furthermore, in comparison with UAE, the extraction technique aforementioned, it has been observed that microwave extraction obtains similar or higher yields in the case of flavonoids (Gao and Liu, 2005; Chen X. J. et al., 2007). For example, Casazza et al., 2010, achieved higher amounts (46.7 mg GAE/g DW) of total flavonoids employing MAE than employing UAE (39.5 mg GAE/g DW) in *Vitis vinifera* wastes. Similar behavior was obtained by Gao and Liu (2005) (yield of flavonoids of 4.1% using MAE and 3.5% using UAE) from cultured cells of *Saussurea medusa* Maxim.

MAE in a closed system is quite similar to the PLE technology, as the solvent is heated and pressurized in both systems (Camel, 2001). According to Søltøft et al. (2009), the efficiencies of PLE was comparable and at the same level as MAE for the extraction of flavonoids in onions. Specifically, about 500  $\mu\text{g}$  quercetin  $\text{g}^{-1}$  dry weight was achieved, showing a significantly better PLE extraction in the case of the quercetin-4-glucoside compound. For example, extraction yield and total flavonoid content under optimal PLE conditions were higher than MAE ( $56 \pm 2\%$ ,  $6.5 \pm 0.2$  mg Eq quercetin/g and  $26 \pm 2\%$ ,  $2 \pm 0.5$  mg Eq quercetin/g dry leaf, respectively) for the extraction of bioactive compounds from *M. oleifera* leaves. However, the antioxidant activity was higher in MAE extracts than PLE ( $16 \pm 1$  Eq Trolox/100 g dry leaf and  $12 \pm 2$  mmol Eq Trolox/100 g dry leaf) (Rodríguez-Pérez et al., 2016). Specifically, these authors highlighted that the extraction method should be selected depending on the target compounds to be isolated. According to their results, PLE was more suitable for extracting phenolic compounds having a higher number of hydroxyl-type substituents (kaempferol diglycoside and its acetyl derivatives or malonyl, hydroxyl, or acetyl glycosylated of quercetin) and those that are sensitive to high temperatures (glucosinolates or amino acids). Therefore, according to these authors, MAE, and PLE seem to be good options to extract bioactive compounds such as flavonoids, with little difference in their yields and due, in many cases, to the target extraction compounds rather than the technique itself. It should be noted that powers used in microwave pretreatment are lower than in PLE because high microwave power values result in lower total dry extract yields due to degradation of the target compounds (Kovačević et al., 2018). However, due to the few articles found in the bibliography where both techniques have been applied under the same matrices and conditions, no general conclusion can be reached.

According to the comparison with the other extraction techniques previously described, although SFE is a promising method in terms of extraction performance, some of its operational attributes are less versatile than in the case of other

techniques, such as MAE. For example, Mustapa et al. (2015) obtained a low yield for the extraction of compounds from the medicinal plant *Clinacanthus nutans* Lindau using SFE, with a value of only 3.19% g/g DM; compared to MAE that obtained an amount of 17.39% g/g DM. The lower SFE yield is probably due to the non-polar nature of the carbon dioxide solvent employed in SFE, which is unfavorable for extracting the abundant polar compounds present in this sample, such as various flavonoids. In supercritical extraction,  $\text{CO}_2$ , the primary solvent used, has low polarity. For these reasons, for the removal of polar compounds, polar solvents must be added, which decreases the extraction selectivity. Furthermore, a high concentration of a polarity modifier can lead to a temperature of the mixture lower than the critical temperature, which cancels the benefit of using supercritical extraction (Camel, 2001).

Bioactive flavonoids are mainly present in edible parts but can also be present in other non-edible parts of the plants, including leaves, stem, and root. Where in some instances, the amount of these compounds is comparable or higher than the amount reported in edible parts of the same plant. It has been widely employed in the extraction of a different kind of matrix, i.e., fruits like grapes and apples, vegetables such as onions and tomatoes, different types of leaves like olive leaves and green tea leaves, or even in blackcurrant marc, among others. It can also be used directly on the fresh sample or after a drying and lyophilization process. Extraction of flavonoids with optimized MAE technique, could not only contribute to the nutraceutical industry (health-promoting foods) but could also aid in decreasing by-product pollution, in the reduction of energy consumption and the creation of new sources of income (Sillero et al., 2018). **Table 3** lists examples of successful MAE applications for the extraction of flavonoids in different matrices in recent years.

## Pressurized Liquid Extraction Fundamentals

Pressurized liquid extraction (PLE) has also been referred to in the literature as pressurized fluid extraction (PFE), accelerated solvent extraction (ASE), and pressurized solvent extraction (PSE). It is an automated technique for extracting solid samples with liquid solvents. When water is used as an extraction solvent, different terms can be used to define the method, including hot water extraction (HWE), subcritical water extraction (SWE), high-temperature water extraction (HTWE), hot water extraction pressurized (PHWE), liquid water extraction or superheated water extraction.

PLE was introduced in 1995 by Dionex Corporation as an alternative to maceration, percolation, sonication, ultrasound, microwave-assisted, soxhlet extraction, and other extraction techniques such as supercritical fluid extraction (SFE) and microwave-assisted extraction. It was initially termed Accelerated Solvent Extraction technology (ASE).

In PLE, environmentally friendly liquid solvents are used at moderated-elevated temperatures and pressures to increase the efficiency of the extraction process. Under PLE conditions, the solvent is kept in a liquid state, providing a better mass transfer of the essential compounds present in the plant matrix to the solvent, as well as the stability of the process (Evstafev

and Chechikova, 2016). The increase of the temperature causes dramatic changes in the physical-chemical properties of water, enhances the solubility of the analytes, breaking matrix-analyte interactions achieving a higher diffusion rate, and especially in its dielectric constant ( $\epsilon$ ). In contrast, the increase of the pressure allows keeps the solvent below its boiling point. Dielectric constant (polarity of the solvent) is a critical parameter in affecting solute-solvent interactions, and in the case of water, increasing the temperature under moderate pressure can mainly decrease this constant. At standard conditions of pressure and temperature, water is a polar solvent with a high dielectric constant ( $\epsilon = 78$ ). Still, at 300°C and 23 MPa, the  $\epsilon$  decreases to 21, which is similar to the value for ethanol ( $\epsilon = 24$  at 25°C) or acetone ( $\epsilon = 20.7$  at 25°C). This means that at moderated-elevated temperatures and moderate pressures, the polarity of water can be reduced considerably and can act as if ethanol or acetone were being employed (Plaza and Turner, 2015; Lachos-Perez et al., 2017; Tena, 2018).

The main advantages of PLE are the following: faster extractions (around 15–50 min), low amount solvent (15–40 mL), no extract filtration required. The main drawbacks are the high cost of the equipment and the need for a thorough optimization of variables to avoid a matrix-dependent efficiency (Wijngaard et al., 2012). PLE, either an aqueous or an organic solvent can be carried out in the static, dynamic mode, or a combination of both. In the static mode, the sample, and solvent kept for a specified time at constant temperature and pressure, whereas in the dynamic mode, the solvent flows through the sample continuously. A more detailed description of the main principles of PLE and the influence in the extraction process of different parameters that affect performance are described in the next section.

### Operating Parameters for Pressurized Liquid Extraction

Several factors that influence the pressurized liquid extraction process, such as sample size, solvent, pressure, temperature, pH, flow rate, and extraction time, must be considered. The parameters with the most significant effect in the PLE process are the type of solvent and the temperature (Wijngaard et al., 2012).

#### Sample size

The size of the particle is a crucial factor. The reduction of the particle size facilitates contact with the solvent and the extraction of the solute from inside the matrix due to the smaller diffusion path (Mustafa and Turner, 2011). Consequently, the extraction process would result in shorter processing time due to the exhaustion of the solute within each part of the matrix.

#### Solvents

The selection of the solvent in the PLE for a solid-liquid system is significant since the desired compounds must have a high solubility in the solvent. The characteristics of the solute and solvent must be identical (Azmir et al., 2013), polar solute in a polar solvent, as well as the non-polar solute, solubilized in a non-polar solvent (Machado et al., 2015). The chemical properties of the solvent must guarantee a higher solubility of the solute, as

well as its selectivity. However, achieving selectivity is a great challenge, and the scientific community has focused on research to optimize the experimental conditions to obtain a specific compound, as shown in **Table 4**.

The use of solvents in this context is based on the concept of green chemistry, that during the development of the extraction process is necessary minimum quantities of solvent (Ibañez et al., 2012), as well as its easy recovery and reused that unlike conventional techniques becomes less sustainable (Mustafa and Turner, 2011; Wijngaard et al., 2012). The type of solvent to be used within the must present characteristics that are less toxic to reduce the environmental and economic impact, favoring a smooth recovery (Azmir et al., 2013). Besides, the few volumes of solvents used in PLE due is a consequence of the combination exerted by high temperature and pressure, reducing the time of the process (Ibañez et al., 2012).

The most used solvents are water and ethanol for PLE, of the most popular methods of extraction according to the solvent used, there is the denomination of extraction with subcritical water, where the solvent is 100% water (Wijngaard et al., 2012). However, in the subcritical state, the application for the extraction of thermally unstable compounds, such as anthocyanins, may be limited. Whose mixtures have also proven to be more 20 effective than traditional extraction solvents, as was already evidenced in some investigations (Machado et al., 2015; Pereira et al., 2019), demonstrating that the mixture of solvents with a moderate polarity has a positive influence on the recovery of phenolic compounds (Xynos et al., 2014).

#### Pressure

The high pressure applied in the PLE is to maintain the solvent in the liquid state, being able to vary the temperature in ranges above the boiling point. The effect of the high pressure of the system gives rise to a phenomenon called penetration, which directs the solvent into the pores of the solid matrix by extracting the analytes (Wijngaard et al., 2012). The effect of high pressure is an essential factor in the changes in the physical-chemical properties of the solvent, such as density, diffusivity, viscosity, and dielectric constant. That is a particular part it improves the penetration phenomenon of the liquid phase in the solid matrix (Mustafa and Turner, 2011). In literature, it is possible to find several studies that report that pressures above of 100 bar increase the PLE yield, from a different matrix, for instance, goldenberry, grape marc, citrus by-products, passion fruit rinds, *Lippia citriodora* leaves (Viganó et al., 2016; Barrales et al., 2018; Corazza et al., 2018; Leyva-Jiménez et al., 2018; Pereira et al., 2019). However, in the case of flavonoid glycosides and aglycones, such as quercetin, luteolin, apigenin, narirutin, naringin, etc., it is possible to obtain high extraction yields at pressures low as 30 bar (Kamali et al., 2016; Cvetanović et al., 2018; Munir et al., 2018).

#### Temperature

The temperature is a critical factor within the PLE, and the thermal effect is of significant influence on the stability of the compounds within the plant matrix. The bioactive compounds can be selectively removed by modifying the temperature; however, the degradation of the thermosensitive compounds can

**TABLE 4 |** Survey on the applications of PLE to obtain flavonoids from natural sources using environmentally-friendly organic solvents.

Sample	Solvent (%)	PLE conditions (mode, reactor volume, extraction time, solvent flow rate)	Temperature (°C)	Pressure (bar)	Target compounds	Yield or recovery	Reference
Goldenberry	Ethanol (70%)	Dynamic, 7.5 mL, 10–60 min, 1–3 mL/min	N/I	100–200	Quercetin Rutin_hydrate Mangiferin	0.57 mg/L 1.20 mg/L 3.57 mg/L	Corazza et al., 2018
Grape marc	Ethanol (50–100%) Water-ethanol acidified	N/I, 50 mL, 220 min, 5 g/min	40–100	100	Anthocyanins	10.21 mg malvidin-3-O-glucoside/g dr	Pereira et al., 2019
Citrus by-products	Ethanol (50–99.5%)	Dynamic, 10 mL, 5–40 min, 2.37 g/min	45–65	100	Hesperidin	19.3 mg/g dry peel	Barrales et al., 2018
Passion fruit rinds	Ethanol (70–100%)	Dynamic, 10 mL, 60 min, 2.7–3 mL/min	30–60	100	Isoorientin Vicenin Orientin Isovitexin Vitexin	118 µg/g dried rind 85 µg/g dried rind 25 µg/g dried rind 34 µg/g dried rind 17 µg/g dried rind	Viganó et al., 2016
Waxy barley	Ethanol (5–20%)	Static, 100 mL, 15–55 min, 2–6 mL/min	135–175	150	Catechin, Naringinin, Morin, Rutin, and Quercetin	N/I	Benito-Román et al., 2015
<i>Dracocephalum kotschy</i>	Methanol	Static and dynamic, 100 mL, N/I, 0.4–0.8	50–80	20–40	Quercetin Luteolin	6.13 mg/g 13.25 µg/g	Kamali et al., 2016
<i>Lippia citriodora</i> leaves	Ethanol (15–85%)	Static, 33 mL, 5–20 min, N/I	40–180	110	Luteolin-7-diglucuronide, apigenin-7-diglucuronide, chrysoeriol-7-diglucuronide, acacetin-7-diglucuronide, methyl quercetin, dimethyl kaempferol, and dimethyl quercetin	N/I	Leyva-Jiménez et al., 2018
<i>Moringa oleifera</i> leaves	Ethanol (55–100%)	Static, N/I, 60–210 min, N/I	110–140	N/I	Quercetin and kaempferol	N/I	Wang et al., 2017

take place at higher temperatures, and consequently promote the formation of undesirable compounds (Wijngaard et al., 2012; Evstafev and Chechikova, 2016; Lachos-Perez et al., 2020). The effect of the temperature generates a high solubility of the analytes extracted in the solvent because the increase in temperature reduces the viscosity resulting in an increase in the extraction rates of the analyte by diffusion to the solvent (Mustafa and Turner, 2011; Evstafev and Chechikova, 2016). However, the high extraction rates are due to a rupture of solute ligations in the matrix due to temperature (Machado et al., 2015).

Among the different studies carried out in extraction, the temperature ranges from 40 to 60°C for optimal extraction of polyphenol compounds. Being the flavonoids within the bioactive compounds, the most stable to the thermal effect, being able to be extracted at temperatures higher than 150°C. Temperature and pressure adjustment guarantees the optimization of the PLE concerning high extraction yields but in conjunction with a reduction of the organic solvent used and shorter process times (Santos et al., 2012; Evstafev and Chechikova, 2016). These characteristics make the PLE as a superior process when compared to other researches that used

conventional techniques to project a larger scale of extraction of polyphenols from food waste by-products (Wijngaard et al., 2012; Evstafev and Chechikova, 2016).

### pH

The effect of the solvent pH, adjusting the temperature or including a buffer, is crucial where target compounds are soluble at selected pH levels. Few studies report the effect of pH in PLE, the works found in literature mention the anthocyanins as the main compound extracted when the pH is altered. Anthocyanins are phenolic compounds belonging to the flavonoid family responsible for the colors of the petals of flowers and fruits; anthocyanins are water-soluble vacuolar pigments that may appear as red, purple, or blue depending on pH values (Bleve et al., 2008; Ren et al., 2020). Pereira et al. (2019) performed PLE for anthocyanins extraction using ethanol-water pH 2.0 (50% w/w) as a solvent. The anthocyanins recovery in acid medium is increased due to their stability in pH from 1.0 to 3.0. The results show that low pH helped to increase their extraction yield.

Espada-Bellido et al. (2018) carried out the extraction of anthocyanins from Mulberry (*Morus nigra* L.) by



PLE, investigating different operating conditions: solvent, temperature, pressure, purge time, pH: 3–7, and flushing, the authors obtained an improvement in the yields of anthocyanins as pH decreased from 7 to 3. However, the yields for total phenolic compounds increased with a pH of 7. Therefore, more studies need to be carried out to investigate the recovery of the extraction of flavonoids by altering the pH.

#### **Flow rate and extraction time**

The flow rate is a parameter in the process of extracting great importance of research, which is directly related to the residence time. Higher flow rates result in shorter residence times of analytes, as well as the rapid extraction of compounds extracted from the plant matrix (Plaza and Turner, 2015; Lachos-Perez et al., 2018). The majority of PLE works use relatively low flow rates (Kamali et al., 2016; Corazza et al., 2018; Pereira et al., 2019) because phenomenologically the desorption and diffusion of the solvent within the pores of the plant matrix used in the extraction process (Plaza and Turner, 2015). Some studies in the literature report flow rates of 0.2, 0.4, 0.6, 0.8, 1 mL/min (Kamali et al., 2016), others report flows of 1.0, 2.0, and 3.0 mL/min for pressurized liquid extraction (PLE) for goldenberry, passion fruit rinds, citrus by-products (Viganó et al., 2016; Barrales et al., 2018; Corazza et al., 2018).

In terms of rapid extraction, the process is more careful, because the thermal effect can form other compounds; the continuous flow of solvent that enters the extraction cells has the objective of extracting the soluble analytes. If the solubility of the compounds in the solvent is limited, the flow velocity must be varied, in the manner of reducing the residence time of the components soluble in water at high temperature, this increase in the flow rate is more effective in terms of using lower amounts of solvent. A study conducted in 2018 reported an extraction time of 60 min for PLE of polyphenols from Goldenberry (Corazza et al., 2018). Another study used a similar extraction time and obtained high yield for PLE of  $\beta$ -glucans and phenolic compounds (Benito-Román et al., 2015). However, it can lead to low solute concentrations within the collected liquid. What originated the use of other operations to reduce the solvent content within the liquid sample to concentrate the extract (Liu et al., 2014).

## **Supercritical Fluid Extraction**

### **Fundamentals, Main Influencing Parameters, and Applications**

Supercritical fluid extraction (SFE) is a green extraction technology that has been widely applied for the recovery of valuable compounds from different materials, both at the laboratory and industrial levels (Herrero et al., 2015). In some cases, laboratory-scale studies were performed to fully recover the compounds of interest for quantification purposes, while in other cases, the aim was to provide optimum conditions for the recovery of bioactive compounds to increase the scale for commercial extraction. The most well-known examples in which scaling has been carried out are decaffeination of coffee beans (Zosel, 1981) and extraction of  $\alpha$ -acids from hops to produce hop resins (Laws et al., 1980).

In SFE, the extractor is in its supercritical state, which means that both pressure and temperature are above their critical values. Supercritical fluids have intermediate properties between those of gas and liquids, which depend on the pressure, temperature, and composition of the fluid. In particular, their viscosity and surface tension is similar to that of liquids. At the same time, the diffusion coefficients are similar to those of gases, which allows for more efficient extractions by diffusing more quickly through the solid matrix (Azmir et al., 2013). These properties make it suitable for the extraction of compounds in a short time with higher yields (Azmir et al., 2013). Also, the density (and hence the solvation power of the fluid) can be adjusted by varying the pressure and temperature, providing the opportunity to theoretically perform highly selective extractions (Camel, 2001). Because of the mentioned advantages, the extraction with supercritical fluid is a process of growing interest in areas such as food, pharmaceutical, and cosmetic industries. This method is a powerful tool in the case of the extraction of natural compounds from food products (Justyna et al., 2017).

A basic SFE system consists of the following parts: a mobile phase tank (generally CO<sub>2</sub>), a pump for transporting and pressurizing the solvent, cosolvent vessel, and pump, a heater for heating the solvent or the supercritical mixture, a pressure vessel where it occurs the extraction, a controller to maintain the high pressure of the system and a collection vessel to collect the extract. A schematic diagram of the typical SFE unit is shown in **Figure 4**. Individual units may have different configurations, instrumentation, valves, by-pass, gas purging systems, and safety features not shown here (Azmir et al., 2013; Yahya et al., 2018).

SFE can be performed in static or dynamic mode. For processing, the raw material is placed in the extractor vessel, in which the temperature and pressure are controlled. The extractor vessel is then pressurized with fluid by the pump. Afterward, the analyte is collected in the collection vial due to solvent depressurizing. The fluid is then rejuvenated and recycled or released into the environment in the last step (Camel, 2001; Yahya et al., 2018).

Although a variety of solvents may be employed in supercritical conditions, such as those mentioned in **Table 5**, carbon dioxide (CO<sub>2</sub>) is by far the most widely used supercritical fluid for the recovery of bioactive compounds from natural matrices (Silva et al., 2016). CO<sub>2</sub> has several advantages, including moderate critical conditions ( $T_c \approx 31^\circ\text{C}$  and  $P_c \approx 74$  bar), inert, non-toxic, non-flammable, non-explosive, environmentally friendly, recognized as safe by the European Food Safety Authority (EFSA) and by the Food and Drug Administration (FDA) of the United States of America. Furthermore, it is cheap and readily available (Herrero et al., 2015; Yahya et al., 2018). Another advantage is that CO<sub>2</sub> is gaseous at ambient temperature and pressure, which makes the recovery of the analyte solvent-free and straightforward. These characteristics are of significant interest for the production of bioactive compounds to be used in the food, pharmaceutical, and cosmetic industry. It avoids subsequent steps to remove the extractor solvent, which are usually needed when other modern extraction techniques are chosen to capture bioactive from natural sources. In addition, SFE using CO<sub>2</sub> allows the

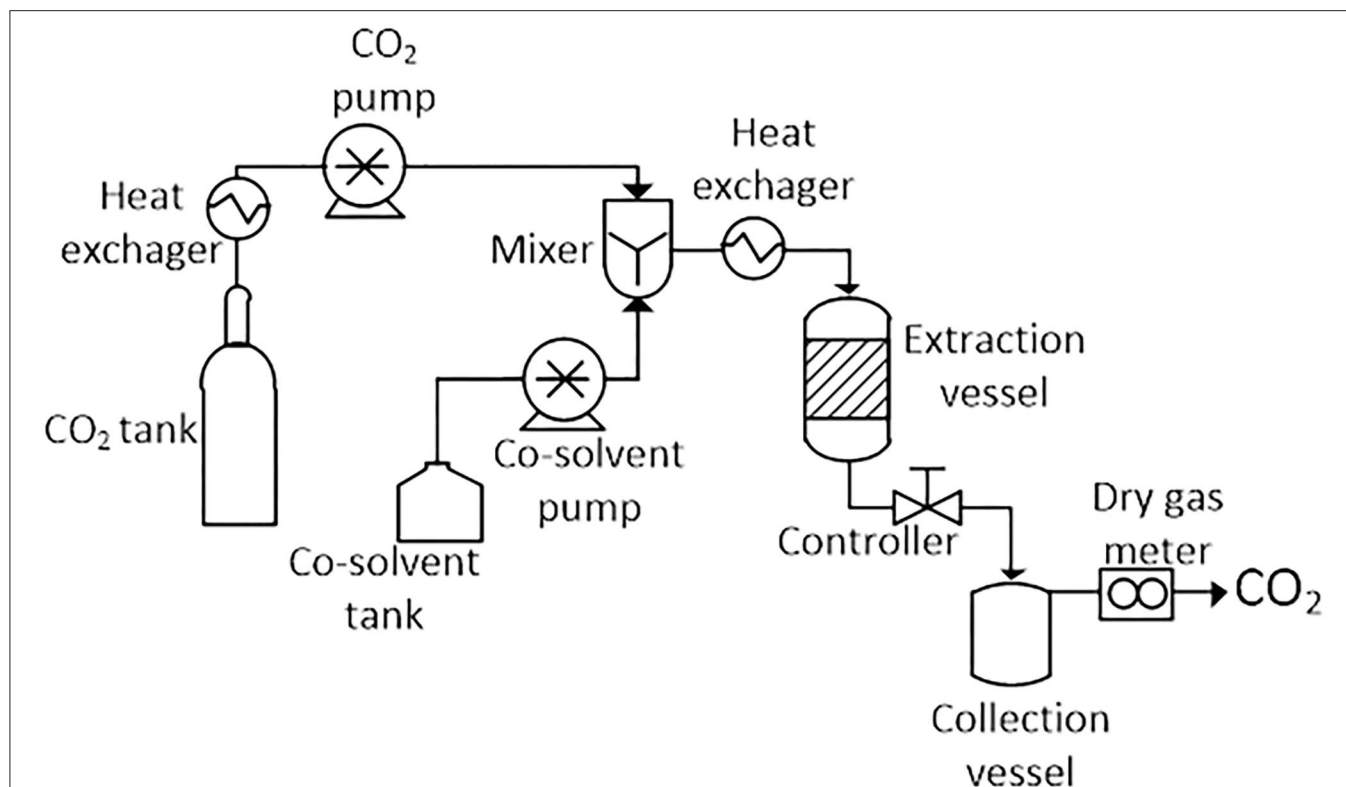


**FIGURE 4** | Schematic diagram of a typical supercritical fluid extractor. Adapted of Azmir et al. (2013) and Yahya et al. (2018).

**TABLE 5** | Critical properties of some pure components used in SFE (Sahena et al., 2009; Silva et al., 2016).

Component	Critical property		
	Temperature (°C)	Pressure (MPa)	Density (g/cm <sup>3</sup> )
Ethylene (C <sub>2</sub> H <sub>4</sub> )	9.4	5.04	0.215
Carbon dioxide (CO <sub>2</sub> )	31.1	7.38	0.470
Ethane (C <sub>2</sub> H <sub>6</sub> )	32.4	4.82	0.203
Nitrous oxide (N <sub>2</sub> O)	36.7	7.17	0.460
Sulfur hexafluoride	45.8	3.77	0.730
Propylene (C <sub>3</sub> H <sub>6</sub> )	91.9	4.60	0.232
Propane (C <sub>3</sub> H <sub>8</sub> )	96.8	4.25	0.217
Freon-134a (CH <sub>2</sub> FCF <sub>3</sub> )	101.1	4.06	0.512
Freon-12 (CCl <sub>2</sub> F <sub>2</sub> )	111.9	4.14	0.565
Acetone (C <sub>3</sub> H <sub>6</sub> O)	235.1	4.70	0.278
Methanol (CH <sub>3</sub> OH)	239.6	8.09	0.272
Ethanol (C <sub>2</sub> H <sub>5</sub> OH)	240.9	6.14	0.276
Ethyl acetate (C <sub>4</sub> H <sub>8</sub> O <sub>2</sub> )	250.2	3.83	0.360
Water (H <sub>2</sub> O)	374.1	22.06	0.322

extraction of easily oxidizable or thermosensitive compounds (which are characteristic of some flavonoids) by operating at low temperatures using a non-oxidizing medium (Herrero et al.,

2010). The only drawback of CO<sub>2</sub> is its low polarity, which makes it ideal for lipid, greasy, and non-polar substances (such as carotenoids, aromas, volatile compounds), but unsuitable for polar flavonoids.

The limitation of the low polarity of CO<sub>2</sub> has been successfully overcome by the use of chemical modifiers or cosolvents, such as methanol, water, acetone, ethanol, and acetonitrile. These cosolvents can increase the polarity of the supercritical fluid mixture, and consequently, the solvation concerning the target bioactive compounds (Azmir et al., 2013; Bubalo et al., 2018; Yahya et al., 2018). These are employed during extraction in small proportions, typically 1–10% (Herrero et al., 2015). Modifiers may be introduced as mixed fluids into the pumping system with a second pump and a mixing chamber (see Figure 3), or by merely injecting the modifier as a liquid in the sample before extraction. The second way is less successful because it leads to the formation of concentration gradients within the sample. The third very rarely applied form is the use of a cylinder tank with modified CO<sub>2</sub> (Bubalo et al., 2018).

Among the cosolvents for SFE, ethanol is considered the best for the extraction and fractionation of bioactive compounds, such as flavonoids, for nutraceutical and food application, due to its lower toxicity and less selectivity when compared to methanol and other organic solvents. Inversely, water is not generally used as the only cosolvent for SFE, primarily because of its low solubility in CO<sub>2</sub> (Bubalo et al., 2018). Therefore, binary mixtures of water and ethanol are generally employed for extracting SFE

**TABLE 6 |** Some representative applications involving the use of SFE for the recovery of flavonoids from natural sources.

Natural source of flavonoids	Solvent	Co-solvent	Extraction mode	T (°C)/P (MPa)	Flow rate	Time (min)	Target compounds	Yield	Reference
Black poplar buds	CO <sub>2</sub>	–	Dynamic	40-60/12-30	2 kg/h	60	Individual flavonoids	0.42–79.56 µg/mg	Jakovljevi et al., 2018
Haskap berry pulp	CO <sub>2</sub>	Water (2.2–5.5 g)	Static + dynamic	35-65/10-52	10 mL/min	15–120	Anthocyanins	16.6–52.7%	Jiao and Kermanshahi, 2018
Brown onion skin	CO <sub>2</sub>	Ethanol 85% (5–15%)	Dynamic	10/40	10 mL/min	120	Quercetin and derivatives	65–118%	Campone et al., 2018
<i>Odontonema strictum</i> leaves	CO <sub>2</sub>	Ethanol 95% (15%)	Static + dynamic	55-65/20-25	15 g/min	210–270	Total flavonoids	10.68–18.92 mg/g	Ouédraogo et al., 2018
Cipó-pucá	CO <sub>2</sub>	Ethanol (0–10%)	Static + dynamic	40-60/20-40	4.52 g/min	210	Total flavonoids	0.28–13.44 mg/g	Salazar et al., 2018
<i>Opuntia ficus indica</i> (L.) Mill	CO <sub>2</sub>	Ethanol (5%)	Dynamic	35-65/20-40	60–100 g/min	120	Isorhamnetin conjugates	12.45–188.07 mg/100 g	Antunes-Ricardo et al., 2017
<i>Citrus unshiu</i> peels	CO <sub>2</sub>	Ethanol (0–50 mol%)	Dynamic	60/30	0.026 mol/min	180	Nobiletin	0.13–0.57 µg/g	Oba et al., 2017
Tea leaves	CO <sub>2</sub>	Ethanol (1–3 g/min)	Static + dynamic	40-60/10-20	8 g/min	60	Total flavonoids	1.87–1.95 mg/mL	Maran et al., 2015
Myrtle leaves	CO <sub>2</sub>	Ethanol	Dynamic	45/23	0.3 Kg/h	120	Quercetin and myricetin	2–8 (10 <sup>–3</sup> ) mg/g	Pereira et al., 2016
<i>Hibiscus sabdariffa</i>	CO <sub>2</sub>	Ethanol (7–15%)	Dynamic	40-60/15-35	25 g/min	90	Methyl-epigallocatechin	0.34–0.53 mg/g	Pimentel-Moral et al., 2018a
Agroindustrial soybean residue	CO <sub>2</sub>	Ethanol (3%)	Dynamic	35-40/40	0.5 Kg/h	–	Total flavonoids	31.3–65.0 mg/100g	Alvarez et al., 2019
Radish leaves	CO <sub>2</sub>	Ethanol	Dynamic	35-50/30-40	0.6 Kg/h	–	Total flavonoids	13.9–21.8 mg/100g	Goyeneche et al., 2018

(Yahya et al., 2018). The properties of the sample and the solutes of interest, the affinity of the application, and the previous results published in the literature are the primary basis for the selection of the best modifier (Azmir et al., 2013). **Table 6** summarizes the most relevant published works in the last 3 years using the SFE technique, using pure supercritical CO<sub>2</sub> and CO<sub>2</sub> mixed with a cosolvent (water and/or ethanol) for the extraction of flavonoids.

It is noted in some of these studies that the use of cosolvent significantly improved the yield of the target flavonoid extraction. For example, (Salazar et al., 2018), achieved higher yields (9.01–13.44 mg QE/g of extract) of total flavonoids employing 10% cosolvent when compared to the conditions in which was used pure CO<sub>2</sub> (0.14–1.08 mg QE/g of extract) and supercritical mixtures with lower cosolvent content (3.70–5.52 mg QE/g of extract). Behavior similar to that was verified by Oba et al. (2017) in the capture of flavonoid nobiletin. Also, the use of modifiers/cosolvents in the SFE process produces extracts with flavonoid yields as good as those produced by other emerging extraction techniques mentioned earlier in this work. Garcia-Mendoza et al. (2017) when extracting anthocyanins from juçara (*Euterpe edulis* Mart.) residue obtained higher extract yields (22.0 mg/g dry residue) using supercritical extraction with CO<sub>2</sub>-water-ethanol (90 CO<sub>2</sub> and 10% cosolvent) compared to the acidified hydroethanolic extract obtained by the PLE technique (7.7 mg/g dry residue). Similarly, Song et al. (2019) noted an improvement in the recovery of kaempferol and quercetin glycosides from Xinjiang jujube (*Ziziphus jujuba* Mill.) leaves, when employing the SFE-CO<sub>2</sub>/ethanol technique compared to UAE extraction.

In addition to the supercritical solvent, modifier nature, modifier proportions, other factors such as physical-chemical characteristics of the vegetable matrix (moisture content, particle size, chemical composition, etc.), solvent flow rate, extraction mode, extraction time, solvent-feed ratio, the porosity of the extraction bed, diameter-extractor length ratio, extractor free volume, and highlighted, pressure and temperature are involved in the extraction process of flavonoids by SFE (Pourmortazavi and Hajimirsadeghi, 2007). In previous papers (Pourmortazavi and Hajimirsadeghi, 2007; Bubalo et al., 2018), there is a detailed review of the influence of these factors/parameters on the SFE system.

In general, the extraction efficiency of bioactive compounds is increased by increasing the pressure and temperature of the supercritical CO<sub>2</sub>, to an ideal level (Molino et al., 2020). It happens, for the reason that both parameters play a significant role in the solubility of solutes in the solvent (Bubalo et al., 2018; Molino et al., 2020). At constant temperature, the increase in pressure causes an increase in the density of CO<sub>2</sub> and its solvation power, which consequently improves the diffusivity and mass transfer of the target compounds into the fluid (Silva et al., 2016; Molino et al., 2020). At constant pressure, by increasing the temperature of the medium, the fluid becomes less viscous, and the vapor pressure of the solutes increases, leading to a rise in the extraction yield (Bimakr et al., 2011; Bubalo et al., 2018). However, there are studies that, for specific temperature ranges employed, have noticed an opposite effect on this. Wang et al. (2008) noted that total flavonoid yield, extracted from the Chinese medicinal plant *Pueraria lobata*, decreased from 16.8

mg/g to 14.2 mg/g when the temperature was changed in the range of 50–60°C. According to reports contained in this work and the specific literature, this happens because a moderate increase in temperature, when applied at relatively low pressure, can lead to a sharp decrease in the density of CO<sub>2</sub> with a consequent reduction in the solubility of the target compounds (Wang et al., 2008; Essien et al., 2020; Molino et al., 2020). A similar effect was observed in the studies of Liu et al. (2011) and Song et al. (2019), which extracted flavonoids from the Asian species *Maydis stigma* and *Ziziphus jujuba* Mill., respectively.

In addition to the ideal temperature and pressure conditions, maximizing the contact of the supercritical solvent with the flavonoid source plant material is necessary to obtain the best efficiency of the SFE extraction. Extraction time, solvent flow rate, and extraction mode (static and dynamic) are variables that directly influence the contact of the solvent with the sample material (Pourmortazavi and Hajimirsadeghi, 2007). The introduction of a static period before dynamic extraction is used to allow the solvent to penetrate the plant matrix and, therefore, improve the mass transfer of the solute to the fluid by diffusivity, besides increasing the yield, and reducing the total extraction time (Alexandre et al., 2020). Static periods between 10 and 30 min are the ones that have been most used to capture phenolic compounds of the flavonoid class (Wang et al., 2008; Liza et al., 2010; Song et al., 2019; Yang et al., 2019). For dynamic extraction, a more extensive range is observed, reaching periods of up to 270 min (Ouédraogo et al., 2018; Yang et al., 2019). However, it is essential to indicate that extraction time is determined by the quantity and composition of the feed raw material. Generally, the extraction yield increases with the increase in the extraction time until the solubility reaches its limit. (Song et al., 2019) found a significant increase in total flavonoids when the time changed from 30 to 120 min. Ouédraogo et al. (2018) observed similar behavior when extracting polyphenols from *Odontonema strictum* leaves. However, in the study by Jiao and Kermanshahi (2018), no significant effect was noted when extracting anthocyanins from haskap berry pulp in periods 15–120 min of static time and 20–60 min of dynamic time.

The CO<sub>2</sub> solvent flow rate or the supercritical mixture (CO<sub>2</sub>-modifier) directly influences the contact time and the mass transfer phenomenon by convection. Typically, an increase in the solvent flow rate increases the extraction capacity by reducing the external resistance to mass transfer and increasing the chances of intermolecular interactions between the solvent and the solutes (Essien et al., 2020; Molino et al., 2020). Ruslan et al. (2018) recovered a higher catechin content (565.38 ppm) from betel nuts at the highest flow rate studied (4 mL/min). However, as noted in a previous study (Ruslan et al., 2015), very high solvent flow rates can substantially reduce extraction yield due to insufficient contact time between the compounds and the extraction fluid (Essien et al., 2020).

As can be seen, in general, all parameters of the SFE process can be adjusted and, depending on the extraction conditions, can interact with each other to maximize the extraction efficiency. For this reason, experimental designs to determine the best extraction conditions in a particular SFE extraction process are widely needed and used so that a systematic study can be



performed with a statistically supported selection of influential variables (Camel, 2001; Azmir et al., 2013; Herrero et al., 2015). The knowledge of these effects is also useful for the economic evaluation of the process to predict the capacity of the process in an increase of scale and to optimize an industrial plant (Bubalo et al., 2018).

## CONCLUSIONS

There is a clear and growing interest in the extraction and isolation of natural products and their applications. The primary importance of modern analytical research is innovative and safe extraction processes, which are economically viable, and environmentally correct for higher recovery of bioactive compounds in shorter process time from natural sources. The advantages of such techniques have been immense in the production of extracts with good quality and yield, lower consumption of solvent, energy, and shorter extraction time. The most appropriate extraction technique depends on plant matrices and the type of compost, and defined selection criteria should be followed. Recent studies have shown that green extraction methods offer excellent alternatives to traditional methods. Many studies are still being carried out in this field, to improve these new green extraction techniques further, with the intention always to reduce the cost of extraction, the time consumed, the quality of the extract, the environmental safety, and health. Also, the combination of extraction methods usually presents advantages to overcome the limitations of a particular approach. Ironically, the massive volume of information available regarding the extraction of flavonoids from the most diverse types of samples makes it difficult to draw overall conclusions. However, the variability of the results reported in the literature for similar compounds is intrinsically related to the sample characteristics, which play a critical role in releasing them to the extraction solvent. Fortunately, our knowledge about the process and how the variables can be

used to control the process is increasing at a fast pace, which is leading to innovative approaches to maximize yields and reduce degradation while at the same time minimizing its environmental impact.

## AUTHOR CONTRIBUTIONS

All authors made a significant contribution to this article. All were involved in the idea and in the writing of specific parts. JC, MS, LS, and MR were responsible for the introduction, ultrasound-assisted extraction, and reviewing whole the manuscript. DL-P, PT-M, and TF-C were responsible for the section of pressurized liquid extraction. MV-E, AG-d-P, and GB were responsible for the microwave-assisted extraction part. AM was responsible for the supercritical fluid extraction part of the manuscript. All authors were involved in the conceptualization and reviewing the manuscript.

## FUNDING

This work was supported by grants 2013/043044 and 2018/14582-5 from the São Paulo Research Foundation (FAPESP). MS is grateful to FAPESP (2016/19930-6 and 2018/17089-8). TF-C is thankful for the financial support received from the São Paulo Research Foundation—FAPESP (2018/05999-0 and 2018/14938-4) and CNPq for the productivity grant (302473/2019-0). This study was financed in part by the Coordenação de Aperfeiçoamento de Pessoal de Nível Superior—Brasil (CAPES)—Finance Code 001 and CAPES-Print 88887.310558/2018-00.

## ACKNOWLEDGMENTS

DL-P is thankful for the financial support received from the São Paulo Research Foundation—FAPESP (2018/23835-4). MR is grateful to CNPq for the productivity grant (303568/2016-0).

## REFERENCES

- Abotaleb, M., Samuel, S. M., Varghese, E., Varghese, S., Kubatka, P., Liskova, A., et al. (2018). Flavonoids in cancer and apoptosis. *Cancers* 11:28. doi: 10.3390/cancers11010028
- Akbari, H. (2019). *Principals of Solar Engineering*, 3rd ed. CRC Press.
- Alara, O. R., Abdurahman, N. H., Abdul Mudalip, S. K., and Olalere, O. A. (2018b). Microwave-assisted extraction of *Vernonia amygdalina* leaf for optimal recovery of total phenolic content. *J. Appl. Res. Med. Aromat. Plants* 10, 16–24. doi: 10.1016/j.jarmap.2018.04.004
- Alara, O. R., Abdurahman, N. H., and Ukaegbu, C. I. (2018a). Soxhlet extraction of phenolic compounds from *Vernonia cinerea* leaves and its antioxidant activity. *J. Appl. Res. Med. Aromat. Plants* 11, 12–17. doi: 10.1016/j.jarmap.2018.07.003
- Alexandre, A. M. R. C., Serra, A. T., Matias, A. A., Duarte, C. M. M., and Bronze, M. R. (2020). Supercritical fluid extraction of *Arbutus unedo* distillate residues—impact of process conditions on antiproliferative response of extracts. *J. CO<sub>2</sub> Util.* 37, 29–38. doi: 10.1016/j.jcou.2019.11.002
- Alvarez, M. V., Cabred, S., Ramirez, C. L., and Fanovich, M. A. (2019). Fluids valorization of an agroindustrial soybean residue by supercritical fluid extraction of phytochemical compounds. *J. Supercrit. Fluids* 143, 90–96. doi: 10.1016/j.supflu.2018.07.012
- Ameer, K., Muhammad Shahbaz, H., and Kwon, J. H. (2017). Green extraction methods for polyphenols from plant matrices and their byproducts: a review. *Compreh. Rev. Food Sci. Food Saf.* 16, 295–315. doi: 10.1111/1541-4337.12253
- Antunes-Ricardo, M., Gutiérrez-uribe, J. A., and Guajardo-flores, D. (2017). Extraction of isorhamnetin conjugates from *Opuntia ficus-indica* (L.) mill using supercritical fluids. *J. Supercrit. Fluid.* 119, 58–63. doi: 10.1016/j.supflu.2016.09.003
- Azmir, J., Zaidul, I. S. M., Rahman, M. M., Sharif, K. M., Mohamed, A., Sahena, F., et al. (2013). Techniques for extraction of bioactive compounds from plant materials: a review. *J. Food Eng.* 117, 426–436. doi: 10.1016/j.jfoodeng.2013.01.014
- Bakirtzi, C., Triantafyllidou, K., and Makris, D. P. (2016). Novel lactic acid-based natural deep eutectic solvents: efficiency in the ultrasound-assisted extraction of antioxidant polyphenols from common native greek medicinal plants. *J. Appl. Res. Med. Arom. Plants* 3, 120–127. doi: 10.1016/j.jarmap.2016.03.003
- Barba, F. J., Zhu, Z., Koubaa, M., Sant'Ana, A. S., and Orlén, V. (2016). Green alternative methods for the extraction of antioxidant bioactive compounds from winery wastes and by-products: a review. *Trends Food Sci. Technol.* 49, 96–109. doi: 10.1016/j.tifs.2016.01.006
- Barrales, F. M., Silveira, P., Barbosa, P. P. M., Ruviaro, A. R., Paulino, B. N., Pastore, G. M., et al. (2018). Recovery of phenolic compounds from citrus

- by-products using pressurized liquids — an application to orange peel. *Food Bioprod. Process.* 112, 9–21. doi: 10.1016/j.fbp.2018.08.006
- Benito-Román, Ó., Alvarez, V. H., Alonso, E., Cocero, M. J., and Saldaña, M. D. A. (2015). Pressurized aqueous ethanol extraction of  $\beta$ -glucans and phenolic compounds from waxy barley. *Food Res. Int.* 75, 252–259. doi: 10.1016/j.foodres.2015.06.006
- Biata, N. R., Mashile, G. P., Ramontja, J., Mketo, N., and Nomngongo, P. N. (2019). Application of ultrasound-assisted cloud point extraction for preconcentration of antimony, tin and thallium in food and water samples prior to ICP-OES determination. *J. Food Comp. Anal.* 76, 14–21. doi: 10.1016/j.jfca.2018.11.004
- Biesaga, M. (2011). Influence of extraction methods on stability of flavonoids. *J. Chromatogr. A* 1218, 2505–2512. doi: 10.1016/j.chroma.2011.02.059
- Bimkr, M., Rahman, R. A., Taip, F., Ganjloo, A., Selamat, J., Hamid, A. A., et al. (2011). Comparison of different extraction methods for the extraction of major bioactive flavonoid compounds from spearmint (*Mentha spicata* L.) leaves. *Food Bioprod. Process.* 89, 67–72. doi: 10.1016/j.fbp.2010.03.002
- Bleve, M., Ciurlia, L., Erroi, E., Lionetto, G., Longo, L., Rescio, L., et al. (2008). An innovative method for the purification of anthocyanins from grape skin extracts by using liquid and sub-critical carbon dioxide. *Sep. Purif. Technol.* 64, 192–197. doi: 10.1016/j.seppur.2008.10.012
- Bosiljkov, T., Dujmić, F., Bubalo, M. C., Hribar, J., Vidrih, R., Brnčić, M., et al. (2017). Natural deep eutectic solvents and ultrasound-assisted extraction: green approaches for extraction of wine lees anthocyanins. *Food Bioprod. Process.* 102, 195–203. doi: 10.1016/j.fbp.2016.12.005
- Bouras, M., Chadni, M., Barba, F. J., Grimi, N., Bals, O., and Vorobiev, E. (2015). Optimization of microwave-assisted extraction of polyphenols from quercus bark. *Ind. Crops Prod.* 77, 590–601. doi: 10.1016/j.indcrop.2015.09.018
- Bubalo, M. C., Vidovic, S., Redovnikovic, I. R., and Joki, S. (2018). New perspective in extraction of plant biologically active compounds by green solvents. *Food Bioprod. Process.* 9, 52–73. doi: 10.1016/j.fbp.2018.03.001
- Camel, V. (2001). Recent extraction techniques for solid matrices—supercritical fluid extraction, pressurized fluid extraction and microwave-assisted extraction: their potential and pitfalls. *Analyst* 126, 1182–93. doi: 10.1039/b008243k
- Campono, L., Celano, R., Lisa, A., Pagano, I., Carabetta, S., Di, R., et al. (2018). Response surface methodology to optimize supercritical carbon dioxide/Co-solvent extraction of brown onion skin by-product as source of nutraceutical compounds. *Food Chem.* 269, 495–502. doi: 10.1016/j.foodchem.2018.07.042
- Carniel, N., Dallago, R. M., Dariva, C., Bender, J. P., Nunes, A. L., Zanella, O., et al. (2017). Microwave-assisted extraction of phenolic acids and flavonoids from physalis angulata. *J. Food Proc. Eng.* 40, 1–11. doi: 10.1111/jfpe.12433
- Casazza, A. A., Aliakbarian, B., Mantegna, S., Cravotto, G., and Perego, P. (2010). Extraction of phenolics from Vitis vinifera wastes using non-conventional techniques. *J. Food Eng.* 100, 50–55. doi: 10.1016/j.jfoodeng.2010.03.026
- Chan, C. H., Yusoff, R., Ngoh, G. C., and Kung, F. W. L. (2011). Microwave-assisted extractions of active ingredients from plants. *J. Chromatogr. A* 1218, 6213–6225. doi: 10.1016/j.chroma.2011.07.040
- Chavan, Y., and Singhal, R. S. (2013). Ultrasound-assisted extraction (UAE) of bioactives from arecanut (*Areca catechu* L.) and optimization study using response surface methodology. *Innov. Food Sci. Emerg. Technol.* 17, 106–113. doi: 10.1016/j.ifset.2012.10.001
- Chemat, F., Rombaut, N., Sicaire, A. G., Meullemiestre, A., Fabiano-Tixier, A. S., and Abert-Vian, M. (2017). Ultrasound assisted extraction of food and natural products. Mechanisms, techniques, combinations, protocols and applications. a review. *Ultrason. Sonochem.* 34, 540–560. doi: 10.1016/j.ulsonch.2016.06.035
- Chemat, F., Vian, M. A., and Cravotto, G. (2012). Green extraction of natural products: concept and principles. *Int. J. Mol. Sci.* 13, 8615–8627. doi: 10.3390/ijms13078615
- Chen, L., Ding, L., Yu, A., Yang, R., Wang, X., Li, J., et al. (2007). Continuous determination of total flavonoids in *Platycladus Orientalis* (L.) franco by dynamic microwave-assisted extraction coupled with on-line derivatization and ultraviolet-visible detection. *Anal. Chim. Acta* 596, 164–170. doi: 10.1016/j.aca.2007.05.063
- Chen, L., Jin, H., Ding, L., Zhang, H., Li, J., Qu, C., et al. (2008). Dynamic microwave-assisted extraction of flavonoids from herba epimedii. *Sep. Purif. Technol.* 59, 50–57. doi: 10.1016/j.seppur.2007.05.025
- Chen, X. J., Guo, B. L., Li, S. P., Zhang, Q. W., Tu, P. F., and Wang, Y. T. (2007). Simultaneous determination of 15 flavonoids in epimedium using pressurized liquid extraction and high-performance liquid chromatography. *J. Chromatogr. A* 1163, 96–104. doi: 10.1016/j.chroma.2007.06.020
- Chirumbolo, S., Björklund, G., Lysiuk, R., Vella, A., Lenchyk, L., and Upyr, T. (2018). Targeting cancer with phytochemicals via their fine tuning of the cell survival signaling pathways. *Int. J. Mol. Sci.* 19, 3568. doi: 10.3390/ijms19113568
- Cigeroglu, Z., Kirbaşlar, S., Ismail, S., Selin, K., and Gökben (2017). Optimization and kinetic studies of ultrasound-assisted extraction on polyphenols from satsuma mandarin (citrus unshiu marc.) leaves. *Iran. J. Chem. Chem. Eng.* 36, 163–171.
- Corazza, G. O., Bilibio, D., Zanella, O., Nunes, A. L., Bender, J. P., Carniel, N., et al. (2018). Pressurized liquid extraction of polyphenols from goldenberry: influence on antioxidant activity and chemical composition. *Food Bioprod. Process.* 112, 63–68. doi: 10.1016/j.fbp.2018.09.001
- Cunha, S. C., and Fernandes, J. O. (2018). Ibañez Extraction techniques with deep eutectic solvents. *TRAC Trends Anal. Chem.* 105, 225–239. doi: 10.1016/j.trac.2018.05.001
- Cvetanović, A., Švarc-Gajić, J., Zeković, Z., Gašić, U., Tešić, Z., Zengin, G., et al. (2018). Subcritical water extraction as a cutting edge technology for the extraction of bioactive compounds from chamomile: influence of pressure on chemical composition and bioactivity of extracts. *Food Chem.* 266, 389–396. doi: 10.1016/j.foodchem.2018.06.037
- Da Porto, C., Porretto, E., and Decorti, D. (2013). Comparison of ultrasound-assisted extraction with conventional extraction methods of oil and polyphenols from grape (*Vitis vinifera* L.) seeds. *Ultrason. Sonochem.* 20, 1076–1080. doi: 10.1016/j.ulsonch.2012.12.002
- Dahmoune, F., Spigno, G., Moussi, K., Remini, H., Cherbal, A., and Madani, K. (2014). *Pistacia lentiscus* leaves as a source of phenolic compounds: microwave-assisted extraction optimized and compared with ultrasound-assisted and conventional solvent extraction. *Ind. Crops Prod.* 61, 31–40. doi: 10.1016/j.indcrop.2014.06.035
- Dean, J. R., Barnabas, I. J., and Fowles, I. A. (1995). Extraction of polycyclic aromatic hydrocarbons from highly contaminated soils: a comparison between Soxhlet, microwave and supercritical fluid extraction techniques. *Anal. Proc. Include. Anal. Commun.* 32, 305–308. doi: 10.1039/ai9953200305
- Deng, C., Yao, N., Wang, B., and Zhang, X. (2006). Development of microwave-assisted extraction followed by headspace single-drop microextraction for fast determination of paeonol in traditional Chinese medicines. *J. Chromatogr. A* 1103, 15–21. doi: 10.1016/j.chroma.2005.11.023
- Destandau, E., Michel, T., and Elfakir, C. (2013). CHAPTER 4. Microwave-assisted extraction. *J. Chromatogr.* 3, 113–56. doi: 10.1039/9781849737579-00113
- Du, F. Y., Xiao, X. H., Luo, X. J., and Li, G. K. (2009). Application of ionic liquids in the microwave-assisted extraction of polyphenolic compounds from medicinal plants. *Talanta* 78, 1177–1184. doi: 10.1016/j.talanta.2009.01.040
- Du, F. Y., Xiao, X. H., and Li, G. K. (2007). Application of ionic liquids in the microwave-assisted extraction of trans-resveratrol from rhizoma polygoni cuspidati. *J. Chromatogr. A* 1140, 56–62. doi: 10.1016/j.chroma.2006.11.049
- Durazzo, A., Lucarini, M., Souto, E. B., Cicala, C., Caiazzo, E., Izzo, A. A., et al. (2019). Polyphenols: a concise overview on the chemistry, occurrence, and human health. *Phytother. Res.* 33, 2221–2243. doi: 10.1002/ptr.6419
- Dzah, C. S. (2014). Influence of fruit maturity on antioxidant potential and chilling injury resistance of peach fruit (*Prunus persica*) during cold storage. *Afr. J. Food Agric. Nutr. Dev.* 14, 9578–9591.
- Dzah, C. S., Duan, Y., Zhang, H., Wen, C., Zhang, J., Chen, G., et al. (2020). The effects of ultrasound assisted extraction on yield, antioxidant, anticancer and antimicrobial activity of polyphenol extracts: a review. *Food Biosci.* 35:100547. doi: 10.1016/j.fbio.2020.100547
- Ekezie, F. G. C., Da Wen, S., and Cheng, J. H. (2017). Acceleration of microwave-assisted extraction processes of food components by integrating technologies and applying emerging solvents: a review of latest developments. *Trends Food Sci. Technol.* 67, 160–172. doi: 10.1016/j.tifs.2017.06.006
- El-Abbassi, A., Kiai, H., Raiti, J., and Hafidi, A. (2014). Cloud point extraction of phenolic compounds from pretreated olive mill wastewater. *J. Environ. Chem. Eng.* 2, 1480–1486. doi: 10.1016/j.jece.2014.06.024
- Esclapez, M. D., García-Pérez, J. V., Mulet, A., and Cárcel, J. A. (2011). Ultrasound-assisted extraction of natural products. *Food Eng. Rev.* 34, 540–560. doi: 10.1007/s12393-011-9036-6
- Espada-Bellido, E., Ferreira-González, M., Barbero, G. F., Carrera, C., Palma, M., and Barroso, C. G. (2018). Alternative extraction method of bioactive

- compounds from mulberry (*Morus nigra* L.) pulp using pressurized-liquid extraction. *Food Ana. Methods* 11, 2384–2395. doi: 10.1007/s12161-018-1218-x
- Essien, S. O., Young, B., and Baroutian, S. (2020). Recent advances in subcritical water and supercritical carbon dioxide extraction of bioactive compounds from plant materials. *Trends Food Sci. Technol.* 97, 156–169. doi: 10.1016/j.tifs.2020.01.014
- Evstafev, S. N., and Chechikova, E. V. (2016). Transformation of wheat straw polysaccharides under dynamic conditions of subcritical autohydrolysis. *Russ. J. Bioorg. Chem.* 42, 700–706. doi: 10.1134/S1068162016070050
- Farzaneth, V., and Carvalho, I. S. (2017). Modelling of microwave assisted extraction (MAE) of anthocyanins (TMA). *J. Appl. Res. Med. Arom. Plants* 6, 92–100. doi: 10.1016/j.jarmp.2017.02.005
- Flannigan, D. J., and Suslick, K. S. (2010). Inertially confined plasma in an imploding bubble. *Nat. Phys.* 6, 598–601. doi: 10.1038/nphys1701
- Fu, X., Belwal, T., Cravotto, G., and Luo, Z. (2019). Sono-physical and sono-chemical effects of ultrasound: primary applications in extraction and freezing operations and influence on food components. *Ultrason. Sonochem.* 60:104726. doi: 10.1016/j.ulsonch.2019.104726
- Galanakis, C.M. (2012). Recovery of high added-value components from food wastes: conventional, emerging technologies and commercialized applications. *Trends Food Sci. Technol.* 26, 68–87. doi: 10.1016/j.tifs.2012.03.003
- Galván, A. S. C., Romero-García, J. M., Castro, E., and Cardona, C. A. (2018). Supercritical fluid extraction for enhancing polyphenolic compounds production from olive wastes. *J. Chem. Technol. Biotechnol.* 2, 463–484.
- Gao, M., and Liu, C. Z. (2005). Comparison of techniques for the extraction of flavonoids from cultured cells of *Saussurea medusa maxim.* *World J. Microbiol. Biotechnol.* 21, 1461–1463. doi: 10.1007/s11274-005-6809-1
- García-Castello, E.M., Rodríguez-López, A. D., Mayor, L., Ballesteros, R., Conidi, C., and Cassano, A. (2015). Optimization of conventional and ultrasound assisted extraction of flavonoids from grapefruit (*Citrus paradisi* L.) solid wastes. *LWT Food Sci. Technol.* 64, 1114–1122. doi: 10.1016/j.lwt.2015.07.024
- García-Mendoza, P., Espinosa-Pardo, F. A., Baseggio, A. M., Barbero, G. F., Junior, M. R. M., Rostagno, M. A., et al. (2017). Extraction of phenolic compounds and anthocyanins from *juçara* (*euterpe edulis mart.*) residues using pressurized liquids and supercritical fluids. *J. Supercrit. Fluids* 119, 9–16. doi: 10.1016/j.supflu.2016.08.014
- Ghasemzadeh, A., Jaafar, H. Z. E., Karimi, E., and Rahmat, A. (2014). Optimization of ultrasound-assisted extraction of flavonoid compounds and their pharmaceutical activity from curry leaf (*Murraya koenigii* L.) using response surface methodology. *BMC Complement. Altern. Med.* 14:138. doi: 10.1186/1472-6882-14-318
- González-Centeno, M. R., Knoerzer, K., Sabarez, H., Simal, S., Rosselló, C., and Femenia, A. (2014). Effect of acoustic frequency and power density on the aqueous ultrasonic-assisted extraction of grape pomace (*Vitis vinifera* L.) - a response surface approach. *Ultrason. Sonochem.* 21, 2176–2184. doi: 10.1016/j.ulsonch.2014.01.021
- Gortzi, O., Lalas, S., Chatzilazarou, A., Katsoyannos, E., Papaconstandinou, S., and Dourtoglou, E. (2008). Recovery of natural antioxidants from olive mill waste water using Genapol-X080. *J. Am. Oil Chem. Soc.* 85, 133–140. doi: 10.1007/s11746-007-1180-z
- Goyeneche, R., Fanovich, A., Rodrigues, C. R., Nicolaob, M. C., and Di Scala, K. (2018). Supercritical CO<sub>2</sub> extraction of bioactive compounds from radish leaves: yield, antioxidant capacity and cytotoxicity. *J. Supercrit. Fluid.* 135, 78–83. doi: 10.1016/j.supflu.2018.01.004
- Grigonis, D., Venskutonis, P. R., Sivik, B., Sandahl, M., and Eskilsson, C. S. (2005). Comparison of different extraction techniques for isolation of antioxidants from sweet grass (*Hierochloa odorata*). *J. Supercrit. Fluids* 33, 223–233. doi: 10.1016/j.supflu.2004.08.006
- Hao, J., Han, W., Huang, S., Xue, B., and Deng, X. (2002). Microwave-assisted extraction of artemisinin from *Artemisia annua* L. *Sep. Purif. Technol.* 28, 191–196. doi: 10.1016/S1383-5866(02)00043-6
- Herrero, M., Mendiola, J. A., Cifuentes, A., and Ibáñez, E. (2010). Supercritical fluid extraction: recent advances and applications. *J. Chromatogr. A* 1217, 2495–2511. doi: 10.1016/j.chroma.2009.12.019
- Herrero, M., Sánchez-Camargo, A. P., Cifuentes, A., and Ibáñez, E. (2015). Plants, seaweeds, microalgae and food by-products as natural sources of functional ingredients obtained using pressurized liquid extraction and supercritical fluid extraction. *Trends Anal. Chem.* 71, 26–38. doi: 10.1016/j.trac.2015.01.018
- Huang, W., Xue, A., Niu, H., Jia, Z., and Wang, J. (2009). Optimised ultrasonic-assisted extraction of flavonoids from folium eucommiae and evaluation of antioxidant activity in multi-test systems *in vitro*. *Food Chem.* 114, 1147–1154. doi: 10.1016/j.foodchem.2008.10.079
- Ibáñez, E., Herrero, M., Mendiola, J. A., and Castro-Puyana, M. (2012). Extraction and characterization of bioactive compounds with health benefits from marine resources: macro and micro algae, cyanobacteria, and invertebrates. *Mar. Bioact. Compd.* 55–98. doi: 10.1007/978-1-4614-1247-2\_2
- Ilbay, Z., Sahin, S., and Büyükkabasakal, K. (2014). A novel approach for olive leaf extraction through ultrasound technology: response surface methodology versus artificial neural networks. *Korean J. Chem. Eng.* 31, 1661–1667. doi: 10.1007/s11814-014-0106-3
- Jakovljević, M., Joki, S., Ku, P., and Jerković, I. (2018). Extraction of bioactive phenolics from black poplar (*Populus nigra* L.) buds by supercritical CO<sub>2</sub> and its optimization by response surface methodology. *J. Pharmac. Biomed. Anal.* 152, 128–136. doi: 10.1016/j.jpba.2018.01.046
- Jha, P., Das, A. J., and Deka, S. C. (2017). Optimization of ultrasound and microwave assisted extractions of polyphenols from black rice (*Oryza Sativa* cv. Poiréton) Husk. *J. Food Sci. Technol.* 54, 3847–3858. doi: 10.1007/s13197-017-2832-0
- Jiao, G., and Kermanshahi, A. (2018). Extraction of anthocyanins from haskap berry pulp using supercritical carbon dioxide: influence of co-solvent composition and pretreatment. *LWT Food Sci. Technol.* 98, 237–244. doi: 10.1016/j.lwt.2018.08.042
- Jin, C., Wei, X., Yang, S., Yao, L., and Gong, G. (2017). Microwave-assisted extraction and antioxidant activity of flavonoids from sedum aizoon leaves. *Food Sci. Technol. Res.* 23, 111–118. doi: 10.3136/fstr.23.111
- Justyna, P., Owczarek, K., Tobiszewski, M., and Namie, J. (2017). Trends in analytical chemistry extraction with environmentally friendly solvents. *Anal. Chem.* 91, 12–25. doi: 10.1016/j.trac.2017.03.006
- Kala, H. K., Mehta, R., Sen, K. K., Tandey, R., and Mandal, V. (2016). Critical analysis of research trends and issues in microwave assisted extraction of phenolics: have we really done enough. *Trends Anal. Chem.* 85, 140–152. doi: 10.1016/j.trac.2016.09.007
- Kalai, S., and Ignasimuthu, N. S. (2018). Separation of catechins from green tea (*Camellia Sinensis* L.) by microwave assisted acetylation, evaluation of antioxidant potential of individual components and spectroscopic analysis. *LWT* 91, 391–397. doi: 10.1016/j.lwt.2018.01.042
- Kamali, H., Khodaverdi, E., Hadizadeh, F., and Ghaziaskar, S. H. (2016). Optimization of phenolic and flavonoid content and antioxidants capacity of pressurized liquid extraction from *dracocephalum kotschyi* via circumscribed central composite. *J. Supercrit. Fluids* 107, 307–314. doi: 10.1016/j.supflu.2015.09.028
- Khan, M. K., Vian, M., Fabiano-Tixier, A. S., Dangles, O., and Chemat, F. (2010). Ultrasound-assisted extraction of polyphenols (flavonone glycosides) from orange (*Citrus sinensis* L.) peel. *Food Chem.* 119, 851–858. doi: 10.1016/j.foodchem.2009.08.046
- Khoddami, A., Wilkes, M. A., and Roberts, T. H. (2013). Techniques for analysis of plant phenolic compounds. *Molecules* 18, 2328–75. doi: 10.3390/molecules18022328
- Kong, Y., Zu, W. G., Fu, Y. J., Liu, W., Chang, F. R., Li, J., et al. (2010). Optimization of microwave-assisted extraction of cajanin stilbene acid and pinostrobin from pigeonpea leaves followed by RP-HPLC-DAD determination. *J. Food Comp. Anal.* 23, 382–388. doi: 10.1016/j.jfca.2009.12.009
- Kovačević, D. B., Maras, M., Barba, F. J., Granato, D., Roohinejad, S., Mallikarjunan, K., et al. (2018). Innovative technologies for the recovery of phytochemicals from *stevia rebaudiana* bertonii leaves: a review. *Food Chem.* 268, 513–521. doi: 10.1016/j.foodchem.2018.06.091
- Koyu, H., Kazan, A., Demir, S., Haznedaroglu, M. Z., and Yesil-Celiktas, O. (2018). Optimization of microwave assisted extraction of *Morus nigra* L. fruits maximizing tyrosinase inhibitory activity with isolation of bioactive constituents. *Food Chem.* 248, 183–191. doi: 10.1016/j.foodchem.2017.12.049
- Kratchanova, M., Pavlova, E., and Panchev, I. (2004). The effect of microwave heating of fresh orange peels on the fruit tissue and quality of extracted pectin. *Carbohydr. Polym.* 56, 181–185. doi: 10.1016/j.carbpol.2004.01.009



- Kumar, S., and Pandey, A. K. (2013). Chemistry and biological activities of Flavonoids: an overview. *ScientificWorldJournal*. 2013:162750. doi: 10.1155/2013/162750
- Lachos-Perez, D., Baseggio, A. M., Mayanga-Torres, P. C., Maróstica, M. R., Rostagno, M. A., Martínez, J., et al. (2018). Subcritical water extraction of flavanones from defatted orange peel. *J. Supercrit. Fluids* 138, 7–16. doi: 10.1016/j.supflu.2018.03.015
- Lachos-Perez, D., Baseggio, A. M., Torres-Mayanga, P. C., Ávila, P. F., and Tompsett, G. A., Maróstica, M., et al. (2020). Sequential subcritical water process applied to orange peel for the recovery flavanones and sugars. *J. Supercrit. Fluids* 160:104789. doi: 10.1016/j.supflu.2020.104789
- Lachos-Perez, D., Brown, A., Mudhoo, A., Martínez, J., Timko, M., Rostagno, M., et al. (2017). Applications of subcritical and supercritical water conditions for extraction, hydrolysis, gasification, and carbonization of biomass: a critical review. *Biofuel Res. J.* 4, 611–626. doi: 10.18331/BRJ2017.4.2.6
- Lamaison, J. L. C., and Carnet, A. (1990). Teneurs en principaux flavonoids des fleurs de *Crataegus monogyna* Jacq et de *Crataegus laevigata* (Poir) D. C. en fonction de la végétation. *Pharm. Acta Helv.* 65, 315–320.
- Laws, D. R. J., Bath, N. A., Ennis, C. S., and Wheldon, A. G. (1980). Hop extraction with carbon dioxide. *U.S. Patent No.* 4,218,491.
- Leong, T., Ashokkumar, M., and Kentish, S. (2011). The fundamentals of power ultrasound—a review. *Acoustics Australia*. 39, 54–63.
- Leyva-Jiménez, F. J., Lozano-Sánchez, J., Borrás-Linares, I., Arráez-Román, D., and Segura-Carretero, A. (2018). Comparative study of conventional and pressurized liquid extraction for recovering bioactive compounds from lippia citriodora leaves. *Food Res. Int.* 109, 213–222. doi: 10.1016/j.foodres.2018.04.035
- Li, J., Wu, C., Li, F., Yu, R., Wu, X., Shen, L., et al. (2019). Optimization of ultrasound-assisted water extraction of flavonoids from psidium guajava leaves by response surface analysis. *Preparat. Biochem. Biotechnol.* 49, 21–29. doi: 10.1080/10826068.2018.1466158
- Li, W., Li, T., and Tang, K. (2009). Flavonoids from mulberry leaves by microwave-assisted extract and anti-fatigue activity. *Afr. J. Agric. Res.* 4, 898–902.
- Li, Y., Li, S., Lin, S. J., Zhang, J. J., Zhao, C. N., and Li, H. B. (2017). Microwave-assisted extraction of natural antioxidants from the exotic gordonia axillaris fruit: optimization and identification of phenolic compounds. *Molecules* 22:1481. doi: 10.3390/molecules22091481
- Liang, Q., Chen, H., Zhou, X., Deng, Q., Hu, E., Zhao, C., et al. (2017). Optimized microwave-assisted extraction combined ultrasonic pretreatment of flavonoids from periploca forrestii schltr and evaluation of its anti-allergic activity. *Electrophoresis* 38, 1113–1121. doi: 10.1002/elps.201600515
- Liaziad, A., Guerrero, R. F. F., Cantos, E., Palma, M., and Barroso, C. G. G. (2011). Microwave assisted extraction of anthocyanins from grape skins. *Food Chem.* 124, 1238–1243. doi: 10.1016/j.foodchem.2010.07.053
- Liu, J., Lin, S., Wang, Z., Wang, C., Wang, E., Zhang, Y., et al. (2011). Supercritical fluid extraction of flavonoids from maydis stigma and its nitrite-scavenging ability. *Food Bioprod. Process.* 89, 333–339. doi: 10.1016/j.fbp.2010.08.004
- Liu, J., Sand ahl, M., Sjöberg, P. J. R., and Turner, C. (2014). Pressurised hot water extraction in continuous flow mode for thermolabile compounds: extraction of polyphenols in red onions. *Anal. Bioanal. Chem.* 406, 441–445. doi: 10.1007/s00216-013-7370-7
- Liu, J. F., Jiang, G. B., and Jönsson, J. A. (2005). Application of ionic liquids in analytical chemistry. *Trends Anal. Chem.* 24, 20–27. doi: 10.1016/j.trac.2004.09.005
- Liza, M. S., Rahman, R. A., Mandana, B., Jinap, S., Rahmat, A., Zaidul, I. S. M., et al. (2010). Supercritical carbon dioxide extraction of bioactive flavonoid from strobilanthes crispus (Pecah Kaca). *Food Bioprod. Process.* 88, 319–326. doi: 10.1016/j.fbp.2009.02.001
- Machado, A. P. F., Pasquel-Reátegui, J. L., Barbero, G. F., and Martínez, J. (2015). pressurized liquid extraction of bioactive compounds from blackberry (*Rubus fruticosus* L.) residues: a comparison with conventional methods. *Food Res. Int.* 77, 675–683. doi: 10.1016/j.foodres.2014.12.042
- Machado, A. P. F., Sumere, B. R., Mekaru, C., Martinez, J., Bezerra, R. M. N., and Rostagno, M. A. (2019). Extraction of polyphenols and antioxidants from pomegranate peel using ultrasound: influence of temperature, frequency and operation mode. *Int. J. Food Sci. Technol.* 54, 2792–2801. doi: 10.1111/ijfs.14194
- Mai, X., Liu, Y., Wang, T., Tang X., Wang, L., Lin, Y., Zeng, H., et al. (2020). Sequential extraction and enrichment of flavonoids from Euonymus alatus by ultrasonic-assisted polyethylene glycol-based extraction coupled to temperature-induced cloud point extraction. *Ultrason. Sonochem.* 66:105073. doi: 10.1016/j.ultsonch.2020.105073
- Mandal, V., and Mandal, S. C. (2010). Design and performance evaluation of a microwave based low carbon yielding extraction technique for naturally occurring bioactive triterpenoid: oleanolic acid. *Biochem. Eng. J.* 50, 63–70. doi: 10.1016/j.bej.2010.03.005
- Maran, J. P., Manikand an, S., Priya, B., and Gurumoorthi, P. (2015). Box-behnken design based multi-response analysis and optimization of supercritical carbon dioxide extraction of bioactive flavonoid compounds from tea (*Camellia sinensis* L.) leaves. *J. Food Sci. Technol.* 52, 92–104. doi: 10.1007/s13197-013-0985-z
- Maran, J. P., Priya, B., Al-Dhabi, N. A., Ponnurugan, K., Moorthy, I. G., and Sivarajasekar, N. (2017). Ultrasound assisted citric acid mediated pectin extraction from industrial waste of Musa balbisiana. *Ultrason. Sonochem.* 35(Pt A), 204–209. doi: 10.1016/j.ultsonch.2016.09.019
- Mason, T. J., and Lorimer, J. P. (2002). *Applied Sonochemistry. The Uses of Power Ultrasound in Chemistry and Processing*. Wiley-VCH. doi: 10.1002/352760054X
- Md Yusof, Huzaimi, A., Gani, S. S. A., Zaidan, U. H., Halmi, M. I. E., and Zainudin, B. H. (2019). Optimization of an ultrasound-assisted extraction condition for flavonoid compounds from cocoa shells (*Theobroma cacao*) using response surface methodology. *Molecules* 24:711. doi: 10.3390/molecules24040711
- Mello, P. A., Barin, J. S., and Guarnieri, R. A. (2014). “Microwave heating,” in *Microwave-Assisted Sample Preparation for Trace Element Analysis*, ed E. M. de Moraes Flores (Santa Maria, RS: Elsevier), 59–75.
- Meullemiestre, A., Breil, C., Abert-Vian, M., and Chemat, F. (2016). Microwave, ultrasound, thermal treatments, and bead milling as intensification techniques for extraction of lipids from oleaginous yarrowia lipolytica yeast for a biojetfuel application. *Bioresour. Technol.* 211, 190–199. doi: 10.1016/j.biortech.2016.03.040
- Miljevic, B., Hedayat, F., Stevanovic, S., Fairfull-Smith, K. E., Bottle, S. E., and Ristovski, Z. D. (2014). To sonicate or not to sonicate pm filters: reactive oxygen species generation upon ultrasonic irradiation. *Aerosol Sci. Technol.* 48, 1276–1284. doi: 10.1080/02786826.2014.981330
- Molino, A., Mehariya, S., Di Sanzo, G., Larocca, V., Martino, M., Leone, G. P., et al. (2020). Recent developments in supercritical fluid extraction of bioactive compounds from microalgae: role of key parameters, technological achievements and challenges. *J. CO<sub>2</sub> Util.* 36, 196–209. doi: 10.1016/j.jcou.2019.11.014
- Moreira, M. M., Barroso, M. F., Boeykens, A., Withouck, H., Morais, S., and Delerue-Matos, C. (2017). Valorization of apple tree wood residues by polyphenols extraction: comparison between conventional and microwave-assisted extraction. *Ind. Crops Prod.* 104, 210–220. doi: 10.1016/j.indcrop.2017.04.038
- Motikar, P. D., More, P. R., and Arya, S. S. (2020). A novel, green environment-friendly cloud point extraction of polyphenols from pomegranate peels: a comparative assessment with ultrasound and microwave-assisted extraction. *Sep. Sci. Technol.* 1–12. doi: 10.1080/01496395.2020.1746969
- Munir, M. T., Kheirkhah, H., Baroutian, S., Quek, S. Y., and Young, B. R. (2018). Subcritical water extraction of bioactive compounds from waste onion skin. *J. Clean. Prod.* 183, 487–494. doi: 10.1016/j.jclepro.2018.02.166
- Mustafa, A., and Turner, C. (2011). Pressurized liquid extraction as a green approach in food and herbal plants extraction: a review. *Anal. Chim. Acta* 703, 8–18. doi: 10.1016/j.aca.2011.07.018
- Mustapa, A. N., Martin, A., Mato, R. B., and Cocero, M. J. (2015). Extraction of phytochemicals from the medicinal plant clinacanthus nutans lindau by microwave-assisted extraction and supercritical carbon dioxide extraction. *Ind. Crops Prod.* 74, 83–94. doi: 10.1016/j.indcrop.2015.04.035
- Nabavi, S. M., Samec, D., Tomczyk, M., Milella, L., Russo, D., Habtemariam, S., et al. (2018). Flavonoid biosynthetic pathways in plants: versatile targets for metabolic engineering. *Biotechnol. Adv.* 38:107216. doi: 10.1016/j.biotechadv.2018.11.005
- Oba, C., Ota, M., Nomura, K., Fujiwara, H., Takito, J., Sato, Y., et al. (2017). Extraction of nobletin from citrus unshiu peels by supercritical fluid and its cre-me diate d transcriptional activity. *Phytomedicine* 27, 33–38. doi: 10.1016/j.phymed.2017.01.014
- Oniszczuk, A., and Podgórski, R. (2015). Influence of different extraction methods on the quantification of selected flavonoids and phenolic



- acids from *tilia cordata* inflorescence. *Ind. Crops Prod.* 76, 509–514. doi: 10.1016/j.indcrop.2015.07.003
- Orsat, V., and Routray, W. (2017). Microwave-assisted extraction of flavonoids. *Water Extract. Bioactive Comp. Plants Drug Dev.* 2017, 221–44. doi: 10.1016/B978-0-12-809380-1.00008-5
- Ouédraogo, J. C. W., Dicko, C., Kinic, F. B., Bonzi-Coulbaly, Y. L., and Dey, E. S. (2018). Enhanced extraction of flavonoids from *odonotoma strictum* leaves with antioxidant activity using supercritical carbon dioxide fluid combined with ethanol. *J. Supercrit. Fluid.* 131, 66–71. doi: 10.1016/j.supflu.2017.08.017
- Palma, M., Barbero, G. F., Piñeiro, Z., Liazid, A., Barroso, C. G., Rostagno, M. A., et al. (2013). CHAPTER 2. Extraction of natural products: principles and fundamental aspects. 58–88. doi: 10.1039/9781849737579-00058
- Pan, G., Yu, G., Zhu, C., and Qiao, J. (2012). Optimization of ULTRASOUND-ASSISTED EXTRACTION (UAE) of flavonoids compounds (FC) from hawthorn seed (HS). *Ultrason. Sonochem.* 19, 486–490. doi: 10.1016/j.ultsonch.2011.11.006
- Pan, X., Niu, G., and Liu, H. (2003). Microwave-assisted extraction of tea polyphenols and tea caffeine from green tea leaves. *Chem. Eng. Proc.* 42, 129–133. doi: 10.1016/S0255-2701(02)00037-5
- Panche, A. N., Diwan, A. D., and Chandra, S. R. (2016). Flavonoids: an overview. *J. Nutr. Sci.* 5:e47. doi: 10.1017/jns.2016.41
- Pashazadeh, B., Elhamirad, A. H., Hajnajari, H., Sharayei, P., and Armin, M. (2020). Optimization of the pulsed electric field -assisted extraction of functional compounds from cinnamon. *Biocatal. Agric. Biotechnol.* 23:101461. doi: 10.1016/j.bcab.2019.101461
- Pasirja, D., and Anand haramakrishnan, C. (2015). Techniques for extraction of green tea polyphenols: a review. *Food Bioproc. Technol.* 8, 935–950. doi: 10.1007/s11947-015-1479-y
- Pereira, D. T. V., Tarone, A. G., Cazarin, C. B. B., Barbero, G. F., and Martínez, J. (2019). Pressurized liquid extraction of bioactive compounds from grape marc. *J. Food Eng.* 240, 105–113. doi: 10.1016/j.jfoodeng.2018.07.019
- Pereira, P., Cebola, M. J., Oliveira, M. C., and Bernardo-Gil, M. G. (2016). Supercritical fluid extraction vs conventional extraction of myrtle leaves and berries: comparison of antioxidant activity and identification of bioactive compounds. *J. Supercrit. Fluid.* 113, 1–9. doi: 10.1016/j.supflu.2015.09.006
- Pimentel-Moral, S., Borrás-Linares, I., Lozano-Sánchez, J., Arráez-Román, D., Martínez-Férez, A., and Segura-Carretero, A. (2018a). Fluids supercritical CO<sub>2</sub> extraction of bioactive compounds from *Hibiscus sabdariffa*. *J. Supercrit. Fluid.* 147, 213–221. doi: 10.1016/j.supflu.2018.11.005
- Pimentel-Moral, S., Borrás-Linares, I., Lozano-Sánchez, J., Arráez-Román, D., Martínez-Férez, A., and Segura-Carretero, A. (2018b). Microwave-assisted extraction for *Hibiscus sabdariffa* bioactive compounds. *J. Pharm. Biomed. Anal.* 156, 313–322. doi: 10.1016/j.jpba.2018.04.050
- Pinela, J., Prieto, M. A., Carvalho, A. M., Barreiro, M. F., Oliveira, M. B. P., Barros, L., et al. (2016). Microwave-assisted extraction of phenolic acids and flavonoids and production of antioxidant ingredients from tomato: a nutraceutical-oriented optimization study. *Sep. Purif. Technol.* 164, 114–124. doi: 10.1016/j.seppur.2016.03.030
- Plaza, M., and Turner, C. (2015). Trends in analytical chemistry pressurized hot water extraction of bioactives. *Trends Anal. Chem.* 71, 39–54. doi: 10.1016/j.trac.2015.02.022
- Pourmortazavi, S. M., and Hajimirsadeghi, S. S. (2007). supercritical fluid extraction in plant essential and volatile oil analysis. *J. Chromatogr. A* 1163, 2–24. doi: 10.1016/j.chroma.2007.06.021
- Ren, F., Nian, Y., and Perussello, C. A. (2020). Effect of storage, food processing and novel extraction technologies on onions flavonoid content: a review. *Food Res. Int.* 132:108953. doi: 10.1016/j.foodres.2019.108953
- Rodríguez-García, C., and Sanchez-Quesada, C. (2019). Dietary flavonoids as cancer chemopreventive agents: an updated review of human studies. *Antioxidants* 8:E137. doi: 10.3390/antiox8050137
- Rodríguez-Pérez, C., Gilbert-López, B., Mendiola, J. A., Quirantes-Pin, R., Segura-Carretero, A., and Ibáñez, E. (2016). Optimization of microwave-assisted extraction and pressurized liquid extraction of phenolic compounds from moringa oleifera leaves by multiresponse surface methodology. *Electrophoresis* 37, 1938–1946. doi: 10.1002/elps.201600071
- Roohinejad, S., Koubaa, M., Barba, F. J., Greiner, R., Orlén, V., and Lebavka, N. I. (2016). Negative pressure cavitation extraction: a novel method for extraction of food bioactive compounds from plant materials. *Trends Food Sci. Technol.* 52, 98–108. doi: 10.1016/j.tifs.2016.04.005
- Rosa, R., Erika, F., and Veronesi, P. (2018). “From field to shelf: how microwave-assisted extraction techniques foster an integrated green approach,” in *Emerging Microwave Technologies in Industrial, Agricultural, Medical and Food Processing*, ed. K. Y. Yeow (Malaysia: University of Technology Malaysia), 179–203. doi: 10.5772/intechopen.73651
- Rostagno, M. A., D'Arrigo, M., Martínez, J. A., and Martínez, J. A. (2010). Combinatory and hyphenated sample preparation for the determination of bioactive compounds in foods. *Trends Anal. Chem.* 29, 553–561. doi: 10.1016/j.trac.2010.02.015
- Rostagno, M. A., Villares, A., Guillaumon, E., García-Lafuente, A., and Martínez, J. A. (2009). Sample preparation for the analysis of isoflavones from soybeans and soy foods. *J. Chromatogr. A* 1216, 2–29. doi: 10.1016/j.chroma.2008.11.035
- Routray, W., and Orsat, V. (2012). Microwave-assisted extraction of flavonoids: a review. *Food Bioproc. Technol.* 5, 409–424. doi: 10.1007/s11947-011-0573-z
- Ruslan, M. S. H., Azizi, C. Y. M., Idham, Z., Morad, N. A., and Ali, A. (2015). Parametric evaluation for extraction of catechin from *Areca catechu* linn seeds using supercritical CO<sub>2</sub> extraction. *J. Technol.* 74, 87–92. doi: 10.11113/jt.v74.4704
- Ruslan, M. S. H., Azizi, C. Y. M., Idham, Z., Yian, L. N., Zaini, M. A. A., and Yunus, M. A. C. (2018). Effect of operating conditions on catechin extraction from betel nuts using supercritical CO<sub>2</sub>-methanol extraction. *Sep. Sci. Technol.* 53, 662–670. doi: 10.1080/01496395.2017.1406947
- Sahena, F., Zaidul, I. S. M., Jinap, S., Karim, A. A., Abbas, K. A., Norulaini, N. A. N., et al. (2009). Application of supercritical CO<sub>2</sub> in lipid extraction - A review. *J. Food Eng.* 95, 240–256. doi: 10.1016/j.jfoodeng.2009.06.026
- Salazar, M. A. R., Costa, J. V., Urbina, G. R. O., Borges, V. M. C., Silva, M. P., Bezerra, P. N., et al. (2018). Fluids chemical composition, antioxidant activity, neuroprotective and anti-inflammatory effects of cipó-puçá (*Cissampelos* L.) extracts obtained from supercritical extraction. *J. Supercrit. Fluids* 138, 36–45. doi: 10.1016/j.supflu.2018.03.022
- Santos, D. T., Veggi, P. C., and Meireles, M. A. A. (2012). Optimization and economic evaluation of pressurized liquid extraction of phenolic compounds from jabuticaba skins. *J. Food Eng.* 108, 444–452. doi: 10.1016/j.jfoodeng.2011.08.022
- Santos, H. M., Lodeiro, C., and Capelo-Martínez, J. L. (2009). “The power of ultrasound,” in *Ultrasound in Chemistry: Analytical Applications*, ed J.-L. Capelo-Martínez (Wiley-VCH Verlag GmbH & Co. KGaA), 1–16.
- Sarfaraizi, M., Jafari, S. M., Rajabzadeh, G., and Galanakis, C. M. (2020). Evaluation of microwave-assisted extraction technology for separation of bioactive components of saffron (*Crocus sativus* L.). *Ind. Crop. Prod.* 145:111978. doi: 10.1016/j.indcrop.2019.111978
- Scarano, A., Chieppa, M., and Santino, A. (2018). Looking at flavonoid biodiversity in horticultural crops: a colored mine with nutritional benefits. *Plants* 7:E98. doi: 10.3390/plants7040098
- Sengar, A. S., Rawson, A., Muthiah, M., and Kalakandan, S. K. (2020). Comparison of different ultrasound assisted extraction techniques for pectin from tomato processing waste. *Ultrason. Sonochem.* 61:104812. doi: 10.1016/j.ultsonch.2019.104812
- Shirsath, S. R., Sonawane, S. H., and Gogate, P. R. (2012). Intensification of extraction of natural products using ultrasonic irradiations-a review of current status. *Chem. Eng. Proc. Proc. Int.* 53, 10–23. doi: 10.1016/j.ccep.2012.01.003
- Sillero, L., Prado, R., and Labidi, J. (2018). Optimization of different extraction methods to obtaining bioactive compounds from larch decidua bark. *Chem. Eng. Transac.* 70, 1369–1374. doi: 10.3303/CET1870229
- Silva, R. P. F., Rocha-Santos, T. A. P., and Duarte, A. C. (2016). Supercritical fluid extraction of bioactive compounds. *Trends Anal. Chem.* 76, 40–51. doi: 10.1016/j.trac.2015.11.013
- Søltoft, M., Christensen, J. H., Nielsen, J., and Knuthsen, P. (2009). Pressurized liquid extraction of flavonoids in onions. *Method Dev. Valid.* 80, 269–278. doi: 10.1016/j.talanta.2009.06.073
- Song, L., Liu, P., Yan, Y., Huang, Y., Bai, B., Hou, X., et al. (2019). Supercritical CO<sub>2</sub> fluid extraction of flavonoid compounds from *Xinjiang Jujube* (*Ziziphus Jujuba* Mill) leaves and associated biological activities and flavonoid compositions. *Ind. Crops Prod.* 139:111508. doi: 10.1016/j.indcrop.2019.111508
- Sookjitsumran, W., Devahastin, S., Mujumdar, A. S., and Chiewchan, N. (2016). Comparative evaluation of microwave-assisted extraction and preheated

- solvent extraction of bioactive compounds from a plant material: a case study with cabbages. *Int. J. Food Sci. Technol.* 51, 2440–2449. doi: 10.1111/ijfs.13225
- Soquetta, M. B., Tonato, D., Quadros, M. M., Boeira, C. P., Cichoski, A. J., Terra, L. M., et al. (2019). Ultrasound extraction of bioactive compounds from *Citrus reticulata* peel using electrolyzed water. *J. Food Proc. Preserv.* 43:e14236. doi: 10.1111/jfpp.14236
- Spigno, G., and De Faveri, D. M. (2009). Microwave-assisted extraction of tea phenols: a phenomenological study. *J. Food Eng.* 93, 210–217. doi: 10.1016/j.jfoodeng.2009.01.006
- Srivastava, J., and Vankar, P. S. (2010). Canna indica flower: new source of anthocyanins. *Plant Physiol. Biochem.* 48, 1015–1019. doi: 10.1016/j.plaphy.2010.08.011
- Tabaraki, R., Heidarizadi, E., and Benvidi, A. (2012). Optimization of ultrasonic-assisted extraction of pomegranate (*Punica granatum* L.) peel antioxidants by response surface methodology. *Sep. Purif. Technol.* 98, 16–23. doi: 10.1016/j.seppur.2012.06.038
- Tena, M. T. (2018). Pressurized liquid extraction reference module in chemistry. *Mol. Sci. Chem. Eng.* doi: 10.1016/B978-0-12-409547-2.14407-5
- Teng, H., Lee, Y. W., and Choi, Y. H. (2013). Optimization of microwave-assisted extraction for anthocyanins, polyphenols, and antioxidants from raspberry (*Rubus Coreanus* Miq.) using response surface methodology. *J. Sep. Sci.* 36, 3107–3114. doi: 10.1002/jssc.201300303
- Tiwari, B. K. (2015). Ultrasound: a clean, green extraction technology. *Trends Anal. Chem.* 71, 100–109. doi: 10.1016/j.trac.2015.04.013
- Tungmunthum, D., Elamrani, A., Abid, M., Drouet, S., Kiani, R., Garros, L., et al. (2020). A quick, green and simple ultrasound-assisted extraction for the valorization of antioxidant phenolic acids from moroccan almond cold-pressed oil residues. *Appl. Sci.* 10:3313. doi: 10.3390/app10093313
- Um, M., Han, T. H., and Lee, J. W. (2018). Ultrasound-assisted extraction and antioxidant activity of phenolic and flavonoid compounds and ascorbic acid from rugosa rose (*Rosa rugosa* Thunb.) fruit. *Food Sci. Biotech.* 27, 375–382. doi: 10.1007/s10068-017-0247-3
- Upadhyay, R., Nachiappan, G., and Mishra, H. N. (2015). Ultrasound-assisted extraction of flavonoids and phenolic compounds from ocimum tenuiflorum leaves. *Food Sci. Biotechnol.* 24, 1951–1958. doi: 10.1007/s10068-015-0257-y
- Vankar, P. S., and Srivastava, J. (2010). Ultrasound-assisted extraction in different solvents for phytochemical study of canna indica. *Int. J. Food Eng.* 6. doi: 10.2202/1556-3758.1599
- Viganó, J., Brumer, I. Z., Braga, P. A. C., da Silva, J. K., Júnior, M. R. M., Reyes, R. G. R., et al. (2016). Pressurized liquids extraction as an alternative process to readily obtain bioactive compounds from passion fruit rinds. *Food Bioprod. Process.* 100, 382–390. doi: 10.1016/j.fbp.2016.08.011
- Vilkhu, K., Manasseh, R., Mawson, R., and Ashokkumar, M. (2011). Ultrasonic recovery and modification of food ingredients. *Ultrasound Technol. Food Bioprocess.* 345–68. doi: 10.1007/978-1-4419-7472-3\_13
- Vinatoru, M., Mason, T. J., and Calinescu, I. (2017). Ultrasonically assisted extraction (UAE) and microwave assisted extraction (MAE) of functional compounds from plant materials. *Trends Anal. Chem.* 97, 159–178. doi: 10.1016/j.trac.2017.09.002
- Wang, J., Zhang, J., Zhao, B., Wang, X., Wu, Y., and Yao, J. (2010). A comparison study on microwave-assisted extraction of *Potentilla anserina* L. Polysaccharides with conventional method: molecule weight and antioxidant activities evaluation. *Carbohydr. Polym.* 80, 84–93. doi: 10.1016/j.carbpol.2009.10.073
- Wang, L., Yang, B., Du, X., and Yi, C. (2008). Optimisation of supercritical fluid extraction of flavonoids from pueraria lobata. *Food Chem.* 108, 737–741. doi: 10.1016/j.foodchem.2007.11.031
- Wang, Y., Gao, Y., Ding, H., Liu, S., Han, X., Gui, J., et al. (2017). Subcritical ethanol extraction of flavonoids from *Moringa oleifera* leaf and evaluation of antioxidant activity. *Food Chem.* 218, 152–158. doi: 10.1016/j.foodchem.2016.09.058
- Wei, X., Chen, M., Xiao, J., Liu, Y., Yu, L., Zhang, H., et al. (2010). Composition and bioactivity of tea flower polysaccharides obtained by different methods. *Carbohydr. Polym.* 79, 418–422. doi: 10.1016/j.carbpol.2009.08.030
- Wijngaard, H., Hossain, M. B., Rai, D. K., and Brunton, N. (2012). Techniques to extract bioactive compounds from food by-products of plant origin. *Food Res. Int.* 46, 505–513. doi: 10.1016/j.foodres.2011.09.027
- Wu, J., Lin, L., and Chau, F. (2001). Ultrasound-assisted extraction of ginseng saponins from ginseng roots and cultured ginseng cells. *Ultrason. Sonochem.* 8, 347–352. doi: 10.1016/S1350-4177(01)00066-9
- Xiang, Z., and Wu, X. (2017). Ultrasonic-microwave assisted extraction of total flavonoids from *scutellaria baicalensis* using response surface methodology. *Pharmac. Chem. J.* 51, 318–323. doi: 10.1007/s11094-017-1606-3
- Xiangnan, L., Huang, J., Wang, Z., Jiang, X., Yu, W., Zheng, Y., et al. (2014). alkaline extraction and acid precipitation of phenolic compounds from longan (*Dimocarpus longan* L.) seeds. *Sep. Purif. Technol.* 124, 201–206. doi: 10.1016/j.seppur.2014.01.030
- Xiao, W., Han, L., and Shi, B. (2008). Microwave-assisted extraction of flavonoids from radix astragali. *Sep. Purif. Technol.* 62, 614–618. doi: 10.1016/j.seppur.2008.03.025
- Xin, L., Yuan, J. P., Xu, S. P., Wang, J. H., and Liu, X. (2008). Separation and determination of secoisolaricresinol diglucoside oligomers and their hydrolysates in the flaxseed extract by high-performance liquid chromatography. *J. Chromatogr. A* 1185, 223–232. doi: 10.1016/j.chroma.2008.01.066
- Xynos, N., Papaefstathiou, G., Gikas, E., Argyropoulou, A., Aligiannis, N., and Skaltsounis, A. L. (2014). Design optimization study of the extraction of olive leaves performed with pressurized liquid extraction using response surface methodology. *Sep. Purif. Technol.* 122, 323–330. doi: 10.1016/j.seppur.2013.10.040
- Yahfoufi, N., Alsadi, N., Jambi, M., and Matar, C. (2018). The immunomodulatory and anti-inflammatory role of polyphenols. *Nutrients* 10:E1618. doi: 10.3390/nu10111618
- Yahya, N. A., Attana, N., and Wahaba, R. A. (2018). An overview of cosmeceutically relevant plant extracts and strategies for extraction of plant-based bioactive compounds. *Food Bioprod. Process.* 2, 69–85. doi: 10.1016/j.fbp.2018.09.002
- Yang, L., Cao, Y. L., Jiang, J. G., Lin, Q., S., Chen, J., et al. (2010). Response surface optimization of ultrasound-assisted flavonoids extraction from the flower of *Citrus aurantium* L. Var. Amara Engl. *J. Sep. Sci.* 33, 1349–1355. doi: 10.1002/jssc.200900776
- Yang, Y. C., Wang, C. S., and Wei, M. C. (2019). Kinetics and mass transfer considerations for an ultrasound-assisted supercritical CO<sub>2</sub> procedure to produce extracts enriched in flavonoids from *scutellaria barbata*. *J. CO<sub>2</sub> Util.* 32, 219–231. doi: 10.1016/j.jcou.2019.04.008
- Yang, Z., and Zhai, W. (2010). Optimization of microwave-assisted extraction of anthocyanins from purple corn (*Zea mays* L.) cob and identification with HPLC-MS. *Innov. Food Sci. Emerg. Technol.* 11, 470–476. doi: 10.1016/j.ifset.2010.03.003
- Yedhu, K. R., and Rajan, K. S. (2016). Microwave assisted extraction of flavonoids from terminalia bellerica: study of kinetics and thermodynamics. *Sep. Purif. Technol.* 157, 169–178. doi: 10.1016/j.seppur.2015.11.035
- Zhang, F., Yang, Y., Su, P., and Guo, Z. (2009). Microwave-assisted extraction of rutin and quercetin from the stalks of *euonymus alatus* (thunb.) sieb. *Phytochem. Anal.* 20, 33–37. doi: 10.1002/pca.1088
- Zhang, L., Shan, Y., Tang, K., and Putheti, R. (2009). Ultrasound-assisted extraction flavonoids from lotus (*Nelumbo nucifera* gaertn) leaf and evaluation of its anti-fatigue activity. *Int. J. Phys. Sci.* 4, 418–422.
- Zhang, Z.-S., Li, D., Wang, L.-J., Ozkan, N., Chen, X. D., Mao, Z.-H., et al. (2007). Optimization of ethanol-water extraction of lignans from flaxseed. *Sep. Purif. Technol.* 57, 17–24. doi: 10.1016/j.seppur.2007.03.006
- Zhao, C. N., Zhang, J. J., Li, Y., Meng, X., and Li, H. B. (2018). Microwave-assisted extraction of phenolic compounds from *melastoma sanguineum* fruit: optimization and identification. *Molecules.* 23:2498. doi: 10.3390/molecules23102498
- Zhao, Z., Liu, P., Wang, S., and Ma, S. (2017). Optimization of ultrasound, microwave and soxhlet extraction of flavonoids from *milletia speciosa* champ and evaluation of antioxidant activities *in vitro*. *J. Food Meas. Charact.* 11, 1947–1958. doi: 10.1007/s11694-017-9577-3
- Zhong, L., Zhang, Y., Chi, R., and Yu, J. (2016). Optimization of microwave-assisted ethanol reflux extraction process of flavonoids and saponins simultaneously

- from radix astragali using response surface methodology. *Food Sci. Technol. Res.* 22, 759–770. doi: 10.3136/fstr.22.759
- Zhou, H. Y., and Liu, C. Z. (2006). Microwave-assisted extraction of solanesol from tobacco leaves. *J. Chromatogr. A* 1129, 135–139. doi: 10.1016/j.chroma.2006.07.083
- Zhou, J., Zhang, L., Li, Q., Jin, W., Chen, W., Han, J., et al. (2019). Simultaneous optimization for ultrasound-assisted extraction and antioxidant activity of flavonoids from sophora flavescens using response surface methodology. *Molecules* 24:112. doi: 10.3390/molecules24010112
- Zosel, K. (1981). Process for the decaffeination of coffee. *Espacenet*. US Patent 4,247,570.

**Conflict of Interest:** The authors declare that the research was conducted in the absence of any commercial or financial relationships that could be construed as a potential conflict of interest.

Copyright © 2020 Chaves, de Souza, da Silva, Lachos-Perez, Torres-Mayanga, Machado, Forster-Carneiro, Vázquez-Espinosa, González-de-Peredo, Barbero and Rostagno. This is an open-access article distributed under the terms of the Creative Commons Attribution License (CC BY). The use, distribution or reproduction in other forums is permitted, provided the original author(s) and the copyright owner(s) are credited and that the original publication in this journal is cited, in accordance with accepted academic practice. No use, distribution or reproduction is permitted which does not comply with these terms.

# Advantages of publishing in Frontiers



## OPEN ACCESS

Articles are free to read  
for greatest visibility  
and readership



## FAST PUBLICATION

Around 90 days  
from submission  
to decision



## HIGH QUALITY PEER-REVIEW

Rigorous, collaborative,  
and constructive  
peer-review



## TRANSPARENT PEER-REVIEW

Editors and reviewers  
acknowledged by name  
on published articles

## Frontiers

Avenue du Tribunal-Fédéral 34  
1005 Lausanne | Switzerland

**Visit us:** [www.frontiersin.org](http://www.frontiersin.org)

**Contact us:** [info@frontiersin.org](mailto:info@frontiersin.org) | +41 21 510 17 00



## REPRODUCIBILITY OF RESEARCH

Support open data  
and methods to enhance  
research reproducibility



## DIGITAL PUBLISHING

Articles designed  
for optimal readership  
across devices



## FOLLOW US

[@frontiersin](https://twitter.com/frontiersin)



## IMPACT METRICS

Advanced article metrics  
track visibility across  
digital media



## EXTENSIVE PROMOTION

Marketing  
and promotion  
of impactful research



## LOOP RESEARCH NETWORK

Our network  
increases your  
article's readership